Bulletin
of
The Geological Society of America

VOLUME 68 September 1957 NUMBER 9

CONTENTS

	Pages
Cretaceous, Paleocene, and lower Eocene geologic history of the northern Mississippi embayment. By Richard G. Stearns	1077–1100
Clay alteration and ore, Temple Mountain, Utah. By Dana R. Kelley and Paul F. Kerr	1101–1116
Uranium-lead method of age determination. Part II: North American localities. By Walter R. Eckelmann and J. Laurence Kulp	1117–1140
Hydrology of Lake Bonneville and sediments and soils of its basin. By A. J. Eardley, Vasyl Gvosdetsky, and R. E. Marsell	1141–1202
Effects of gamma radiation on the experimental deformation of calcite and certain rocks. By John Handin, D. V. Higgs, D. R. Lewis, and P. K. Weyl	1203–1224

Subscription $15.00 per year.
Printing Office: Mt. Royal & Guilford Aves., Baltimore 2, Md.
Communications for publications should be addressed to The Geological Society of America, Dr. H. R. Aldrich, Secretary, 419 West 117 Street, New York, N. Y.
Please give notice of change of address 4 weeks in advance. Claims for nonreceipt of the Bulletin of a given month must be sent to the Secretary of the Society before the end of the second succeeding month.

Entered as second-class matter at the Post Office at Baltimore, Md., under the Act of Congress of July 16, 1894.
Accepted for mailing at special rate of postage provided for in Section 1103 Act of October 3, 1917, authorized on July 8, 1918.

PAPERS IN PRESS FOR FORTHCOMING ISSUES

GEOLOGIC EVOLUTION OF THE BEARTOOTH MOUNTAINS, MONTANA AND WYOMING. PART 1: ARCHEAN HISTORY OF THE QUAD CREEK AREA. By F. Donald Eckelmann and Arie Poldervaart

WEATHERING OF GRANITE AND ASSOCIATED EROSIONAL FEATURES IN HONG KONG. By Bryan P. Ruxton and Leonard Berry

MINERALOGY, PETROGRAPHY, AND RADIOACTIVITY OF REPRESENTATIVE SAMPLES OF CHATTANOOGA SHALE. By Thomas F. Bates and Erwin O. Strahl

UPLAND GRAVELS OF SOUTHERN MARYLAND. By John Schlee

GEOLOGY OF THE COCHISE HEAD AND WESTERN PART OF THE VANAR QUADRANGLES, ARIZONA. By F. F. Sabins

GEOLOGICAL AND GEOPHYSICAL SYNTHESIS OF THE TECTONICS OF PORTIONS OF BRITISH COLUMBIA, THE YUKON TERRITORY, AND ALASKA. By Pierre St. Amand

ANTHRACITIC COAL FROM THE PRECAMBRIAN UPPER HURONIAN BLACK SHALES OF THE IRON RIVER DISTRICT, NORTHERN MICHIGAN. By S. A. Tyler, E. S. Barghoorn, and L. P. Barrett

STRATIGRAPHY AND STRUCTURE OF THE ST. ALBANS AREA, NORTHWESTERN VERMONT. By A. B. Shaw

PEBBLE AND SAND LITHOLOGY OF THE MAJOR WISCONSIN GLACIAL LOBES OF THE CENTRAL LOWLAND. By Richard C. Anderson

STRUCTURE AND PETROLOGY OF THE CARIBOU LAKE INTRUSIVE BODY, ONTARIO, CANADA. By Gerald M. Friedman

BULLETIN OF THE GEOLOGICAL SOCIETY OF AMERICA
VOL. 68, PP. 1077–1100, 21 FIGS. SEPTEMBER 1957

CRETACEOUS, PALEOCENE, AND LOWER EOCENE GEOLOGIC HISTORY OF THE NORTHERN MISSISSIPPI EMBAYMENT

By Richard G. Stearns

Abstract

Subsurface data show that in the northern Mississippi Embayment Cretaceous, Paleocene, and lower Eocene deposition occurred in a single sedimentary cycle.

The cycle began with Cretaceous deposition of nonmarine Tuscaloosa gravel, restricted in area. Marine advance and depositional limits reached a maximum in the Paleocene with the deposition of Porters Creek Clay, which once generally extended beyond the embayment limits. Deposition ended in the early Eocene with nonmarine Wilcox beds, now restricted to the subsurface near the embayment axis. Uplift and erosion resulting in marked truncation followed to complete the cycle.

Overlying middle Eocene Claiborne Group beds overlap all the lower Eocene Wilcox Group and part of the Paleocene Midway Group, all around the northern end of the embayment north of the Tennessee-Mississippi border.

Within the cycle five advances and regressions of the sea, which are illustrated by stratigraphic cross sections and a series of paleogeographic maps, are recorded.

The pattern of contemporary subsidence of the embayment is shown on four isopach maps, which indicate that the present trough shape of the embayment appeared during latest Cretaceous and persisted through the Paleocene and early Eocene.

Subsidence of the embayment trough strongly influenced geography from late Paleocene through early Eocene. During this time the sea occupied bays that followed the embayment axis. A delta was prominent in western Kentucky and northwestern Tennessee during Late Cretaceous and late Paleocene.

CONTENTS

TEXT

	Page
Introduction	1078
General statement	1078
Present investigation	1078
Previous investigations	1078
Acknowledgments	1081
Geology	1081
Surface geology	1081
Correlations	1081
Environmental relationships	1084
General statement	1084
Back-beach clay and sand	1084
Shallow-water near-shore sand	1085
Deeper-water clay and shale	1085
Isopach and lithofacies maps	1085
General statement	1085
Map of Cretaceous rocks below "X point"	1088
Map of Cretaceous rocks above "X point"	1089
Map of Paleocene rocks	1089
Map of lower Eocene rocks	1090
Paleogeography of the Cretaceous, Paleocene, and lower Eocene	1090
Gulfward environmental and stratigraphic changes	1090
Major oscillations	1092
Paleogeographic maps	1093
General statement	1093
Lowermost Cretaceous	1093
Upper Cretaceous transgression	1094
Upper Cretaceous regression	1094
Paleocene maximum transgression	1095
Upper Paleocene regression	1095
End of the Paleocene	1097
First lower Eocene transgression	1097
Second lower Eocene transgression	1099
Second lower Eocene regression	1099
Conclusions	1099
References Cited	1100

ILLUSTRATIONS

Figure	Page
1.—Generalized geologic map	1082
2.—Relations of electric-log subdivisions of this report to formations and major subdivisions	1083
3.—Locations of wells used in this report	1084
4.—Index map showing the locations of stratigraphic cross sections on Figures 5 and 6	1085
5.—Stratigraphic correlation section showing environmental relationships from Bolivar County, Mississippi, to Paducah, Kentucky	1086

Figure Page
6.—Stratigraphic correlation section showing environmental relationships from White County, Arkansas, to Madison County, Tennessee 1087
7. Isopach and sand-shale ratio map of Cretaceous rocks below "X point" 1088
8.—Isopach and sand-shale ratio map of Cretaceous rocks above "X point" 1089
9.—Isopach and sand-shale ratio map of the Midway Group (Paleocene) 1090
10.—Isopach and sand-shale ratio map of the Wilcox Group (Lower Eocene) 1091
11.—Correlation of typical logs and lithologies showing environmental and stratigraphic variations 1092
12.—Transgressive and regressive oscillations during deposition of the Cretaceous, Midway, and Wilcox 1092
13.—Paleogeography of the lowermost Cretaceous 1093
14. Paleogeography during the Upper Cretaceous transgression 1094
15.—Paleogeography during the Upper Cretaceous regression 1095
16.—Paleogeography during the Paleocene maximum transgression 1096
17.—Paleogeography during the upper Paleocene regression 1096
18.—Paleogeography at the end of the Paleocene 1097
19.—Paleogeography during the first lower Eocene transgression 1098
20.—Paleogeography during the second lower Eocene transgression 1098
21.—Paleogeography during deposition of the latest preserved lower Eocene 1099

TABLES

Table Page
1. Electric-log correlations 1079

Introduction

General Statement

The Mississippi Embayment is an extension of the Coastal Plain and reaches into the interior as far north as Cairo, Illinois. Almost complete preservation of the original extent of many stratigraphic units from Cretaceous through Eocene makes this region of considerable interest in both stratigraphy and historical geology.

Lateral variations from marine to nonmarine beds here furnish a rare opportunity to investigate the shifting patterns of paleogeography. Lateral variations in thickness also furnish the opportunity to investigate the shifting tectonic patterns of the embayment as it assumed the form reflected in its present area.

Present Investigation

This investigation is a part of Tennessee's ground-water program carried out in cooperation with the United States Geological Survey. Western Tennessee, which is part of the Mississippi Embayment, is the area where the largest potential supplies of ground water exist. Inasmuch as drill holes are scarce in western Tennessee, it was believed desirable to gather data from other States of that province in order to understand better the distribution of aquifers in Tennessee.

Many stratigraphic units here are for the most part restricted to the subsurface, and some are buried. Information used in constructing the maps contained in this report is almost exclusively from bore holes (Fig. 3). Unfortunately, poor drilling records and lack of sampling render many bore holes useless. The only consistent record throughout the area is electric logs of wells, many of which have no other stratigraphic information. Such logs are used for the correlation and lithologic interpretation of this report.

Previous Investigations

Although many workers have investigated sediments of this area, few have worked primarily with the subsurface, and still fewer with electric logs.

Brown (1947) correlated many wells in Mississippi by both samples and electric logs. The present work in Mississippi is based on his publication. His correlations in Bolivar County, Mississippi, are the standard for Eocene correlations used herein.

Renfroe (1949) correlated many wells in eastern Arkansas, and his correlations are in agreement with those of Brown. The electric and lithologic log of the Cockburn-Robinson No. 1 well (Table 1) serves as a reference section for correlation in eastern Arkansas.

The stratigraphic cross section of West Tennessee by Schneider and Blankenship (1950) was the first published electric-log correlation for that part of the State. The U. S. Geological Survey–Tennessee Division of Geology test wells in that section are heavily relied upon for the relationship between lithology and electric-log patterns.

Caplan (1954) described the subsurface geology of northwest Arkansas with particular reference to oil and gas possibilities. Stratigraphic units, particularly in the Cretaceous,

TABLE 1.—ELECTRIC-LOG CORRELATIONS
(Depths in feet)

ARKANSAS

No.	Well name and number	Location	Total depth	Elev. (msl)	Base "500-ft. sand"	Base "1,400-ft. sand"	Top Cretaceous	"X Point"	Top Paleozoic
1	Stone-Hopkins 1	28-16N-2E	744	258					669
2	Crenshaw-Goldman 1-A	6-15N-2E	726	255			422		
4	Ramsey-Singer 1	35- 9N-4E	3512	210	1020	1400	2170		2880
5	Cross-Rhodes 1	20- 8N-2E	2500	220	750	1060	1820		
6	Davis-DeMange 1	22- 8N-7E	5022	224	1005	1583	2400		3190
7	Stanley-Danner 1	18- 8N-9E	3352	225		1620	2525		3305
8	Cross-Newman 1	28- 7N-1E	2070	215	875	1060	1870		
9	Cross-Surrat 1	33- 7N-2E	2548	220	960	1275	2060		
10	Irene-Nevils 1	14- 6N-6W	1323	200	85		562		660
11	Irene-Self 1	28- 6N-5W	2170	210	95		832		988
12	Taubman-Peel 1	26- 6N-3W	1600	200	485	590	1395		1575
13	Manning-Park 1	4- 6N-5E	4452	205			2450		3275
14	Ramsey-Sanderson 1	15- 6N-7E	3503	212	1150	1720	2585	3345	3500
15	Tatum-Miller 2	7- 5N-2W	1744	215	745	875	1681		
16	Tatum-Nathan 1	18- 5N-2W	1785	197	688	880	1618		
17	Manning-Gregg 1	20- 5N-5E	3988	205	1240	1620	2525	3303	3390
19	Barnwell-Thombaugh 1	8- 4N-1W	2672	214	1070	1319	2122	2625	2670
20	Petroleum-Caples 1	17- 4N-1W	2725	214	1100	1380	2194		2725
21	Hargraves-Peters 1	21- 4N-1W	2505	205	1105	1380	2230		
22	Wier-Lynn 1	7- 4N-1E	2792	205	1155	1360	2262		
23	Martin-Stewart 1	3- 3N-5W	3240	210	640	740	1590		1876
24	Sohio-Gann 1	22- 3N-3W	3164	170	1030	1240	2120	2645	2645
25	Silver-Chambers 1	17- 2N-7W	1980	227	600		1340		1465
26	Cockburn-Robinson 1	14- 2N-1E	3643	203	1432	1840	2750	3415	3545
27	Victory-Clayton 1	10- 1N-5W	3383	220	1185	1465	2230		
28	Curtis-West-Day 1	1- 1N-5W	2876	222	1170	1449	2230		2703
29	Ryan-McCollum 1	24- 2S-5W	3731	215	1660	2065	2905		3530
30	Rambo-Nivens 1	16- 3S-8W	3102	206	1620	1860	2670		3075
31	Flesh-Rosencrantz 1	2- 3S-6W	3633	219	1740	2090	2940		3463
32	McAlester Co. -Howe 1	27- 3S-2E	4574	171	1605	2350	3455	4280	4459
33	Youngblood-West 1	24- 4S-2W	4183	185	1865	2390	3446	4160	4183
34	McAlester Co. -Welch 1	24- 4S-2E	4953	174	1705	2425	3503	4338	4522
35	Foha-Miller 1	33- 5S-4W	4558	190	2115	2760	3690	4402	4518
36	Blackwell-Fox 1	23- 5S-3W	4372	195	2050	2585	3565	4275	4335
37	Columbia-Victoria 1	34- 8S-3W	4915	174	2150	2950	3895	4700	4875
38	Allaum-Moore 1	34- 9S-10W	3821	268	1925	2350	3250		
39	Lion-Holderfield 1	21-10S-9W	4606	223	1945	2340	3280		3920
40	Lion-Clinton 1	10-10S-8W	4204	262	2095	2590	3558		4200
41	Lion-Reef 1	25-11S-9W	4248	185	1970	2410	3292		4000
42	Magnolia-Sturgis 1	30- 9N-3W	5994	217					495
43	States-LaFerney 1	25- 6N-8W	4821	230					330
44	Layton-Layton 1	17- 2N-7W	1411	295	590		1335		
45	Continental-Dewitt 1	32- 5S-2W	4520	195	2040	2710	3675	4395	4510
46	Wadley-Brown 1	33- 5S-3W	4543	197	2115	2770	3695	4400	4540
47	Continental-Cunningham 1	3- 6S-2W	4607	196	2020	2635	3690	4422	4607
48	Martin-Parnell 1	25- 6S-5W	2125	234	1270		1640		2010
49	Seaboard-Anderson-Tully 1	30-10S-1E	4819	153	2115	2800	3745	4510	4795
50	Delta-Grief 1	32-10S-1W	5295		2155	2855	3715	4490	4855
51	Seaboard-Core Hole B	14-10N-2E	2114	239	545	800	1540		2090
52	Seaboard-Core Hole A	19-10N-2E	1983	235	455	700	1430		1980
53	Seaboard-Core Hole C	8- 9N-2E	2125	232	600	850	1570		2120
54	Seaboard-Core Hole F	11- 2N-2W	3153	182	1245	1530	2450		3090
55	Seaboard-Core Hole J	28- 1S-7W	2590	200	1260	1520	2290		2530
56	Seaboard-Core Hole K	11- 3S-4W	3916	200	1770	2240	3200		3915

KENTUCKY

No.	Well name and number	Location	Total depth	Elev. (msl)	Base "500-ft. sand"	Base "1,400-ft. sand"	Top Cretaceous	"X Point"	Top Paleozoic
3a	Roof 1	McCracken Co.		475	176				
3b	Reidland Water Dist.	"		400			100		
3c	West Paducah School	"		355			150		340

TABLE 1—*Continued*

MISSISSIPPI No.	Well name and number	Location	Total depth	Elev. (msl)	Base "500-ft." sand	Base "1,400-ft." sand	Top Cretaceous	"X Point"	Top Paleozoic
1	Union-Withers 1	18- 2S- 9W	4884	220	1030	1708	2500	3335	3540
2	Johnson-Pritchard 1	28- 4S- 7W	2955	235	775	1245	1950	2719	2800
3	Cullet-Nabors 1	36- 7S- 3E	1416	425				530	1102
4	Richardson-Robbins 1	3- 8S- 1E	3479	400			420	930	1732
7	Blevins-Water 5	16- 9S- 8W	2457		620	1158	2010		
8	Adams-Lewellen 1	9-10S- 1W	4006	569			625±	1200±	1785
9	Guiberson-Lyon 1	3-10S- 3E	2233	500				565	1255
11	Grasty-Lumber Co. 1	7-10S-10E	3538	349					362
13	Onyette-Austin 1	1-11S- 6W	2134	250		622	1385	1960	
14	Ellison-Neely 1	28-11S- 5E	4271	315					945
15	Michael-Temple 1	8-11S- 7E	1762	341					550
20	Honolulu-Davis 1	22-12S- 1E	3325	315			320	815	1700
21	Union-Dinsmore 1	28-12S- 3E	4447	422				535	1420
22	Sinclair-Epperson 1	13-12S- 3E	2962	429				430	1330
24	Davidor-Gladney 1	24-12S- 4E	2656	360				185	1110
26	Hutchings-Stone 1	29-12S- 5E	2507	378				150	1060
27	Carter-Abernathy 1	29-12S- 5E	3491	350				125	1103
28	Carter-Crane 1	31-13S- 1E	9237	392			520	992	2255
29	Carter-Fowler 1	22-13S- 2E	4906	327			139	600	1800
30	Magnolia-Pierce 1	22-13S- 7E	8003	309					1055
31	Magnolia-Snow 1	27-13S- 7E	4769						740
36	Killam-Chennault 1	14-14S- 2E	2787	300				602	1875
37	Carter-Pulliam 1	24-14S- 4E	7029	304				160	1325
38	Carter-Baskin 1	19-14S- 5E	5186	320				135	1310
39	Shell-Gelling 1	34-14S- 6E	5022	328					1122
41	Shell-Holmes A-1	25-14S- 6E	3595	271					1125
44	Union-Henderson 1	22-15S- 4E	10557	437				315	1750
45	Union-Lenoir 1	29-15S- 6E	5826	250					1220
47	Union-Sanders 1	22-15S- 6E	6059	288					1120
50	Union-Rye 1	27-15S- 6E	5529	297					1085
53	Union-Watson 1	31-15S- 7E	6417	278					985
55	Atlantic-Myers 1	31-15S-18W	5751	215					630
57	Carter-McFadden 1	36-16S- 5E	9580	205					1430
59	Henson-Green 1	10-17N- 9E	4517	387			1220		4275
60	Hunt-Phillips 1	33-18N- 3E	4211		990±	1630±	2610		
61	Hunt-Winters 1	28-18N- 3E	5955		1000±	1600±	2580		5950
62	Henson-Stafford	33-18N- 9E	4387	379			1190		4245
63	Gulf-Parker 1	23-19N- 7E	5086	394			1450	1950	4430
64	Allen-Nowell 1	2-19N-13E	4975	268				370	2310
65	Atlantic-Dunning 1	12-19N-16E	9243	184				260	1290
66	Exchange-Wildwood 1	6-20N- 1E	5330		1030	1625	2530	3210	5260
68	Gulf-Cason 1	2-21N- 1W	5900	145	1030	1590	2555	3245	5070
69	Young-Kennedy 1	23-21N- 1E	3278	144	863	1430	2365	3020	
70	Henderson-Greer 1	36-21N- 5E	3479			820	1630	2160	
71	Adams-Avent 1	26-22N- 4E	4030	304	510	980	1825	2418	
72	Lockhart-Lamon 1	22-22N- 6E	2765	294	60	560	1428	1992	
73	Lockhart-Fite 1	25-22N- 6E	3787	324		528	1398	1945	3630
74	Killam-Dattel 1	18-23N- 7W	5118		1975	2645	3650	4433	4972
75	Hunt-Rayner 1	4-23N- 5W	5057	150	1645	2360	3350	4100	5000
76	LaRue-Westbrook 1	18-23N- 2W	4296	136	1255	1902	2890	3608	
77	Williams-Conn. Life 1	28-23N- 5E	3006	201		600	1530	2080	3600
78	Holmans-Thomas 1	18-24N- 7W	4661	159	1850	2595	3558	4322	4588
79	Phillips-Perthshire 1	2-24N- 7W	6009	164	1805	2530	3525	4325	4700
80	Marshall-Ogilvie 1	32-24N- 2E	3976	145	738	1220	2070	2705	
81	Stewart-McRee 1	25-24N- 6E	2960	205		258	1140	1700	
82	Ogg-Bardwell 1	5-25N- 3E	3659	245	500	1108	1930	2535	3355
83	Airmont-Boyle 1	33-25N- 7E	2841	415		337	1160	1690	
84	Honolulu-Davis 2	27-12S- 1E	8390	369			363	870	1760
85	Gulf-Basden 1	20- 7S- 5E	5010	367				125	730
86	Salmon-Wilson Est. 1	29- 9S- 3E	4504	470				600	1250
87	Salmon-Patterson 1	12-11S- 1E	5904	352			340	845	1640
88	Magnolia-Warren 1	26-11S- 3E	7419	513				545	1350
90	Young-Parker 1	18-20N- 3W	4431	133	1605	2440	3430	4150	
91	Young-McClain 1	9-20N- 3W	4467	130	1535	2310	3290	4000	
92	Seaboard-Chicago Mill 1	9-23N- 8W	4785	150	2000	2755	3660	4455	4735

TABLE 1—*Concluded*

MISSOURI

No.	Well name and number	Location	Total depth	Elev. (msl)	Base "500-ft." sand	Base "1,400-ft." sand	Top Cretaceous	"X Point"	Top Paleozoic
1	Strake-Russell 1	24-19N-11E	2158	271	732	1200	1710		2062
2	City Steel-Water? 1	26-17N-11E	2350		904	1597	2170		

TENNESSEE

No.	Well name and number	Location	Total depth	Elev. (msl)	Base "500-ft." sand	Base "1,400-ft." sand	Top Cretaceous	"X Point"	Top Paleozoic
1	Henderson-Fields 1	Dyer	3240	260	1040	1530	2200		2780
2	T-1-F (U. S. G. S.)	Fayette	2582	318	615	1050	1632	2255	2530
3	Hay-Morrison 1	Fayette	2722	411				1675±	1993
4	LaZaros-Beasley 1	Fayette	1767		180	270	775	1475±	1758
5	Watson-Holt 2	Gibson	2355	319	725	970	1460	1950±	2000
6	Maquire-Moore 1	Haywood	2181	445			1275	1865±	2120
8	Corley-Vaughan 1	Lake	2590	289	1140	1590	2100		2430
9	Pure-Gray 1	Lauderdale	3289	303	795?	1242?	1750		2440
10	Gear-Lee 1	Lauderdale	2832	329	1000	1465	1925		2648
11	T-1-M (U. S. G. S.)	Madison	1106	570	140		400	936±	1072
12	T-2-M (U. S. G. S.)	Madison	1289	351	225		520	1100±	1270
13	Lion-Bateman 1	Shelby	2865	250	975	1410	2080		2810
14	Owen-Crumpler 1	Shelby	3010	390	890	1350	2030	2840	3039
15	Pure-McGregor 1	Tipton	2753	270	550?	1050±	1950		2550
16	Nance-Donaldson 1	Hardeman	3780	357			90	750±	1002
17	Benz-Hays 1	Lake	2263	293	1010	1420	1920		2260
18	Memphis	Shelby	1512	247	1055	1480			

are treated in more detail than in the present report. This report includes several correlation sections and an isopach map of the Cretaceous.

Stearns and Armstrong (1955) published a brief general report on the stratigraphy of the northern Mississippi Embayment. They first proposed the relationship between lithology and environment used herein. The report also includes electric-log correlations, isopach and sand-distribution maps, and structure contour maps. The present investigation represents a revision and extension of their work.

Grohskopf (1955) described the subsurface geology of the Mississippi Embayment area of southeast Missouri.

Acknowledgments

The writer is indebted to many people for aid and guidance. Seaboard Oil Company furnished lithologic and electric logs of its core holes in Arkansas. Carter Oil Company also provided electric logs of several of its core holes in Woodruff, Prairie, and White counties, Arkansas. Establishment of electric-log correlations is for the most part due to the generosity of these organizations.

Guidance by W. D. Hardeman, State Geologist of Tennessee, and the support and advice of E. M. Cushing, District Engineer, Ground Water Branch, U. S. Geological Survey, Memphis, Tennessee, are particularly appreciated.

Many of the interpretations of this project were resolved during discussions with the writer's colleagues, including R. M. Richardson and R. F. Schreurs of the U. S. Geological Survey, and F. M. Alexander of the Tennessee Division of Geology.

C. W. Wilson, Jr., of Vanderbilt University, critically read the manuscript and contributed many valuable suggestions.

R. J. Floyd, of the Tennessee Division of Geology, did the final manuscript editing.

GEOLOGY

Surface Geology

Figure 1 is a generalized geologic map of the region. Cretaceous beds and Paleocene Midway Group beds crop out almost all around the embayment edge. Strata of the lower Eocene Wilcox Group crop out only in northern Mississippi. Elsewhere, the Wilcox and upper Midway beds are overlapped by middle Eocene Claiborne Group beds. In part of Arkansas the Claiborne overlaps not only the Wilcox, but also the Midway and Cretaceous.

Correlations

Five major contacts are recognized on electric logs: (1) base of the "500-foot" sand of the Memphis area (Schneider and Cushing, 1948), (2) base of the "1400-foot" sand of the Memphis

area, (3) top of the Cretaceous System, (4) a point within the Cretaceous System referred to herein as "X point," and (5) top of Paleozoic rocks. Electric-log correlations of these five contacts are the main basis of this report. The

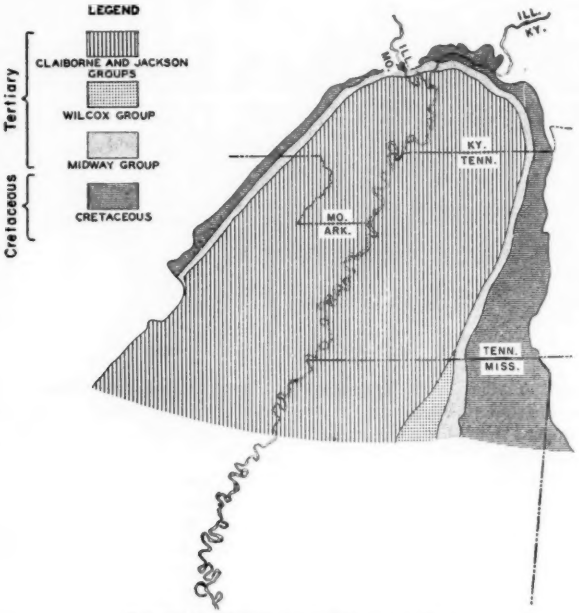

FIGURE 1.—GENERALIZED GEOLOGIC MAP

position of these contacts on a generalized electric log is shown in Figure 2. Table 1 gives the drilled depth to each of these contacts for all the wells used.

The base of the "500-foot" sand is a distinct break that divides the Eocene Series into two units, the Wilcox Group below and the Claiborne and Jackson groups above. This contact coincides with the top of the Wilcox of Brown (1947, Pl. 5) in Bolivar County, Mississippi; Renfroe (1949, Pl. 3) in Lee County, Arkansas; and Schneider and Blankenship (1950) in Fayette and Shelby counties, Tennessee.

As used in this report the Wilcox (lower Eocene) extends from the base of the "500-foot" sand to the base of the "1400-foot" sand. The top of the Porters Creek Clay (Paleocene) is customarily used as the boundary between the Wilcox and Midway (Caplan, 1954, p. 95), and in some wells near the Mississippi River the "1400-foot" sand does directly overlie Porters Creek. Elsewhere, however, as much as 200 feet of sandy beds intervene. This interval is included here with the Paleocene Midway rather than the lower Eocene Wilcox, because it grades laterally into Porters Creek Clay.

The Paleocene Series extends from the base of the "1400-foot" sand downward to the top of the Cretaceous System. The Cretaceous top has been established in Arkansas (Renfroe, 1949) and in Tennessee on the basis of fossils. It can be extended to other areas, because this contact corresponds to traceable "kicks" on electric logs. The Cretaceous top does not follow a sand-shale contact but occurs within sands in some areas and within shales in others.

The "X point" (Fig. 2), a slight but characteristic electric-log "kick," divides the Cretaceous System into two units. Both units are of Late Cretaceous age. The "X point" is easily recognized in northeastern Mississippi, and in other areas its approximate position can be traced by the many minor similarities of the electric logs. It occurs in the interval between

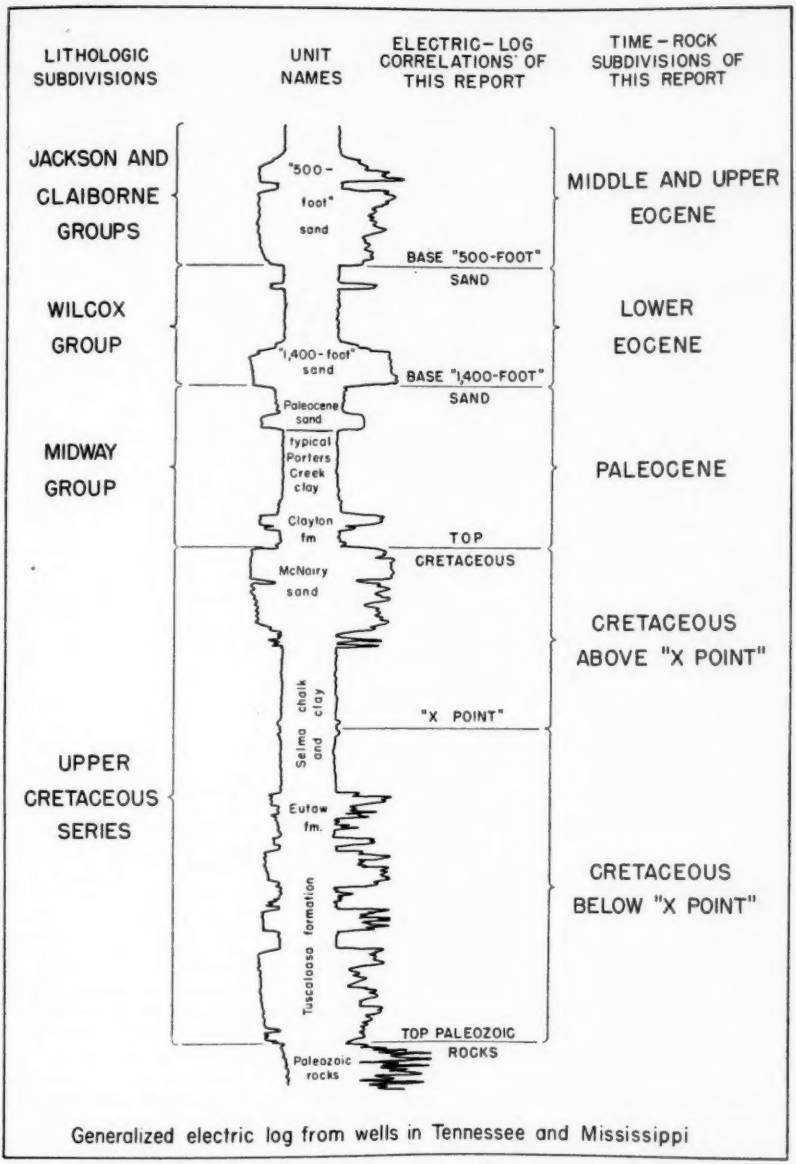

FIGURE 2.—RELATIONS OF ELECTRIC-LOG SUBDIVISIONS OF THIS REPORT TO FORMATIONS AND MAJOR SUBDIVISIONS

the two principal sandy zones in the Cretaceous. The Ripley Formation and its prominent McNairy Sand Member, is above the "X point," and the Tuscaloosa and Eutaw formations are below the "X point" and immediately above rocks of Paleozoic age.

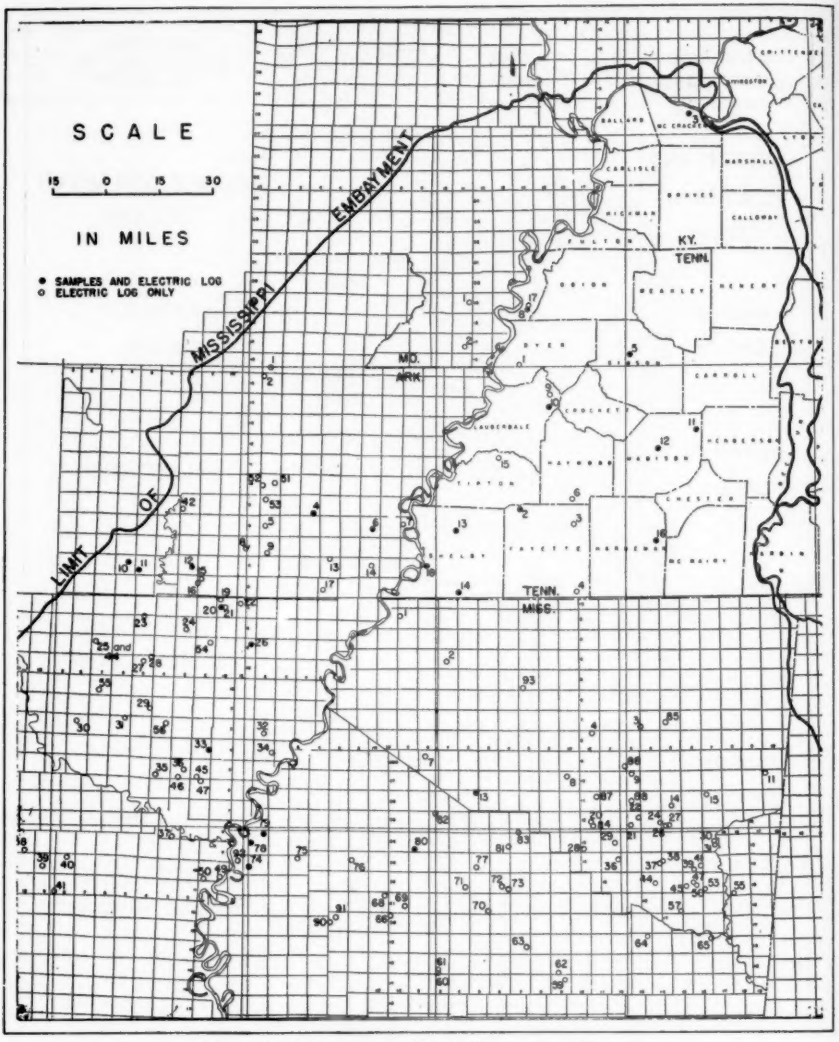

FIGURE 3.—LOCATIONS OF WELLS USED IN THIS REPORT

Environmental Relationships

General statement.—Examination of samples from selected wells (Fig. 3) and changes observable on electric logs suggested general environmental relationships (Stearns and Armstrong, 1955). Although criteria are available for a complex subdivision within some units in certain areas, division was restricted to three sedimentary environment types that best illustrate the inferred relationships. The three subdivisions are back-beach clay and sand, shallow-marine near-shore sandy beds, and deeper-marine clay and shale. Generalized distribution of these types is presented in cross section on Figures 5 and 6. The locations of these cross sections are shown on Figure 4.

Back-beach clay and sand.—Back-beach beds

consist of tan, white, pink, and light-gray clay, lignite, and discontinuous sand. The clay beds commonly bear leaf imprints, and glauconite is absent. Such units are difficult to correlate in detail by means of electric logs, even in closely spaced wells, because they are not persistent laterally.

Shallow-water near-shore sand.—Shallow-water near-shore sand is characterized by good sorting, by the presence of glauconite, and by the presence of marine fossils in some clay interbeds. Such sand tends to have a "blanket" distribution in contrast to back-beach sand bodies which are local and discontinuous. Where shallow-water sand beds grade vertically or laterally into back-beach beds, they commonly contain abundant wood fragments and lignitic material, but where they grade into deeper-water clay beds they may contain glauconite. The "1400-foot" sand is believed to be an example of the shallow-water near-shore deposits.

Deeper-water clay and shale.—The deeper-water clay and shale is characteristically medium gray to dark gray and contains marine fossils, calcareous beds, and glauconite. Drill cuttings are commonly prismatic in shape. Because these clay beds are shown by characteristic patterns on the electric logs, they may be subdivided and widely traced in the subsurface. Slight but characteristic "kicks" in the otherwise monotonous clay-shale pattern were used to trace the "X point" through a predominantly shaly Cretaceous section (Figs. 5, 6).

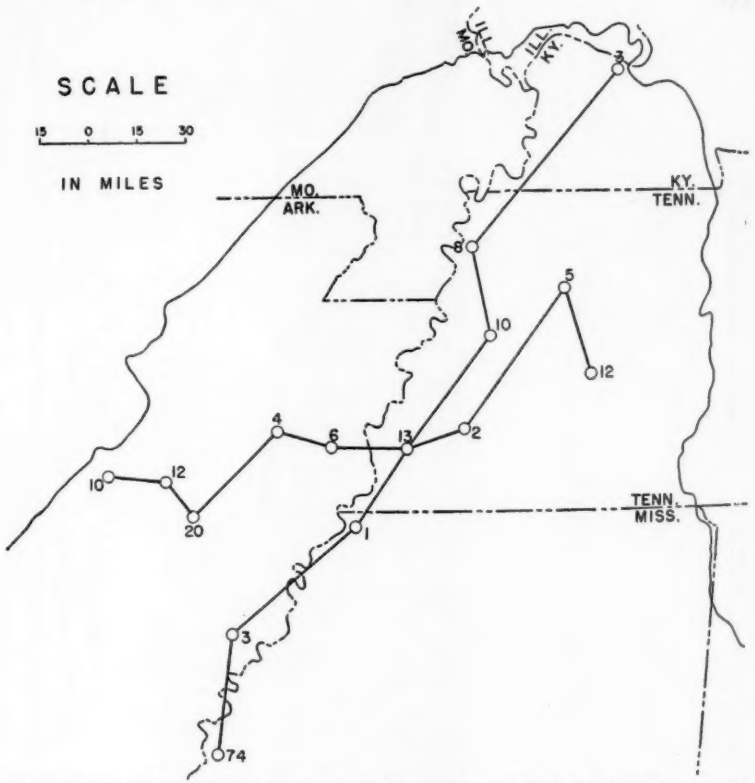

FIGURE 4.—INDEX MAP SHOWING THE LOCATIONS OF STRATIGRAPHIC CROSS SECTIONS ON FIGURES 5 AND 6

Isopach and Lithofacies Maps

General statement.—Sand-shale ratios were prepared by using both electric logs and sample

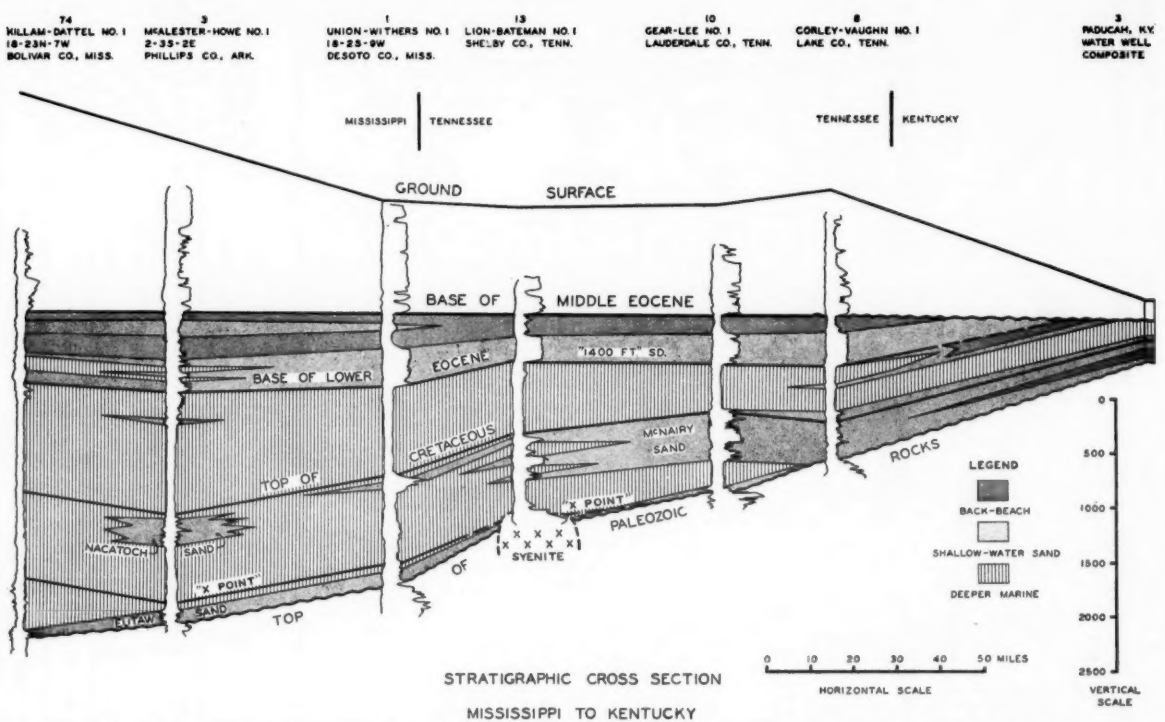

STRATIGRAPHIC CROSS SECTION

MISSISSIPPI TO KENTUCKY

FIGURE 5.—STRATIGRAPHIC CORRELATION SECTION SHOWING ENVIRONMENTAL RELATIONSHIPS FROM BOLIVAR COUNTY, MISSISSIPPI, TO PADUCAH, KENTUCKY

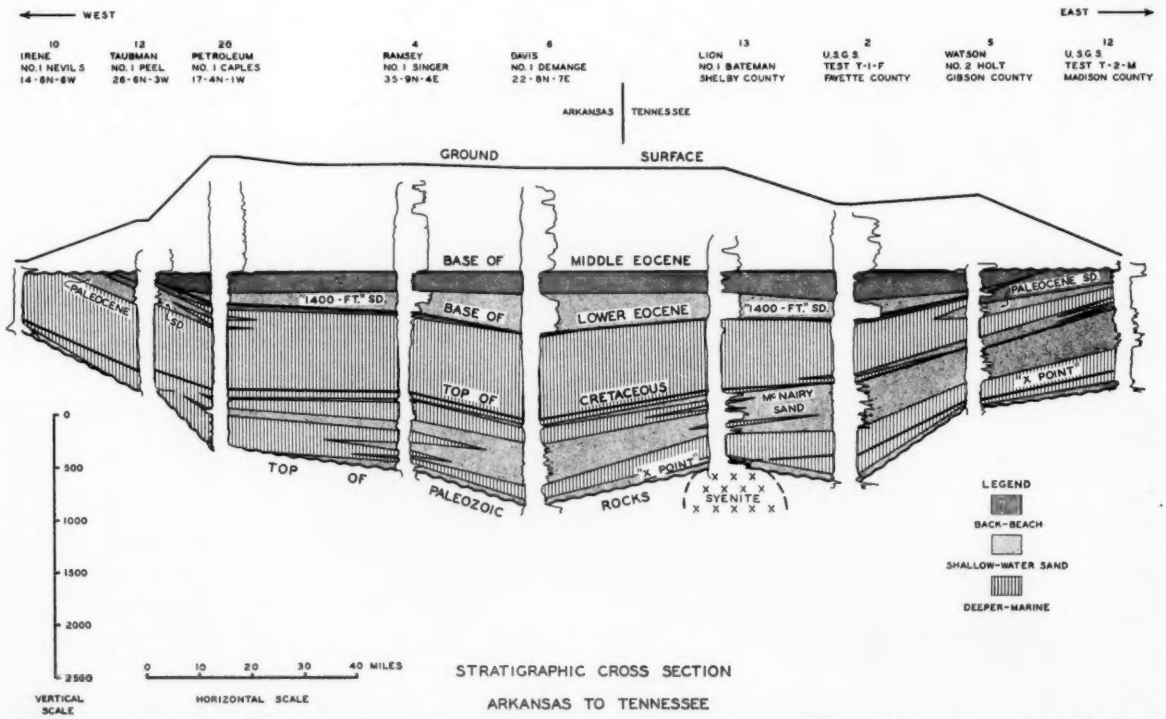

FIGURE 6.—STRATIGRAPHIC CORRELATION SECTION SHOWING ENVIRONMENTAL RELATIONSHIPS FROM WHITE COUNTY, ARKANSAS, TO MADISON COUNTY, TENNESSEE

data. For each unit the number of feet of coarser clastic material (shown in the logs by high resistivity and low self potential) was divided by the number of feet of shale or clay (low resistivity and high self potential). Values of the sand-shale ratios indicate the number of feet of sand per foot of shale. Lignite, ironstone, and chalk were included in the fine clastics.

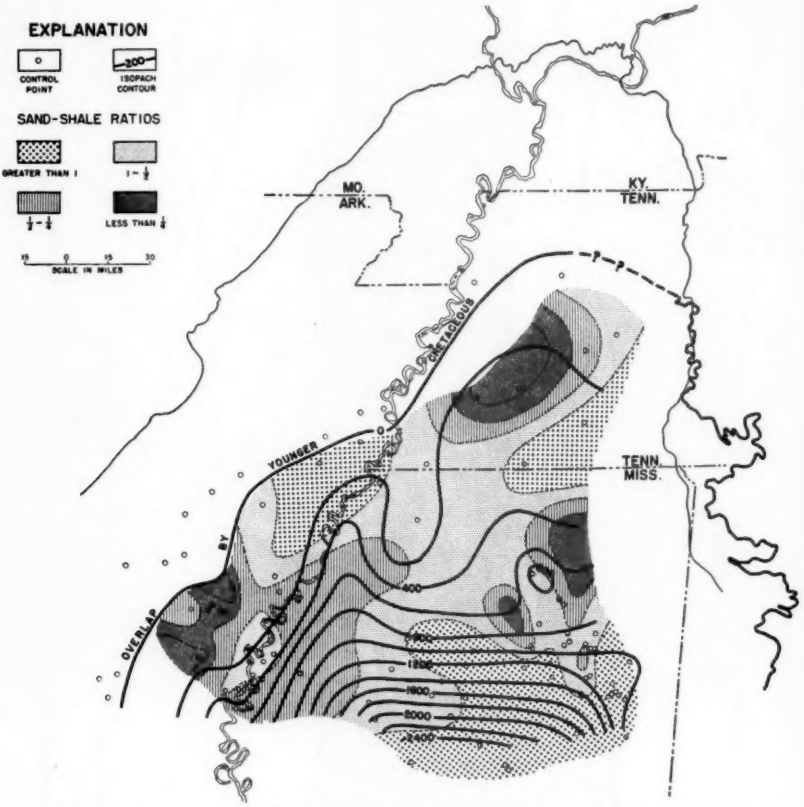

FIGURE 7.—ISOPACH AND SAND-SHALE RATIO MAP OF CRETACEOUS ROCKS BELOW "X POINT"

The maps should be examined with the correlation sections (Figs. 5, 6), because sand-shale ratios give only an average picture of the sand and do not indicate the vertical distribution of sand within the section or the cause for lateral changes in the sand-shale ratios.

Map of Cretaceous rocks below "X point" (*Fig.* 7).—The map of Cretaceous units below the "X point" has a markedly different pattern from all overlying units. At the northwest zero line these older Cretaceous rocks are overlapped. Beyond that line younger Cretaceous units overlie Paleozoic rocks. There is major southward thickening of the Cretaceous where the Tuscaloosa Formation is well developed in Mississippi. The eastward isopach trend here is parallel to the Coastal Plain trend. Evidently the Mississippi Embayment did not assume its present form until after these rocks were deposited.

Northwest of the 600-foot isopach line, variations of the sand-shale ratio generally indicate changes in the development of basal sands in the older Cretaceous rocks. Southeast of this line the higher ratios are due to gravel in the Tuscaloosa Formation.

Map of Cretaceous rocks above "X point" (*Fig. 8*).—Throughout latest Cretaceous time, progressive westward overlap continued. Beyond the zero line in Arkansas, the top of the zero edge in Arkansas, high values show that sands other than the McNairy are locally well developed. All these sands are considered to be shallow-water deposits. Sand in the Cretaceous

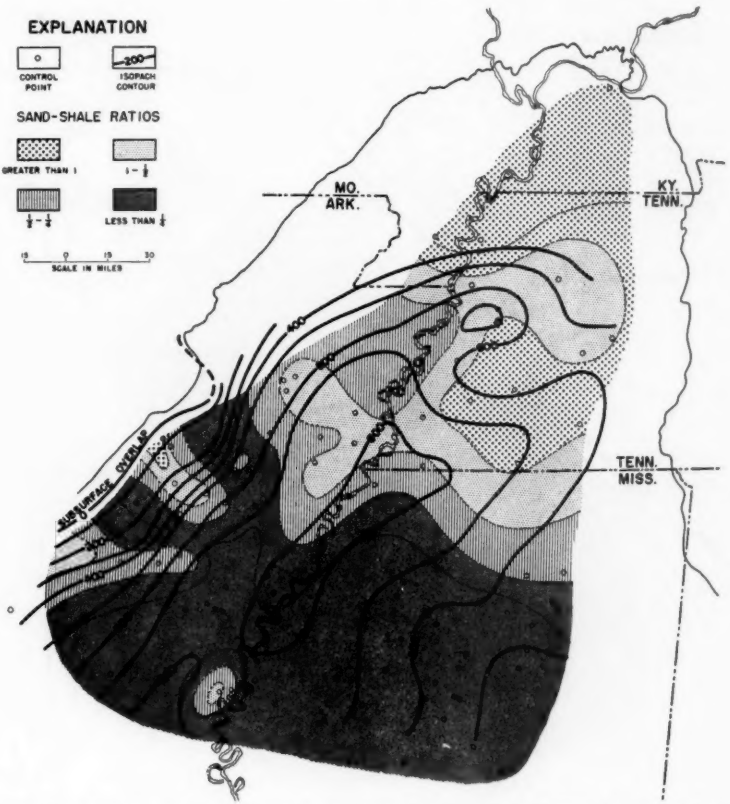

FIGURE 8.—ISOPACH AND SAND-SHALE RATIO MAP OF CRETACEOUS ROCKS ABOVE "X POINT"

Cretaceous is overlapped by Paleocene units that locally rest directly upon Paleozoic rocks. Also, at this time the axis of maximum deposition was along the present Mississippi River, where it persisted in overlying beds. The presence of this axis indicates the beginning of the Mississippi Embayment tectonic trend as opposed to the older Coastal Plain eastward trend (Fig. 7).

The high sand-shale ratios to the north in Tennessee, Kentucky, and northeast Arkansas show the distribution of the McNairy Sand Member of the Ripley Formation. Near the above the "X point" diminishes to the south and disappears in Mississippi.

Map of Paleocene rocks (*Fig. 9*).—This map has an isopach pattern similar to that of Figure 8. Owing to the large proportion of Porters Creek Clay in this interval, sand-shale ratios are low. The increase in the ratios to the north in Tennessee, Missouri, and Kentucky is due to sand at the base of the section. In this area the underlying McNairy Sand Member is also well developed. Higher ratios to the east in Mississippi result from marked increase in sand as marine clay in the upper part of the Porters

Creek grades laterally into shallow-water and back-beach sandy beds.

Map of lower Eocene rocks (*Fig. 10*).—The map of lower Eocene rocks has approximately the same isopach pattern as shown by Figure 9. to greater relative thickness of the "1400-foot" sand.

Lower sand-shale ratios to the east and west are due to gradation of the shallow-water "1400-foot" sand into lignitic clays of the back-

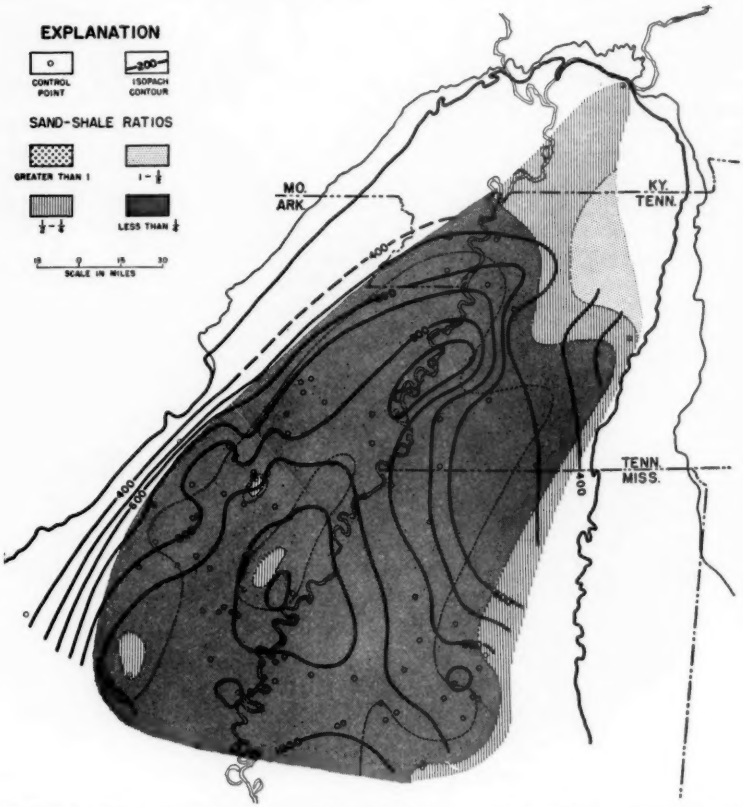

FIGURE 9.—ISOPACH AND SAND-SHALE RATIO MAP OF THE MIDWAY GROUP (PALEOCENE)

The zero line to the west, north, and northeast represents overlap of this unit by the base of the overlying "500-foot" sand. A shallow basin to the south is closed by the 700-foot isopach. Another minor basin is developed in the extreme northeast corner of Arkansas.

Sand-shale ratios show a marked high to the north and along the axis of the Mississippi Embayment. High values in the north, where the total thickness is less than 500 feet, are due to the truncation of the upper shaly part of the section, leaving only the "1400-foot" sand. High ratios southward along the axis are due beach environment. The lignitic clays also overlie the sand in most of the area. To the south, beds of deeper-water clay occur within the sand, but these are too thin to affect the pattern.

PALEOGEOGRAPHY OF THE CRETACEOUS, PALEOCENE, AND LOWER EOCENE

Gulfward Environmental and Stratigraphic Changes (*Fig. 11*)

Figure 11 shows four representative sections in which environmental types are superimposed

on electric logs. These also show the main correlation lines. Three important relationships are demonstrated.

(1) Both oldest and youngest beds occur in the gulfward section. Northward, these disappear as a result of onlap at the base and truncation at the top.

(2) Deeper-water beds dominate the gulfward section, but northward there is a lateral facies change from deeper-marine beds to transitional beds of sand and back-beach material.

(3) Only back-beach sediments and sand occur at the base and top, except where postdepositional truncation has been most severe at the thinnest section in McCracken County, Kentucky.

The same changes that occur northward along the axis of the Mississippi Embayment also occur eastward and westward up the sides of the embayment.

The three types of material within this sequence invariably maintain their proper relative sequence. Deeper-water sediments are always separated from back-beach material by shallow-water near-shore sand in the vertical succession of each well. Lateral variations occur in the same manner between closely spaced wells and also appear to occur between more widely spaced wells.

It is therefore assumed that facies variations occurred throughout the region in this regular manner, and facies correlations and the main electric-log correlations result in the stratigraphic section shown on Figure 12. These same relationships are shown in more detail on Figures 5 and 6.

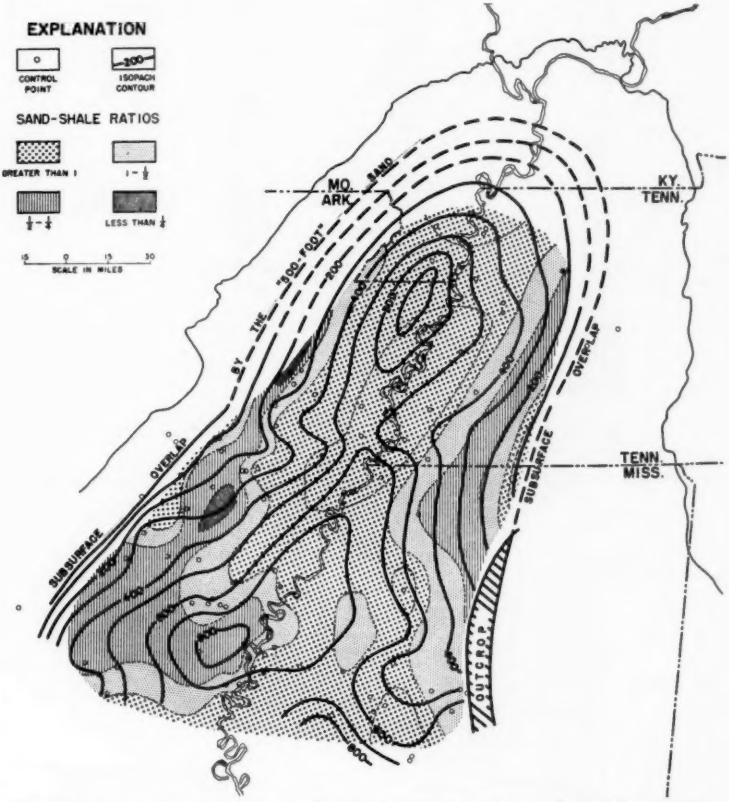

FIGURE 10.—ISOPACH AND SAND-SHALE RATIO MAP OF THE WILCOX GROUP (LOWER EOCENE)

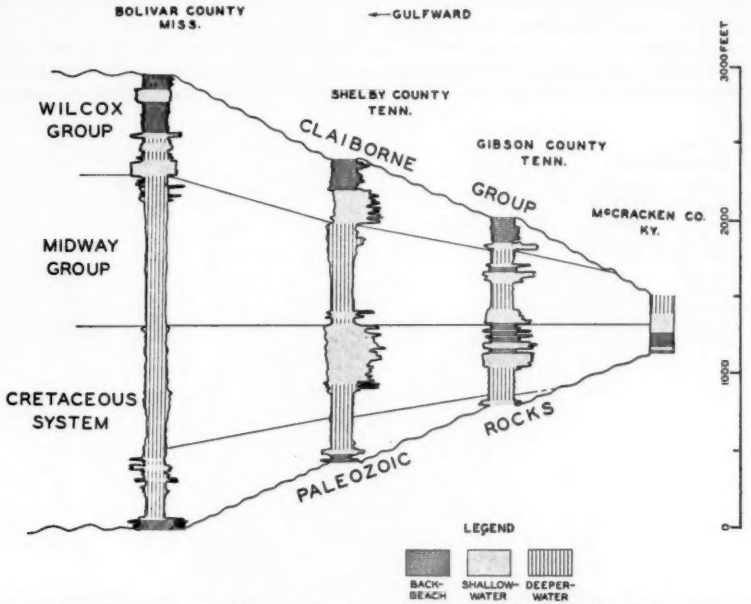

FIGURE 11.—CORRELATION OF TYPICAL LOGS AND LITHOLOGIES SHOWING ENVIRONMENTAL AND STRATIGRAPHIC VARIATIONS

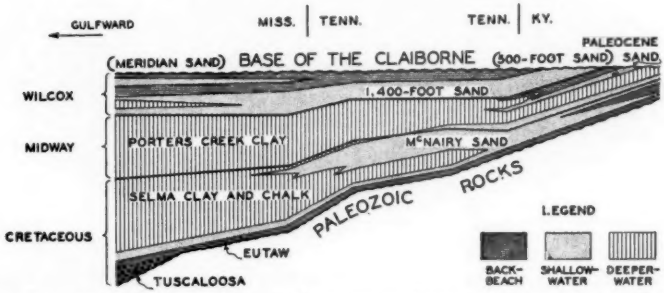

FIGURE 12.—TRANSGRESSIVE AND REGRESSIVE OSCILLATIONS DURING DEPOSITION OF THE CRETACEOUS, MIDWAY, AND WILCOX

Marine Oscillations (Fig. 12)

The Cretaceous, Paleocene (Midway), and lower Eocene (Wilcox) deposits constitute a single sequence bounded above and below by major unconformities. Within this sequence there is no lithologically recognized unconformity, and five major marine oscillations are known.

The first oscillation occurred during deposition of the transgressive Tuscaloosa Formation, Eutaw Formation, and Selma Chalk, and the regressive McNairy Sand Member of the Ripley Formation. The second oscillation began during latest Cretaceous, reached its maximum transgression during the Paleocene with deposition of the Porters Creek Clay, and ended with deposition of the regressive unnamed sand herein referred to as the Paleocene sand. A third oscillation occurred during deposition of uppermost Paleocene, where the Porters Creek Clay is repeated and overlies the Paleocene

sand. The fourth oscillation is dominated by transgressive "1400-foot" sand. During the fifth and last transgressive oscillation an unnamed sand was deposited. This sand occurs only as far north as the Mississippi-Tennessee border.

FIGURE 13.—PALEOGEOGRAPHY OF THE LOWERMOST CRETACEOUS

Paleogeographic Maps (Figs. 13–21)

General statement.—In construction of the series of paleogeographic maps, it was assumed that maximum transgressions, as well as maximum regressions, are approximately synchronous. The oscillations themselves are in turn founded on a partly observed and partly inferred facies correlation of the three sedimentary environment types.

The maps show the distribution of the three sedimentary environment types at each horizon chosen. These horizons are shown on Figure 2. The shore line, shown by a heavy line, is drawn as an approximation at the boundary between shallow-water sand and back-beach beds.

Two separate phenomena are responsible for the patterns shown on the maps. First, regardless of lithology, the limits of deposition are controlled by tectonic behavior of the area of deposition. Second, the distribution of facies within the area of deposition is controlled not only by subsidence but by rate of sedimentation and perhaps also by sea-level change.

Isopach maps reflect the tectonic pattern of the area. The degree to which environments parallel isopach patterns is of interest because it indicates control, or lack of control, of paleogeography by contemporary structural movements in the embayment area.

Lowermost Cretaceous (Fig. 13).—After a long period of erosion, the cycle began with deposition of nonmarine (?) Tuscaloosa gravel on eroded Paleozoic rocks. It is debatable whether the Tuscaloosa is actually nonmarine, but its interbeds of red clay and position below the transitional Eutaw make this the most logical interpretation.

Distribution of the Tuscaloosa is totally dissimilar to the embayment pattern but is similar to the isopach map including it (Fig. 7). It is perhaps significant that the zero edge of the Tuscaloosa, except near the Mississippi River,

approximately follows the truncated edge of Mississippian rocks. This may mean that the tectonic pattern of the embayment area during Tuscaloosa deposition was a continuation of the earlier uplifts that resulted in exposure of beds as old as Cambrian by erosion before being covered by Cretaceous in northwest Tennessee and southeast Missouri (Grohskopf, 1955, Pl. 3).

Upper Cretaceous transgression (*Fig. 14*).—Succeeding the nonmarine Tuscaloosa, the transitional Eutaw and marine Selma were deposited in an advancing sea. This is not the maximum transgression but is at an arbitrary horizon of the "X point" that can be traced on electric logs. A map at an earlier horizon would show the shore line farther southeast, and a map at a higher horizon would show the shore line farther northwest.

Deeper-water clay and chalk dominate this map. There is only a narrow rim of shallow-water sand and back-beach sediments, so that marine transgression and spread of limits of sedimentation practically coincide. This picture is identical in trend with the edge of the isopach map (Fig. 7), because this is the horizon chosen as the top of that isopach interval.

Upper Cretaceous regression (*Fig. 15*).—During the Upper Cretaceous the sea regressed in the northeast part of the embayment. Over most of the region shallow-water sand of the McNairy spread over the Selma chalks and clays. Selma deeper-water deposition continued to the south.

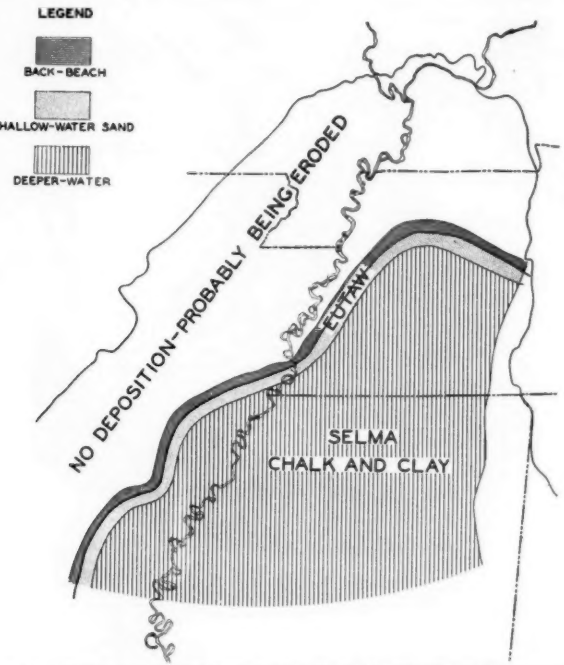

FIGURE 14.—PALEOGEOGRAPHY DURING THE UPPER CRETACEOUS TRANSGRESSION

Environment patterns on this horizon are largely dissimilar to the isopach lines of the interval including it. There is a suggestion of the Mississippi Embayment shape in the distribution of Selma deeper-water sediments, and the shore line parallels isopach lines near the zero edge adjacent to the nondeposition area in Arkansas. The northeast termination of that nondeposition area is a present offset of the embayment edge (Fall Line) in Arkansas. This feature controlled the shore line as well as the pattern of onlap. It also influenced deposition later in the Paleocene.

Discordance with the isopach lines of Figure

8 occurs to the northeast where the shore line trends northwestward across the isopach trough. This situation in that northeast area indicates more rapid sedimentation, which drove the sea back by filling the basin as rapidly as it subsided. That this area was a delta, or deltas, is strongly suggested by the lithofacies pattern on Figure 8, which suggests that sand was debouched into the trough in southwest Tennessee and in western Kentucky.

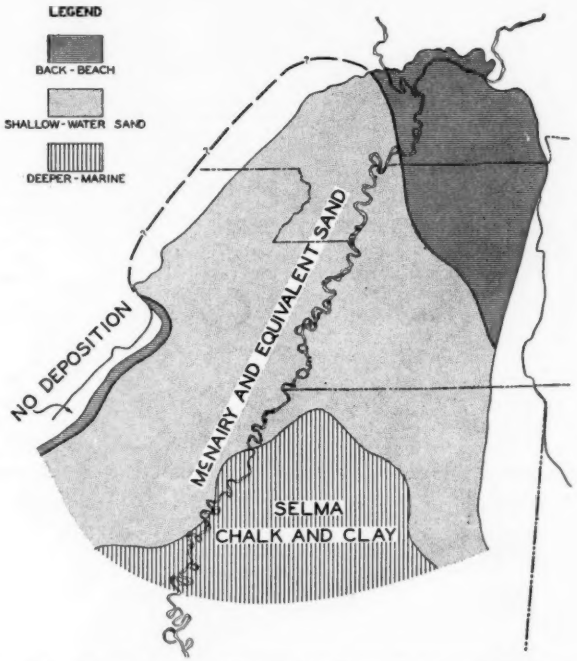

FIGURE 15.—PALEOGEOGRAPHY DURING THE UPPER CRETACEOUS REGRESSION

Northwest basal Cretaceous onlap, which started in earlier times, had by this time covered almost all the Mississippi Embayment with Cretaceous sediments. Onlap was slower in that part of Arkansas labeled "no deposition." There, onlap continued after the time represented by this map and into the Paleocene.

Paleocene maximum transgression (*Fig. 16*).—During the Paleocene the sea reached its maximum transgression. Shore-line and back-beach facies are not found within the present embayment limits for these rocks; only the deeper-water beds extend to the outcrop completely around the Mississippi Embayment. How far the sea advanced beyond this present erosional limit is conjectural.

Onlap, which started during the Cretaceous, finally covered the entire basin. In the small area of Cretaceous nondeposition in Arkansas, Paleocene Porters Creek Clay overlaps the Cretaceous and rests directly on Paleozoic rocks.

Upper Paleocene regression (*Fig. 17*).—During the late Paleocene the sea regressed and for the first time formed a wide bay. A "rim" of shallow-water sand was deposited along its shore, but in the bay deeper-water deposition of Porters Creek Clay continued.

Environment patterns are strongly reminiscent of the Upper Cretaceous regression (Fig. 15) except that sand is much less widespread, and an east shore line is visible for the first time in Mississippi. The shore line to the west and north is nearly identical in position with that earlier shore line. The offset of the Fall Line in Arkansas again influenced deposition. Here, the Paleocene sand and the shore line swing northwestward. The earlier Cretaceous deltaic con-

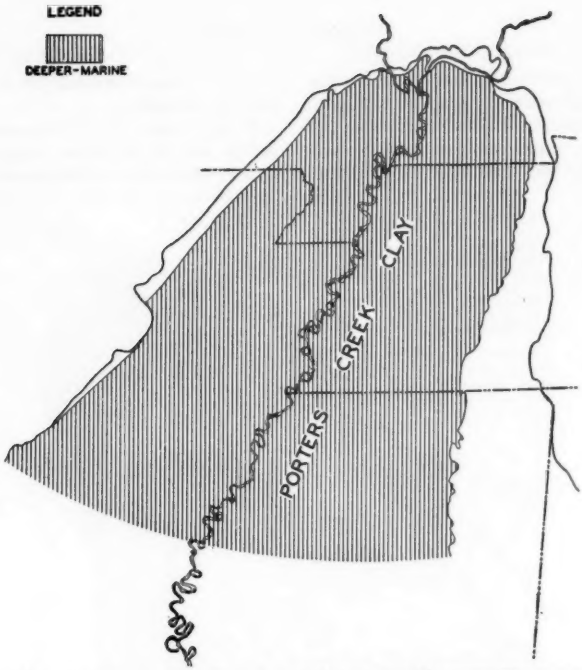

FIGURE 16.—PALEOGEOGRAPHY DURING THE PALEOCENE MAXIMUM TRANSGRESSION

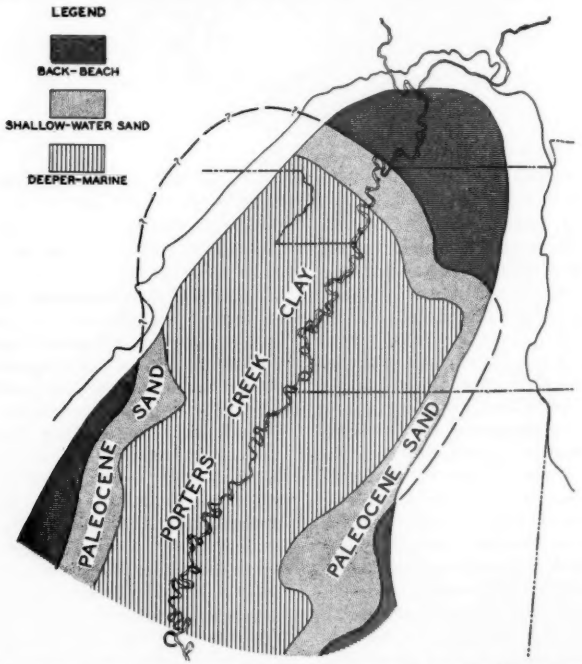

FIGURE 17.—PALEOGEOGRAPHY DURING THE UPPER PALEOCENE REGRESSION

dition to the northeast also was revived at this time.

Although deeper-water Porters Creek Clay crops out around the Mississippi Embayment

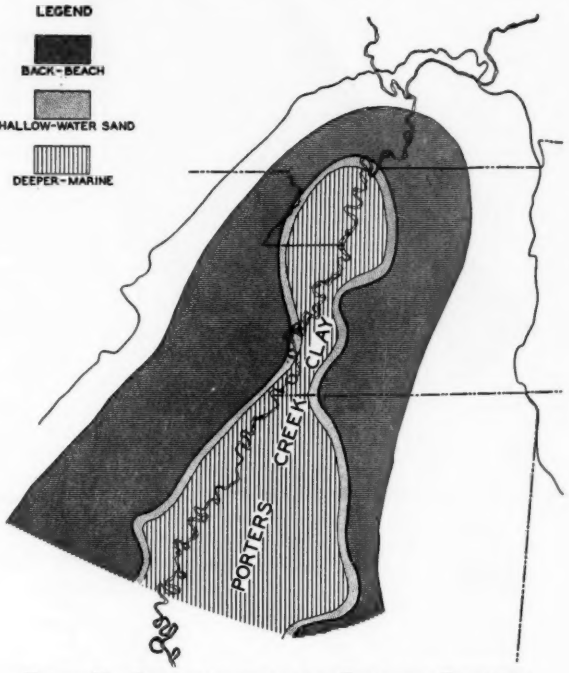

FIGURE 18.—PALEOGEOGRAPHY AT THE END OF THE PALEOCENE

edge, this upper horizon is truncated and overlapped by the Claiborne everywhere except Mississippi and a small adjacent area in Tennessee. Succeeding horizons of uppermost Paleocene and the lower Eocene are progressively more restricted to the trough of the embayment. Edges of the facies patterns on Figure 17 and succeeding maps are the inferred lines of truncation of each horizon beneath the overlapping Claiborne.

End of the Paleocene (*Fig. 18*).—Before the end of the Paleocene there was a slight transgression (not shown on a map), but by the end of the Paleocene the sea had assumed the shape of a long narrow bay extending along the axis of the Mississippi Embayment. In this bay, deposition of Porters Creek Clay continued. Lignitic back-beach sediments are predominant elsewhere, and shallow-water sand is of little significance.

The marine bay closely follows the isopach trough of Figure 9. This horizon is more restricted in area than that of the preceding map (Fig. 17). It is overlapped by Claiborne everywhere except in southernmost Tennessee and in Mississippi. (Fig. 1.)

First lower Eocene transgression (Fig. 19).—At the beginning of the lower Eocene the sea again advanced to occupy an open bay similar to that of Figure 17, and a widespread blanket of shallow-water sand was deposited. Back-beach sediments occur to the east and west, but sediments deposited at the northern shore line have been eroded, and Claiborne there rests unconformably on the "1400-foot" sand. Deeper-water clays occur only in the embayment trough far to the south.

Following deposition of the "1400-foot" sand the sea withdrew (not shown on a map), and lignites overlie this sand even in the center of the trough. This is the most widespread lower Eocene horizon but it crops out only in Mississippi. Elsewhere, it is overlapped by Claiborne,

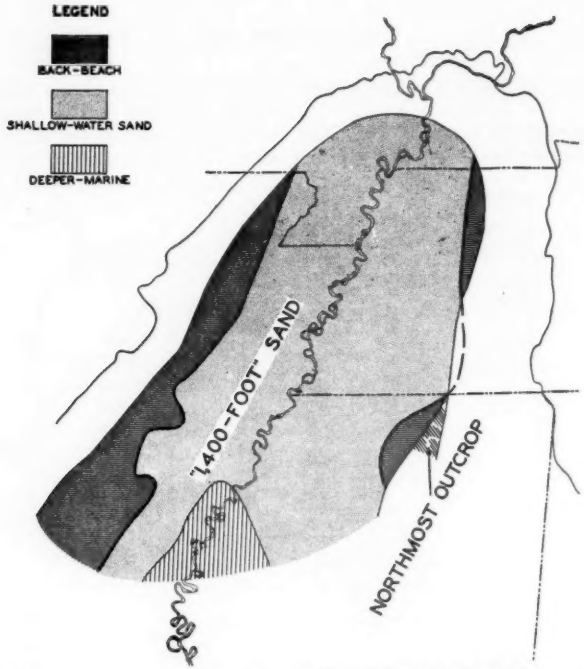

FIGURE 19.—PALEOGEOGRAPHY DURING THE FIRST LOWER EOCENE TRANSGRESSION

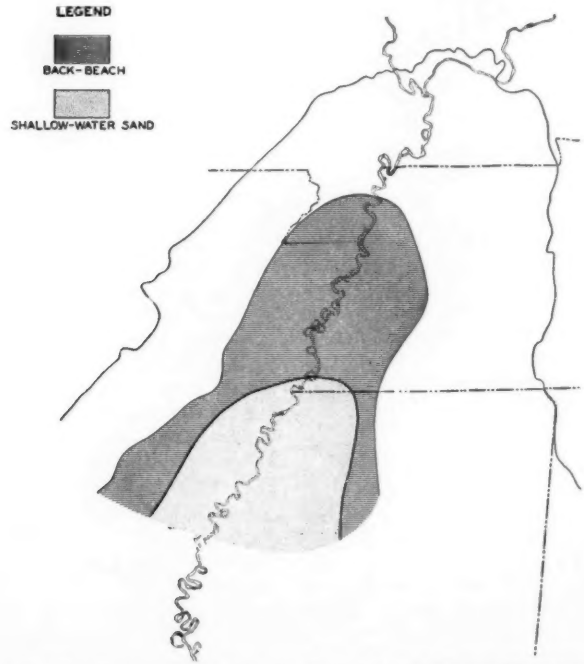

FIGURE 20.—PALEOGEOGRAPHY DURING THE SECOND LOWER EOCENE TRANSGRESSION

and still higher horizons of the lower Eocene are progressively restricted to the trough.

Second lower Eocene transgression (*Fig. 20*).—The sea invaded again for the last time during the lower Eocene. It advanced only as far north as the southwest corner of Tennessee and left as a record an unnamed glauconitic sand; no deeper-water beds occur here. Beds of this age do not crop out anywhere in the area studied.

Second lower Eocene regression (*Fig. 21*).—Following this advance, the sea withdrew, as shown by uppermost lower Eocene beds which contain lignite throughout the region.

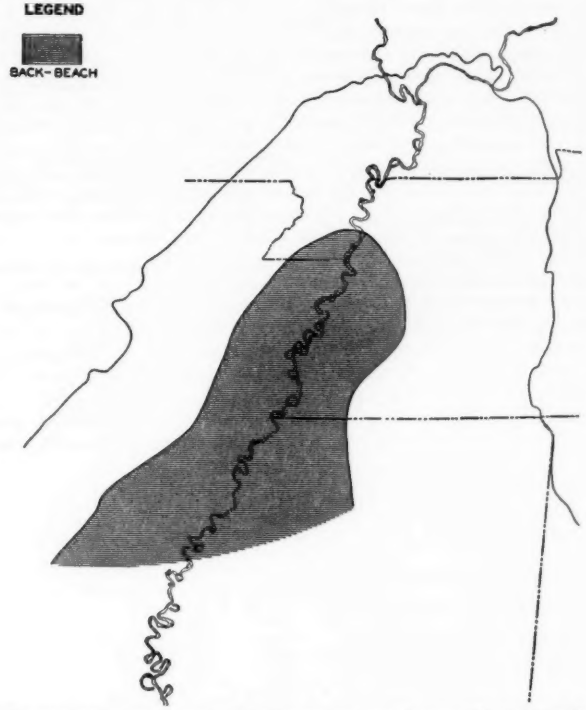

FIGURE 21.—PALEOGEOGRAPHY DURING DEPOSITION OF THE LATEST PRESERVED LOWER EOCENE

CONCLUSIONS

In the northern Mississippi Embayment, Cretaceous, Paleocene, and lower Eocene sediments were deposited in a single sedimentary cycle bounded above and below by truncating unconformities. The cycle is broken within only by the disconformity at the Cretaceous-Paleocene boundary.

Nonmarine or shore-facies material is lacking at the Cretaceous-Paleocene boundary, except where it was deposited both above and below the contact, as in northwest Tennessee. This suggests to the writer that in the northern embayment this boundary represents not a withdrawal of the sea, but a "stillstand" in which constant geographic conditions persisted while deposition was lacking or very slow. Slight deposition is suggested by widespread glauconite and phosphatic material at and near this boundary.

At the lower boundary of the cycle, Cretaceous and Paleocene beds rest upon Paleozoic rocks ranging in age from Cambrian to Pennsylvanian. At the upper boundary the lower Eocene Wilcox Group is overlapped by beds of the middle Eocene Claiborne Group around the end of the Embayment north of the Tennessee-Mississippi border.

Within the cycle, five advances and regressions of the sea are recorded. The geographic patterns of these advances and regressions were

strongly influenced by contemporary structural movements in the region. The earliest (late Cretaceous) advance was from the southeast. The second (Paleocene) advance extended beyond the embayment limits; its pattern is unknown because the shore facies is not present. During the last three advances (late Paleocene through lower Eocene) the sea occupied bays that followed the Embayment axis.

The structural trough shape of the Embayment appeared during latest Cretaceous and persisted through early Eocene.

References Cited

Brown, G. F., 1947, Geology and artesian water of the alluvial plain in northwestern Mississippi: Miss. Geol. Survey Bull. 65, 424 p.

Caplan, W. M., 1954, Subsurface geology and related oil and gas possibilities of northeastern Arkansas: Ark. Div. Geology Bull. 20, 124 p.

Grohskopf, J. G., 1955, Subsurface geology of the Mississippi Embayment of southeast Missouri: Mo. Geol. Survey, v. 37, 2d ser., 133 p.

Renfroe, C. A., 1949, Petroleum exploration in eastern Arkansas with selected well logs: Ark. Geol. Survey Bull. 14, 159 p.

Schneider, Robert, and Blankenship, R. R., 1950, Subsurface geologic cross section from Claybrook, Madison County, to Memphis, Shelby County, Tennessee: Tenn. Div. Geology Prelim. Chart 1

Schneider, Robert and Cushing, E. M., 1948, Geology and water-bearing properties of the "1,400-foot" sand in the Memphis area, a progress report: U. S. Geol. Survey Circ. 33, 13 p.

Stearns, R. G., and Armstrong, C. A., 1955, Post-Paleozoic stratigraphy of western Tennessee and adjacent portions of the upper Mississippi Embayment: Tenn. Div. Geology Rept. Inv. 2, 29 p.

Tennessee Division of Geology, Nashville, Tennessee

Received by the Secretary of the Society January 14, 1957

BULLETIN OF THE GEOLOGICAL SOCIETY OF AMERICA
VOL. 68, PP. 1101-1116, 3 FIGS., 2 PLS. SEPTEMBER 1957

CLAY ALTERATION AND ORE, TEMPLE MOUNTAIN, UTAH

By DANA R. KELLEY AND PAUL F. KERR

ABSTRACT

The Moss Back Sandstone at Temple Mountain, Utah, exhibits abundant argillic alteration in the grain interstices. Near collapse features and close to ore zones the principal clay minerals, kaolinite and illite, become more abundant. Aggregate birefringence and particle size appear to increase. Specific types of illite also develop. Mixtures of 1M and $2M_1$ mica polymorphs are typical. The $2M_1$ mica-clay polymorph also becomes a more abundant constituent of mixtures. Near collapse areas, microvermicular aggregate growths of kaolinite become common.

In unaltered and nonore-bearing sediments, the $2M_1$ mica-clay polymorph has not been observed. Where scattered detrital flakes of $2M_1$ muscovite are found along bedding planes in the unaltered sediments, they appear to be breaking down to a 1M structure.

Hydrothermal synthesis of micas by Yoder and Eugster (1955) has shown the transition of 1M to $2M_1$ mica polymorphs which appears to occur between 200° C. and 350° C. at 15,000 p.s.i. water pressure. The illite at Temple Mountain which contains the $2M_1$ polymorph is believed to have been deposited by hydrothermal solutions accompanying urano-organic ore deposition. Natural conduits for circulation appear to have been provided by the collapse features and by fractures. The source of the clay-forming elements is probably not only the original interstitial material but also includes detrital feldspar replaced during the development of ore masses.

CONTENTS

TEXT

	Page
Introduction	1101
Acknowledgements	1102
Argillization of the Moss Back Sandstone	1102
Normal lithology	1102
Weathering	1103
Extent of argillization	1104
Status of "illite" and mica polymorphs	1105
Mica polymorphs at Temple Mountain	1106
General statement	1106
X-ray diffractometer curves	1107
X-ray microcamera photography of thin sections	1109
Distribution of mica-clay polymorphs	1110
Significance of mica-clay polymorphs	1112
Formation of kaolinite	1113
Source of clay-forming elements in the Moss Back Sandstone	1114
Summary and conclusions	1115
References cited	1116

ILLUSTRATIONS

Figure	Page
1. Interstitial cement of Moss Back Sandstone	1103
2. Line sketches of argillization surrounding ore zones	1111
3. Replacement of detrital feldspar and clay in ore zones and argillization surrounding ore, Moss Back	1114

Plate	Facing page
1. X-ray microcamera patterns of interstitial aggregates	1112
2. Argillization in the Moss Back and collapse.	1113

TABLES

Table	Page
1. Microscopic estimates of intergranular alteration	1104
2. X-ray microcamera measurements	1105
3. Significant polymorph spacings	1107
4. X-ray diffraction of mica clays	1108
5. Microcamera polymorph reflection	1110
6. Alteration of detrital $2M_1$ muscovite	1110
7. X-ray diffraction measurements of mica clay in silty mudstones	1112
8. X-ray microcamera values for kaolinite	1113

INTRODUCTION

A study of the Temple Mountain uranium-mining district, Utah, began in 1954. It has been divided into three parts. A description of the collapse features (Kerr, Bodine, Kelley, and Keys, 1957) has been published. An examination of the alteration (Bodine, 1956, Ph.D. the-

sis, Columbia Univ.) is in its final stages, and a preliminary report on the mechanism of emplacement of urano-organic ore (Kelley and Kerr, 1956) is being revised for publication. A brief discussion of phases involved in the mechanism of ore emplacement has been published (Kerr and Kelley, 1956).

Temple Mountain is located along the southeastern side of the San Rafael Swell in Emery County, Utah, 44 miles southwest of Green River. The swell is an asymmetric anticlinal fold which trends northeastward; it has steep dips along the eastern side and a gradual slope to the west. A description of the geologic setting of Temple Mountain and the San Rafael Swell in general is given in the report on the collapse features (Kerr, Bodine, Kelley, and Keys, 1957). Urano-organic materials constitute the ore.

Most of the workable deposits of urano-organic ore are found in the Moss Back Sandstone Member of the Chinle Formation, although prospects and mineralization occur above and below. Associated alteration has received particular attention, and argillization is the dominant type. Ten ore localities in the Temple Mountain mining district and one non-ore locality outside the district were selected for laboratory investigation. Study of these localities is believed to provide data with a significant bearing on the mechanism of mineralization involved. However, systematic collecting and the accompanying analysis of a considerable number of clay-alteration suites would be required to evaluate a three-dimensional pattern of argillization with relation to ore and collapse features.

X-ray diffraction and microscopic examination were the main techniques employed. Study of thin sections of the Moss Back Sandstone shows interstitial aggregates of illite, kaolinite, and sulfates which have been identified with the X-ray microcamera. In order to remove the considerable quantities of detrital material, bulk samples were elutriated in distilled water, and −0.01 mm particle-size fractions were collected. X-ray diffractometer measurements of these fractions confirm the mineral assemblage identified (Fig. 1) with the X-ray microcamera. In order to establish the mica polymorphs of the mica clay (illite), bulk samples were elutriated in distilled water to obtain a 2-micron fraction. X-ray diffractometer measurements of these fine-clay fractions indicated that nearly all the detrital material in the sandstone had been removed. All previously identified aggregates were present. However, the concentration of illite increased sufficiently, relative to the other mineral components, to identify the mica polymorph. In order to facilitate comparison of the structural modifications of the mica clays, the X-ray spacings of the other minerals present in the 2-micron fraction have been eliminated in the tables of X-ray diffraction measurements (Table 4; Table 7). Standard glycolation procedures were employed on the 2-micron fraction for determining the presence of mixed-layer clays. In all analyses, the experimental conditions were essentially uniform.

Acknowledgments

The writers wish to express their appreciation to Dr. H. D. Glass of the Illinois Geological Survey and Dr. H. S. Yoders Jr., of the Geophysical Laboratory for the discussion of mica polymorphs and mixed-layer clays which has aided this study.

Argillization of the Moss Back Sandstone

Normal Lithology

The Moss Back Member of the Chinle Formation includes small lenses of silty mudstone, conglomeratic beds, and predominant, poorly sorted, medium- and coarse-grained sandstones. Optical examination indicates that the principal detrital minerals, not including those constituting the mudstones, are subrounded to subangular quartz, chalcedony, orthoclase, microcline, oligoclase, and andesine. A distinctive sheen along bedding surfaces of fine-grained sandstones is imparted by detrital muscovite.

The normal sedimentary clay matrix contains minor amounts of material generally termed illite, or hydromuscovite. Slightly coarser-grained materials are ordinarily referred to as sericite. Fine particles of quartz, kaolinite, and some calcite are intermixed with the clay. A few sulfates are found. Accessories include apatite, zircon, tourmaline, epidote, sphene, and spinel. Coalified wood fragments and wholly or partially silicified logs are found in places. The fragments are commonly flattened, or otherwise distorted, along bedding planes and minor lithologic contacts. The abundance of these components varies with lithology. The coarser sediments contain more feldspar and

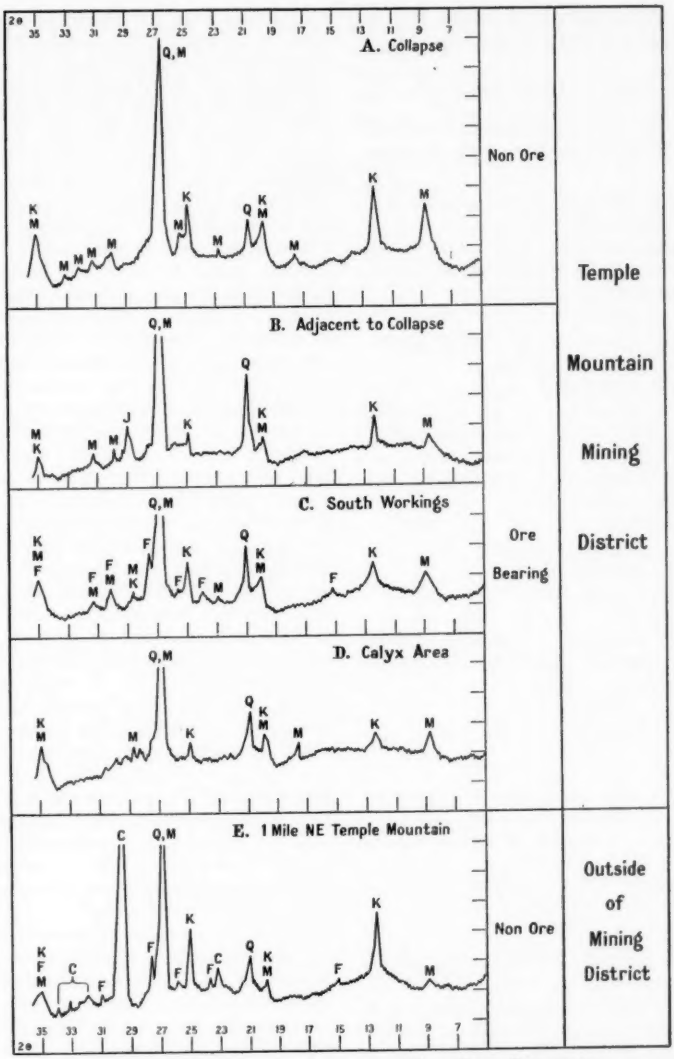
2θ
35 33 31 29 27 25 23 21 19 17 15 13 11 9 7
A. Collapse
B. Adjacent to Collapse
C. South Workings
D. Calyx Area
E. 1 Mile NE Temple Mountain
Non Ore
Ore Bearing
Non Ore
Temple Mountain Mining District
Outside of Mining District

FIGURE 1.—INTERSTITIAL CEMENT OF MOSS BACK SANDSTONE

X-ray diffraction scanning of the minus 0.01 fraction. Cu/Ni, 1°/minute. M-Mica, K-Kaolinite, Q-Quartz, C-Calcite, F-Feldspar, J-Jarosite.

chalcedony than the dominant sandstones, and the finer sediments contain more clay.

Weathering

Surficial bleaching is produced by weathering where organic materials, particularly the hydrocarbons, are involved. It reflects, in part, reduction of the iron present in the sediments as hematite, goethite, siderite, and jarosite, associated with alteration and mineralization by the impregnated hydrocarbons. Near the collapse features where urano-organic material is observed, bleaching tends to outline clay

areas and the development of sulfates with the decomposition of pyrite and marcasite.

Extent of Argillization

The host rock of the urano-organic ore commonly contains considerable argillic alteration; clay-mineral distribution is apparently related to ore. The volume of the alteration in the matrix has been estimated by point counts with the microscope of a large number of equally measured thin-section fields (each 1.0 mm in diameter) from nine selected localities. A summary of the volume relations of one of these localities is shown in Table 1. Unaltered and unmineralized sandstone contains an average of 80 per cent detrital minerals, 18 per cent interstitial clay, and 2 per cent opaque material. The latter includes nonuranium-bearing organic substances and minor pyrite. In altered rock surrounding the ore mass, the average content of detrital minerals drops as low as 45 per cent. At the same time, the interstitial clay may increase to as much as 50 per cent. The average opaque content, including nonuranium organic substances with minor pyrite and urano-organic ore, increases to about 5 per cent, or locally up to a maximum of 10 per cent. The loss in detrital minerals appears balanced by the gain in alteration clays. A corresponding study of the other localities reveals a similar relationship and substantiates the conclusion that matrix alteration increases close to ore.

TABLE 1.—MICROSCOPIC ESTIMATES OF INTERGRANULAR ALTERATION

Moss Back Sandstone surrounding urano-organic materials, Camp Bird Mines, Temple Mountain, Utah

Lithologic unit	Description	Estimated volume per cent		
		Detrital content	Interstitial material	Organic materials and metallic minerals
Upper conglomeratic sandstone	Pyritic near vitrain. Nonore	25*	25*	50*
	Altered near vitrain and fusain. Nonore	70	25	5
Lower sandstone	Ore mass	45–60	1–5†	25–55†
	Altered about ore mass. Nonore	45–75	15–50	2–10
	Unaltered "dead-oil sand." Nonore	80	18	2

* A decrease in interstitial and detrital material results from pyritic replacement.

† Emplacement of ore causes a decrease in interstitial material.

Finely mixed mica clay and kaolinite commonly form the clay fraction. Minor sulfates appear to represent subsequent mineralization. A decrease in the detrital content and the interstitial clays in the ore mass results from replacement by the opaque urano-organic ore. A slight increase in interstitial clays is noticed in altered sediments near carbonized wood fragments (vitrain and fusain) above the ore mass. Quantitative estimates of volume for this increase were not attempted, because the unaltered sediments about fragments of vitrain commonly contain considerable amounts of replacement pyrite (Table 1). Most of the bleaching reflects oxidation during the period of alteration and mineralization. Some of the pyrite has been altered to jarosite, which is intimately mixed with the interstitial clays.

Significant mixtures of illite, kaolinite, quartz, small amounts of sulfates, chalcedony, carbonates, and feldspar are characteristic of alteration accompanying uranium mineralization in the Moss Back Sandstone. In general, the concentration of one or more of these minerals in the interstitial mixed aggregates indicates the intensity of alteration as shown in five diffractometer curves, representative of a group of 20 (Fig. 1). Away from mineralized areas, the interstitial cement of barren Moss Back Sandstone consists dominantly of calcite and kaolinite with fine particles of granular quartz (Fig. 1*E*). Illite is a minor constituent, and sulfates are negligible. In ore zones, most of the interstitial cement is introduced illite and recrystallized kaolinite (Fig. 1*C-D*). Minor amounts of jarosite, alunite, carbonates, and chalcedony are scattered through the clay. Adjacent to ore bodies and bordering the collapse features, the alteration of the Moss Back reflects an increase in illite and kaolinite with mixed jarosite and possibly other sulfates (Fig. 1*B*). Sharp basal X-ray reflections (Fig. 1*A*) also show an increase in the crystallinity of the clays within the collapse. Away from the ore, the sulfates diminish or disappear.

The fineness of the mixtures of clay minerals and sulfates in the intergranular alteration of the sandstone is indicated by some of the X-ray microcamera patterns of clay patches less than 100 microns in diameter in thin section (Table 2). These patterns yield more than one of the major clay-sized mineral components—mica, kaolinite, or sulfate.

TABLE 2.—X-RAY MICROCAMERA MEASUREMENTS
Mixed clay minerals in Moss Back strata

Alteration about ore pod, Camp Bird Mines*		Minerals	Alteration about vitrain, Camp Bird Mines*		Minerals
d (Å)	I		d (Å)	I	
10.58†	5	Mica	10.05	5	Mica
.....	.....	.....	7.19	5	Kaolinite
5.86	4	Jarosite	.....	.....	.....
5.09	9	Mica, jarosite	5.03	1	Mica
4.47	2	Mica	4.50	7	Mica, kaolinite
.....	.....	.....	4.29	6	Quartz
.....	.....	.....	4.15	5	?Mica, kaolinite
.....	.....	.....	3.87	1	?Mica, kaolinite
.....	.....	.....	3.54	5	Kaolinite
3.33	2	Mica	3.30	10	Quartz, mica
3.07	9	Jarosite, ?mica	.....	.....	.....
2.86	1	Jarosite, ?mica	2.28	1	Mica
2.53	3	Jarosite, mica	2.54	6	Kaolinite, mica
.....	.....	.....	2.36	1	Kaolinite, mica
2.26	2	Jarosite, mica	.....	.....	.....
.....	.....	.....	2.14	1	Mica
1.95	1	Jarosite, mica	1.97	2	Kaolinite, mica

* Copper radiation, nickel filter.
† Above normal value because of warping of flat film.

Status of "Illite" and Mica Polymorphs

Grim, Bray, and Bradley (1937) proposed the name "illite" for the fine-grained, micalike minerals in argillaceous sediments. They suggested (p. 816) the name "as a general term for the clay mineral constituent of argillaceous sediments belonging to the mica group." Recently, Yoder and Eugster (1955, p. 254) stated

> ". . . the term illite should be used only as a field term as Grim *et al.* originally proposed. When identification is made of the material or materials, the polymorph of the mica should be specified, and note made of the clay mineral with which it may have formed mixed layers. Proof has yet to be obtained that the materials now called illite are not all mixed-layer structures."

Recent opinions indicate that most illite represents mixed-layer structures made up of mica and montmorillonite, or mica and chlorite, and even vermiculite (Foster, 1956, p. 57–67; Weaver, 1956). Weaver (1956, p. 202), in discussing the distribution and identification of mixed-layer clays in sedimentary rocks, states,

> "From an examination of over 6,000 sedimentary rock samples from all over the United States ranging in age from Cambrian to Recent it is estimated that over 70 per cent of the samples contain some variety of mixed-layer clay."

Although most illite is mixed-layer mica, Levinson (1955) demonstrated that polymorphism may exist among specimens called illite (or hydrous mica) which yield identifications as 3T, $2M_1$, 1M, and disordered 1Md structures.[1] It may be true that the fine, mixed,

[1] There is some doubt that the Fithian, Illinois illite, has a disordered structure. It may represent an extremely fine-grained 2M polymorph (H. Glass, personal communication). Fithian illite reported by Yoder and Eugster (1955) was found to be a mixture of mixed-layer 1Md, montmorillonite, and $2M_1$ polymorphs.

clay-sized particles of the mica polymorphs and mixed-layer mica polymorphs with montmorillonite, chlorite, or vermiculite, previously called illite or hydromuscovite, are mineralogically micas. However, in addition to the identification of the mica polymorphs, some modification of rock nomenclature is needed to distinguish between the clay-sized mica polymorphs and large crystals of the same polymorphs, which may occur together and may have considerable genetic significance in argillic alteration. The occurrence and origin of the two types may differ to such an extent that the term $2M_1$ mica polymorph is inadequate to indicate whether a material identified consists of $2M_1$ detrital muscovite flakes, as found scattered in the sediments, or fine interstitial $2M_1$ "mica clay" formed during hydrothermal alteration. In order to clarify this discussion, the subspecies terms illite and mica clay will be utilized for the mica polymorphs in the alteration clays to distinguish them from the detrital muscovite flakes in the sediments.

Discussion of numerous layered silicate structures can be found in the literature. An excellent list of references dealing with such studies in the mica and mica-clay groups is available in Yoder and Eugster (1955), Grim (1953), and Grim, Bradley, and Brown (1951).

Basically, structural changes in dioctahedral micas involve two major processes: (1) the isomorphous replacement of CaAl for KSi (tetrahedral position) and simplified Mg, Fe, and Al for each other (octahedral position) (Foster, 1956, p. 57–67), and (2) polymorphic changes resulting from the stacking of the mica layers. In the mica lattice, each layer contains structurally combined two opposed ($AlSi_3$)-O tetrahedral sheets external to one Al-OH octahedral sheet; potassium ions between the layers make up a deficiency in positive charge which is due to substitution of CaAl for KSi in the tetrahedral position. The various mica polymorphs represent systematic glide or other types of displacements between the consecutively stacked mica layers, in which unit-cell symmetry (repetition) occurs only where a particular number of layers are involved, depending on the polymorph.

The hexagonal symmetry of the ($AlSi_3$)-O sheets permits intervals of rotation of 60° in the basal plane. This allows stacking of adjacent ($AlSi_3$)-O tetrahedral sheets in a fixed series of alternative positions (Hendricks and Jefferson, 1939; Smith and Yoder, 1956), which may be summarized as follows (Smith and Yoder, 1956):

Mica Polymorphs

Structural nomenclature	*Rotation on basal plane*	*Space group*
1M	0°	$C_{2/m}$
2O	180°	$C_{cm}2_1$
3T	120° or 240° (mirror images)	$P3_112$ or $P3_212$
$2M_1$	120° and 240° (alternating)	$C_{2/c}$
6H	60° or 300° (mirror images)	$P6_122$ or $P6_522$
$2M_2$	60° and 300°	$C_{2/c}$

The 2O and 6H polymorphs have not been found in nature. The very few higher polymorphs encountered in nature (as in 12M, 18M, 8Tc) are possibly due to the operation of a spiral growth mechanism.

The layer stacking is essentially random in the disordered one-layer polymorph (1Md = one-layer monoclinic disordered) and is systematically repetitive in the one-layer ordered structure (1M). The unit cell contains a single layer. In the two-layer polymorphs (2M) the unit cell contains two layers. The three-layer, trigonal mica structure (3T), $2M_2$, and higher polymorphs probably would not occur in the mica clays at Temple Mountain (Yoder and Eugster, 1955; Smith and Yoder, 1956), and none of the X-ray diffraction patterns suggests they are present.

Mica Polymorphs at Temple Mountain

General statement.—Since the mica-clay polymorphs at Temple Mountain are poorly crystallized, determinations present a problem. Ordinary methods of separation yield limited concentrations which are commonly intimate physical mixtures of illite with kaolinite, fine quartz, and, in some, sulfates and feldspars. Sulfates are only partially removed by leaching. Fortunately, X-ray diffractometer curves of the 2-micron elutriated fractions supplemented by X-ray microcamera patterns yield criteria for identification.

The most characteristic diffraction angles of the various mica polymorphs occur between 2θ values of approximately 20° and 34° for copper radiation (Grim, Bradley, and Brown, 1951). Most reference data to identify the polymorphic forms of mica in this region are based on patterns of synthetic material published by Yoder and Eugster (1955, Fig. 10; Tables 3, 4, p. 243–247), although some pre-

viously published patterns of natural mica polymorphs are available. The duplication of synthetic mica by natural mica is structurally exact. X-ray reference data on synthetic material are preferable to the data on natural material, in view of reduced variation in the synthetic crystallization of mica. An outline (Table 3) of the distinguishing spacing d (Å) of the various mica polymorphs between 22° and 32° 2θ derived from Yoder and Eugster (1955, p. 246), is given.

X-ray diffractometer curves.—X-ray-diffraction patterns used for the determination of mica-clay polymorphs were obtained with a North American Philips diffractometer, using copper radiation and a nickel filter, at a goniometer speed of .5-degree 2 θ per minute. Resolution was sufficient in most cases to separate mica clay from other mineral reflections. Where resolution was inadequate, the examination of intensities in some cases revealed a masked reflection. Only peaks yielding unique data were used for polymorph identification. X-ray-diffraction patterns for 8 selected samples from 5 localities, out of a total of 20 samples from 8 localities (Table 4) summarize a study of interstitial mica clay in the Moss Back Sandstone at Temple Mountain based on mica-polymorph determinations. All samples used for preparing the 2-micron fraction for mica-clay polymorph determinations were free from detrital muscovite, as determined by prior microscopic examination of thin sections. Therefore, the $2M_1$ polymorph spacings obtained are not likely to represent contaminant detrital muscovite flakes. X-ray reflections below 1.98 Å for the various clay minerals are not presented.

Polymorph interpretations as shown in the various columns for the diffractometer patterns are as follows (Table 4*A*):

1. D.D.H. no. 1, depth 11.2 feet. Mica clay, quartz, and kaolinite occur in altered sandstone along the flopover, Temple Mountain collapse. Here the minerals are not associated with urano-organic ore. The 3.68, 3.49, 3.24, 2.98, and 2.85 Å spacings with weak intensities suggest a mixture of 1M and $2M_1$ polymorphs. (*See* Table 3.) The absence of the 3.07 Å reflection suggests more $2M_1$ than 1M. Mica-clay is too dispersed for a microcamera pattern.

2. From altered sandstone in workings within the collapse along the east side of Temple Mountain. Mica clay, quartz, and kaolinite are shown. The sample is not associated with urano-organic ore. The 3.74, 3.50, 3.26, 2.99, 2.87, and 2.83 Å spacings are indicative of a $2M_1$ polymorph. Absence of the 3.89 Å reflection and moderate intensitie suggests a mixture as above with considerably more $2M_1$ than 1M mica. Mica clay is too dispersed for a microcamera pattern.

3a. Camp Bird mines bordering west collapse. Kaolinite, mica clay, and quartz in relatively unaltered sandstone below urano-organic ore pod. There is not sufficient mica clay to make an analysis of mica polymorphs with the X-ray diffractometer, but the microcamera gives a pattern of mica clay.

TABLE 3.—SIGNIFICANT POLYMORPH SPACINGS

1Md	1M	$1M > 2M_1$*	$2M_1 > 1M$*	$2M_1$
.....	.....	3.93w	.....	.....
.....	.....	3.91w	3.91w	3.889m
.....	.....	3.74w	3.78m	3.735m
Weak to absent	3.66s	3.70s	3.70w	.....
.....	.....	3.53m	3.52s	3.500s
3.35vs	3.356vs	3.35vs	3.35vs	3.351vs
.....	.....	3.24m	3.22s	3.208s
.....	.....	.....	3.14w	.....
Weak to absent	3.073s	3.09s	3.09m	.....
.....	.....	3.03m	3.00s	2.999s
Absent	2.929w	2.93w	.....	.....
.....	.....	2.86m	2.88m	2.871m
.....	.....	2.81w	2.81w	2.803w

* Approximate spacings estimated from Yoder and Eugster (1955, Fig. 10, p. 246).

vs = very strong, s = strong, m = moderate, w = weak.

3b. Same locality as 3a. Mica clay, quartz, kaolinite, and minor jarosite and feldspar from strongly altered sandstone occur surrounding urano-organic ore pods. The polymorph spacings are 3.69 Å equals 1M or $1M > 2M_1$, 3.50 Å equals $2M_1$ or $2M_1 > 1M$, and 2.99 Å equals $2M_1$ or $2M_1 > 1M$. Absence of 2.87 and 2.80 Å spacings suggests a mixture of 1M and $2M_1$ polymorphs. The microcamera pattern shows mica clay with possible minor jarosite.

3c. Same locality as 3a. Mica clay is associated with a pod of urano-organic ore. There is not sufficient material to make an analysis of mica polymorphs with the X-ray diffractometer, but the microcamera pattern indicates mica clay.

4a. Incline no. 1, south workings, Clayx mine area. Chrome mica clay and quartz occur adjacent to a fault and near urano-organic ore in altered sandstone. Both a powder-camera pattern and a microcamera pattern were obtained of mica clay. The 3.78, 3.50, 2.99, and 2.81 Å reflections of the powder-camera pattern are indicative of a $2M_1$ polymorph. Although the 1M polymorph spacings are lacking, the low intensity of the $2M_1$ reflections suggests a $1M–2M_1$ polymorph mixture. More detailed work on the chrome-bearing mica clays (Kerr and Hamilton, in press) reveals some of the characteristic 1M polymorph lines.

TABLE 4.—X-RAY DIFFRACTION OF MICA CLAYS, MOSS BACK SANDSTONE, TEMPLE MOUNTAIN, UTAH

A. Selected Diffractometer Measurements*

Collapse				Collapse Border				Calyx Mining Area							
1. $2W_1 > 1M$		2. $2W_1 > 1M$		3a.		3b. $1M-2W_1$		3c.		4a. $1M-2W_1$		4b. $1M-2W_1$		5. $1M-2W_1$		Inferred Polymorphs
Non-ore		Ore		Non-ore		Ore Border		Ore		Fault Border		Fault Ore		Bedding Ore		Major Reflections of Mica Polymorphs**
d(Å)	I	d(Å)	I	d(Å)	I	d(Å)	I	d(Å)	I	d(Å)	I	d(Å)	I	d(Å)	I	d(Å) I
9.82	10	10.1	9			9.9	10			10.1	10	10.0	10	10.0	10	10.0 basic 10
4.95	3											5.0	2			5.0 basic 3-5
4.44	6x	4.47	>10x			4.45	6x			4.49	5	4.46	9x			4.48 basic 2-9
4.33	1x	4.37	3x													4.30-4.37, 1M, $2W_1$ 1-3
4.07	1x															4.11, 1M, $2W_1$ 1-2
						3.86	4x							3.86	5x	3.89, $2W_1$ 2-4
		3.74	2							3.78	1	3.76	3s			3.76, $2W_1$ 3
3.68	2					3.69	4					3.69	2			3.65, 1M 6
3.49	2	3.50	4			3.50	4			3.50	1	3.47	5s	3.45	3	3.50, $2W_1$ 4-5
3.32	> 10wx	3.34	> 10wx	(Mica-clay fraction inadequate)		3.34	>10wx	(Mica-clay fraction inadequate)		3.36	>10wx	3.33	>10wx	3.33	>10wx	3.35 basic >10
3.24	1	3.26	3			3.23	5s?			Unmasked		3.23	11s	3.25	4s?	3.21, $2W_1$ 4-5
						3.09	6y					3.08	1	3.10	5	3.08, 1M 5-6
2.98	2	2.99	3			2.99	4			2.99	1	2.99	5s	2.99	3	2.99, $2W_1$ 4-5
2.85	1	2.87	2									2.89	3s	2.89	4	2.87, $2W_1$ 3-4
		2.83	1							2.81	1	2.84	2			2.80, $2W_1$ 2-3
														2.70	2	2.69, 1M 1-3
2.55	>10y	2.58	>10x			2.62	4x			2.58	6	2.56	>10xs	2.57	10x	2.56-2.58 basic 8-9
2.48	1x															2.51, $2W_1$ 2
2.45	3w					2.45	8w			2.45	2w	2.45	9w	2.45	5w	2.45 basic 1-3
2.37	2x	2.38	4x			2.38	2x			2.39	1	2.38	3x	2.39	3x	2.38 basic 2-5
2.27	2xw	2.24	3xw			2.28	4xw			2.28	1w	2.28	7xw	2.27	5xw	2.25, 1M, $2W_1$ 1-4
2.23	2w					2.23	4w			2.23	1w	2.23	3	2.21	3	2.21 basic 1
2.13	3w	2.15	2w			2.13	6w			2.13	4w	2.12	7w	2.13	6w	2.15 basic 1-2
1.99	3x	1.98	4x			1.98	8x			1.99	2	2.01	3x	1.99	3x	1.99 basic 3-8

B. Selected Micro-Camera Measurements***

1.		2.		3a. 1Md		3b. $1M-2W_1$		3c. $2W_1 > 1M$		4a. $1M-2W_1$		4b. $2W_1-1M$		5. Plus 1M		Inferred Polymorphs
				d(Å)	I	d(Å)	I	d(Å)	I	d(Å)	I	d(Å)	I	d(Å)	I	d(Å) I
				9.9	9	10.0	9	9.9	10	9.9	10	10.0	10	10.1	10	10.0 basic 10
				5.0	1	5.0	5y	5.0	1	4.9	1	4.93	1	4.92	1	5.0 basic 3-5
				4.49	9	4.49	7	4.48	8	4.48	7	4.48	6	4.48	9	4.48 basic 2-9
								3.86	1							3.78-3.89, $2W_1$ 2-4
												3.70	1			3.66-3.76, 1M, $2W_1$ 3-6
		3.32	9w	3.30	2	3.33	9	3.32	10	3.32	10w	3.32	3	3.32	3	3.35 basic >10
				3.07	4y	3.12	1							3.04	2	2.99-3.08, $2W_1$, 1M 4-6
				2.84	1	2.85	1	2.87	1	2.89	1					2.80-2.99, $2W_1$ 2-5
		2.54	8	2.54	4	2.57	9	2.57	8	2.56	5			2.56	3	2.56, basic 8-9
		2.47	1											2.42	1	2.45, basic 1-3
		2.37	1	2.32	1	2.39	5	2.36	1	2.41	2					2.38, basic 2-5
		2.24	1			2.25	1			2.26	1					2.21-2.25, basic, 1M, $2W_1$ 1-4
						2.15	3	2.16	1	2.16	1					2.15, basic
				1.98	1	1.98	1	1.97	2	1.99	1	1.97	1	1.98	1	1.98, basic 3-8

* All are diffractometer patterns except No. 4a, which is a powder camera photograph. Copper radiation, nickel filter. Only mica spacings are listed. Where resolution is insufficient for separation, the mica lines are wholly or partially masked by the following minerals: w-Quartz, x-Kaolinite, y-Jarosite, z-Feldspar. All intensities are recalculated on the basis of 10 maximum for 10.0 Å spacing.

** Spacings and range in intensities of major mica-polymorph reflections are based on Yoder and Eugster (1955). Major polymorph spacings are underlined.

*** Philips micro X-ray-diffraction camera. Exposures of 100-micron diameter patches of mica clay cut from thin sections and mounted on duco film. Average film to sample distance 12.6 mm. Corrections made for slight buckling of duco strip. Intensities decrease toward higher angles and are not relative as photograph is on flat film. Copper radiation. Nickel filter.

4b. Locality same as 4A. Mica clay, quartz, kaolinite, and minor feldspar from altered sandstone fragments occur along a fault associated with urano-organic ore. The only unmasked spacings are 3.69 Å, which equals 1M or $1M_1 > 2M$; 3.08 Å, which equals 1M or $2M_1$; and 2.84 Å which equals $2M_1$ or $2M_1 >$ 1M. Although feldspar masks most of the possible $2M_1$ polymorph lines, mixtures of $2M_1$ sericite and feldspar, as well as the intensity of the 3.47 and 2.99 Å spacings, indicate that $2M_1$ polymorph reflections occur. The material is therefore interpreted as a 1M–$2M_1$ polymorph mixture. The microcamera pattern is one of mica clay and possibly minor quartz.

5. Calyx mine no. 3. Mica clay, quartz, and kaolinite, and possibly minor feldspar are associated with urano-organic ore in altered sandstone. The 3.45, 3.10, 2.99, and 2.89 Å spacings and the absence of the 3.74 and 3.66 Å spacings, together with moderate intensities of these lines, suggest again a mixture of 1M and $2M_1$ polymorphs. Microcamera patterns were taken of the mica clay.

Similarly, polymorph determinations of all X-ray-diffractometer patterns were made. Before sample preparation, all materials were noted microscopically to be fine intergranular mixtures. Both oriented and nonoriented 2-micron fractions were investigated by X-ray diffraction. After obtaining the 2-micron fraction by elutriation, oriented samples were prepared for determining mixed-layer material by allowing the particles to settle out of water on a glass slide. Unoriented material was prepared by filtering the water-suspended fraction, then lightly grinding the material for 10 minutes, and finally filling a diffractometer holder with the powder. Mica-polymorph determinations were made only on the unoriented material. Therefore fineness of particles and preferred orientation were eliminated as serious factors in the interpretation of differences in polymorphic mixtures. Consequently, the differences in polymorphic mixtures reflect natural differences in the structure of the mica clays and not differences in orientation and fineness of particles due to nonuniform preparation of samples, or to significantly large differences in initial particle size of the intergranular mica clay. However, as in the case of the Fithian, Illinois illite, the over-all fineness of the Temple Mountain mica clay compared with sericite may be reflected by relatively low intensities for polymorph reflections and a broadening of the 10.0 Å peak.

The Temple Mountain green chrome mica clay (Kerr and Hamilton, 1957) shows no doublet, and only slight asymmetry, of the basal 10.0 Å reflection. No shift of this line on glycolation has been observed. Thus either the mica is not structurally intermixed with montmorillonite, or the expanded lattice material is present as less than 10 per cent (Weaver, 1956). The mica clays outside the Temple Mountain mining district are probably "normal" mixed-layer structures which have not been influenced by the hydrothermal solutions which produced the clay and ore at Temple Mountain.

Optical studies of the relationship of clay to ore and other minerals were made. The general fineness of the clay minerals and their intermixture and frequent staining by secondary iron and oxidized hydrocarbon interfered with the determination of optical properties. However, with the microscopic study, careful selection of 100-micron (0.1 mm) patches of relatively pure clay areas in thin sections was made with a microscope. The selected patches were transferred to duco strips and mounted and aligned for X-ray diffraction with a Philips micro X-ray-diffraction camera (Hirsch, 1955 p. 278–297).

X-ray micro-camera photography of thin sections.—Partial powder patterns are possible with a microcamera. Reflection intensities decrease rapidly toward higher angles, and closely spaced reflections usually are inseparable. These disadvantages are offset by careful selection of small patches of relatively pure mineral aggregate (the "powder") for identification and petrographic correlation.

A group of selected microcamera patterns (Pl. 1) is shown. Despite the small film size, the characteristic lines of various interstitial aggregates can be observed without magnification (the most intense line for single mineral aggregates is shown). The possibility of natural orientation has been considered. Patches selected for X-ray diffraction were observed to be optically unoriented and contained clays of comparable particle size. Thin sections were cut normal to bedding to reduce possible variations due to fineness and orientation. Patterns were run with nickel-filtered copper radiation, using an initial film to sample distance of 12.6 mm, which was later corrected for a slight buckling of the duco strip and flat film. Exposure time was between 5½ and 8 hours. Only slight background and line darkening was noticed for an 8-hour pattern, compared with the same pattern run for 5½ hours.

*** Philips micro X-ray-diffraction camera. Exposures of 100-micron diameter patches of mica clay cut from thin sections and mounted on duco film. Average film to sample distance 12.6 mm. Corrections made for slight buckling of duco strip. Intensities decrease toward higher angles and are not relative as photograph is on flat film. Copper radiation. Nickel filter.

Fairly consistent results were obtained, and differences in spacings are believed to be due to polymorphic variations. Where comparison was possible, diffractometer patterns of the same sample were found to be confirmatory.

X-ray microcamera spacings of mica clays, as represented in the six samples shown in Table 4*B*, are representative of various mica reflections. The spacings at 10.0, 5.0, 4.48, 3.32 and 2.56 Å, and those which occur sporadically at higher-angle reflections are the basic mica

TABLE 5.—MICROCAMERA POLYMORPH REFLECTIONS

Line occurring between (d(Å))	Interpreted as representing the following possible polymorph lines (d(Å))
2.84–2.89	2.80 plus 2.87 = $2M_1$; or 2.80 plus 2.87 plus 2.99 = $2M_1$.
3.04–3.12	2.99 = $2M_1$ plus 3.08 = 1M; or 3.08 = 1M.
3.62–3.70	3.66 = 1M; or 3.66 = 1M plus 3.74 = $2M_1$.
3.86	3.74 plus 3.89 = $2M_1$.

lines. However, the other spacings that occur between 2.84 and 2.89 Å, 3.04 and 3.12 Å, 3.62 and 3.70 Å, and in the region of 3.86 Å are interpreted as representing the various characteristic mica-polymorph reflections (Table 5). The closely spaced microcamera reflections are generally inseparable and combine to form a single reflection at a spacing determined by the distance of the separation and relative intensities of the lines.

The writers used this tabulation and the relative intensities of characteristic polymorph spacings to index patterns tentatively in terms of polymorphs; the procedure employed for complete diffractometer patterns (Table 4*B*) was used.

Distribution of Mica-Clay Polymorphs

Illite found in a few places in the interstices between grains in unaltered and unmineralized Moss Back outside the Temple Mountain mining area is too scarce for an estimate of polymorphs. X-rays merely reveal a basic pattern of low intensity, and most of this pattern is masked by an abundance of kaolinite and sedimentary quartz. At the Camp Bird mines in unaltered and unmineralized sandstone near the collapse, detrital muscovite flakes, flattened on bedding planes, are surrounded by a small halo of illite which appears to have slightly higher aggregate birefrigence and particle size than the normal interstitial illite (Fig. 2*E*). The edges of the mica laths are altered and at places merge with the surrounding illite. Powder patterns of the hand-picked

TABLE 6.—ALTERATION OF DETRITAL $2M_1$ MUSCOVITE CAMP BIRD MINES, MOSS BACK SANDSTONE

Detrital $2M_1$ muscovite*		1M mica clay surrounding detrital $2M_1$ muscovite†		1Md–1M mica clay; interstitial†	
d(Å)	I	d(Å)	I	d(Å)	I
9.71	10	10.1	10	9.9	9
4.94	6	5.0	1	5.0	1
4.47	7	4.48	9	4.49	9
3.86	3	...	..	....	..
3.70	3	...	..	....	..
....	...	3.62	6	....	..
3.46	4	...	..	....	..
3.30	10[a]	3.33	8	3.32	9[a]
3.16	7	...	..	....	..
....	...	3.05	5	....	..
2.96	6	...	..	....	..
....	...	2.90	1	....	..
2.83	5	...	..	....	..
2.76	1	...	..	....	..
2.54	10	2.57	7	2.54	8
2.44	3[a]	2.43	1	2.47	1
2.37	4	...	..	2.37	1
....	...	...	..	2.24	1
2.13	10[a]	...	..	....	..
1.99	10	1.99	1	1.98	1

* Debye Scherrer powder camera. Copper radiation, nickel filter. Picked from hand specimen.

† Philips micro X-ray-diffraction camera. Copper radiation, nickel filter. Intensity decreases toward higher angles.

detrital flakes indicate the $2M_1$ polymorph. Microcamera patterns indicate that the associated illite surrounding the detrital muscovite is 1M, and that the normal interstitial illite is 1Md (Table 6). The spatial relationships suggest the disordering of $2M_1$ detrital muscovite to 1M illite in unaltered and unmineralized sediments. The $2M_1$ polymorph in intergranular mica clay has not been identified in unaltered and unmineralized sediments.

Mica clay markedly increases toward urano-organic masses; in a few places it forms rims or stringers which outline coalescing ore masses

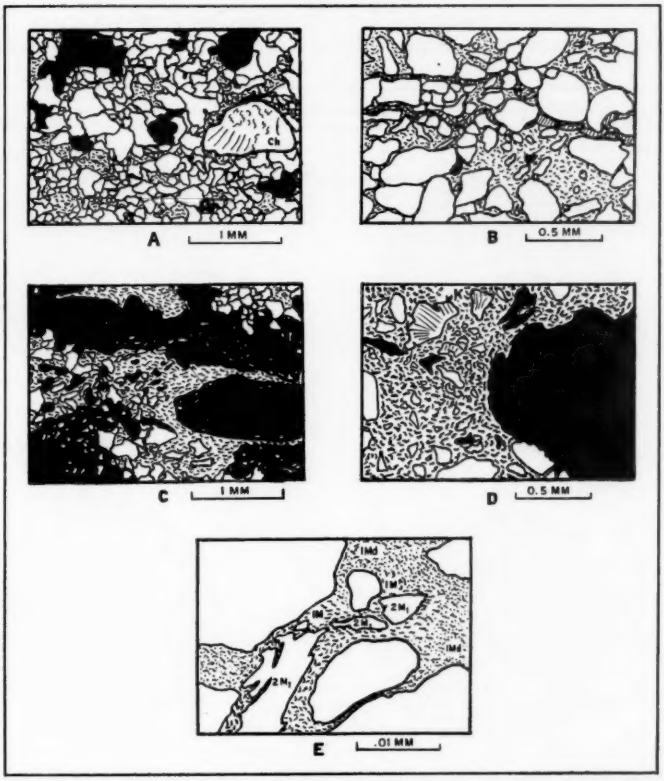

FIGURE 2.—LINE SKETCHES OF ARGILLIZATION SURROUNDING ORE ZONES IN MOSS BACK

Detritals outlined: Clay (dominantly illite and kaolinite)—dashed; Urano-organic material—black; Chalcedony—Ch; Vermicular kaolinite flakes—K.

A. Unaltered sandstone, Calyx mine No. 3. Interstitial clay patches. B. Unaltered sandstone, Camp Bird mines. Interstitial clay and detrital muscovite along bedding planes (crosshatched). C. Clay alteration surrounding coalescing ore, Calyx mine No. 3. D. Clay alteration surrounding ore, Camp Bird mines. Large vermicular patches of kaolinite and illite intermixed with jarosite (heavy dashes). E. Unaltered sandstone, Camp Bird mines. Detrital $2M_1$ muscovite partially surrounded by 1M illite in interstitial 1Md illite.

(Fig. 2*A*, *C*; Pl. 2). Aggregate birefringence appears to increase slightly from values below .020 to approximately .030. Particle size also appears to increase slightly. Within ore zones, the kaolinite-illite rims of sedimentary clay pellets and galls are altered to almost pure illite.

Near and within the collapse, there is a similar increase in abundance, aggregate birefringence, and apparently particle size of illite toward ore (Fig. 2*B*, *C*). More illitization seems to occur about ore zones near and within the collapse in the Moss Back than at localities away from the collapse.

Both X-ray-diffractometer and microcamera patterns indicate that the illite associated with the alteration and mineralization in the Moss Back at Temple Mountain consists of mixtures of one- and two-layer polymorphs (Table 4). Increased abundance of the more ordered two-layer structure toward ore is suggested at the Camp Bird mines bordering the collapse (Table 4, 3a–c). Similarly, the illite intermixed with kaolinite, quartz, and in some places minor sulfates in mudstones underlying Moss Back ore and present within the ore as splits and galls, yields X-ray-diffraction patterns of mixed 1M and $2M_1$ polymorphs (Table 7). Determination of an increase in the abundance of the $2M_1$ polymorph in the mixtures toward the collapse or toward ore in these argillites is

TABLE 7.—SELECTED X-RAY DIFFRACTION MEASUREMENTS

Mica clays in greenish-gray silty mudstone of the Moss Back and Upper Monitor Butte members, Temple Mountain.

Collapse				Calyx Mine Area			
1. 1M-2M$_1$		2. 2M$_1$> 1M		3. 1M-2M$_1$		Inferred Polymorphs	
Non-Ore*		Ore*		Non-Ore*		Major Reflections of Mica Polymorphs**	
d(Å)	I	d(Å)	I	d(Å)	I	d(Å)	I
9.90	10	10.1	10	9.90	10	10.0 basic	10
4.98	1^{y}	4.95	4	4.97	4	5.0 basic	3-5
4.46	6^{x}	4.45	>10^{x}	4.45	>10^{x}	4.48 basic	2-9
		4.10	2^{x}			4.11, 1M, 2M$_1$	1-2
		3.84	4^{x}			3.89, 2M$_1$	2-4
		3.75	1			3.74, 2M$_1$	3
3.65	2					3.66, 1M	6
2.49	2^{y}	3.47	4	3.50	3	3.50, 2M$_1$	4-5
3.34	>10^{wx}	3.32	>10^{wx}	3.33	>10^{wx}	3.35 basic	>10
3.24	2	3.25	4	3.24	3	3.21, 2M$_1$	4-5
3.05	1	3.04	4^{y}	3.12	1	3.08, 1M	5-6
2.96	3^{y}	2.96	4	2.97	2	2.99, 2M$_1$	4-5
2.86	2	2.85	3	2.89	1	2.87, 2M$_1$	3-4
		2.78	2			2.80, 2M$_1$	2-3
				2.70	3	2.69, 1M	1-3
2.56	7^{x}	2.56	>10^{xy}	2.57	7^{x}	2.56-2.58 basic	8-9
				2.49	1^{x}	2.51, 2M$_1$	2
2.45	7^{w}	2.43	2^{w}	2.45	4^{w}	2.45 basic	1-3
2.37	2^{x}	2.37	6^{x}	2.37	3^{x}	2.38 basic	2-5
2.28	4	2.29	10^{wxy}	2.28	3^{wx}	2.25, 1M, 2M$_1$	1-4
2.20	1^{w}			2.20	1	2.21 basic	1
2.13	7^{wy}	2.14	2^{w}	2.13	4^{w}	2.15 basic	1-2
1.99	3^{xy}	1.98	8^{xy}	1.99	3^{x}	1.99 basic	3-8

* Copper radiation, nickel filter. Only mica spacings are listed. Where resolution is insufficient for separation the mica lines are wholly or partially masked by the following minerals: w-Quartz, x-Kaolinite, y-Jarosite for no. 2 and Alunite for no. 1. All intensities are recalculated on the basis of 10 maximum for the 10.0 Å spacing.

** Spacings and range in intensities of major polymorph reflections are based primarily on Yoder and Eugster (1955). Major polymorph spacings are underlined.

1. D.D.H. No. V-1, 340 feet. Collapse. Moss Back or Upper Monitor Butte Member silty mudstone breccia fragments. Not associated with urano-organic materials. Mica clay, quartz, kaolinite, and alunite.

2. From Moss Back Member in fault associated with urano-organic ore. East side of Temple Mountain collapse. Mica clay, quartz, kaolinite, and jarosite.

3. "Underclay" beneath urano-organic ore at base of Moss Back Sandstone, Calyx Hole mine no. 3. Mica clay, quartz, and kaolinite.

not possible, because of their sporadic distribution.

A study of argillaceous lithologies in the Chinle, below and above the Moss Back, indicates increased ordering of the mica clay from 1Md-1M mixtures in unaltered sediments, through 1M–2M$_1$ mixtures in partially altered rocks, to mixtures containing predominantly the 2M$_1$ polymorph in altered sediments bordering the collapse features.

Significance of Mica-Clay Polymorphs

Yoder and Eugster (1955, p. 246) consider that ". . . the transition of 1M to 2M appears to be between 200° C. and 350° C. at 15,000 p.s.i. water pressure" for synthetic materials. Under natural conditions, the crystallization of the 2M$_1$ polymorph may occur at temperatures below or above the range suggested, because of indeterminable effects of catalytic minerals under variable conditions of temperature, pressure, and ion concentration. It is generally believed, however, that progressive metamorphism of sediments leads to the transformation of 1Md to 1M to 2M$_1$ for mica clays (Yoder and Eugster, 1955; Smith and Yoder, 1956). Smith and Yoder (1956, p. 229) state,

"Although materials called illite and hydrous mica may contain micas having any structure or may even be mixtures, only that portion of the micas having a 1Md or a 1M structure is believed by Yoder and Eugster (1955) to be indicative of a low temperature environment."

X-RAY MICROCAMERA PATTERNS OF INTERSTITIAL AGGREGATES, MOSS BACK SANDSTONE

FIGURE 2

FIGURE 4

FIGURE 1

FIGURE 3

ARGILLIZATION IN THE MOSS BACK AND COLLAPSE

Yoder and Eugster (1955, p. 249) report mixed single- and double-layer polymorphic illites and hydromicas from the following localities:

Fithian, Illinois. Pennsylvanian underclay. "Illite." Mixed-layer 1Md plus montmorillonite and 2M.

Morris, Illinois. Underclay. "Illite." Mixed-layer 1Md plus montmorillonite, 2M, and quartz.

Mineral Jo mine, Jo Dandy Mining Group, Paradox Valley, Montrose, Colorado. Salt Wash Member (?) of the Morrison Formation. "Hydromica." Mixed-layer 1Md plus montmorillonite and 2M.

The occurrences listed above are between mixed-layer disordered mica with montmorillonite and $2M_1$ mica. These clays may have formed after deposition or may represent the original constituents of the sediment.

The lack of mixed-layer mica and montmorillonite at Temple Mountain and the common occurrence of 1M with $2M_1$ polymorphs indicate a greater amount of ordering than is shown above. The concentration of illite in the Moss Back near ore deposits and collapse features probably is not a product of diagenetic origin. The presence of the ordered single-layered structure with the $2M_1$ polymorph—the latter apparently increasing in concentration toward ore and the collapse—indicates elevated temperatures, on the basis of data on the production of synthetic micas, and supports the hydrothermal conditions postulated for the emplacement of urano-organic ore.

Formation of Kaolinite

Kaolinite is the dominant clay mineral in the unaltered and nonore-bearing Moss Back Sandstone. It occurs in interstices as an original constituent of the sediments before mineralization. Like the illite, the kaolinite shows changes toward ore-bearing strata, major faults, and collapse structures. In altered zones near or within the collapse features, the concentration, frequency of vermicular forms, and large aggregate flakes increase near ore (Fig. 2 *B*, *D*; Pl. 2).

TABLE 8.—X-RAY MICROCAMERA VALUES FOR KAOLINITE

Salt and pepper kaolinite		Aggregate flakes		Well-crystallized kaolinite*		Poorly crystallized kaolinite*	
d(Å)	I	d(Å)	I	d(Å)	I	d(Å)	I
7.14	10	7.15	10	7.15	10	7.15	10
4.48	6	..	..	4.45	4	4.45	8
....	..	4.38	2b	4.35	6	4.36	2
....	..	..	..	4.17	6	..	..
....	..	..	..	4.12	3	4.14	2
4.05	7†	..	..	....	..	..	..
....	..	..	..	3.837	4	..	..
3.75	1	..	..	3.734	2	..	..
3.58	9	3.57	9	3.566	10	3.57	10
....	..	3.32	1	3.365	4	..	..
....	..	3.10	1	3.138	2	..	..
2.58	5	2.53	2b	2.553	8	2.55	7
....	..	..	..	2.521	4	2.50	7
2.48	5	..	..	2.486	9	..	..
....	..	..	..	2.374	7	2.375	7
2.35	5b	2.36	2b	....	..	..	..
....	..	..	..	2.331	10	2.325	8b
2.29	4	..	..	2.284	9	..	..
....	..	..	..	2.243	1	..	..
2.18	1	..	..	2.182	3	..	..
....	..	..	..	2.127	2	..	..
....	..	..	..	2.057	1	..	..
1.994	1	1.98	1b	1.985	7	2.977	4

* Grim (1953).
† Not identified.
b = broad line.

X-ray-diffraction patterns were sufficiently resolved to indicate that both the "salt and pepper" and vermicular forms have the spacings

PLATE 2. ARGILLIZATION IN THE MOSS BACK AND COLLAPSE

FIGURE 1.—Camp Bird mines bordering the Temple Mountain collapse. Moss Back Sandstone. Aggregate vermicular flakes of kaolinite in intermixed salt and pepper kaolinite and illite surround ore pod. Nicols crossed. × *ca.* 20

FIGURE 2.—Camp Bird mines bordering the Temple Mountain collapse. Moss Back Sandstone. Large vermicular kaolinite being partially replaced by surrounding intermixed kaolinite, illite, and ore (black). Edge of ore pod. Nicols crossed. × *ca.* 20.

FIGURE 3.—D.D.H. V-1, 340 feet. Temple Mountain collapse. Development of intermixed kaolinite and illite with large vermicular kaolinite in siltstone from breccia zone. Nicols crossed. × *ca.* 30.

FIGURE 4.—D.D.H. V-1, 340 feet. Temple Mountain collapse. Development of interstitial illite and kaolinite and alteration of orthoclase in poorly sorted sandstone from breccia zone. Nicols crossed. × *ca.* 30.

of well-crystallized kaolinite (Grim, 1953 p. 88). This can be seen in X-ray microcamera patterns of the two types (Table 8).

Relationships between the two clay minerals show the following paragenesis from earliest to latest:

(1) Diagenetic interstitial salt and pepper kaolinite with scattered patches and stringers of illite and a few small vermicular flakes of kaolinite

(2) Increased concentration of illite intermixed with salt and pepper kaolinite

(3) Continued increase of illite with first, development of small aggregate vermicular flakes, and, finally, large vermicular flakes of kaolinite

(4) Increased development of illite with some replacement of the larger flakes of kaolinite; emplacement of ore

Source of Clay-Forming Elements in the Moss Back Sandstone

The collapsed features appear to have been major channels for the hydrothermal solutions, as shown by the concentrations of dolomite and siderite around the collapse areas and the increased argillization near by in the Moss Back. The clays associated with the ore and collapse alteration suggest that silica and potassium were transported from materials penetrated and may not have originated with the hydrothermal solutions.

In unaltered Moss Back Sandstone, micro-

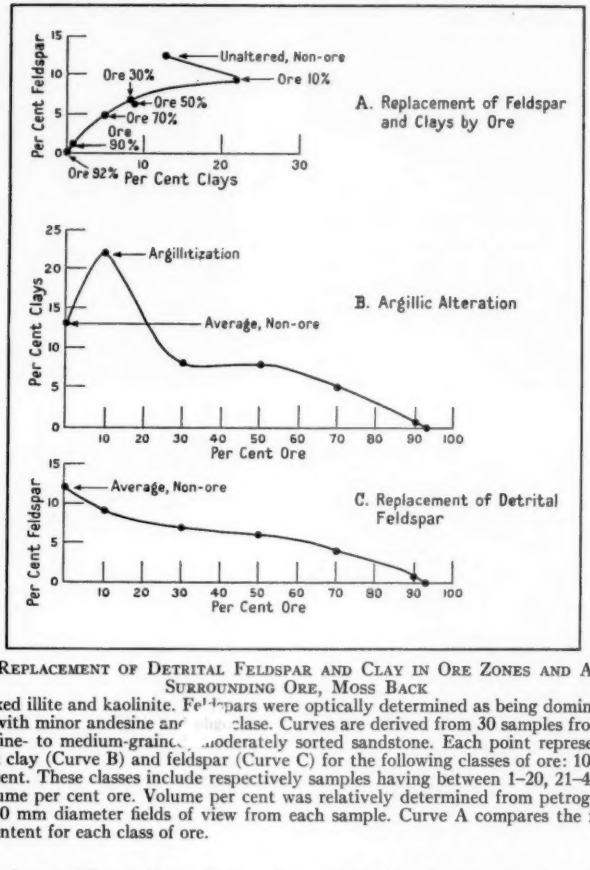

FIGURE 3.—Replacement of Detrital Feldspar and Clay in Ore Zones and Argillization Surrounding Ore, Moss Back

Clays are mixed illite and kaolinite. Feldspars were optically determined as being dominantly orthoclase and microcline with minor andesine and oligoclase. Curves are derived from 30 samples from nine localities of comparable fine- to medium-grained moderately sorted sandstone. Each point represents the average volume per cent clay (Curve B) and feldspar (Curve C) for the following classes of ore: 10, 30, 50, 70, and 90 volume per cent. These classes include respectively samples having between 1–20, 21–40, 41–60, 61–80, and 81–100 volume per cent ore. Volume per cent was relatively determined from petrographic examination of many 1.0 mm diameter fields of view from each sample. Curve A compares the feldspar content with the clay content for each class of ore.

scopic estimates indicate that original interstitial clay material averages about 13 per cent of the rock by volume. The original detrital feldspar content is about the same.

The relative increase in clay content because of alteration is noteworthy. Within ore zones away from the collapse, the average content of interstitial material in the rock ranges between 12 and 30 per cent; in faults away from the collapse, between 20 and 40 per cent; and in or near the collapse, between 25 and 50 per cent.

The replacement of interstitial clay and feldspar, the extent of argillic alteration, and the replacement of detrital feldspar are illustrated graphically in Figure 3. In peripheral ore zones containing less than 20 per cent uranoorganic material and metallics, there is an average increase in concentration of interstitial material of 11 per cent and an average decrease in detrital feldspar of only 3 per cent of the rock. However, within the ore zones where uranoorganic materials and metallic minerals make up between 20 and 90 per cent, the interstitial cement has decreased on the average about 5 per cent, and the detrital feldspar about 6 per cent, from normal, unaltered, nonore sediments. Thus there is a total increase of interstitial material (dominantly clays) on the order of 11 per cent surrounding ore zones, whereas a corresponding total of approximately 14 per cent of the interstitial material and detrital feldspar has been removed within ore zones. Because of the intimate mixing of the clay minerals, it is not feasible to arrive at these figures for individual minerals. However, it is apparent that there was probably sufficient potassium, aluminum, and silica in the sediments to account for the production of clays surrounding ore masses during replacement. The following observations substantiate the above hypothesis:

(1) The argillic phase of alteration is mainly characteristic of the Moss Back Sandstone, the remainder of the Chinle, and upper Moenkopi sediments.

(2) Argillization is associated with ore and alteration bordering and within the collapse where evidence of replacement of original sediments is strongest.

(3) No large bodies of relatively pure clay are present that may not have been originally argillaceous lithologies containing sufficient aluminum, potassium, and silica to account for reconstitution of clay minerals during alteration.

(4) Ore associated with silicified limestones (believed to be correlative with the Kaibab) in drill holes in the collapse contains only slight amounts of interstitial clay.

(5) The Moenkopi argillite adjacent to the collapse shows little, if any, evidence of removal of clay constituents. The quantities of clay added to sandstones near ore and collapses are smaller than would be expected if extensive solution of the Moenkopi had taken place and elements had been transported upward from below the Chinle.

Summary and Conclusions

A study of the urano-organic ore in the Moss Back Sandstone Member of the Chinle at Temple Mountain appears to reveal a significant spatial relationship between the ore and the associated intergranular argillic alteration. Although systematic collecting and accompanying analysis of more ore localities would be necessary to establish a complete three-dimensional pattern of argillization, the current study is believed to provide data with a significant bearing on the mechanism of mineralization.

Unaltered and nonore sandstone contain dominantly salt and pepper kaolinite, with scattered patches of 1Md and 1M illite. The $2M_1$ mica-clay polymorph is apparently lacking. Detrital $2M_1$ muscovite, present along bedding planes in these sediments in some places appears to be breaking down to 1M mica clay.

Toward masses of ore and collapse features, the intergranular kaolinite and illite become more abundant. Aggregate birefringence and particle size also appear to increase slightly. Mixtures of 1M and $2M_1$ mica polymorphs of the mica clay are typical. The $2M_1$ mica polymorph also becomes a more abundant constituent of the mixtures. In and near collapses, vermicular forms of kaolinite are more common. Furthermore, mixed-layer clays, typical of unaltered sediments, do not appear in the Temple Mountain mining district.

Hydrothermal synthesis of micas has shown that the transition of the 1M to the $2M_1$ mica polymorph appears to occur between 200° C. and 350° C. at 15,000 p.s.i. water pressure (Yoder and Eugster, 1955, p. 246). It may be inferred that the illite associated with the ore at Temple Mountain is the type one would expect to be deposited by the hydrothermal solutions accompanying urano-organic deposition. The clay-forming elements apparently were derived from the original interstitial clay and detrital feldspar during mineralization of the sediments. Collapse structures and fractures

represent the feeders from which the altering solutions migrated out along the permeable sandstones of the Chinle and Wingate—particularly the Moss Back ore horizon.

The features of argillization, involving subtle changes in the structure of the clay minerals, developed during this study of a well-known plateau locality, may be applicable to the determination of centers of uranium mineralization elsewhere on the Colorado Plateau.

References Cited

Foster, M. D., 1956, Correlations of dioctahedral potassium micas on the basis of their charge relations: U. S. Geol. Survey Bull. 1036-D, 67 p.

Grim, R. E., Bradley, W. F., and Brown, G., 1951, The mica clay minerals, p. 138–172 *in* Brindley G. W., *Editor*, X-ray identification and crystal structures of clay minerals: London, Mineralog. Soc., Clay Mineral Group, 345 p.

Grim, R. E., Bray, R. H., and Bradley, W. F., 1937, The mica in argillaceous sediments: Am. Mineralogist, v. 22, no. 7, p. 813–829

Grim, R. E., 1953, Clay mineralogy: N. Y., McGraw-Hill Book Co., 384 p.

Hendricks, S. B., and Jefferson, M. E., 1939, Polymorphism of the micas: Am. Mineralogist, v. 24, p. 729–771

Hirsch, P. B., 1955, X-ray microbeam techniques, p. 278–297 *in* Peiser, H. S., Rooksby, H. P., and Wilson, A. J. C., *Editors*, X-ray diffraction by polycrystalline materials: London, Inst. of Physics, 725 p.

Kelley, D. R., and Kerr, P. F., 1956, Emplacement of uraniferous hydrocarbons at Temple Mountain, Utah: U. S. Atomic Energy Comm. Ann. Rep., June 30, 1955, to April 1, 1956, 79 p.

Kerr, P. F., and Hamilton, P. K., in press, Chrome mica clay, Temple Mountain, Utah: Am. Mineralogist

Kerr, P. F., and Kelley, D. R., 1956, Urano-organic ores of the San Rafael Swell, Utah: Econ. Geology, v. 51, p. 386–391

Kerr, P. F., Bodine, M. W., Kelley, D. R., and Keys, W. S., 1957, Collapse features, Temple Mountain uranium area, Utah: Geol. Soc. America Bull., v. 68, p. 933–982

Levinson, A. A., 1955, Studies in the mica group: polymorphism among illites and hydrous micas: Am. Mineralogist, v. 40, p. 41–49

Smith, J. V., and Yoder, H. S., Jr., 1956, Experimental and theoretical studies of the mica polymorphs: Mineralog. Mag., v. 31, no. 234, p. 209–235

Weaver, C. E., 1956, The distribution and identification of mixed-layer clays in sedimentary rocks: Am. Mineralogist, v. 41, p. 202–221

Yoder, H. S., Jr., and Eugster, H. P., 1955, Synthetic and natural muscovites: Geochim. Cosmochim. Acta, v. 8, no. 5/6, p. 225–280

The Texas Company, Farmington, N. Mex.; Department of Geology, Columbia University, New York, N. Y.

Manuscript Received by the Secretary of the Society, December 6, 1956

BULLETIN OF THE GEOLOGICAL SOCIETY OF AMERICA
VOL. 68, PP. 1117–1140 SEPTEMBER 1957

URANIUM-LEAD METHOD OF AGE DETERMINATION

PART II: NORTH AMERICAN LOCALITIES

BY WALTER R. ECKELMANN AND J. LAURENCE KULP

ABSTRACT

Many new isotopic age determinations by the uranium-lead method have been made on most of the important North American localities from which primary uranium minerals have been reported. With the aid of other published isotopic U-Pb age measurements the writers attempted to interpret the most probable age for each locality and to assign a reasonable uncertainty to that age. The recognition of differential lead loss, the relation of alteration to mineral type, the importance of radon leakage for young samples, and the potential analytical errors make it timely to conduct such a re-evaluation. Among the well-established ages are: Spruce Pine district, North Carolina, 360 ± 20 m.y.; Portland, Connecticut, 265 ± 10 m.y.; Front Range, Colorado, 59 ± 5 m.y.; Black Hills, South Dakota, 1620 ± 20 m.y.; southeast Manitoba, 2650 ± 100 m.y.; Lake Athabasca, Saskatchewan, 1900 ± 50 m.y.; and the Wilber-force area, 1050 ± 20 m.y. Other probable ages are Bedford, New York, 350 m.y.; Colorado Plateau, 60 m.y.; Coeur d'Alene, 1200 m.y.; and Great Bear Lake, Northwest Territories, 1500 m.y. Although there may have been several regional metamorphic events in the Appalachian Province in the Precambrian, the post-Cambrian effects appear at only two periods centering on 260 m.y. and 360 m.y. The Grenville metamorphism appears limited to a narrow time interval about 1050 m.y. ago. The Front Range and Colorado Plateau uranium mineralization may have been one event occurring about 60 m.y. ago.

CONTENTS

TEXT

	Page
Introduction	1118
Acknowledgments	1118
Experimental procedures	1118
New experimental data	1118
Evaluation of ages of North American localities	1121
Southern Appalachians	1122
Spruce Pine district, North Carolina	1122
Other southern localities	1125
New England and eastern New York	1126
Portland, Connecticut	1126
Bedford, New York-Branchville, Connecticut	1126
Colorado	1127
Front Range	1127
Colorado Plateau	1128
Idaho	1129
Sunshine Mine, Coeur d'Alene district	1129
South Dakota	1130
Black Hills	1130
Other western localities	1131
Canada	1131
Manitoba	1131
Northwest Territories	1133
Great Bear Lake	1133
Other areas in the Northwest Territories	1133
Saskatchewan-Alberta	1136
Lake Athabasca region	1136
Ontario	1136
Wilberforce area	1136
Conclusions	1138
References cited	1138

TABLES

Table	Page
1. Chemical analyses	1119
2. Raw isotopic data	1121
3. New isotopic ages of primary uranium minerals	1122
4. Common leads used for correcting raw isotopic data	1123
5. Isotopic ages of Spruce Pine, North Carolina, uranium minerals	1124
6. Chemical ages of uranium minerals from Spruce Pine pegmatite district, North Carolina	1125
7. Isotopic ages of uranium minerals from Middletown, Connecticut	1126
8. Isotopic ages of cyrtolite from Bedford, New York	1127
9. Isotopic ages of pitchblende from the Colorado Front Range	1128
10. Isotopic ages of primary uranium minerals from the Colorado Plateau	1129
11. Isotopic ages of pitchblende from Sunshine Mine, Idaho	1130
12. Isotopic ages of uraninite from the Ingersoll pegmatite, Black Hills, South Dakota	1131

13. Ages of minerals from various western localities 1131
14. Isotopic ages of minerals from the Huron Claim, Manitoba 1132
15. Isotopic ages of pitchblende from Eldorado Mine, Great Bear Lake 1133
16. Isotopic ages of minerals, Saskatchewan-Alberta 1134
17. Isotopic ages of Saskatchewan-Alberta pegmatites 1137
18. Isotopic ages of minerals, Grenville province 1137

Introduction

The advances in the understanding of the uranium-lead method of age determination that have occurred during the past few years, and the fundamental character of this method in geochronometry make it important to re-examine the previously reported ages from the North American localities and to compare these with new data. The relative importance of lead, uranium, and thorium loss, radon leakage, and the common-lead correction can be well-defined in many cases, making it possible to interpret discordant ages in terms of the time of formation of the mineral and its subsequent history. Since each radioactive mineral appears to show a unique pattern of discordance if altered (Kulp and Eckelmann, 1957), the analysis of more than one mineral type from a locality provides much interlocking data which can be used to estimate times of formation and alteration.

The experimental measurements given in this paper were made on new material from the various localities. The experimental study included radon-leakage measurements and tests for radioactive equilibrium in addition to the necessary chemical and isotopic analyses. The principles derived in the investigation of the Lake Athabasca region (Eckelmann and Kulp, 1956) are applied to the data from all the laboratories in an attempt to determine the most probable age that may be assigned with the present state of knowledge.

Acknowledgments

This research has been supported by the Research Division of the Atomic Energy Commission under Contract AT(30-1)-1114. Prof. P. F. Kerr initially encouraged the study and put at the writers' disposal his personal collection of uranium minerals as well as those of the Columbia Systematic Collection. The late J. P. Marble contributed valuable advice and provided portions of some of the identical lead salts measured by Prof. A. O. Nier. Prof. Brian Mason, Curator of Mineralogy, American Museum of Natural History, and Profs. Horace Winchell and John Rodgers of Yale University were most generous in providing excellent specimens for study. Discussions with Drs. R. D. Russell, G. R. Tilton, G. L. Bate, W. S. Broecker, P. W. Gast, and B. J. Giletti were most helpful.

The preparation of lead tetramethyl from lead chloride was performed by J. E. Gaetjen, M. Trautman, and R. E. Nuckolls. H. R. Owen and G. L. Bate were responsible for the design and construction of the mass spectrometer. W. Knox assisted in the electronic maintenance of the instrument.

The co-operation of Dr. C. J. Rodden and Dr. P. J. Tregoning of the Atomic Energy Commission, New Brunswick Analytical Laboratory, was an important factor in the completion of this study. M. Trautman, D. S. Miller, E. Hodges, and W. Knox assisted in the technical phase of the program.

Experimental Procedures

The specimens utilized in this study were pitchblende, uraninite, samarskite, uranothorite, galena, and clausthalite. The lead, uranium, and thorium contents of these minerals were determined by wet-chemical methods. In addition lead was separated and purified as the chloride.

The mass spectrometer and the technique of isotopic analyses of lead as the tetramethyl have been described by Bate, Miller, and Kulp (1957). The isotopic abundances of most of the samples were obtained from the Pb $(CH_3)_3^+$ spectra. The use of Pb $(CH_3)_3^+$ spectra instead of the Pb^+ spectra removes the necessity of Hg^{204} corrections, which are troublesome in samples of low Pb^{204}. The use of the Pb $(CH_3)_3^+$ spectra also reduces the hydride correction and thus increases the precision of the Pb^{204} abundance.

The method and equipment involved in measurement of radon leakage have been described by Giletti and Kulp (1955, p. 482–484). The procedure for analyzing Pb^{210} has also been described (Kulp, Broecker, and Eckelmann, 1953, p. 21).

New Experimental Data

The chemical analyses for the samples involved in this study are given in Table 1. Each of these elemental analyses was run at least twice. Most of the lead analyses were run three

TABLE 1.—CHEMICAL ANALYSES*

Sample No.	Locality	Per cent U†	Per cent Th	Per cent Pb
K-3	Mitchell Co., N.C.	9.95±.02	1.265±.01	0.42±.02
K-4	Wiseman Mine, Spruce Pine District, N. C.	13.06±.03	1.11 ±.033	0.603±.01
K-6	Richards Mine, Gilpin Co., Colo.	47.88±.05	0.10 ±.01	1.34 ±.01
K-7	Contact Lake, N.W.T.	19.46±.03	2.51 ±.01	0.22 ±.02
K-8	German and Belchin Mine, Central City, Colo.	64.66±.05	0.73 ±.01	0.18 ±.01
K-16	Eldorado Mine, (151 Stope), Saskatchewan	6.61±.02	---	1.40 ±.01
K-18	Eldorado Mine (913 Stope), Saskatchewan	48.85±.05	---	8.39 ±.05
K-19	Nicholson Mine, No. 2 Shaft, Saskatchewan	44.31±.02	---	4.91±.02
K-41	Ace Mine, Saskatchewan	16.90±.02	<.01	3.34±.03
K-46	Ace Mine, Saskatchewan	30.05±.05	<.01	5.47±.03
K-58	ABC Adit, Nesbitt Labine, Saskatchewan	12.74±.02	<.01	.63±.01
K-64	Cardiff Township, Ontario	50.57±.05	---	8.63±.03
K-68	Lee Lake, Lac-LaRonge Saskatchewan	50.70±.02	---	4.62±.03
K-71	Wood Calhoun Mine, Gilpin Co., Colo.	62.03±.01	.335±.01	.39±.01
K-96-1	McKinney Mine, Mitchell Co., N.C.	7.53±.02	.27 ±.01	.41±.02
K-96-2	McKinney Mine, Mitchell Co., N.C.	7.30±.02	.30 ±.01	.34±.005
K-101	Sunshine Mine, Idaho	3.32±.02	.015	.535±.005
K-105	Flat Rock Mine, Spruce Pine, N.C.	74.16±.05	.45±.01	3.68±.04
K-106	Mars Hill, N.C.	0.15±.01	6.12±.02	.06±.01

TABLE 1.—Continued

Sample No.	Locality	Per cent U†	Per cent Th	Per cent Pb
K-109	Huron Claim, Manitoba	6.09±.03	1.49±.04	2.12±.03
K-113	Viking Lake, Saskatchewan	26.36±.12	8.10±.03	7.98±.03
K-120-a	Black Hills, S.D.	53.16±.06	2.87±.02	14.44±.05
K-120-b	Black Hills, S.D.	63.18±.06	8.55±.02	14.38±.06
K-124	Petaca, N.M.	9.04±.09	1.78±.02	.35±.02
K-125	Spinelli Quarry, Glastonbury, Conn.	6.04±.04	2.86±.04	.27±.005

* These analyses were performed by the New Brunswick Analytical Laboratory of the A.E.C. Lead and thorium analyses were made by Dr. W. Bergholz; uranium analyses were made by Mr. W. Peavy.

† Each analytical value of U, Th, and Pb represents a minimum of two independent determinations.

times. The stated errors indicate the standard deviation. The raw isotopic data for the same samples are shown in Table 2. These were also run at least twice on different days. Many were run three or four times. Again the stated error represents the standard deviation. Table 3 gives the isotopic ages corrected only for common lead, and Table 4 gives the isotopic composition of the common leads used in making the calculations for Table 3. In those cases where no representative common lead for the area was available a theoretical common lead, based on the age of the mineral, was used. The 206/204, 207/204, 208/204 vs. time curves used to calculate the theoretical common lead at any age were based on the isotopic composition of original lead (4.5 b.y. age) of 1:9.5:10.3:29.2 and a modern lead of 1:18.9:15.7:38.9. It was also assumed that the U/Pb and Th/Pb ratios in the source environment of uranium minerals have not changed appreciably during earth history.

The errors stated in Table 3 are derived from an evaluation of all factors involved in the determination of the age. In the case of the Pb^{206}/U^{238} and Pb^{207}/U^{235} ages for samarskite, the dominant error in the Pb^{207}/Pb^{206} is due to the error in the abundance of Pb^{207}. This is a combination of the errors in the isotopic analysis and the uncertainty in the common-lead correction. The Pb^{207}/Pb^{206} age in the low age range, *i.e.*, <500 m.y., is extremely sensitive to small changes in the Pb^{207}/Pb^{206} ratio. For example, as little as 1 per cent radon leakage in a mineral 100 m.y. old would cause the Pb^{207}/Pb^{206} age to be high by 25 m.y. One per cent error in the isotopic abundance of Pb^{207} caused by mass spectrometer discrimination could produce the same error.

The uncertainty in the U^{235} half life, *i.e.*, 2 per cent, is not included in the stated error, although this could cause a considerable spread in the ages for a young sample. The concordant ages for some of the older localities suggest that the half life of U^{235} is known to better than ±2 per cent. The error in the other half lives appears to be less than 1 per cent.

The largest contribution to the error in 210/206 age is from the half life of Pb^{210}. Radioactive impurities in the extracted lead will make this age obtained from the 210/206 ratio appear too young. The particular samples reported here appear to be free from this effect. The large error in the 208/232 age is due in some cases to the small thorium concentration which results in large uncertainty in the radiogenic Pb^{208} abundance.

The constants employed in making the calculations in this paper were: $N^{238}/N^{235} = 137.7$, $T - 1/2\ U^{238} = 4.51 \times 109$ yrs., $T -$

TABLE 2.—RAW ISOTOPIC DATA

Sample No.	204	206	207	208
K-3	.034 ± .003	90.9 ± .1	5.45 ± .09	3.65 ± .03
K-4	.040 ± .004	91.3 ± .2	5.63 ± .09	3.15 ± .07
K-6	.97 ± .01	44.88 ± .2	16.63 ± .05	37.52 ± .10
K-7	< .01	92.3 ± .2	7.50 ± .20	.27 ± .03
K-8	.57 ± .01	65.7 ± .1	11.78 ± .04	21.97 ± .20
K-16	.12 ± .01	86.4 ± .1	9.27 ± .15	4.26 ± .10
K-18	.21 ± .01	82.6 ± .1	9.66 ± .05	7.52 ± .04
K-19	< .02	92.4 ± .1	7.25 ± .10	.32 ± .02
K-41	.073 ± .001	88.11 ± .06	9.69 ± .07	2.12 ± .02
K-46	.091 ± .007	89.77 ± .11	9.69 ± .08	.50 ± .01
K-58	.028 ± .004	92.6 ± .1	6.36 ± .06	1.21 ± .02
K-64	.010 ± .004	85.3 ± .2	6.63 ± .08	8.01 ± .08
K-68	.035 ± .015	87.06 ± .05	9.63 ± .06	3.34 ± .07
K-71	.33 ± .02	78.8 ± .2	9.59 ± .20	11.35 ± .06
K-96-1	.030 ± .003	92.43 ± .11	5.24 ± .03	2.32 ± .03
K-96-2	.057 ± .001	90.95 ± .09	5.64 ± .02	3.36 ± .02
K-101	.361 ± .005	76.70 ± .07	10.73 ± .04	12.21 ± .05
K-105	< .004	94.60 ± .04	5.04 ± .03	.352 ± .008
K-109	.014 ± .001	81.80 ± .08	13.32 ± .02	4.86 ± .14
K-113	.029 ± .004	86.4 ± .3	10.51 ± .18	3.07 ± .03
K-120-a	< .008	89.88 ± .05	8.85 ± .03	1.27 ± .02
K-120-b	.015 ± .001	89.63 ± .05	8.96 ± .04	1.39 ± .02
K-121	.0145 ± .0004	93.68 ± .06	5.25 ± .04	1.06 ± .09
K-124	.124 ± .007	83.88 ± .07	7.47 ± .07	8.54 ± .05
K-125	.088 ± .004	79.18 ± .20	5.41 ± .05	15.41 ± .20

$1/2\ U^{235} = 7.13 \times 10^8$ yrs., and $T - 1/2\ Th^{232} = 1.39 \times 10^{10}$ yrs.

EVALUATION OF AGES OF NORTH AMERICAN LOCALITIES

In this investigation an attempt has been made to synthesize and interpret published data on primary uranium- and thorium-bearing minerals from North American localities for which isotopic measurements have been reported. Some of the earlier chemical ages are noted where they are pertinent to the discussion. Where possible, earlier data are recalculated, and probable errors assigned. In

some cases there is a considerable difference between the common-lead correction if Pb^{208} rather than Pb^{204} is used as a base. If a thorium analysis indicates negligible radiogenic Pb^{208}, this is preferred for the common-lead correction.

If the calculation of an average age for a particular isotopic ratio was warranted, the reciprocal of the square root of the error for each sample was used as a weighting factor unless otherwise stated. This procedure is justified if the differences appear to be due to experimental procedures rather than alteration effects in the mineral. The error assigned to this average age for a single isotopic ratio is the standard deviation of the mean.

The data in this paper are complete to date and supersede earlier published results (Kulp, Bate, and Broecker, 1954; Kulp, Broecker, and Eckelmann, 1953; Kulp, Bate, and Giletti, 1955; Eckelmann and Kulp, 1956).

TABLE 3.—NEW ISOTOPIC AGES OF PRIMARY URANIUM MINERALS
(In million years)

Sample No.	206/238	207/235	207/206	210/206	208/232
K-3	282±13	292±17	405±60		170±10
K-4	307±6	312±13	380±80	325±15	205±50
K-6	56±1	62±6	320±230		
K-7	840±5	960±15	1220±50	882±35	
K-8	51±1	54±2	305±100		
K-16	1230±10	1305±15	1405±15	1230±40	
K-18	1010±5	1100±10	1240±20	1042±40	
K-19	730±5	845±10	1140±25		
K-41	1185±10	1335±10	1630±20		
K-64	1015±5	1038±15	1060±30		
K-68	565±5	868±10	1750±30		
K-71	35±1	42±2	430±130		
K-96-1	367±18	353±20	300±40	335±12	400±80
K-96-2	314±10	316±10	342±20		302±30
K-101	805±10	860±20	1035±35		
K-105	345±4	345±5	372±20	322±12	
K-109	1860±10	2150±20	2510±25		1355±50
K-113	1525±10	1720±15	1870±20		445±25
K-120-a	1615±5	1615±5	1622±10		1370±20
K-120-b	1390±5	1460±5	1610±15		1030±25
K-121			355±15		
K-124	240±5	310±5	875±30		180±7
K-125	257±8	258±8	292±35	292±30	257±8

SOUTHERN APPALACHIANS

Spruce Pine District, North Carolina

The Spruce Pine pegmatite district in the metamorphic complex of western North

Carolina has been the subject of detailed geologic study (Kulp and Brobst, 1956). Since this area provides a key to the regional geology of a major part of the Blue Ridge Province in North Carolina, the definition of the time of the pegmatite intrusion is important. The formation of the pegmatites appears to have concluded the metamorphic history of the region.

Tables 5 and 6 are a compilation of the age determinations on uranium and thorium minerals from this district. The common-lead composition used to correct these samples was that of Henderson, North Carolina (Table 4). These data present an interesting array which suggests the following:

(1) The essential agreement of the Pb^{206}/Pb^{210} and Pb^{206}/U^{238} ages shows that these samples are now in equilibrium, and no large change in the radon leakage has occurred during the last 100 years. Experimental measurements of the radon leakage of several of these specimens gave a value of less than 0.1 per cent at room temperature for the samarskite and less than 1 per cent for the K-105 uraninite.

(2) The average values of ages for K-3, 4, 96-2, and 105 derived from each of the various isotopic ratios agrees within the errors. Uncertainties in the U^{235} half life and a possibility of isotopic discrimination by the mass spectrometer could account for a part of numerical separation that is observed in this age range. Pb^{207}/Pb^{206} ages are extremely sensitive to small errors. A 2 per cent error in the value of Pb^{207} of a 300 m.y. old sample changes this age approximately 40 m.y.

(3) The main source of error in the chemical analyses of samarskite data is probably due to the small lead content (~0.4 per cent). The only sample that afforded the opportunity for a highly quantitative lead analysis was the uraninite from Flat Rock Mine (K-105). This sample had a lead analysis of 3.67 ± .04 per cent and gave uranium-lead ages of corre-

TABLE 4.—COMMON LEADS USED FOR CORRECTING RAW ISOTOPIC DATA

Sample Location	204	206	207	208	Reference
Middletown, Conn.	1.33(8) ±.005	25.10 ±.06	21.19 ±.05	52.37 ±.08	Bate and Kulp (1955)
Average Colo.	1.35 ±.01	25.00 ±.06	21.10 ±.05	51.20 ±.07	Bate and Kulp (1955)
Great Bear Lake, N. W. T.	1.464 ±.004	23.61 ±.08	22.59 ±.07	52.34 ±.05	Bate and Kulp (1955)
Deer Trail, Utah	1.38 ±.02	24.93 ±.10	21.52 ±.10	52.25 ±.06	Bate and Kulp (1955)
Lake Athabasca, Saskatchewan	1.543 ±.004	22.15 ±.04	23.09 ±.06	53.22 ±.06	Bate and Kulp (1955)
Ace Mine, Lake Athabasca, Saskatchewan	1.026 ±.007	41.05 ±.08	19.86 ±.05	38.06 ±.09	Bate and Kulp (1955)
Eganville, Ontario	1.21 ±.005	28.21 ±.06	19.39 ±.06	51.19 ±.08	Bate and Kulp (1955)
St. Eugene Mine, Idaho	1.442 ±.006	23.76 ±.05	22.26 ±.05	52.54 ±.07	Bate and Kulp (1955)
Tucson Mountains Ariz.	1.350 ±.007	25.00 ±.06	21.15 ±.04	52.50 ±.07	Nier (1939)
Sunshine Mine, Idaho	1.428 ±.005	24.05 ±.06	21.99 ±.05	52.53 ±.07	Bate and Kulp (1955)
Henderson, N. C.	1.348 ±.005	25.05 ±.04	21.27 ±.03	52.33 ±.04	Bate and Kulp (1955)

spondingly low errors. The average 207/206 age from the samarskite, which of course does not depend on the chemical analysis, is 350 m.y., in good agreement with those directly determined on the uraninite.

assigned because of the lack of detailed information on procedures and replicate analyses. Since there appears to be only minor common lead in these uranium-bearing pegmatite minerals, it is not surprising perhaps that

TABLE 5.—ISOTOPIC AGES OF SPRUCE PINE, NORTH CAROLINA, URANIUM MINERALS

(In million years)

Sample No.*	Mineral and Location	206/238	207/235	207/206	208/232	210/206
K-3	Samarskite (Mitchell Co.)	282±13	292±17	405±60	170±10	-
K-4	Samarskite (Wiseman Mine)	307±6	312±13	380±80	205±50	325±15
K-96-1	Samarskite (McKinney Mine)	367±18	353±20	300±40	400±80	355±12
K-96-2	Samarskite (McKinney Mine)	314±10	316±10	342±20	302±30	-
K-105	Uraninite (Flat Rock Mine)	344±4	346±5	372±15	-	322±12
K-121	Gummite (Flat Rock Mine)	-	-	355±20	-	-
	Uraninite (Mitchell Co.)			355±20		
	Uraninite (Chestnut Flat Mine)			(375±10)		
Arithmetic average and average deviation		323±30	324±27	361±28	268±90	334±15
Weighted average		323	325	362	250	334

* All K samples are from this paper.
† Published by Collins et al. (1954) and recalculated.
** Aldrich et al. (1956). Apparently reasonably concordant ages were obtained.

(4) K-96-1 suggests an erroneously high lead analysis, since there was no evidence of weathering or leaching, which tend to remove uranium preferentially to lead and produce such an age pattern.

(5) The low 208/232 ages suggest some lead loss, since in uraninite (Kulp and Eckelmann, 1957, p. 157) thorium lead appears to be more sensitive to this phenomenon.

Table 6 shows the assays obtained by earlier workers on minerals from the Spruce Pine district. These are all "chemical" ages without isotopic analyses and were done on apparently unaltered specimens. No errors have been

chemical analyses on these minerals dating back before the discovery of radioactivity yield ages that broadly agree with the latest isotopic measurements.

The age of 590 m.y. obtained by Bliss on the Deer Park monazite appears impossibly high (Table 6). The Deer Park pegmatite is surrounded by the pegmatites which supplied all the other dates in these tables. There is no geologic evidence for two periods of pegmatite intrusion in the center of the Spruce Pine district. Since the Deer Park pegmatite probably has an age of about 360 m.y., the monazite which Bliss analyzed by the same procedure

used by Marble and Kroupa must either contain common lead or have an erroneous chemical analysis. Because the writers' isotopic analysis on the identical Mars Hill specimen showed no evidence of appreciable common lead, the analytical problem appears to be the source of the anomaly. Although the question cannot be considered finally settled, the weight of the evidence points to a single age for the Spruce Pine pegmatites.

It is concluded that the last regional metamorphic event in the Spruce Pine district and possibly in a large area of the Blue Ridge Province reached a climax 360±20 m.y. ago. This date is presumably around the Ordovician-Silurian boundary and generally equivalent in time to the Taconic disturbance in New England.

Other Southern Localities

Although there are no other localities in the Southern Appalachians for which isotopic data have been published, it is of interest to compare some of the available chemical ages with the Spruce Pine data.

A very old analysis of a uraninite from Marietta, South Carolina, by Hillebrand (1891, p. 386) gives an apparent age of 330 m.y., in good agreement with the Spruce Pine age. The pegmatites around Marietta are also a result of the last phase of metamorphic activity and are not far east of the strike of the Spruce Pine and Franklin-Sylva district pegmatite swarms.

A chemical age (Pb-α) (Larsen, Keevil, and Harrison, 1952, p. 1050) on two zircons from Statesville, North Carolina (~50 miles west of Spruce Pine), in the Piedmont gave 306 and 345 m.y., which again averages close to the Spruce Pine measurements. Finally, several Pb-α ages were determined on zircons and monazites from quartz monazites and pegmatites from Toluca, Shelby County, Alabama, giving 442, 426, 399, and 395 m.y. Whether these ages are higher because of common-lead contamination, or whether they truly represent an earlier metamorphism than the Spruce Pine pegmatite intrusion, cannot be decided from

TABLE 6. CHEMICAL AGES OF URANIUM MINERALS FROM SPRUCE PINE PEGMATITE DISTRICT, NORTH CAROLINA

(In million years)

Locality	Mineral	Age	Reference
Spruce Pine	Uraninite	340	Føyn (1938)
Spruce Pine	Uraninite		Lane (1942)
	Outside	330	
	Middle	340	
	Core	350	
Flat Rock Mine	Uraninite		Hillebrand (1891)
	A	350	
	B	365	
Flat Rock Mine	Uraninite	345	Boltwood (1907)
Stony Point (Mitchell Co.)	Uraninite	310	von Foullon (1883)
	Average uraninites	340 ± 10	
Deer Park Mine	Monazite	590	Bliss (1944)
Mars Hill	Monazite	*640	Marble (1936)
		*635	Lane (1937)
		*235 ± 70	This paper (K-106)

* Identical powder used for all 3 analyses

the data at hand. The localities are separated by 300 miles and different rock environments, but they lie on the same general trend in the Southern Appalachians.

New England and Eastern New York

Portland, Connecticut

Table 7 gives the isotopic ages obtained by Wasserburg and Hayden (1955, p. 56), Nier *et al.* (1941, p. 113), and the present study for the pegmatite swarm located in the vicinity of Portland, Connecticut. The errors have been estimated from the data of the original papers. The common lead used for the correction was the Middletown, Connecticut, galena (Table 4). Geologically all these pegmatites, which intrude the Bolton schist, appear to be the same age (Stugard, 1953). The excellent agreement between the Pb^{206}/U^{238} and the Pb^{207}/U^{235} ages for three separate samples involving two different minerals run at three laboratories and the fact that the isotopic ratios trend in the opposite direction for two apparently fresh specimens of uraninite strongly suggest that no significant alteration loss has occurred. This is verified by the fact that within the experimental errors the Pb^{207}/Pb^{206} ages agree with the Pb^{206}/U^{238} and the Pb^{207}/U^{235} ages. In this case even the Pb^{208}/U^{232} ratio which is more susceptible to lead loss than the other ratios gives essentially the same age within the errors. The chemical ages on uraninite and monazite (Fenner, 1932, p. 333; Hillebrand, 1891, p. 386; Føyn, 1938, p. 17; Hecht and Kroupa, 1936, p. 103) are in broad agreement. They yield ages ranging from 267–320 m.y. and suggest minor common-lead contamination in some cases.

The writers conclude that the time of the Portland pegmatite formation was 265±10 m.y. ago and is one of the well-established points on the geologic time scale. A Devonian age has been suggested for the Bolton schist, which is not inconsistent with the absolute age and may support a correlation of the later metamorphic activity in this region with the Acadian disturbance. The geological relationship strongly suggests a pre-Upper Carboniferous age for these pegmatites.

Table 7.—Isotopic Ages of Uranium Minerals from Middletown, Connecticut

(In million years)

Locality	Mineral	206/238	207/235	207/206	208/232	Reference
Strickland Quarry	Uraninite	268±3	266±3	250±25	239±12	Wasserburg and Hayden (1955)
Spinelli Quarry	Samarskite	252±3	254±8	271±75	267±10	Nier et al. (1941)
Spinelli Quarry	Samarskite	257±8	258±8	292±35	257±8	K-125 (This paper)
Arithmetic average		259	259	271	254	
Weighted average		260±6	260±5	270±17	255±12	

Bedford, New York-Branchville, Connecticut

This group of pegmatites presumably represents a geological event distinct from that which produced the Portland pegmatites. The samples of cyrtolite (zircon containing uranium and rare earths) from Bedford, New York (Table 8), which were analyzed for uranium, thorium, and lead by Muench (1931, p. 356) are identical with those used by Nier (1939, p. 159) for lead isotopic measurements. The cyrtolite was found to occur in pegmatite dikes intrusive into the Manhattan schist and may date the climax of the metamorphic cycle which produced these rocks. Both samples of unweathered cyrtolite came from the same dike and were originally used by Muench (1931; 1936) to see if the same chemical age could be obtained from two independent analyses

on material of identical geologic age and occurrence.

The data of Nier have been recomputed using the Middletown, Connecticut, common lead (Table 4). The common-lead correction was done in two ways, based on Pb^{204} in one case and Pb^{208} in the other. If the ages calculated using the Pb^{204} as the common-lead indicator are assumed valid, the age distribution might be interpreted to mean slight lead loss. A minor error in the lead analyses would explain the differences among the uranium-lead ages. This interpretation would yield a probable age as equal or greater than 420 ± 20 m.y. Muench (1931, p. 356) showed that the thorium concentration of cyrtolite I was less than 2 mg per gm of uranium; hence the Pb^{208} can be used for the common-lead correction. The isotopic ages corrected in this manner show an opposite trend. The most probable age is about 350 m.y., but the uncertainty must be ±30 m.y. at this time. Potassium-argon age determinations on the Manhattan schist at the laboratory indicate the time of formation to be 360–380 m.y. ago.

Thus the Bedford, New York, cyrtolites have essentially the same ages as the Spruce Pine, North Carolina, pegmatites, and both may reflect an orogenic cycle (along the entire length of the Appalachians) that was culminated by pegmatite intrusions.

TABLE 8.—ISOTOPIC AGES OF CYRTOLITE FROM BEDFORD, NEW YORK
(In million years)

Mineral	206/238	207/235	207/206	Reference
	Common lead correction based on Pb204			
Cyrtolite II	352±4	365±7	392±35	Nier (1939)
Cyrtolite I	333±3	342±10	428±55	Nier (1939)
	Common lead correction based on Pb 208			
Cyrtolite II	350±3	341±4	305±20	Nier (1939)
Cyrtolite I	331±3	326±4	321±20	Nier (1939)

COLORADO

Front Range

Although pitchblende has been reported at many places in the Front Range, quantitative uranium-lead analyses were made only from the deposits in Gilpin and Larrimer counties. Available data are shown in Table 9. The ages were calculated by using the Pb^{208} content for the common-lead correction, since the concentration of thorium in all cases was negligible. The isotopic composition of the common lead used was that from a galena at Idaho Springs, Colorado, but any normal modern common lead would have given essentially the same result. The common lead in the lead minerals of this area does not show evidence of contamination with radiogenic lead, so that this correction is not a major source of uncertainty.

Pb^{206}/Pb^{210} ages for K-6 and K-8 were 61±3 and 58±3 m.y. respectively, indicating that the minerals were essentially in equilibrium at the time of collection. Radon-leakage measurements at room temperature on these two samples gave 2.5 and 8.6 per cent respectively. Radon leakage of other fine pitchblende samples ranges from 1 to 10 per cent.

Since the Pb^{207}/U^{235} age is always greater than the Pb^{206}/U^{238} and the specimens were free of apparent surface weathering, uranium leaching is not a dominant factor. The radon leakage would tend to bring the ages from the three isotopic ratios together. The radon leakage measured in the laboratory is probably maximal, since the minerals have been near the surface throughout most of their history; hence this may be a reasonable correction. In the case of K-8, for example, the radon-leakage correction would bring the Pb^{206}/U^{238} age up to 55±1 and the Pb^{207}/Pb^{206} age down to 114± 100. If it is assumed that this factor would make the ages concurrent, then the Pb^{207}/U^{235}

ages would suggest deposition during a period ranging between 42 and 75 m.y. ago. This is not considered likely for several reasons:

(1) In the case of K-6 and certainly K-71 the radon leakage might not be large enough to bring the ages into agreement.

The high sensitivity of the 207/206 age in this range and the correspondingly low sensitivity of the difference between the 206/238 and 207/235 ages make it difficult to be certain of the factor or factors that are mainly responsible for the observed variations. A combination of

TABLE 9.—ISOTOPIC AGES OF PITCHBLENDE FROM THE COLORADO FRONT RANGE

(In million years)

Location	Pb^{206}/U^{238}	Pb^{207}/U^{235}	Pb^{207}/U^{206}	Total lead per cent	Reference sample no.
Wood Mine Gilpin Co.	35 ± 1	42 ± 2	430 ± 130	.39	K-71 (This paper)
Wood Mine Gilpin Co.	55 ± 1	56 ± 2	150 ± 110	1.03	Nier et al. (1941)
Wood Mine Gilpin Co.	63 ± 1	64 ± 2	114 ± 70	.78	Stieff et al. (1953)
Iron Mine Gilpin Co.	65 ± 1	70 ± 3	280 ± 100	.89	Stieff et al. (1953)
Richards Mine Gilpin Co.	56 ± 1	62 ± 6	320 ± 230	1.34	K-6 (This paper)
German Mine Gilpin Co.	51 ± 1	54 ± 2	315 ± 100	.79	K-8 (This paper)
Gilpin Co.	59 ± 1	61 ± 2	170 ± 100	.64	Nier et al. (1941)
Copper King Mine (1) Larrimer Co.	55 ± 2	56 ± 2	170 ± 100	.23	Phair and Levine (1952)
Copper King Mine (2) Larrimer Co.	71 ± 4	75 ± 5	280 ± 200	.19	Phair and Levine (1952)

(2) The geologic evidence is against multiple deposition in a single mine over a time interval of 15–20 m.y.

(3) The poor reproducibility on replicate lead analyses suggests that the lead determination is a major source of error.

The quantity of lead in samples K-71 and the Copper King was small (Table 9), and these samples gave the largest age spread.

The writers conclude that a single period of deposition occurred, the age of which is given by the average of Pb^{207}/U^{235} ages, *i.e.*, 59±5 m.y. Further work is needed in which more elaborate analytical techniques are employed. isotopic dilution analysis for U and Pb, radon-leakage measurements on each sample, and a search for old radiogenic lead should resolve the anomalies. Even with this additional information the true age probably will be inside the limits stated above.

Colorado Plateau

Table 10 gives the results of Steiff *et al.* (1953, p. 18–19) on primary uranium minerals from the Colorado Plateau, calculated with the use of Pb^{208}, as an indicator of the common lead present and the Tucson Mountain common

lead value of Nier *et al.* (1941, p. 115). The samples containing more than 0.1 per cent uranium were analyzed volumetrically and the lead content determined colorimetrically. Duplicate volumetric and colorimetric analyses were reproducible to within 2–3 per cent. Stieff *et al.* (1953, p. 1) suggest systematic errors caused by the inability of the mass spectrometer to resolve the lead peaks and thus increase the Pb^{207}/Pb^{206} ratio. This does not appear to be the major source of the high Pb^{207}/Pb^{206} ratios, since the Lamont mass spectrometer, using a different technique altogether, gave similar results on the Front Range samples. They also suggest that some lead minerals from the plateau have a composition that indicates a component of old (450 m.y.) radiogenic lead. If the most highly contaminated common lead is used for the correction instead of the Tucson Mountain sample the Pb^{207}/Pb^{206} ratios are reduced, although the Pb^{206}/U^{238} ratios are not strongly affected. However, complete agreement is still not obtained. It is possible that in this area, radon leakage plus the presence of old radiogenic lead which accompanied the pitch-blende-bearing solution must be considered. A value of 70 m.y. was the mean Pb^{206}/U^{238} age of all the pitchblendes after correction for Pb^{208}. The data of Table 10 show the variations in age of pitchblende specimens from one mine, Monument No. 2. The fluctuations are almost as large as those observed for all the samples of Stieff *et al.* (1953, p. 17). It is probable that the plateau uranium mineralization occurred about 60 m.y. ago simultaneously with that in the Front Range and that the great variety of apparent ages is due to the interaction of alteration effects and analytical difficulties. It is most difficult to separate these effects in the very young pitchblendes because of the extreme sensitivity of the Pb^{207}/Pb^{206} age. Despite the problems due to alteration there is little question that the ores were deposited much later than the sedimentary rocks in which they are found.

TABLE 10.—ISOTOPIC AGES OF PRIMARY URANIUM MINERALS FROM THE COLORADO PLATEAU*

Mine	206/238 Age in m.y.	Radiogenic 207/206 Ratio	Per cent lead	Approximate per cent radiogenic lead
Cato	62	$.050^5$	55	94
Grey Dawn	71	$.050^1$	.77	77
Monument No. 2	84	$.051^0$	.925	83
Monument No. 2	98	$.052^2$	1.17	82
Monument No. 2	60	$.053^6$	.75	74
Happy Jack	65	$.050^0$	.74	90
Shinarump	74	$.055^7$	1.43	41

* Data of Stieff et al. (1953) recalculated using Pb^{208} and the Tucson Mountain common lead (Nier, 1939)

IDAHO

Sunshine Mine, Coeur d'Alene District

Two different specimens of pitchblende from this mine have been analyzed isotopically (Table 11). These samples contain high and variable concentrations of common lead, greater than 24 per cent (Table 2). This is due to extremely fine galena mixed in the pitchblende. In this case the common-lead correction introduces a rather large error because of the uncertainty in the isotopic composition of the common lead that should be used in the correction. Kerr and Kulp (1952, p. 87) assumed an isotopic composition for the common lead that was essentially that of Great Bear Lake galena and based their calculations on the Pb^{204}. Two improvements can be made in their calculation (Table 11). First, a common lead can be chosen for the correction from the Sunshine Mine itself. Second, the absence of thorium in the samples makes it preferable to base the common-lead correction on the Pb^{208} abundance. The results emphasize the sensitivity of the ages to the common-lead correction in those cases where the concentration for

common lead is high. The lower common lead in K-101 makes the results from this sample more reliable if the Pb^{204} is used for the common-lead correction.

Radon-leakage measurements on a number of pitchblende concentrates from the Sunshine Mine give values ranging from 1 to 4 per cent. Four per cent is probably a maximum value or the true leakage, since it should be less in the compressed state under the surface. Therefore it appears that lead loss is the dominant factor in producing the anomalous ages. The period of lead loss must have occurred more recently than 700 m.y. ago. It probably occurred at Laramide time when other hydrothermal deposits were formed in the vicinity. If this is true, then the Pb^{207}/Pb^{206} age is nearly correct, and the time of deposition is 1100–1200 m.y. ago. The isotopic composition of galena samples from the Sunshine Mine (Table 4; Farquhar and Cummings, 1954, p. 12) is consistent over a vertical range of 3500 feet and suggests an age of 1030±290 m.y. in excellent agreement with the uranium-lead ages.

TABLE 11.—ISOTOPIC AGES OF PITCHBLENDE FROM SUNSHINE MINE, IDAHO

(In million years)

Errors as expressed assume that proper common-lead isotopic composition has been used.

Sample	206/238	207/235	207/206	Reference or sample*
Uraninite	712±10	785±15	885±50	Kerr and Kulp (1952)
Uraninite	700±10	830±15	1190±30	Kerr and Kulp (1952) Recalculated
Uraninite	805±10	860±20	1035±35	K-101 (This paper)

* Data obtained by using Sunshine Mine galena (Pb^{208})

SOUTH DAKOTA

Black Hills

Although the pegmatites of the Black Hills have been subjected to intensive field study by Paige (1924), Darton and Paige (1925), and Runner (1928) and since 1900 have been known to contain various minerals, it was not until 1955 that isotopic ages from this important locality were determined.

Paige (1924) showed that the pegmatite intrusions occur principally in the southeastern part of the Precambrian area which in itself is an elliptical body approximately 55 miles long and 20 miles wide. The largest mass of pegmatite complex (Harney Peak "granite") lies also in the southern area, and this body is surrounded by a zone of varying width in which the schistosity follows the contact and along which many parallel dikes have been injected.

Table 12 gives the isotopic ages of Wetherill *et al.* (1956, p. 293) and of the present study on separate specimens of uraninite. The specimen studied at Lamont was cut by fracture-filled veins of secondary uranium minerals. These were separated out as much as possible, but the separation was not complete because of the microsize of the veins. Sample K-120b contained visible alteration products, but K-120a was megascopically clean.

The excellent consistency in the uranium-lead and lead-lead ages of the K-120a unaltered specimens and the agreement of the Pb^{207}/Pb^{206} age at 1620 for all three samples suggest that a real age has been obtained. The low age given by the Pb^{206}/U^{238} ratio may reflect slight lead removal even in the case of K-120a. Tilton (1956) found that in some cases Pb^{206} is leached preferentially from radioactive minerals of high uranium/thorium ratio. It can be concluded that the Black Hills pegmatites were intruded 1620±20 m.y. ago.

If the Pb^{206}/U^{238} ages are accepted as real, the time of lead loss must have been less than 1030 m.y. ago. If additional minerals can be found which were more profoundly affected, it might be possible to fix the time of this event

TABLE 12.—ISOTOPIC AGES OF URANINITE FROM THE INGERSOLL PEGMATITE, BLACK HILLS, SOUTH DAKOTA
(In million years)

Description	206/238	207/235	207/206	208/232	Reference
Fresh	1615±5	1615±5	1622±10	1370±20	K-120a (This paper)
Slightly altered	1390±5	1460±5	1610±15	1030±20	K-120b (This paper)
Fresh	1580±30	1600±20	1630±30	1440±75	Wetherill et al. (1956)

TABLE 13.—AGES OF MINERALS FROM VARIOUS WESTERN LOCALITIES
(In million years)

Locality	Mineral	206/208	207/235	207/206	208/238	Reference
Petaca, N. M	Samarskite	240±5	310±15	875±30	180±7	K-124 (This paper)
Dixon, N. M. (Harding mine)	Microlite	916	996	1180	--	Carnegie Institution*
Bagdad, Ariz.	Zircon	630	770	1210	270	Carnegie Institution*
Quartz Creek, Colo.	Zircon	930	1130	1540	515	Carnegie Institution*
Las Vegas, N. M.	Monazite	1730	1675	1340	770	Nier et al. (1941)

* Carnegie Institution, Annual Report of the Director of the Geophysical Laboratory, 1954-1955. Work done by G. R. Tilton, G. L. Davis, T. R Aldrich, G. W. Wetherill

with greater certainty (Eckelmann and Kulp, 1956). Since the Pb^{207}/Pb^{206} ages appear constant at this locality for samples of considerably different Pb^{206}/U^{238} and Pb^{208}/U^{232} ages, it is possible that the lead loss was recent and may have been a result of weathering. The correlation of the low Pb^{206}/U^{238} age with the obvious weathering products in the specimen supports this view.

Other Western Localities

All these specimens (Table 13) show evidence of lead loss, and the Las Vegas, New Mexico, monazite shows uranium loss. The samarskite, which is from the same group of pegmatites as the microlite, appears the most profoundly affected. The most probable age at the present time is: Petaca pegmatite district ($\leq$1200 m.y.), Bagdad granite ($\leq$1200 m.y.), Quartz Creek pegmatites ($\leq$1540 m.y.), and the Las Vegas locality ($\leq$1340 m.y.).

CANADA

Manitoba

There are several groups of pegmatites about 50 miles east and northeast of Winnipeg, Manitoba. The age relations between these pegmatites and associated rock bodies have not been established, but the initial determinations suggest great antiquity.

Isotopic measurements have been reported on uraninite by Nier (1939, p. 159), Cummings *et al.* (1955, p. 64), and in this paper, and on

a monazite (Nier *et al.*, 1941, p. 113) from the Huron Claim which lies about 1 mile south of the Winnipeg River near Pointe du Bois (Table 14). The diversity of ages obtained from the various isotopic ratios shows evidence for uranium loss in the monazite and lead loss in all three samples.

TABLE 14.—ISOTOPIC AGES OF MINERALS FROM THE HURON CLAIM, MANITOBA

(In million years)

Mineral	Pb^{206}/U^{235}	Pb^{207}/U^{235}	Pb^{207}/Pb^{206}	Pb^{208}/U^{232}	Reference
Uraninite	1564	1985	2475	1273	Nier et al. (1941)
Monazite	3217	2839	2590	1827	Nier et al. (1941)
Uraninite	1650±10	2170±15	2505±20	1360±45	K-109 (This paper)
Uraninite	-	-	2580±100	-	Cummings et al. (1955)
Uraninite*	-	-	2535±100	-	Cummings et al. (1955)

* Identical to salt that Nier analyzed

Holmes (1949) suggested that the Pb^{206}/U^{238}, Pb^{207}/U^{235}, and Pb^{207}/Pb^{206} discrepancies of the monazite could be resolved if there occurred a 29 per cent loss of radon and a recent 60 per cent lead loss. In this way he obtained 1985 m.y. as the most likely age, *i.e.*, essentially the same as the Pb^{207}/U^{235} age for the uraninite. Collins, Farquhar, and Russell (1954, p. 20) accounted for the variation by assuming recent loss of 42 per cent of the radiogenic lead in the uraninite and 22 per cent loss of uranium in the monazite. They attached no significance to Pb^{208}/U^{232} age and suggested that the "best estimate" of the age of the uraninite and monazite is about 2500 m.y., *i.e.*, essentially the average of the Pb^{207}/Pb^{206} age of both minerals.

Although fine-grained pitchblendes can approach 10 per cent radon leakage under unusual circumstances, coarsely crystalline pegmatitic uraninites have generally less than 1 per cent and rarely exceed 2 per cent. A sample of uraninite from the Huron Claim gave a radon-leakage value of .50±.06 per cent. Thus radon leakage probably did not cause significant change in the isotopic ratios.

It is concluded that the Pb^{207}/Pb^{206} ages are minimal, that the monazite has undergone sufficient surface weathering to remove some of the uranium but probably not the less soluble thorium, and that lead removal occurred at some time in the past when the regional temperature was elevated. If the alteration was a regional effect it must have affected all specimens, since they came from the same small pegmatite. If it is assumed that only one period of lead loss occurred in the past, then the isotopic ages show: (1) This event occurred less than 1270 m.y. ago. (2) Pb^{208} was removed preferentially to Pb^{206} in the uraninite. (3) Pb^{208} was removed more easily in the uraninite than in the monazite. (4) More Pb^{206} and Pb^{207} were extracted from the uraninite than the monazite. (5) More uranium than Pb^{206} and Pb^{207} was removed from the monazite. The agreement in the Pb^{207}/Pb^{206} ages in these three samples does suggest recent alteration.

This locality would merit further study. Measurements on a large number of samples of radioactive minerals might make a closer definition of those events possible. Because of the scarcity of the radioactive minerals in pegmatite areas it is unlikely that secondary lead minerals will be found containing the exsolved radiogenic lead, as at Lake Athabasca.

The age of the Huron Claim pegmatite which intrudes the metasedimentary Rice Lake Series is therefore at least 2500 m.y. Extrapolating from the relative loss of lead isotopes in these three samples a provisional age is taken as 2650±100 m.y.

Northwest Territories

Great Bear Lake

Of the 11 samples from the Eldorado Mine at Great Bear Lake that have been analyzed isotopically for lead, only three were accompanied by chemical analyses (Table 15). Two of these, K-16 and K-18, give 206/210 ages that agree with the 206/238 ages and thus demonstrate present radioactive equilibrium. Also Collins *et al.* (1954, p. 6) reported seven Pb^{207}/Pb^{206} ages ranging from 1240 to 1440 m.y., and Aston (1933, p. 542) reported one at 1170 m.y. The measured radon leakage on these two samples was less than 1 per cent; hence this correction will not affect the ages appreciably.

As in the case of Lake Athabasca (Eckelmann and Kulp, 1956) it appears that effects subsequent to deposition have caused lead loss. Since the discordance in the ages is not related to depth in the mine, current weathering is not the cause of lead loss. From the available isotopic ratios, this effect does not seem to have been very extensive. The absence of thorium in these pitchblendes and the low common-lead content of most of the Great Bear Lake samples makes it desirable to use the Pb^{208} and the Great Bear Lake common lead (Table 4) as a basis for the common lead correction. This was employed in recomputing the data of Collins *et al.* (1954) and Nier (1939).

It is concluded that the initial pitchblende deposition occurred at least 1450 m.y. ago, probably closer to 1500 m.y. The major lead loss appears to have occurred less than 1000 m.y. ago. Since the pitchblende cuts an early diabase in this area, which in turn intrudes the Echo Bay group, the latter may approach the age of the Lake Athabasca Series rocks in the Goldfields region.

Other Areas in the Northwest Territories

Lead isotopic data were obtained on two samples of pegmatitic uraninite from the Stark Lake area, which is about 130 miles east of Yellowknife. The Pb^{207}/Pb^{206} ages for the Rag and Rex properties are 1700 ± 30 and 1850 ± 40 m.y. respectively (Collins, Lang, Robinson, and Farquhar, 1952, p. 30). If these are truly contemporaneous here again is evidence of lead loss such that the time of pegmatite intrusion is at least 1850 m.y. The pegmatites are overlain unconformably by the sedimentary Great Slave group (Barnes, 1951). K-7, a Contact Lake (Northwest Territories) uraninite, gives a 207/206 age of 1220 ± 50 m.y. but also shows a lead-loss pattern.

A number of samples have been analyzed from the Hottah Lake area, about 80 miles south of the Eldorado mine. Chemical ages by Bruner (1936, p. 266; 1937, p. 369) and Baxter and Averill (1937, p. 705) were 315 and 385 m.y. respectively. A Pb^{207}/Pb^{206} age by Collins *et al.* (1954, p. 6) from the Isabella Claim gave 580 ± 60 m.y. Nier (1939, p. 159) did a complete analysis on a pitchblende from Beaverlodge, Northwest Territories, near Hottah Lake. This has been recomputed using Pb^{208} for the basis of the common-lead correction, giving Pb^{206}/U^{238} = 340 m.y., Pb^{207}/U^{235} = 380 m.y., and Pb^{207}/Pb^{206} = 680 m.y. This pitchblende cuts the Snare group which has been correlated with the Echo Bay group in the Great Bear Lake region.

TABLE 15.—ISOTOPIC AGES OF PITCHBLENDE FROM ELDORADO MINE, GREAT BEAR LAKE, NORTHWEST TERRITORIES

(In million years)

Mineral	206/238	207/235	207/206	210/206	Reference
Pitchblende	1230±10	1305±15	1405±45	1230±40	K-16 (This paper)
Pitchblende	1010±5	1100±10	1240±20	1040±40	K-18 (This paper)
Pitchblende*	1220±10	1275±15	1395±20	-	Nier (1939)

* Recomputed on basis of Pb^{208}

TABLE 16.—ISOTOPIC AGES OF MINERALS, SASKATCHEWAN-ALBERTA
(In million years)

Mineral and location	206/238	207/235	207/206	210/206	Reference
Pitchblende Concentrate (Nesbitt Labine)	220±5	285±10	820±60	-	K-36
Pitchblende Concentrate (Nesbitt Labine)	325±5	365±10	615±60	315±8	K-37
Pitchblende Concentrate (ABC Adit)	335±15	395±15	730±30	355±8	K-58†
Pitchblende Concentrate (American Mine)	265±4	375±6	1110±40	-	K-38
Pitchblende Concentrate (Beaver Lodge)	325±5	390±15	750±35	340±8	K-28
Pitchblende Concentrate (Pitch Ore Group)	1005±10	1255±20	1650±20	955±25	K-30
Pitchblende * Concentrate (Beaver Lodge)	335	380	685	-	Nier(1939)
Pitchblende (Eagle Mine)	1420±10	1450±10	1530±20	1440±35	K-14
Pitchblende (Eagle Mine)	1375±10	1480±15	1610±40	1345±30	K-24
Pitchblende (Eagle Mine)	895±5	975±10	1140±30	890±25	K-26
Pitchblende (Fish Hook Bay)	1485	1650	1850±50	-	Collins et al. (1954)
Pitchblende Concentrate (Martin Lake)	765±5	935±30	1365±10	800±20	K-31
Pitchblende Concentrate (Martin Lake)	850±5	935±10	1140±35	-	K-33
Pitchblende Concentrate (Martin Lake)	1140±5	1305±10	1585±35	1060±35	K-32
Pitchblende (Martin Lake)	190	260	940±30	-	Collins et al. (1954)
Pitchblende (Bolger)	444	437	400±50	-	Collins et al. (1954)

TABLE 16.—Continued

Mineral and location	206/238	207/235	207/206	210/206	Reference
Pitchblende Concentrate No. 2 (Nicholson)	860±5	970±10	1220±15	-	K-25
Pitchblende Concentrate (Ace Mine)	1185±12	1335±10	1630±20	-	K-41†
Pitchblende Concentrate (Ace Mine)	1515±10	1675±10	1840±20	-	K-42
Pitchblende Concentrate (Ace Mine)	1315±10	1550±10	1860±20	-	K-44
Pitchblende Concentrate (Ace Mine)	1280±10	1490±10	1780±20	1280±30	K-45
Pitchblende Concentrate (Ace Mine)	1120±5	1255±15	1537±30	-	K-46†
Pitchblende Concentrate (Ace Mine)	255±5	320±6	820±35	275±8	K-48
Pitchblende Concentrate (Ace Mine)	850±15	1095±20	1600±40	860±25	K-49
Pitchblende Concentrate (Ace Mine)	1570±10	1665±10	1780±20	1560±40	K-50
Pitchblende Concentrate (Ace Mine)	715±10	815±20	1065±60	-	K-51
Pitchblende Concentrate (Ace Mine)	220±10	395±15	1585±30	-	K-53
Pitchblende Concentrate (Ace Mine)	1550±10	1630±10	1795±15	1535±45	K-54
Pitchblende Concentrate (Ace Mine)	1170±10	1400±10	1760±35	1200±30	K-55
Pitchblende Concentrate (Ace Mine)	775±5	920±15	1300±40	755±20	K-34
Pitchblende (Nicholson)	730±5	845±10	1140±25		K-19†

* Based on Pb^{208} common lead correction

† These samples first reported in this paper. Raw chemical and isotopic data for the other K samples given in Eckelmann and Kulp (1956)

Possibly these deposits are much younger than those at Great Bear Lake. However, apparent ages as low as this were obtained in the Lake Athabasca region where it appears quite clear that the true age of deposition was about 1900 m.y. Therefore possibly these Hottah Lake deposits were emplaced at the same time as those at Great Bear Lake (1500 m.y.?), but they were subjected to greater lead loss. If this is the case, the major lead loss occurred less than 330 m.y. ago.

Saskatchewan-Alberta

Lake Athabasca Region

In the last decade numerous uranium deposits have been discovered and developed in the region of Lake Athabasca, particularly centering in the Goldfields, Saskatchewan area. Here the pitchblende cuts the relatively unmetamorphosed Lake Athabasca Series (consisting mainly of arkoses and basalts) which lie unconformably on a thin plate of plastically deformed gneiss and schist of the Tazin Series. In addition to metalliferous pitchblende deposits, uranium minerals have been found in several pegmatites in the Tazin Series within 100 miles of the Goldfields region.

An intensive study of samples from this region involving complete chemical and isotopic analyses was reported in the preceding paper of this series (Eckelmann and Kulp, 1956). The isotopic ages obtained from that study and the other samples that have had complete chemical and isotopic data by the Toronto group are given in Table 16.

The interpretation derived by Eckelmann and Kulp (1956) from the isotopic ratios of the pitchblende samples and the isotopic composition of the associated galenas and clausthalites was that the initial deposition of the pitchblende took place about 1900 m.y. ago, after which at least two periods of lead loss occurred, one about 1200 m.y. ago and the other about 200 m.y. ago; the latter possibly spread over the time range 150–400 m.y. ago. The data also could be satisfied by additional periods of lead removal. The Toronto data in Table 16 fit in well with this interpretation and add data from other mines and prospects in the district. Sample 58 T from the Bolger mine appears to be a case of 100 per cent lead removal (*i.e.* complete recrystallization) around 400 m.y. ago. If the data are recalculated using the Pb^{208} as an indicator of common lead, the ages give the following spread: Pb^{206}/U^{238} = 445 m.y., Pb^{207}/U^{235} = 430 m.y., and the Pb^{207}/Pb^{206} = 360 m.y. This recalculation is permissible because of the very low abundance of thorium (.0026 per cent) relative to lead (0.38). The spread in ages could be due to the chemical analysis.

In this region there does not appear to be a strong geographical effect on the quantity of lead removed. Specimens from the Ace Mine alone show as wide a range in the quantity of lead removed as in the mines from different parts of the district. The writers suggest therefore that the process of lead removal may require regional elevation of temperature, but that the degree of alteration which occurs depends on very local factors such as porosity of the rocks, availability of water, and sulphide ion concentration of the adjacent water.

The Toronto group (Collins *et al.*, 1954) also reported Pb^{207}/Pb^{206} ages on about 30 additional specimens. These ages fall between about 1700 m.y. and 680 m.y. in much the same distribution as the samples which were analyzed both chemically and isotopically.

Table 17 gives the isotopic ages on samples from three pegmatites which should date the regional metamorphism of the Tazin Series. The geological relationship given above suggests that it should be equal to or older than the pitchblende. The low Pb^{206}/U^{238} age for the uraninite from Lac La Ronge verifies a major recrystallization subsequent to 565 m.y. ago.

Ontario

Wilberforce Area

The pegmatites of eastern Ontario have yielded a considerable number of uranium minerals. These pegmatites apparently represent the last significant metamorphism of the Grenville rocks in this area.

The isotopic ages obtained by several investigators for minerals from the Grenville Province are given in Table 18. The uraninite samples at and near Wilberforce give essentially the same age. The low Pb^{208}/U^{232} ages suggest a slight lead loss. The high value of the Pb^{206}/U^{238} and Pb^{207}/U^{235} ages for the Nier sample may be due to a 5–10 per cent error in the lead analysis or some uranium loss due to weathering. The Lamont (K-64) sample of Table 18 was hard and fresh and showed no evidence of alteration. Taking the Pb^{207}/Pb^{206} age as most reliable, the most probable age is 1050 ± 20 m.y. There is no reason to assume that these pegmatites near Wilberforce came

TABLE 17.—ISOTOPIC AGES OF SASKATCHEWAN-ALBERTA PEGMATITES
(In million years)

Mineral and location	206/238	207/235	207/206	208/232	Reference
Uraninite (Viking Lake)	1850	1880	1920	1670	Wasserburg and Hayden (1955)
Uranothorite (Viking Lake)	1525±10	1720±15	1870±20	445±25	K-113 (This paper)
Uraninite (Lac La Ronge)	565±5	868±10	1750±30	-	K-68 (This paper)

TABLE 18.—ISOTOPIC AGES OF MINERALS, GRENVILLE PROVINCE
(In million years)

Mineral and location	206/208	207/235	207/206	208/232	Reference
Uraninite (Wilberforce)	1015±5	1038±15	1060±30		K-64 (This paper)
Uraninite (Wilberforce)	1077	1062	1035	983	Nier (1939)
Uraninite (Cardiff Township)	1000	1020	1085	870	Wasserburg and Hayden (1955)
Uraninite (Blackstone Lake)	994	993	982	897	Wasserburg and Hayden (1955)
Uraninite (Conger Township)	1000	1015	1030	1010	Nier et al. (1941)
Uraninite (Parry Sound)	1002	1005	1030	945	Nier et al. (1941)
Thucolite (Parry Sound)	265	317	430	245	Nier et al. (1941)
Uraninite (Besner)	770	800	860	845	Nier (1939)
Thucolite (Besner)	262 •	275	440	250	Nier et al. (1941)
Uraninite (Besner)	770	785	825	845	Cummings et al. (1955)
Zircon (Natural Bridge, N. Y.)	1025	1065	1140	-	Carnegie Institution

in at significantly different times. Collins *et al.* (1954, p. 10) reported Pb^{207}/Pb^{206} ages on four samples of uraninite from Wilberforce ranging from 1032 to 1100 m.y., but the errors on the higher values were much larger than the lower two at 1032 and 1040 m.y. The uranium-lead and lead-lead ages are not in good agreement for the thucolite (Nier, *et al.* 1941, p. 113) and the uraninite from Besner (Nier, 1939, p. 159). The thucolite apparently is more sensitive to alteration. Ellsworth (1931, p. 577) originally analyzed the Besner uraninite sample and described it as intimately associated with thucolite which appears to have partly replaced the uraninite in some instances. He was unable to separate the very small veins of thucolite from the uraninite and therefore it might be expected that the ages of the uraninite in this case would be lowered by the presence of the thucolite. The Parry Sound uraninite was fresh and apparently free of thucolite and gave an age identical with Wilberforce. Collins *et al.* (1954, p. 10) reported two Pb^{207}/Pb^{206} ages on euxenite and fergusonite from Calabogie and Madawaska at 1010 ± 70 and 960 ± 50 respectively.

The zircon from Natural Bridge, New York, appears to be somewhat older and may not be related to the Wilberforce-Parry Sound pegmatite development. The pitchblende in the Sault St. Marie area of western Ontario (Collins *et al.*, 1954, p. 9) also appears to predate the Wilberforce event giving Pb^{207}/Pb^{206} ratios suggesting an age of at least 1200 m.y.

Conclusions

The new isotopic age measurements on specimens from a variety of North American localities have produced new information about the principles and application of the uranium-lead method of age determination. It is concluded that when properly interpreted, isotopic studies on uranium minerals will define both the initial time of deposition and a portion of the subsequent history of the mineral. Some uranium minerals yield essentially concordant ages from the various isotopic ratios, but many do not. Among those that do not and are not obviously weathered, lead-loss appears to be the dominant cause yielding the pattern $206/238 < 207/235 < 207/206$. Radon leakage may be important in producing the discrepancies in the case of very young minerals. Except for very young minerals the Pb^{207}/Pb^{206} age is the most reliable. However, in order to evaluate quantitatively the absolute age of a given locality, it is necessary to analyze a number of samples, since the Pb^{207}/Pb^{206} age of any given sample is minimum.

The new data from this and other laboratories interpreted in terms of current knowledge of the uranium method have helped to refine the age of a number of important localities in North America. In certain cases this analysis has required a major change in the accepted age for a locality, but in other cases it remains essentially the same. The most important development is the extension of the Precambrian time scale. Examples of this change are:

(1) The Belt Series of Montana and Alberta were thought to be very late Precambrian (possibly 600 m.y.). The data from the Sunshine Mine pitchblende and galena which cuts the Belt Series rocks show that they are at least 1190 m.y. in age.

(2) The unmetamorphosed Lake Athabasca Series, previously considered late Precambrian, is cut by 1900 m.y. old pitchblende. This series lies unconformably on plastically deformed Tazin Series.

(3) The pegmatites of southeast Manitoba which represent the last major metamorphic event in the area were previously thought to be about 1.9 b.y. old, but the new work suggests 2.6 b.y. as a more likely date.

The ages of cyrtolite from the Bedford, New York, pegmatites (350 m.y.) which intrude the Manhattan schist, the uraninite from the pegmatites at Branchville, Connecticut (350 m.y.), and the uraninite and samarskite from the Spruce Pine, North Carolina, pegmatites (360 m.y.), suggest that these may represent a single event throughout the Appalachian Province. The Portland, Connecticut, pegmatite values indicate renewed activity at this locality more recently (265 m.y. ago).

Advances in understanding of the uranium-lead method contribute to the broad problems in geology as well as the geochronometry of local areas. The data already obtained suggest areas where further isotopic studies will add to present knowledge of the geologic periods and eras and the processes which have resulted in the present structural features of the continents.

References Cited

Aldrich, L. T., Wetherill, G. W., Tilton, G. R., and Davis, G. L., 1956, Half-life of Rb^{87}: Phys. Rev., v. 103, p. 1045–1047

Aston, F. W., 1933, The isotopic constitution and

atomic weights of lead from different sources: Royal Soc. Proc., v. 140, p. 535–543

Barnes, F. Q., 1951, Snowdrift map-area, Northwest Territories: Canada Geol. Survey Paper, 51–6, p. 1–30

Bate, G. L. and Kulp, J. L., 1955, Variations in the isotopic composition of common lead and the history of the crust of the earth: Lamont Geol. Observatory Tech. Rept., Contract AT(30–1)-1114, p. 1–124

Bate, G. L., Miller, D. S., and Kulp, J. L., 1957, Isotopic analysis of tetramethyllead: Anal. Chem., v. 29, p. 84–88

Baxter, G. P., and Averill, M. E., 1937, The lead-uranium ratio of Beaver Lodge pitchblende: Am. Chem. Soc. Jour., v. 59, p. 705

Bliss, A. D., 1944, Radioactive substances III. The analysis and age of a North Carolina monazite: Am. Jour. Sci., v. 242, p. 327–330

Boltwood, B. B., 1907, On the ultimate disintegration products of the radio-active elements, I: Am. Jour. Sci., ser. 4, v. 23, p. 77–88

Bruner, F. H., 1936, Uraninite from the Hottah Lake: Am. Mineralogist, v. 21, p. 265–266

—— 1937, Contributions to the determinations of the exact age of a Canadian uraninite: Jour. Phys. Chem., v. 41, p. 365–373

Collins, C. B., Farquhar, R. M., and Russell, R. D., 1954, Isotopic constitution of radiogenic leads and the measurement of geologic time: Geol. Soc. America Bull., v. 65, p. 1–21

Collins, C. B., Lang, A. H., Robinson, S. C., and Farquhar, R. M., 1952, Age determinations for some uranium deposits in the Canadian Shield: Geol. Assoc. Canada Proc., v. 63, p. 15–41

Cummings, G. L., Wilson, J. T., Farquhar, R. M., and Russell, R. D., 1955, Some dates and subdivisions of the Canadian Shield: Geol. Assoc. Canada Proc., v. 7, pt. II, p. 27–79

Darton, N. H., and Paige, S., 1925, Central Black Hills folio, S. D.: U. S. Geol. Survey, Geol. Atlas, Folio 219

Eckelmann, W. R., and Kulp, J. L., 1956, The uranium-lead method of age determination. Part I: The Lake Athabasca problem: Geol. Soc. America Bull., v. 67, p. 33–54

Ellsworth, H. V., 1931, Uraninite from Henvey Township, Parry Sound district, Ontario: Am. Mineralogist, v. 16, p. 576–579

Farquhar, R. M., and Cummings, G. L., 1954, Isotopic analyses of anomalous lead ores: Royal Soc. Canada Trans., v. 48, ser. 3, sec. 4, p. 9–16

Fenner, C. N., 1932, The age of a monazite crystal from Portland, Connecticut: Am. Jour. Sci., ser. 5, v. 23, p. 327–333

Foullon, H. von, 1883, Über Verwitterungsproducte des Uranpecherzes: Verh. k. k. geol. Reichsanst, no. 6, p. 95–96

Føyn, E., 1938, Über einige Verhältnisse in Uranmineralien: Skrift Norsk. Videnskaps, Akad. Oslo: I Mat-Naturo. KI, no. 4, p. 1–61

Giletti, B. J., and Kulp, J. L., 1955, Radon leakage from radioactive minerals: Am. Mineralogist, v. 40, p. 481–496

Hecht, F., and Kroupa, E., 1936, Die Bedeuting der Quantitativen Mikroonalyse Radioaktiver Mineralien für Geologische Zeitmessung: Zeit. Anal. Chem., v. 106, p. 82–103

Hillebrand, W. F., 1891, On the occurrence of nitrogen in uraninite and on the composition of uraninite in general: Am. Jour. Sci., ser. 3, v. 40, p. 384–394

Holmes, A., 1949, Lead isotopes and the age of the earth: Nature, v. 163, p. 453–456

Kerr, P. F., and Kulp, J. L., 1952, Precambrian uraninite, Sunshine Mine, Idaho: Science, v. 115, no. 2978, p. 86–88

Kulp, J. L., Bate, G. L., and Broecker, W. S., 1954, Present status of the lead method of age determination: Am. Jour. Sci., v. 252, p. 345–364

Kulp, J. L., Bate, G. L., and Giletti, B. J., 1955, New age determinations by the lead method: Geol. Assoc. Canada Proc., v. 7, pt. II, p. 15–24

Kulp, J. L., and Brobst, D. A., 1956, Geology of the Bakersville-Plumtree area Spruce Pine district, North Carolina: U. S. Geol. Survey Mineral Inv. Field Studies Map MF 97

Kulp, J. L., Broecker, W. S., and Eckelmann, W. R., 1953, Age determination of uranium minerals by the PB^{210} method: Nucleonics, v. 11, p. 19–21

Kulp, J. L., and Eckelmann, W. R., 1957, Discordant U-Pb ages and mineral type: Am. Mineralogist, v. 42, p. 154–164

Lane, A. C., 1937, Report of the Committee on the Measurement of Geologic Time, 1936–37: Nat. Research Council Ann. Rept., 77 p.

—— 1942, Report of the Committee on the Measurement of Geologic Time, 1941–42: Nat. Research Council Ann. Rept., 68 p.

Larsen, E. S., Keevil, N. B., and Harrison, N. C., 1952, Method for determining the age of igneous rocks using accessory minerals: Geol. Soc. America Bull., v. 63, p. 1045–1052

Marble, J. P., 1936, Possible age of monazite from Mars Hill, N. C.: Am. Mineralogist, v. 21, p. 456–457

Muench, O. B., 1931, The analysis of cyrtolite for lead and uranium: Am. Jour. Sci., ser. 5, v. 21, p. 350–357

—— 1936, The lead uranium ratio of Henvey cyrtolite: Am. Chem. Soc. Jour., v. 58, p. 2433–2434

Nier, A. O., 1939, The isotopic composition of radiogenic leads and the measurement of geological time, II: Phys. Rev., v. 55, p. 153–163

Nier, A. O., Thompson, R. W., and Murphy, B. F., 1941, The isotopic constitution of lead and the measurement of geological time III: Phys. Rev., v. 60, p. 112–116

Paige, S., 1924, Geology of the region around Lead, South Dakota, and its bearing on the Homestake ore body: U. S. Geol. Survey Bull. 765, 58, p.

Phair, G., and Levine, H., 1952, Notes on the differential leaching of uranium, radium and lead from pitchblende in H_2SO_4 solutions: Econ. Geology, v. 48, p. 358–369

Runner, J. J., 1928, Intrusion mechanics of the Harney Peak batholithic granite (Abstract): Geol. Soc. America Bull., v. 39, p. 186

Stieff, L. R., Stern, T. W., and Milkey, R. G., 1953, A preliminary determination of the age of some uranium ores of the Colorado plateaus by the lead-uranium method: U. S. Geol. Survey Circ. 271, p. 1–19

Stugard, F., 1953, Geological map of part of Glastonbury and Middle Haddan quadrangles,

Conn.: U. S. Geol. Survey Trace Elements Inv. Rept. 233

Tilton, G. R., 1956, The interpretation of lead-age discrepancies by acid-washing experiments: Am. Geophys. Union Trans., v. 37, p. 224–230

Wasserburg, G. L., and Hayden, R. J., 1955, A^{40}/K^{40} dating: Geochim. et Cosmochim. Acta, v. 7, p. 51–60

Wetherill, G. W., Tilton, G. R., Davis, G. L., Aldrich, L. T., 1956, New determinations of the age of the Bob Ingersoll pegmatite, Keystone, S. D.: Geochim. et Cosmochim. Acta, v. 9, p. 292–297

Carter Research Laboratories, Tulsa. Oklahoma; Lamont Geological Observatory, Columbia University, Palisades, New York

Manuscript Received by the Secretary of the Society, May 21, 1956

Lamont Geological Observatory Contribution No. 257

BULLETIN OF THE GEOLOGICAL SOCIETY OF AMERICA
VOL. 68, PP. 0000-0000, 20 FIGS., 4 PLS. SEPTEMBER 1957

HYDROLOGY OF LAKE BONNEVILLE AND SEDIMENTS AND SOILS OF ITS BASIN

By A. J. EARDLEY, VASYL GVOSDETSKY, AND R. E. MARSELL

ABSTRACT

The total salt in the Bonneville basin in the form of salt crusts, salt water in clays, and salt in the Great Salt Lake brine is about 6 billion tons. The annual rate of addition of new salt by the inflowing rivers is about 1 million tons. Thus the time of accumulation since the last overflow should be 6000 years approximately, but C^{14} analyses indicate a time in excess of 30,000 years. The writers believe that the wind is responsible for the removal of the salt from the basin floor.

Should Great Salt Lake rise 20–30 feet it would spill at Lakeside into the Great Salt Lake Desert; the lake's surface would suddenly increase two times and produce a stabilized lake level. A major beach about 45 feet above Great Salt Lake is vividly impressed on the topography; it is believed to be related to the Great Salt Lake Desert expansion.

Cores from Great Salt Lake indicate that the last fresh-water lake existed from about 23,000 years to 13,500 years ago. This correlates with C^{14} analyses of tufa at the Stansbury level.

Soils of several ages and varieties are recognized and in their relations to the various lake deposits and associated river terraces support the other evidence from which the following chronology of lake stages is postulated:

Alpine stage (5050 feet ±)—first high-level lake, possibly Kansan
Low lake stage—possibly Sangamon-Illionian-Yarmouth
Bonneville-Provo 1 stage (5135 feet ±)—Tazewell-Iowan, overflow stage
Low-lake stage—Brady
Provo 2 stage (4820 feet ±)—Cary
Low lake stage—Two Creeks
Stansbury stage (4470 feet ±)—about 23,000 to 13,500 years ago. Mankato
Gilbert stage (4245 feet ±)—about 10,000 to 8000 years ago. May be a minor pluvial maximum or a stability level in the recession of the lake.
Altithermal—about 6000 years ago

CONTENTS

TEXT

	Page
Introduction	1142
Principal contributions	1142
Authorship and acknowledgments	1143
Hydrology	1143
Surface areas	1143
Volumes	1143
Salt content	1143
Salinity at different levels	1146
Annual saline accession and age considerations	1147
Analysis of salinity data	1149
Precipitation changes and lake-level fluctuations	1152
Precipitation—evaporation economy	1152
Lake-level adjustment to precipitation	1152
Temperature changes related to precipitation	1153
Expansions of Lake Bonneville	1155
Significance of thresholds and expansions	1155
Great Salt Lake Desert expansion	1155
Expansions near the Stansbury level	1161
Elevations of Stansbury water planes	1163
Meaning of multiple shore lines	1164
Sedimentary record	1165
Preliminary considerations	1165
Alpine and Bonneville deposits	1165
Provo deposits	1166
Stansbury deposits	1168
Gilbert deposits	1169
Great Salt Lake sediments	1169
Soils of Bonneville Basin	1171
Significance and scope of investigation	1171
Definitions	1171
Types of soils recognized	1172
Post-Alpine Pre-Stansbury soils	1172
Characteristics and general relations	1172
Soils of the Bacchus area	1173

Soils of Emigration Creek Valley 1179
Soil at mouth of Parleys Canyon 1179
Soils of the lower Sevier River Valley 1179
Old soils in the Alpine area 1185
Soil of Terminal Reservoir 1186
Post-Stansbury soils 1186
Occurrence and nature 1186
Lower Jordan River flood plain 1187
Soils of Big Cottonwood Creek flood plain 1190
Soils of Emigration Creek Valley 1191
Pre-Alpine soils 1191
Occurrence 1191
Spring Canyon exposure 1192
Foothill Boulevard occurrence 1193
Bacchus exposure 1193
Significance and interpretation 1193
Mountain soils 1194
Soils of mountainous areas 1194
Soils of Deer Creek Canyon 1194
Soils of Silver Lake cirque basin 1195
Correlation of soils 1196
Chronology of Lake Bonneville stages 1196
Succession of stages 1196
Ages of younger pluvial maxima 1197
Age of Alpine Formation 1197
Proposed correlations 1200
References cited 1200

ILLUSTRATIONS

Figure — Page

1. Extent of Lake Bonneville at intervals up to 4500 feet above sea level 1144
2. Volume, area, and salinity of Lake Bonneville up to 4500 feet 1145
3. Relation of salt accession, volume fluctuation, and removal of salt by wind in Bonneville Basin 1150
4. Salt economy of the Great Salt Lake drainage region and the Great Salt Lake Desert 1151
5. Relation of precipitation to lake-level fluctuation, Great Salt Lake 1153
6. Relation of temperature to rainfall in Great Salt Lake drainage basin 1154
7. Map of lower Jordan River Valley 1158
8. Transverse profiles of lower Jordan River Valley 1160
9. Threshold elevations and area of expansions of Lake Bonneville 1162
10. Elevations of shore lines along east and south margins of Great Salt Lake 1163
11. Bonneville and Provo beach features 1166
12. Stansbury beach deposits 1168
13. Great Salt Lake sedimentary record and deposits of Danger Cave 1170
14. Soils at Bacchus pit and east Salt Lake City 1173
15. Terraces and soils of the lower Sevier River Valley 1180
16. Meanders of the Sevier River near Delta-Melville reservoir 1181
17. Soils, terraces, and deposits of lower Jordan River Valley 1189
18. Soils of Parleys and Emigration creeks and the Bacchus area 1192
19. Relation of moraines 3 and 2 to Alpine silts 1197
20. Graphs showing proposed chronology of Lake Bonneville 1198

Plate — Following page

1. Gilbert beaches at north end of Stansbury Range
2. Gilbert beaches on Antelope Island and Crater Island 1160
3. Vertical aerial photograph of Lake Bonneville beaches on east piedmont of Pilot Range
4. Red-brown soil in east Salt Lake City

TABLES

Table — Page

1. Area, volume, and salinity of Lake Bonneville at various levels 1145
2. Skeletal composition of the Bacchus pit soils 1175
3. Mechanical composition of the Bacchus pit soils 1175
4. Specific gravity of skelton and coarse soil in the Bacchus Pit 1176
5. Chemical analyses of the Bacchus pit soils 1177
6. Mechanical composition of the Sevier Valley soils 1182
7. Specific gravity of skeleton and coarse soil in living soil at Leamington Bridge 1183
8. Hygroscopic moisture and carbonates of Sevier Valley soils 1184
9. Mechanical composition of lower Jordan Valley flood-plain soils 1187
10. Carbonates in lower Jordan Valley flood-plain soils 1188
11. Mechanical composition of flood-plain soils at head of Big Cottonwood Creek 1191
12. Skeletal composition of red-brown fossil soil in Spring Canyon 1193
13. Skeletal composition of Deer Creek fossil soil 1195
14. Mechanical composition of Deer Creek fossil soil 1195
15. Specific gravity of skeleton and coarse soils in Deer Creek 1195
16. Correlation chart of pluvial and glacial stages 1199

INTRODUCTION

Principal Contributions

The history of Lake Bonneville proposed by Gilbert (1890) was not challenged for 50 years, but now much new information incident to extensive quarrying of the beach sands and gravels, drilling of many water wells, use of micropaleontology in dating sediments, and recognition and interpretation of fossil soils, has made it clear that the lake history is more complicated than Gilbert proposed. The chief con-

tribution here is new information on the hydrology and soils of the Bonneville basin and the cored sediments of Great Salt Lake.

Authorship and Acknowledgments

Gvosdetsky is responsible for the work on the soils. He had been assisted in the preparation of two separate reports on the subject by H. Bowman Hawkes of the Department of Geography, University of Utah (Gvosdetsky and Hawkes, 1953; 1956).

Marsell collected numerous data on the glacial and lake deposits, particularly of the Wasatch Piedmont over the past 30 years. He mapped the deposits along the course of the Salt Lake City Aqueduct and mapped in detail the deposits at the mouths of Big Cottonwood and Little Cottonwood canyons. He is responsible chiefly for those parts of the article that deal with the higher lake deposits and glacial moraines.

The sections on hydrology, precipitation, and lake-level fluctuations, expansions of Lake Bonneville, and the sedimentary record in Great Salt Lake were prepared by Eardley. He organized and wrote the manuscript and attempted to adapt the independent studies of Gvosdetsky and Marsell to his; undoubtedly the interpretations are colored by his own thinking.

D. J. Jones checked several samples for microfossils and helped on the interpretation of the lake deposits. Meyer Rubin of the U. S. Geological Survey and Wallace Broecker of Columbia University kindly made the C^{14} analyses, and Jesse B. Jennings, University of Utah, advised on archeological aspects. The sedimentary record of Great Salt Lake is by Joseph Schreiber, Jr. (Ph.D. thesis, Univ. Utah, in preparation). The authors profited much from association with Jack Feth of the U. S. Geological Survey who worked in the Ogden area on assignment to the Bureau of Reclamation for 2 years.

Gvosdetsky did part of his work by aid of a grant from The Geological Society of America, and he and Eardley had separate grants from the Research Fund of the University of Utah for various aspects of the project.

Hydrology

Surface Areas

Figure 1 charts the extent of Lake Bonneville in intervals up to 4500 feet above sea level. The mean lake level in historical times is about 4200 feet. The lake has fluctuated through 19 feet, with a high in 1873 of 4211 feet and a low of 4192 in 1934.

A 5-mile-square grid was superposed on the map, and the areas at different levels were computed by counting the squares and fractions of squares.

Figure 1 shows an isobath at 4245 in the Great Salt Lake area but at 4230 in the Great Salt Lake Desert area. This is a result of an analysis of the expansion of the lake over the desert and will be dealt with below. All available topographic maps, railroad grade elevations, and photo-index sheets were used in making the compilation.

Volumes

Lake volume was computed on the assumption that the shape approximates an average of a cone and a wedge. The area times the depth divided by 3 is the formula for a cone; the area times the depth divided by 2 is the formula for a wedge. The volume of Great Salt Lake, if computed by this method, would be the area times the greatest depth divided by $2\frac{1}{2}$. In computing volume from one level to the next, for instance from 4300 to 4400 feet, the formula would be: (volume up to 4300) + (area at 4300 × 100 feet) + (difference in area at levels 4300 and 4400 × 100 divided by $2\frac{1}{2}$).

A unit equal to 1 square mile in area and 100 feet thick is convenient to use with the data at hand. One unit of volume would be 640 × 100 or 64,000 acre feet of water.

In the above method, the more vertical divisions or isobaths (contours) used, the more accurate will be the volume computations. Table 1 shows the results, and Figure 2 shows volume change related to area change.

Salt Content

If Great Salt Lake rose 100 feet to the 4300-foot level, the salt of the Great Salt Lake brine would be contained in the water, and the salt of the Bonneville Flats salt crust and the Pilot Valley salt crust would also be dissolved. A great amount of salt is held in the clays of the Great Salt Lake Desert and in the clays under and bordering Great Salt Lake; in time much of this would be held in the greater lake's waters. Appreciable salt is held in the silts and clays of Lake Bonneville at elevations considerably above the desert-floor clays. In attempting to compute the lake's salinity at any

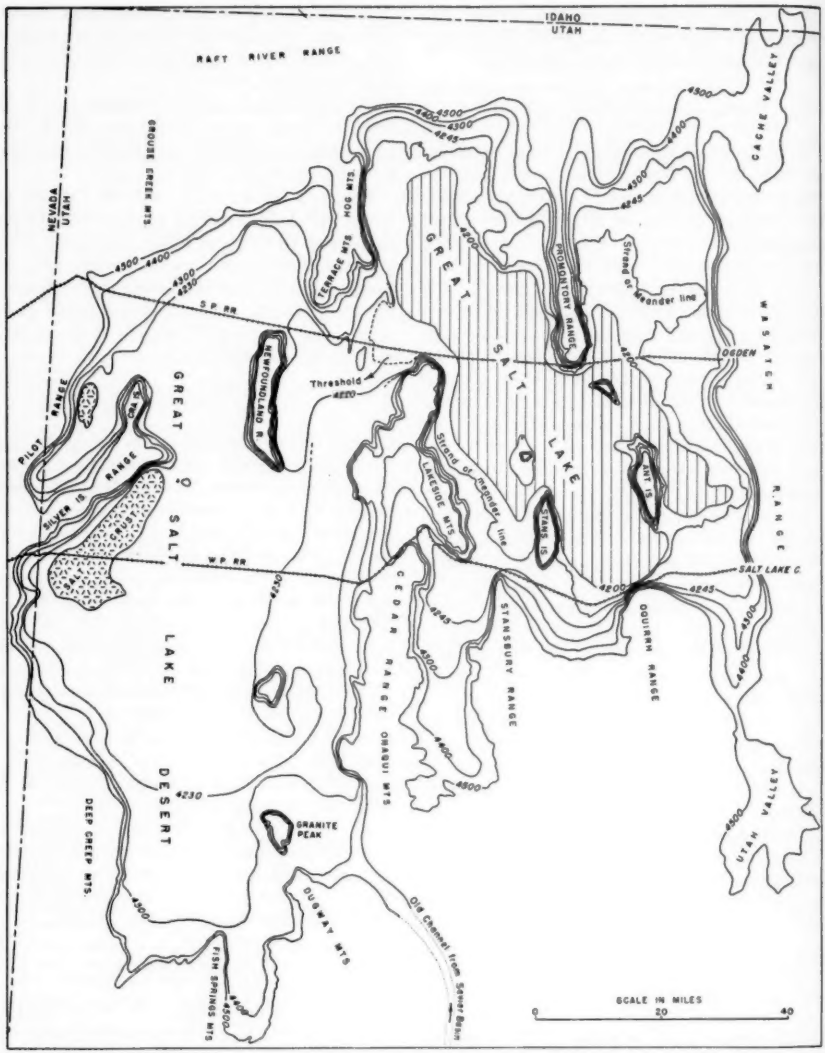

FIGURE 1.—EXTENT OF LAKE BONNEVILLE AT INTERVALS UP TO 4500 FEET ABOVE SEA LEVEL

level all these sources of salt must be considered. However, the total salt now in the basin is not an accurate measure of the salt present in the lake's waters in the past, for two reasons: (1) the streams draining into the basin are adding annually a sizable and measurable increment, and (2) the wind is removing annually a sizable but apparently not directly measurable amount. These factors will be considered below. For the immediate purpose of approximating salinities of the lake at higher levels the effect of the wind in removing salt from the basin and the gradual accumulation of the salt by stream inflow are neglected; past salinities are determined on the basis that the salt now present was in solution at different levels and volumes in the past.

Salt in Great Salt Lake may be approximated

TABLE 1.—AREA, VOLUME, AND SALINITY OF LAKE BONNEVILLE AT VARIOUS LEVELS

Elevation Above Salt Lake (feet)	Surface Area (square miles)	Volume in Units (1 square mile X 100 feet)	Salinity† (per cent)
5135 ± (Bonneville)	19,750*	112,800	
4820 ± (Provo)	15,000*	59,600	Outlet Stage
4500	9700	21,850	0.2
4400	8750	12,000	0.4
4300	7300	4280	1.2
4245	5000	1750	2.6
4230	4500	1100	4.8
4220	2500	600	7.7
4200	1650	203	23.0

* Gilbert's figures

† If lake should rise with present salt inventory

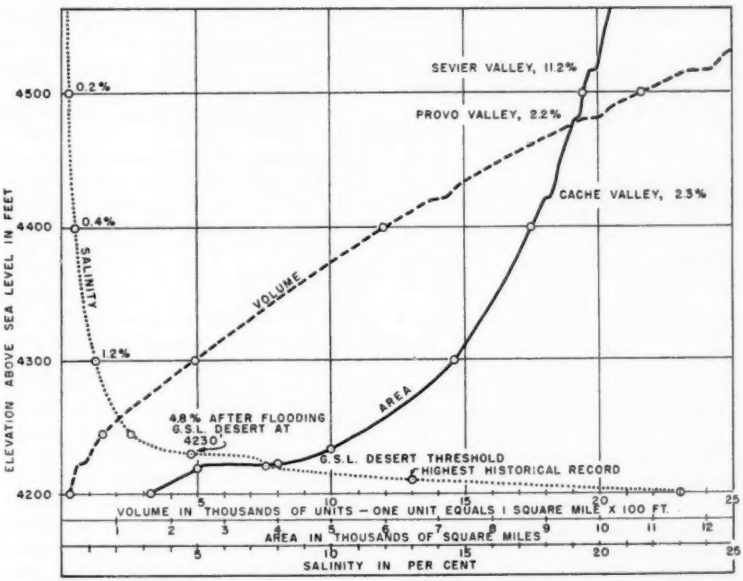

FIGURE 2.—VOLUME, AREA, AND SALINITY OF LAKE BONNEVILLE UP TO 4500 FEET
Percentage figures after Sevier, Provo, and Cache valleys indicate amount of expansion

as follows: 203 (units) × 64,000 (acre feet per unit) × 43,560 (cu. feet/acre foot) × 62.5 (lbs./cu. foot) × 1.17 (specific gravity at 23 per cent salinity) × $\frac{.23 \text{ (per cent salinity)}}{2000 \text{ (lbs./ton)}}$ = 4,760,000,000 tons (approximate) NaCl and Na_2SO_4.

Salt in the Bonneville salt crust (also known as the Salduro Marsh) may be calculated as follows:

Area of salt crust—150 square miles

Maximum thickness—3.5 feet; assumed to wedge out at margin

Brine in crust up to ¼ of total volume; specific gravity of crust 1.87

96.2 per cent of crust soluble

Therefore:

150 (square miles) × 3.5 (feet thick) × 640 (acres per square mile)

$$\times \frac{43{,}560 \times 62.5 \text{ (lbs./sq. foot)} \times 1.87 \text{ (specific gravity)} \times .962 \text{ (soluble)}}{2\tfrac{1}{2} \times 2000}$$

= 329,000,000 tons (approximate), mostly NaCl with some Na_2SO_4, KCl, and MgCl

Salt in the Pilot Valley salt crust may be computed as follows:

$$\frac{21 \times 1.75 \times 640 \times 43{,}560 \times 62.5 \times 1.87 \times .962}{2\tfrac{1}{2} \times 2000}$$

= 23,000,000 tons approximately

Salt in the clays under and around Great Salt Lake may be approximated as follows:

(1) Consider that the salt clays extend to "meander line" of Clarence King's map which had area of 2100 square miles (Gilbert, 1890).

(2) Consider that salt in clays in center of lake extends to depth of 18 feet and to 5 feet at edge.

(3) Consider salinity of water in clays 100 grams per liter, and about 30 per cent water and 70 per cent clay by weight. Then salts are about 3 per cent of weight of wet clay.

Therefore:

$$\frac{2100 \times 640 \times 43{,}560 \times (18\text{–}5) \times 62.5 \times .03}{2\tfrac{1}{2} \times 2000}$$

= 285,000,000 tons approximately

Plus

$$\frac{2100 \times 640 \times 43{,}560 \times 5 \times 62.5 \times .03}{2000}$$

= 274,000,000 tons approximately

Total 285,000,000 + 274,000,000 = 559,000,000 tons in clays under Great Salt Lake. This figure is approximate and may be excessive because of the depth of saturation assumed.

Salt in the clays of the Great Salt Lake Desert are calculated on the basis of 405 shallow borings and analyses by Nolan (1927, p. 25–44). Data are as follows:

(1) A layer of clay at least 5 feet thick contains brine.

(2) Within a central area of 1400 square miles the clays are made up of 27 per cent water, 3 per cent salt, and 70 per cent clay by weight.

(3) In an outer area of 800 square miles the clays contain about 1.8 per cent salt, also wet with brine to a depth of at least 5 feet.

Therefore:

$$\frac{1400 \times 640 \times 43{,}560 \times 5 \times 62.5 \times .03}{2000}$$

= 183,000,000 tons (approximate)

Plus

$$\frac{800 \times 640 \times 43{,}560 \times 5 \times 62.5 \times .018}{2000}$$

= 63,000,000 tons (approximate)

Total 183,000,000 + 63,000,000 = 246,000,000 tons in clays

Total salt in Great Salt Lake Desert:

329,000,000 tons Bonneville salt crust
23,000,000 tons Pilot Valley salt crust
246,000,000 tons in desert clays
598,000,000 tons total

Total salt in Great Salt Lake and in underclays:

4,760,000,000 tons in Great Salt Lake brine
559,000,000 tons in Great Salt Lake underclays
5,319,000,000 tons total

Total salt present today in the lower part of the Bonneville basin:

5,900,000,000 tons (approximate).

The figures on the amount of salt in the clays are approximate and are subject to correction of 25 per cent more or less. The figures for the salt in the lake and the salt crusts may be subject to smaller error but are still only approximations.

Hunt *et al.* (1953, p. 31–35) recognized the presence of considerable soluble salts in the silts and clays of the lake at former high levels. The near-shore sediments of the Alpine and Provo formations, at elevations 4500–5100 feet in Utah Valley, contain water-soluble salts up to 0.75 per cent, of which, on an average, about one-third may exist as NaCl. The rest is some combination of calcium, magnesium, and potassium with carbonate and sulfate. The sediments carrying the salts are 100 feet thick in places. If the lake should rise to the Provo level (4820 feet) some of this salt would go into solution and must be considered part of the present total salt inventory of the Lake Bonneville basin. The writers conclude below that most of the salt is secondary and has accumulated by wind transportation after the lake subsided. Accordingly, it would not be considered part of the lake's inventory at the last Provo stand.

Salinity at Different Levels

Since the volumes at different levels and the total salt content are known, the salinity at different levels can be computed. The salinity of the Great Salt Lake at different levels

through which it has fluctuated in historical times was measured. At 4200 feet the salinity is 23 per cent; at 4211 it is 13 per cent. The lake will overflow into the Great Salt Lake Desert at about 4221 feet and by 4245 feet will have covered all the area of highly saline clays, so that the Bonneville salt crust and the salt in the clays will be in solution. If the lake should rise quickly and take all the salt of salt pans and underclays into solution, the salinity at 4245 feet will be 2.6 per cent, at 4300 feet 1.2 per cent, at 4400 feet 0.4 per cent, and at 4500 feet 0.2 per cent (Table 1; Fig. 2).

Annual Saline Accession and Age Considerations

GREAT SALT LAKE: Any attempt to compute the amount of sodium salts discharged into the lake each year will result in uncertain conclusions because of insufficient discharge and salinity data on the streams draining into the lake. In Bear River a salinity measurement at the Utah-Wyoming State line showed 124.3 ppm, at Lewiston 211.3 ppm, and at Corinne 797.4 ppm (Thorne and Thorne, 1951; Grover, 1935). A rapid increase in salinity is thereby indicated, which seems normal, but a good part of this is picked up by the river while it flows over the lower bottom lands of old Lake Bonneville and may not be a new contribution to the salt content of the lake. As in Utah lake and Jordan River the salt content has increased several times since the introduction of agriculture, and thus much of the salt being flushed from the lower lake beds is part of the existing inventory. If the intermediate station is representative of the addition of new salt to the lake, and if this figure represents the average salinity of the stream through its seasonal fluctuations, which is not known, then the following computation indicates the amount of salt carried into the lake each year by the Bear River.

Discharge per year, 211.3 ppm × 1.56 million acre feet, is 330 acre feet (density of 1) of salt. The volume of salt would be half of this amount.

For the other major streams flowing into the lake the salt added is as follows:

Jordan River at Lehi:
784 ppm × 0.30 million acre feet = 235 acre feet salt

Ogden River at Ogden:
195 ppm × 0.15 million acre feet = 29 acre feet salt

Weber River at Devil's Slide:
159 ppm × 0.38 million acre feet = 60 acre feet salt

Total 654 acre feet salt

Acre feet may be changed to tons as follows:

$$\frac{654 \times 43{,}560 \times 12.5}{2000} = 887{,}358 \text{ tons salt per year}$$

Salt in the above computations means all the Na, K, Cl, and SO_4 in solution.

The inflow of the four rivers listed above accounts for slightly less than two-thirds of the total water added to the lake each year (Peck, 1951, M.A. thesis, Univ. Utah, p. 42). Inflow unaccounted for includes many shore-line springs and seeps which are impressive on aerial photos. The largest spring known to the writers is Timpie Springs at the northwest end of the Stansbury Range. Its flow was measured on June 25, 1956, through two 36-inch concrete flumes under the highway and found to be about 2.3 cubic feet per second. A sample of the water had a salinity of 0.88 per cent or 8800 ppm and tasted very salty. The spring, therefore, contributes the following salts to the lake each year:

$$\frac{2.3 \times 60 \times 60 \times 24 \times 365 \times .0088 \times 62.5}{2000}$$

$$= 20{,}000 \pm \text{tons}$$

Timpie Springs contributes about 2000 acre feet of water to the lake each year, but this is only $\frac{1}{300}$ of the total spring or "ground-water" inflow as computed by Peck (1951, M.A. thesis, Univ. Utah). If the rest of the inflow unaccounted for carries 300 ppm of salt, then the total annual salt contribution will be:

$$\frac{300 \text{ ppm.} \times 0.6 \text{ million acre feet} \times 43{,}560 \times 62.5}{2000}$$

$$= 240{,}000 \pm \text{tons}$$

Although there are many uncertainties in the above estimates of salt added to the lake each year during the past 50 years, the grand total of all additions is about 1,100,000 tons per year.

If the total salt in Great Salt Lake and the Great Salt Lake Desert, including the salt-saturated clays, and the rate of accession are known, then the accumulation time may be computed as follows:

$$\frac{5{,}819{,}600{,}000 \text{ tons}}{1{,}100{,}000 \text{ tons}} = 5300 \pm \text{years}$$

Carbon-14 dates at Danger Cave indicate that the lake fell below the 4300-foot level more than 11,000 years ago, and the lake history (Fig. 20) suggests that the water surface may have fallen for the last time below the Provo outlet approximately 30,000 years ago. Thus the figure 5300 years seems too small. Even admitting appreciable error in the basic data from which the figure was computed another factor is needed to explain the difference. This factor seems to be the ability of the wind to drift and carry finely divided salt from the salt crusts and saline clay flats of the desert floor to surrounding areas of the drainage basin and to regions outside the basin. Occasional "salt" storms in Salt Lake City coat windows and cars with salt and silt. On the salt flats salt drifts like fine snow across the highways and makes driving hazardous. No way is known of measuring directly the amount of salt removed by the wind, but observations suggest that the amount is appreciable. Whereas the streams concentrate the salt, the winds disperse it.

Sevier Lake. The effect of the wind is conspicuous in the Sevier Desert and Sevier Lake region, as shown from the following computations. The only data available are from Gilbert (1890, p. 224) who states that the salt crust was 4 inches thick in 1880 and covered about 47 square miles. The composition of the crust, though not important in figuring tonnage, was dominantly sodium chloride and sodium sulfate. Therefore:

$$\frac{47 \times 640 \times 43{,}560 \times .33 \text{ (4 in.)} \times 62.5 \times 2}{2\tfrac{1}{2} \times 2000} = 1{,}076{,}000 \pm \text{tons}$$

The above amount is small and seems incorrect if calculated on another basis. Gilbert (1890, p. 225) states that in the northern part the lake had a water surface in 1872 of 188 square miles and a maximum depth of 15 feet. Salinity of the brine was 8.64 per cent. It is remarkable that such a lake could have dried up in 6 years. It was nearly dry in 1880 (Gilbert, 1890, p. 226), and local residents reported that it was dry during the fall of the 2 preceding years. Gilbert attributed the decline to a turn toward aridity (Great Salt Lake reached its greatest height in 1872 and 1873 and dropped 6.5 feet by 1880) and to the extensive use of the Sevier and San Pitch waters for irrigation.

In the lake of 1872 the salt content was:

$$\frac{188 \times 640 \times 43{,}560 \times 15 \times 62.5 \times .0864}{2.5 \times 2{,}000} = 84{,}600{,}000 \text{ tons}$$

This is 80 times as much as computed from the data of the salt crust. Of course, much of the salt in the 1872 lake was in the clays and not in the centralized salt crust, about 45 square miles in area. Yet there would be many times more salt at present if the lake had the volume and salinity that Gilbert describes. The inconsistency could be checked by surveying the salt crust again.

The salt in the underclays may be computed as follows, if the area of the salt-saturated lake bed is the same as Gilbert's figure for the lake in 1872, and if the salinity of the underclays is half of that of the brine as given by Gilbert. It is also assumed that the salt-saturated clay is 5 feet thick and that it is 30 per cent water by weight.

$$188 \times 140 \times 43{,}560 \times 5 \times 62.3 \times .0125 \text{ (per cent salt in clay)} = 10{,}000{,}000 \pm \text{ tons salt in clays}$$

This figure would be the same whether related to the salt-crust calculation or to the 1872 lake.

The saline content of the Sevier River, the only measurable discharge into the lake, is determined at the Delta Reservoir (Thorne and Thorne, 1951) as: Na, 344 ppm; K, 19 ppm; Cl, 460 ppm; SO_4, 407 ppm; Ca, 64 ppm.

Total salinity, not including Ca, is 1230 ppm. This is very high, and much of the salt is picked up by the Sevier River and its major tributary, the San Pitch, in their lower courses. The writers and Dr. Wm. Lee Stokes (Personal communication) believe that much of this salt comes from the Jurassic Arapien Shale of San Pete Valley within the lower drainage areas of the basin.

The flow of the Sevier River has been gauged as follows:

Near Juab—average 22 years (1911–1933)—289 sec. feet
Below Gunnison—average 16 years (1917–1933)—248 sec. feet
Near Vermillion—average 19 years (1914–1933)—129 sec. feet
Below Piute Dam—average 21 years (1912–1933)—274 sec. feet
Near Kingston—average 19 years (1914–1933)—160 sec. feet

Present dams and irrigation prevent much of the Sevier River water from reaching Sevier Lake; hence the above flow records must be the basis for estimation of the amount that reached the lake before human occupation of the region. The streams were at a century high in 1872, and much of the water reached the lake,

judging from its size at the time, even though irrigation had started. The flow near Juab was measured during an average precipitation period, judging from the fluctuation cycles of Great Salt Lake, and is 289 sec. feet. The flow would have been considerably more if irrigation had not been practiced, yet some of the flow would have been lost before reaching the lake while flowing about 70 miles over desert floor from Juab. Possibly a flow of 300 sec. feet in pre-agriculture time would be a liberal figure, and 200 sec. feet would be a conservative figure. Taking a flow of 200 sec. feet that reached the lake with a salinity of 1230 ppm, the annual accession would be

$$\frac{200 \times 60 \times 60 \times 24 \times 365 \times 1230 \times 62.5}{1{,}000{,}000 \times 2{,}000}$$

$= 240{,}000\pm$ tons Na, K, Mg, Cl, and SO_4 per year.

If the total salt content on the basis of the 1872 lake is 84,600,000 tons + 10,000,000 tons = 94,600,000 tons, then the accumulation time would be

$$\frac{94{,}600{,}000}{240{,}000} = 400\pm \text{ years}$$

On the basis of the salt-crust computation the age would be

$$1{,}076{,}000 + 10{,}000{,}000 = 11{,}076{,}000$$

and

$$\frac{11{,}000{,}000}{240{,}000} = 50\pm \text{ years}$$

It is postulated below that the lake last sank below the 4500-foot level and abandoned the Sevier Lake depression about 13,500 years ago. Both 400 years and 50 years are much too short, apparently, and one must conclude either that the method of salt accession in determining the time necessary for the salt to accumulate is grossly inaccurate or that most of the salt has been blown out of the depression. The difference in the results of the two methods of calculation of the salt content suggests that neither can be relied upon until the extent and thickness of the salt crust has been resurveyed. Use of the method of salt accretion in determining the age of Great Salt Lake has little value in light of the above inconsistencies. The only apparent value in the computations is the assurance that large quantities of salt are being added to the lake each year and that equally large tonnages may be extracted commercially without measurably decreasing the salt content.

Analysis of Salinity Data

PROBLEMS: Since the salt (Na, K, Cl, and SO_4) accumulated gradually after the lake last fell below the Provo outlet at Red Rock Pass, it would be an error to consider in solution at that early stage all the salt that has been introduced by the streams in the subsequent history of the lake. One must account for gradual introduction of salt as well as for the fluctuations in lake level and volume. Removal of salt by wind and addition of airborne ocean salt to the drainage basin must also be taken into account. Although all four factors are imperfectly known a method of computation can be worked out, and a graph of the lake's changing salinity can be prepared on the basis of certain assumptions taken from previous calculations.

SALT FALL OUT IN RAIN: Considerable data are at hand regarding salt spray from the oceans, the transportation of salt by wind as spray and as microscopic salt crystals, and salt fallout in the rain. (*See* Goldschmidt, 1954.) No information is available, however, on the salt content of rain and snow in the Salt Lake region. The amount may be estimated by analogy with similar regions. For instance at Coolgardie, West Australia (Goldschmidt, 1954, p. 592), 400 miles from the west coast, with a rainfall of 10 inches, the fall out is 0.404 mg/cm² of chlorine per year. At Perth on the west coast the fall out is 3.40 mg/cm²/year. This is about the magnitude expected along the California coast and in the Great Salt Lake region. Fall out is about 0.35 in Iowa, which is much farther away from the Pacific Ocean source, so that it may be as much as 0.7 mg/cm²/year in the Salt Lake area. For the figure, 0.34 mg/cm², the fall out of NaCl in the drainage area of the Bear, Ogden, Weber, and Jordan rivers would be about 250,000 tons per year. For the higher figure it would be about 500,000 tons per year.

The area of the Great Salt Lake and the Great Salt Lake Desert and surrounding drainage area is about the same as that of the four rivers drainage area, so it, also, would receive 250,000–500,000 tons of salt per year from fall out.

Considerable water-soluble matter has been detected in the silts and clays of Utah Valley (Hunt *et al.*, 1953, p. 31–35). The Alpine beds in general contain less than the Provo beds. Hunt considers that the soluble salts reflect the composition of the water in which the particles settled. He says (p. 35):

"The high-level and near-shore deposits in the Alpine formation, where this condition most likely

prevailed contain 0.75 percent water soluble salts. The salinity of the water during the Alpine stage, therefore, may have been in the order of several thousand parts per million."

present the total soluble content is about 1000 ppm, and according to Clarke (1924, p. 159) it was about one-fourth this much before irrigation; only a small part of this was NaCl. It

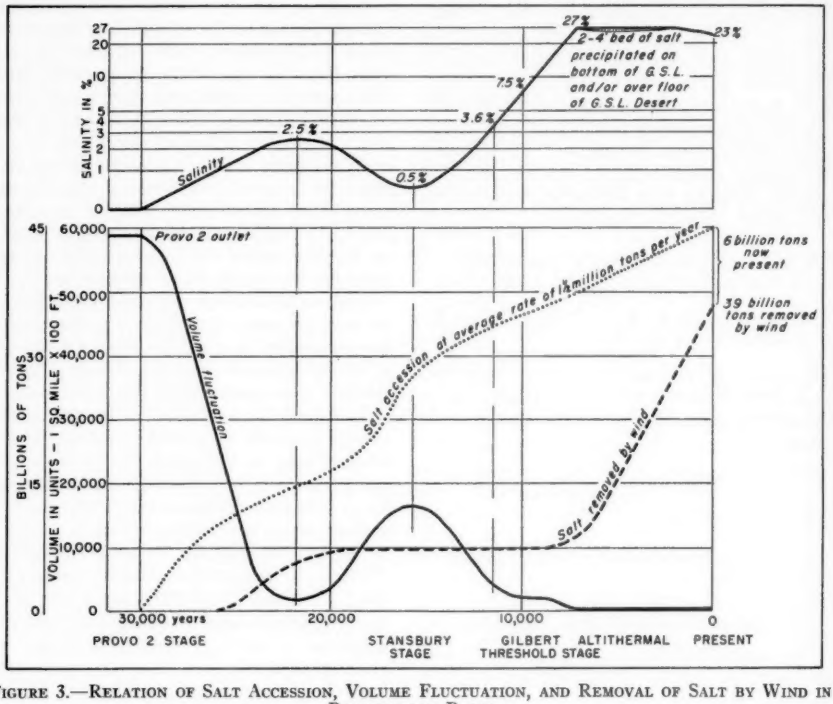

FIGURE 3.—RELATION OF SALT ACCESSION, VOLUME FLUCTUATION, AND REMOVAL OF SALT BY WIND IN BONNEVILLE BASIN

He also concludes that the salinity of the Provo stage waters, before desiccation and lowering to the Stansbury stage, probably had about the same salinity as the water of the Alpine stage. The relation of the analysis to the conclusion is not explained, but if several thousand means 5000, a salinity of 0.5 per cent would be suggested. About one-third of this is NaCl (1953, p. 32, Table 7). Curves drawn by the writers suggest a salinity of 0.5 per cent (NaCl and Na_2SO_4) about 15,000 years later at the Stansbury stage, by which time considerable increase in salinity over that of the previous overflow stage would have occurred. The lake waters during an overflow stage, however, would have almost the same composition as the inflowing rivers. Utah lake, a small overflow lake, before the settlement of the valley contained fresher water than it does now. At seems impossible that Lake Bonneville at the close of the overflow Provo 2 stage could have carried as much as 5000 ppm, even if only one-third were NaCl and Na_2SO_4. Hunt read the manuscript of the present paper and recognized the factor of wind-spread salt over the exposed lake beds. High sodium chloride and sodium sulfate content in Great Salt Lake and large amounts of sodium, potassium, and magnesium carbonates and sulfates in the silts and clays seem to indicate secondary processes of salt accretion after accumulation of the sediments.

INTEGRATION OF ACCESSION, LAKE FLUCTUATIONS, AND ABLATION: Figure 3 shows the relation of salt accession in Lake Bonneville, its volume fluctuations, and the removal of salt by wind action (ablation). Figure 4 shows the debits and credits of the salt economy as postu-

lated on previous pages. The volume fluctuations are determined by relating the level changes shown on Figure 20 to the volume curve of Figure 2. Average rate of increase of virgin salt is assumed to be 1,000,000 tons annually by the rivers and 1,000,000 tons annually by the rain fall out. Recycled salt brought in by the rivers is calculated to be about 1,500,000 tons annually. The annual rate of 1,000,000 tons of river-borne salt would quickly it would have a salinity of 0.3 per cent. As it fell to the 4300-foot level, below Danger Cave, where one of the oldest human camp sites in North America has been identified (Jennings, 1953, p. 184), it would have had a salinity of 3.6 per cent, but if it should rise again quickly to this elevation it would have a salinity of 1.2 per cent. The salinity as the lake fell to the Gilbert level (4245 feet) was 7.5 per cent, but if it rose to that level suddenly it would have a

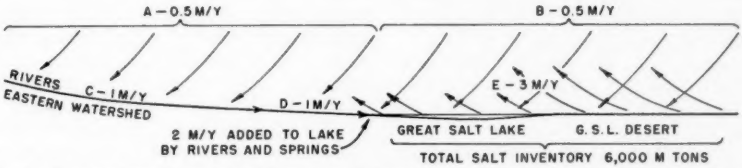
A – 0.5 M/Y
B – 0.5 M/Y
RIVERS
EASTERN WATERSHED
C – 1 M/Y
D – 1 M/Y
E – 3 M/Y
2 M/Y ADDED TO LAKE BY RIVERS AND SPRINGS
GREAT SALT LAKE
G. S. L. DESERT
TOTAL SALT INVENTORY 6,000 M TONS

FIGURE 4.—SALT ECONOMY OF THE GREAT SALT LAKE DRAINAGE REGION AND THE GREAT SALT LAKE DESERT

Salt picked up by the rivers in D is considered part of the existing inventory and is not counted in the conclusion that salt is being removed from the system at present about twice as fast as it is added.

A, B—Atmospheric fall out derived from Pacific Ocean

C—Salt derived from leaching of soils and rock mantle. Most of this may be fall-out salt

D—Salt derived from salt left in lake-bottom sediments plus fall-out salt from Great Salt Lake and Great Salt Lake Desert.

E—Salt picked up from Great Salt Lake and Great Salt Lake Desert by wind and carried out of the basin

0.5 M/Y = Half a million tons of salt per year

B + C times 30,000 years = 45,000 M tons added since Provo 2 outlet stage

have been increased during high stages and decreased during low stages, because these fluctuations result from greater and smaller stream runoff with presumably greater and smaller contributions of salt. The increases and decreases as shown on the curve of Figure 3 are estimated. The writers assume that the salinity will not become great enough to leave much salt on the silt and clay flats surrounding the lake until the lake sinks below the Gilbert level at 4245 ± feet. Hence nearly all the salt has been removed from the lake's waters in the last 8000 to 10,000 years, particularly during the altithermal and postaltithermal stages.

If the average annual rate of salt accession has been 1,500,000 tons, then 45 billion tons of salt has been added in the last 30,000 years. Since only about 6 billion tons is accounted for, it is assumed that 39 billion has been removed by the wind. The ablation curve is constructed on this basis.

SALT IN BONNEVILLE WATERS: As a result of integration of the three curves the salinity at the Stansbury stage, about 15,000 years ago, is determined as 0.5 per cent. With the present salt in Great Salt Lake and the Great Salt Lake Desert, if the lake should rise to the Stansbury salinity of 2.6 per cent. The difference is striking and if true demonstrates that threshold overflow from Great Salt Lake during the Gilbert level stand could have added to the large salt pan in the Great Salt Lake Desert.

The salinity curve (Fig. 3) indicates that saturation would have been reached at a time when the amount of salt was 2½ times as much as now. Since 40 per cent of the total at this time now remains, then it appears that 60 per cent was precipitated out during the altithermal. This would leave a salt crust over the floor of Great Salt Lake 3–4 feet thick; if spread over the Great Salt Lake Desert as well, it would be about 2 feet thick. This crust, principally over the Great Salt Lake Desert and around the margins of Great Salt Lake, has been removed, presumably, by the wind. It may be postulated, therefore, that the Bonneville salt crust was once much more extensive than it is now and is rapidly diminishing.

THE ABLATION POTENTIAL: The writers postulate that the wind removes about 3,000,000 tons of salt annually from Great Salt Lake and its surrounding salt flats and from the Great Salt Lake Desert. This is carried by the wind out of the drainage basin. A formula developed

by Hutchinson (1953, p. 418) indicates that the fall out decreases exponentially with distance from source. Using the formula, Dr. M. A. Cook (Personal communication) concludes that only 7 per cent of the amount that becomes airborne leaves the basin and that the rest is spread over the basin. The problem is difficult to pursue because the amount that becomes airborne is not determined by the formula, and the direction or directions of transportation—which would provide an index of the distribution of wind-blown salt within and outside the basin—are not easily determinable.

CONCLUSIONS: The conclusions drawn from Figure 3 are built on weak supports. The volume curve is probably correct to within 10 per cent. The salt-accession curve is far from certain. New salinity measurements for each month of the year of the main streams that enter the lake should be made and correlated with discharge. More measurements of salt discharge in springs should be made. The atmospheric fall-out data need careful check by field measurements. The writers feel that the figure of 2,000,000 tons per year might need to be changed by a factor of 50 per cent. The fluctuations along the curve are guesses and are at best relative.

According to the figure of present fluviatile salt accession and carbon-14 dates the amount of salt now present is far less than it should be, and the difference is assigned simply to wind removal. The total amount of salt brought in by the streams may not be new salt derived from the weathering of bedrock of the Bonneville drainage basin but may be recycled salt swept from the drying salt pans and salt flats by the wind to higher areas of the basin and brought back by the streams. This contingency was considered when the computations were made, but the problem needs more study.

The curves are based on the history of level fluctuations of Lake Bonneville, and a number of geomorphologists may hesitate to accept the chronology proposed in this paper. The conclusions regarding salinities of past lake stages, therefore, are valuable principally as a guide for future study.

Precipitation Changes and Lake-Level Fluctuations

Precipitation-Evaporation Economy

In most closed basins occupied by a lake, the lake level is subject to fluctuations; that of Great Salt Lake has fluctuated through nearly 19 feet in historical times. The fluctuations are assigned to imbalance of additions and subtractions of water from year to year. Gilbert (1890, p. 171) visualized the factors governing the fluctuations as follows: additions are: direct precipitation and inflow, principally by the Bear River, Jordan River, Weber River, and Ogden River; subtractions are due to evaporation, and above the 4800-foot level to overflow. Subsequent studies have been summarized by Peck (1951, M.A. thesis, Univ. Utah), who concludes that in addition to direct precipitation and stream inflow, a sizable contribution comes from ground-water movement into the lake. After analyzing the precipitation data in the Great Salt Lake watershed, stream flow into the lake, diversions, lakes, and reservoirs of the basin, and evaporation from the surface of the lake, Peck concluded that the fluctuation of the lake level of any year is due to the precipitation of the past 4 years. The effect of the immediate year is the most pronounced; if expressed by carry-over factors with the current year as 1.00, the preceding 4 years are:

Current year	1.00
First previous year	0.30
Second previous year	0.02
Third previous year	0.04
Fourth previous year	0.10
Fifth through seventh previous years	0.00

Over a period of about 1 year the lake rises or falls about 20 per cent in response to the preceding year's precipitation. The precipitation this year, for instance, will have very little effect on the lake during the second and third year hence, but in the fourth year it will be responsible for about 7 per cent of the lake's rise or fall.

Lake-Level Adjustment to Precipitation

Study of precipitation changes and the fluctuations of level of Great Salt Lake contributes to understanding past fluctuations of Lake Bonneville. Data from Peck's study (1951, M.A. thesis, University of Utah) is plotted in Figure 5. His "total index of precipitation" is the sum of the seasonal index and the carry-over effects for the preceding years. He weighted the precipitation of each station in the basin according to its station weight, its location (group weight), and the time of year (monthly weight) and added this total to the effects of previous years. He concludes that the average annual recorded rainfall of the drainage basin of Great Salt Lake is 15.6

inches, and this relates approximately to his index of 250.

The co-ordinate, "change in lake level," indicates how much the lake rose or fell each year. The graph indicates: (1) If the precipitation should increase 3 inches per year (from 15.6 to 18.6) the lake level will rise 1.2 feet per year. In 30 years, if this increase should hold, the lake would lap at the base of West High School and would cover the lower sections of Salt Lake City. (2) If precipitation should increase 0.54 inches per year (3.4 per cent) the lake would rise 0.2 feet per year. In 100 years it would rise 20 feet and in 1000 years 200 feet. In 2500 years it would rise to the 4500-foot mark and flood Cache and Utah valleys.

In historical time the fluctuations in precipitation have changed through nearly 8 inches with apparent minor half cycles (maximum to minimum and minimum to maximum) of 7.7 years and major cycles of about 25 years. The longest sustained change was a general decrease in precipitation from 1873 to 1903.

Thus, the lake is delicately adjusted to precipitation changes; presumably, Lake Bonneville also responded markedly to precipitation changes in the past.

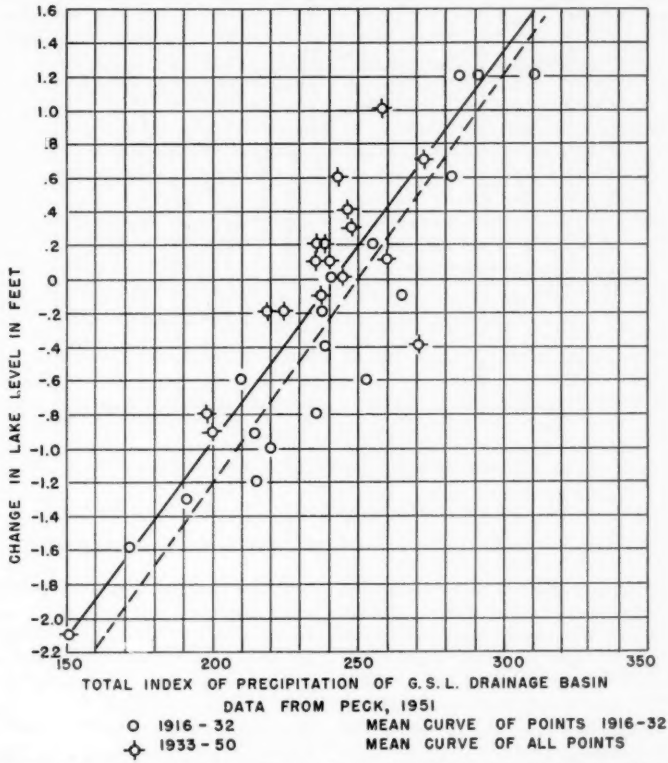

FIGURE 5.—RELATION OF PRECIPITATION TO LAKE-LEVEL FLUCTUATION, GREAT SALT LAKE

Temperature Changes Related to Precipitation

The effect of temperature change on precipitation is particularly pertinent to an understanding of past climatic changes. Peck's study includes precipitation data but not temperature data. Dr. J. Vern Hales, Department of Meteorology, University of Utah, supervised the gathering of temperature data from the records of the U.S. Weather Bureau, matched the data with the precipitation data, and analyzed the results.

Reports from 3 of the 21 stations used by Peck do not include temperature, but reports from the remaining 18 stations include concurrent temperature and precipitation records

Figure 6 shows relation of temperature to rainfall and provides a means of converting one to the other. In general it shows that a fall of 1°F. in annual temperature would be associated

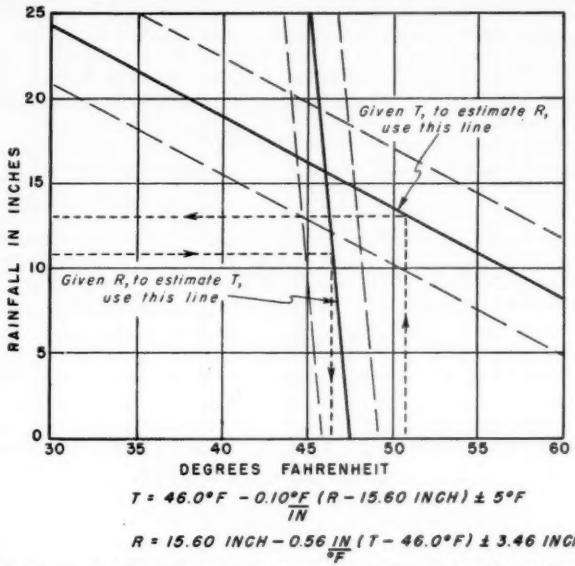

FIGURE 6.—RELATION OF TEMPERATURE TO RAINFALL IN GREAT SALT LAKE DRAINAGE BASIN

for periods ranging from 20 to 45 years. The annual average temperatures of these stations were correlated individually with the annual total precipitation and recorded to give linear correlation coefficients ranging from +0.18 to −0.49. Only two values were positive. The average, weighing each station correlation with the weighting coefficient assigned by Peck and adjusted for deletion of the 3 stations without temperature records, is −0.23. Although this correlation coefficient is small, it indicates that the relation of temperature to precipitation in the region can be estimated. The following equation, using Peck's weighting coefficients, expresses the relation:

$$R = 15.60 \text{ inches} - 0.56\ (T\text{-}46.0°F) \pm 3.46 \text{ inches}$$

where 15.60 is the average annual precipitation, and 3.46 is the standard error of the precipitation estimate.

This equation is valid only in the temperature range and in the precipitation range for which it was developed, viz., the variations of weather observed in the Great Salt Lake drainage basin during the last 40 years.

with an increase in precipitation of about 1 inch, but each year a standard error of 3.46 inches must be entertained; however, the graph shows an approach to quantitative calculations.

The association of greater annual precipitation with lower annual temperatures is indicated by charts published by Visher (1954). The charts show that in the western interior region from Yuma to Salt Lake and to Spokane there is a definite relation of lower temperature to higher precipitation. Temperature changes are not necessarily the controlling factor, because if the general storm tracks shifted their courses southward from west to east across the Rocky Mountains, the temperatures in any one place would probably drop. This phenomenon could be regional, but a shift in the regional weather pattern seems reasonably tied to a world-wide change.

If the relations in the Great Salt Lake drainage basin are a key to world-wide temperature changes, then it may be concluded that a general drop in temperature of ½°F., if sustained, would result in a rise of Great Salt Lake of 0.2 feet per year, and in 2500 years a rise of 300

feet. This would create another Lake Bonneville at the Stansbury level. The above conclusion is based on the assumption that decrease in temperature to rise in lake level is linear, and this is incorrect because the area of evaporation increases as the lake rises (Fig. 2), and the rate of evaporation increases as salinity decreases. Analysis of the data on the fluctuations of Great Salt Lake yields an average figure and does not provide a trend reflecting increasing evaporation rate and increasing area of evaporation. For the above reasons the conclusion that a decrease in temperature of ½°F will bring on a glacial stage is undoubtedly too low.

Emiliani (1955) shows that the ocean-bottom waters of low latitudes fluctuated through 6°C. in temperature during the Pleistocene. Others (Flint, 1947, p. 501) suggest that the maximum amplitude of fluctuation of air temperature was probably of the order of 10°C., so that the figure ½°F. is considerably smaller than others have postulated.

The climatic change is considered abrupt, but a change would undoubtedly occur gradually. Accordingly, the time to consummate a certain rise in the lake for a given temperature decrease is too short.

Expansions of Lake Bonneville

Significance of Thresholds and Expansions

The Bonneville Basin is made up of a number of basins, which are of three kinds. Some are closed and have internal drainage. If in or near the Wasatch Mountains where rainfall is heaviest, these may fill and overflow into the main body of water. If farther west in the more arid country, the main body of water may reach the threshold first and spill into the local closed basin. Some have a continuous downslope into the major basin, yet a slight fluctuation of lake level floods or drains a large area. In the closed and open basins the water enters or leaves through a relatively narrow inlet, and in the closed basin the elevation of the inlet is important. Evaporation is increased in proportion to the expanded area. This will retard a further rise in the lake, especially if precipitation is only slightly higher than evaporation. Some time will lapse after the expansion before precipitation again exceeds evaporation and the lake level begins to rise. In the normal course of events the climate becomes moister slowly, the lake rises slowly, and a sudden expansion into a basin causes a stillstand in the level of the lake for a certain time. The chief factor determining the length of time the level will hold constant is the size of the basin into which the lake expands. Other factors are the presence or absence of perennial streams flowing into the basin and the presence or absence of a lake in the basin. A basin like Utah Valley, which receives a major stream of the Bonneville Basin, the Provo River, would probably be flowing into the main basin; it would have trenched its threshold and would fill as rapidly as the main lake rose. The expansion of the lake over the floor of such a valley would probably have only a slight retarding effect on the main lake's rise. The flatness of the local valley's floor, its size, and its aridity determine the retarding influence on the rise of the main lake.

The Bonneville Basin is more arid in the central and western parts than in the eastern part. If the threshold basin is in the more arid part which has no perennial streams, an expansion into it will have a marked effect on the lake.

When the lake falls and abandons a closed basin or relicts an open basin, the area of evaporation is suddenly decreased, and precipitation for a while will equal evaporation. Again the lake level is stationary. Therefore, a number of stillstands of Lake Bonneville may have occurred long enough for the lake's waves and currents to carve and build beaches of recognizable size. A stationary water level and resultant beach caused by a basin expansion do not indicate climatic maxima or minima. This seems a principle of sufficient importance to explore thoroughly in trying to unravel the lake's history.

Great Salt Lake Desert Expansion

HYDROLOGY: If Great Salt Lake rose about 21 feet to an elevation of approximately 4221 feet it would spill into the Great Salt Lake Desert; with a rise of 9 feet more the water area would be increased from 2500 square miles to about 5000 square miles. (*See* Fig. 1.)

The spillway or threshold lies west of Lakeside on the Southern Pacific Railroad. Elevations along the roadbed surveyed by the railroad are accurate in relation to themselves but are not tied carefully to U.S. Geological Survey or U.S. Coast and Geodetic Survey benchmarks. The lowest elevations seem to be just north of the Newfoundland Mountains, where the roadbed elevations indicate a lake-bed elevation of about 4221 feet. Aerial photos and observations

from the air indicate also that this is probably the threshold into the Great Salt Lake Desert. The area east of the Newfoundland Range seems low and especially moist (Nolan, Pl. 3); possibly water spilled into the Desert around the south end of the range also.

The engineering staff of the Western Pacific Railroad supplied records of elevations along the roadbed from the Cedar Mountains to Wendover at the Utah-Nevada state line. From the 4230 contour (Fig. 1) the old lake bed falls gently and apparently continuously to the salt-crust area which various sources report at 4211–4214 feet above sea level. The railroad engineers favored the higher figure. In any case, the basin of the Great Salt Lake Desert has a closure of 7–10 feet below the 4221-foot contour and presents an ideal example of the bar theory of salt formation. The salinity of Great Salt Lake at the 4220-foot level would be 7.7 per cent, and water of this salinity flowing into the very arid desert would readily be concentrated to the point of precipitation. The Bonneville salt pan or crust, also called the Salduro salt crust, is a natural consequence.

The valley between the Pilot Range and Desert Range also has a salt pan, and examination of photo-index sheets shows that the spillway is at the northern end of the Desert Range and seems to be only a few feet above the desert floor. Small rivulets drain both ways from the low threshold.

ASSOCIATED BEACHES: Because of the stabilizing influence on lake level of expansion into or withdrawal from the Great Salt Lake Desert the 4221-foot mark should be one of the important beach-forming lake levels; a search was made for shore features at this elevation. The lake waters impinged on bedrock and steep slopes at the 4221-foot level in only a few places. For the most part the lake shores on its own gently sloping bottom deposits, and beach features are not so conspicuous as at higher elevations; yet a distinct and strong beach exists. This low-level beach is not at the expected 4221-foot elevation but at 4240–4245 feet, and a contour around Great Salt Lake at the 4245-foot level has been drawn (Fig. 1) to mark this beach.

Figure 7 is a map of the southeastern margin of Great Salt Lake and the Jordan River Valley and shows the 4245-foot beach and associated terraces of the Jordan River.

The first locality studied is in sections 14 and 15, T. 3 N., R. 1 W., about 2½ miles west of Farmington. The Farmington quadrangle topographic map shows a northwestward-extending escarpment whose base is at 4240 feet. The top of the escarpment is 5–25 feet above the base. The low cliff is interpreted to be wave cut because of the uniform level of the base and because little evidence of any deposit exists. The bench land into which the waves are presumed to have cut is composed of the silts and very fine sands of the Weber delta; hence the paucity of sand and gravel is explained. A dark-brown soil 6–12 inches thick covers the tan silts above the wave-cut cliff and seems to have evolved in part before the beach was cut.

The next locality where a wave-cut beach is believed to occur is northward from the northwest corner of the Beck's Spur. (*See* Salt Lake City North quadrangle, sections 2 and 11, T. 1 N., R. 1 W.; Fig. 7.) Beginning at the refinery of the Standard Oil Company of California, immediately to the east of the railroad tracks of the Union Pacific Railroad, a low cliff rises 5–10 feet from an elevation of 4240 feet and continues northward for about 4 miles. The base of the cliff holds at the 4240 elevation for 2½ miles northward to a pond in section 35, T. 2 N., R. 1 W., north of which the base follows at about 4245 feet. The escarpment thus defined has been taken as a fault scarp of recent origin (Gilbert, 1890, p. 349) and has been considered an extension of the Warm Springs fault by students of ground water in the area. The Becks Hot Springs, 1 mile south of the refinery, lie on a southward projection of the scarp and are believed to issue along the fault. The major normal fault at this locality is about 600 feet east of the hot springs; its scarp follows around the base of the bedrock slope and rises and falls as various gentle relief features are crossed. The persistence of the base of the low scarp on the west, however, at the 4240- to 4245-foot level, here and west of Farmington, leads the writers to regard it as a wave-cut cliff and bench and to mark the stabilizing of the lake's level at the threshold elevation of the Great Salt Lake Desert expansion.

A third conspicuous feature of the lake shore at the 4240- to 4245-foot level is a combination split and barrier beach running due east of Magna. (*See* Magna quadrangle, sections 26, 27 and 28, T. 1 S., R. 2 W.) The spit begins at an alluvial slope off the northeast corner of the Oquirrh Range and extends nearly 3 miles eastward; between the spit and the piedmont slope is a lagoon, and its bottom is about 5 feet below the crest of the spit. A secondary highway follows the crest of the spit which is

uniformly 4251–4253 feet above sea level. The spacing of the contours here on the lakeward side of the spit suggests a water plane at about 4245 feet. The spit is about 400 feet wide and is composed of coarse sand to pebble-sized gravel.

A fourth conspicuous feature of the lake at about the 4250-foot elevation is a spit extending to the southwest from Mills Junction in section 16, 17, 19, and 20 of T. 2 S., R. 4 W., Tooele County. This spit complements the spit east of Magna in that it has been built westward from the north end of the Oquirrh Mountains. U. S. Highway 40 to San Francisco runs along the crest of the sandy and gravelly spit, which ranges from 4261 to 4263 feet in elevation and is therefore 10 feet higher than the Magna spit. (*See* U.S. Geological Survey topographic map of part of Tooele County.)

A spring-fed pond lies on the lee side and is part of a rather broad marshy lagoon. The Mills Junction bar was recognized by Antevs (1952, p. 94; 1955, p. 326) who assigned it to a rise of the lake from a previous low. The strongest beaches in the Great Lakes region were formed by a rising lake, and from this point of view there is good reason in Antevs' deduction. A study of the main, low Jordan River terrace, however, indicates that the lake held at about the 4240–4245 foot level for a long time; the writers are therefore prone to associate the Mills Junction bar, the Magna bar, and the wave-cut cliffs north of Becks Hot Springs and west of Farmington with the Great Salt Lake Desert expansion.

The crest of the Mills Junction bar is 10 feet higher than the Magna bar, and the difference may be explained by recent faulting or by the fact that the waves built one bar higher than another. Recent faulting has been noted along the west side of the Oquirrh Mountains, but at a locality several miles south of the Mills Junction bar; hence faulting is not believed to have elevated the bar. However, it might be reasoned that the Mills Junction bar, facing directly the northwesterly waves, which Gilbert postulated as the strongest and most persistent, would be built higher than the Magna bar.

The north end of the Stansbury Range, like the Oquirrh, has a spit extending westward, over part of which runs U.S. Highway 40. The spit is composed principally of sand and has little gravel. No complementary lagoon exists. At the site of a telephone relay house and a nearby railroad cut through the sand body, the irregular accumulations suggest sand-dune activity. No detailed topographic maps of the area exist; hence accurate elevations along the spit are not available, and the form could not be clearly analyzed.

A number of small bars across re-entrants are at approximately 4240 feet, as are beaches at the base of steep slopes at the north end of the Stansbury Range. They seem to be features of the Great Salt Lake Desert expansion level, but without accurate elevations the correlations are uncertain. Some of the bars and beaches appear to be a little higher than 4240 feet (Pl. 1).

A strong beach at the 4245-foot level occurs on the west side of Antelope Island. It is as strong as the next-higher Stansbury beach; the desert vegetation and a slight modification by alluviation and erosion give it an appearance equally as old as the Stansbury. The clean gravels and boulders of the crisp modern storm beach below, free of vegetation, are in contrast to the rather smooth alluvium of the 4245-foot beach.

Figure 2 of Plate 2 illustrates a wave-notched headland at the Gilbert level on the southwest end of Antelope Island.

Beaches at the Gilbert level are prominent around Silver Island Range and its northern end, Crater Island See (Pl. 2, fig. 1). Accurate elevations are not available in this area, and exact elevations of the beach at various points are not known. However, the visible difference in elevation of the beach and the adjacent salt flats indicates that the beach marks the Gilbert level.

JORDAN VALLEY TERRACE: The recently published Salt Lake City South and Midvale quadrangles show the Jordan River to be meandering in a flood plain about 40–45 feet below adjacent bench lands in sections 14 and 15 of T. 2 S., R. 1 W. This locality is about 2 miles southwest of Murray. The flood plain ranges from half a mile to a mile wide and has a local relief of 5–10 feet. The bench above the incised river is in places a mile wide on either side, but locally, because of lateral shifting of the river, has been cut away so that pronounced slopes rise from the terrace rim eastward to the base of the Wasatch Range and westward to the base of the Oquirrh Range.

Upstream (southward) the incision increases to 70 feet near Riverton Station in section 26, T. 3 S., R. 1 W., and to 85 feet at the southwest corner of section 14, T. 4 S., R. 1 W. (Jordan Narrows quadrangle).

Downstream the depth of incision decreases gradually, so that at 33rd South Street, Salt Lake City, it has nearly disappeared. The last traces of the terrace and the bench lands here

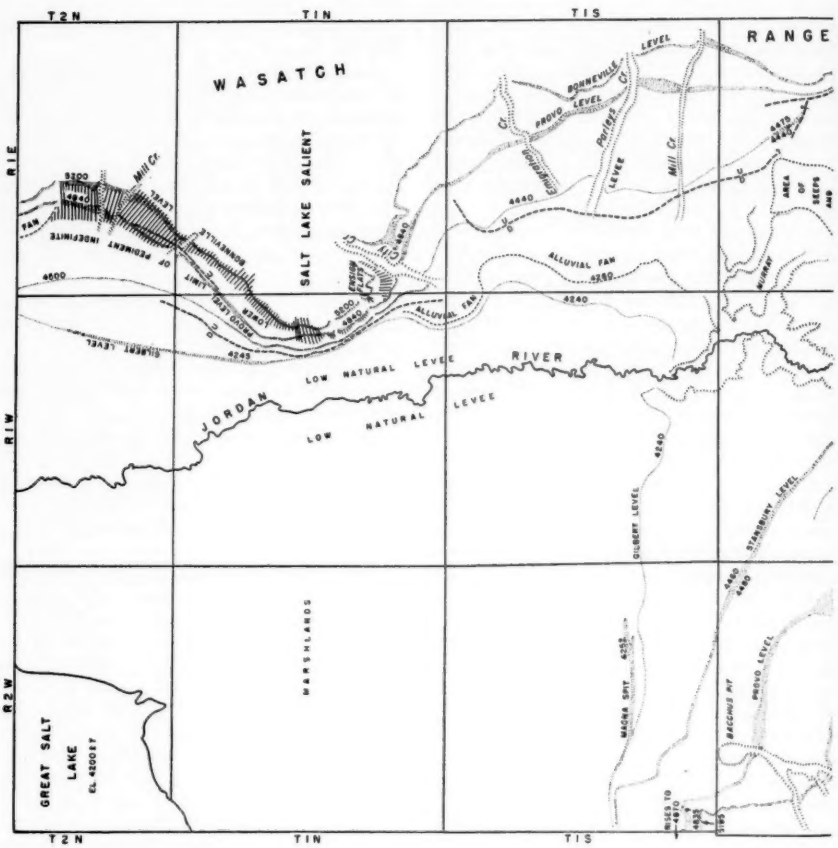
T2N
T1N
T1S
R1E
R1W
R2W
WASATCH
SALT LAKE SALIENT
RANGE
Mill Cr.
BONNEVILLE LEVEL
PROVO LEVEL
Provo Cr.
Bonneville Cr.
Provo Levee
Mill Cr.
ALLUVIAL FAN
ALLUVIAL FAN
SILVER LAKE LEVEL
LOW NATURAL LEVEE
LOW NATURAL LEVEE
JORDAN RIVER
GILBERT LEVEL
STANSBURY LEVEL
MARSHLANDS
GREAT SALT LAKE
EL. 4200±?
MAGNA SPIT
BACCHUS BAY
PROVO LEVEL
RISES TO 4870
4200
4240
4245
4440
4600
4800
4820
4840
4850
4870

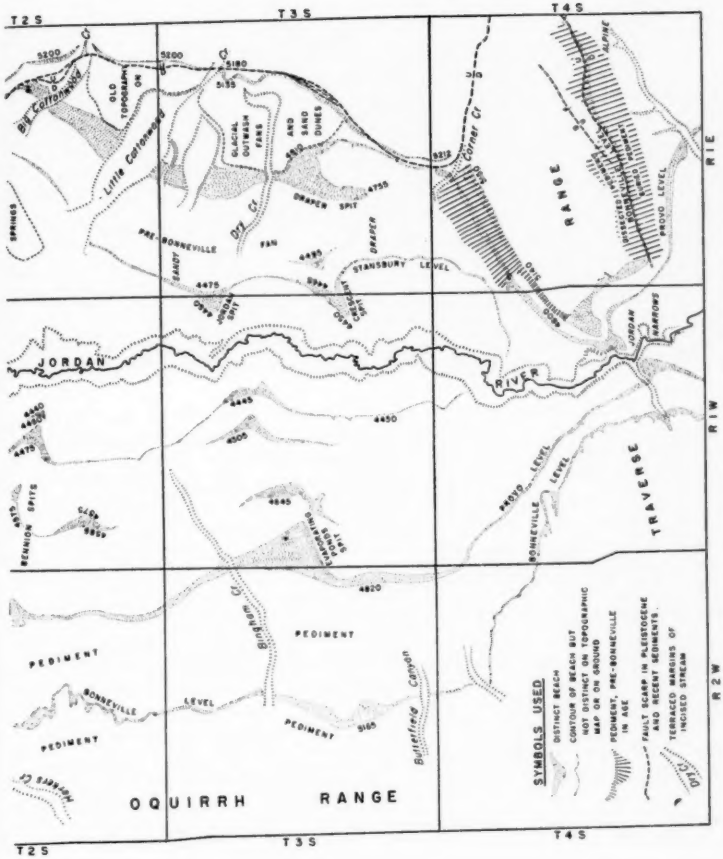

FIGURE 7.—MAP OF LOWER JORDAN RIVER VALLEY
Showing beaches of Lake Bonneville, terraces of the Jordan River Valley, and associated features.

are at an elevation of 4250–4255 feet. Other contours to the north seem to continue the bench gently downward to elevations of 4230 feet. At this point the terrace bench and the from Bluffdale northward. This settlement is 3 miles north of the Jordan Narrows. Considerable sediment was probably transported to the trough of the valley by subaqueous currents,

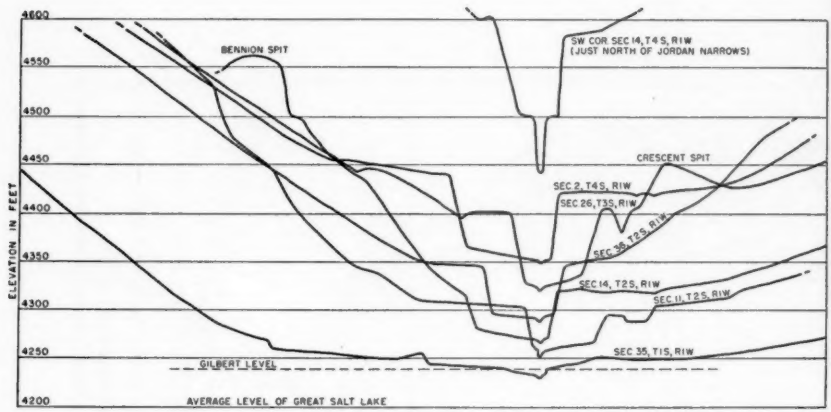

FIGURE 8.—TRANSVERSE PROFILES OF LOWER JORDAN RIVER VALLEY

flood plain merge. A series of transverse profiles (Fig. 8) illustrates the terrace from the lowest expression upstream nearly to the constricture of the Jordan Narrows. According to the foregoing data on the main terrace of the Jordan River the benchland, which was the bottom of the valley before dissection, sloped gently from the Jordan Narrows at an elevation of 4580 feet or a little less.

The history of the Jordan Valley bottom before dissection is tied to the lake at higher levels. The map of Jordan Valley (Fig. 7) shows four spits whose nearly flat tops range from 4445 to 4465 feet in elevation. The nearly level tops of the spits toward their points may not represent the level of the water in which they were built, because these distal ends may have accumulated slightly under water. The water level was probably not much higher, however, than 4465 feet, which presumably is one of the Stansbury levels. Jordan Valley bottom (now the tread of the main terrace) was under water and the sediment was probably supplied partly from the spits and partly from wave activity on the immediate shores. Jordan River flowed out of clear-water lake (enlarged Utah Lake) and would have derived sediments only from the Narrows section, which it was undoubtedly deepening at the time. Irregularities of the valley bottom between the Oquirrh and the Wasatch ranges were filled and smoothed out, and the transverse profile was established in the form of a broad and very gently curved surface, concave upward. The manner of alluviation of the bottom of dams is believed to apply here. The wave-built spits at several elevations are the only interruptions in the smooth bottom slope.

If the lake fell rather rapidly from the 4465-foot level to the 4245-foot level and then held stationary for a while, the Jordan River would have trenched the bottom somewhat, especially headward toward the Jordan Narrows. Then, when the lake fell to its present level, the

PLATE 1.—GILBERT BEACHES AT NORTH END OF STANSBURY RANGE

FIGURE 1.—Gilbert beach at north end Stansbury Range.

FIGURE 2.—Gilbert, Stansbury, and Provo beaches at north end Stansbury Range.

PLATE 2.—GILBERT BEACHES ON ANTELOPE ISLAND AND CRATER ISLAND

FIGURE 1.—Gravel spit at Gilbert level on southwest side of Crater Island. (*See* Figure 1).

FIGURE 2.—Gilbert beach on southwest end of Antelope Island.

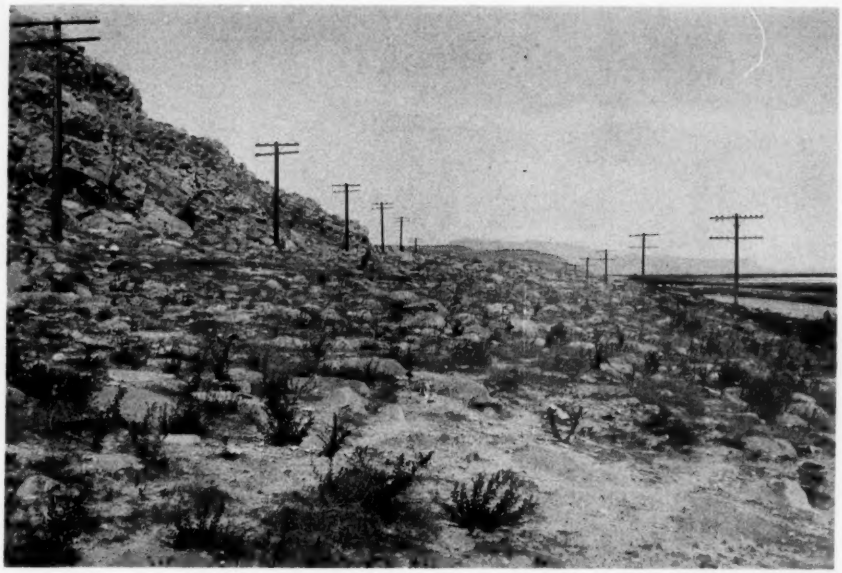

FIGURE 1

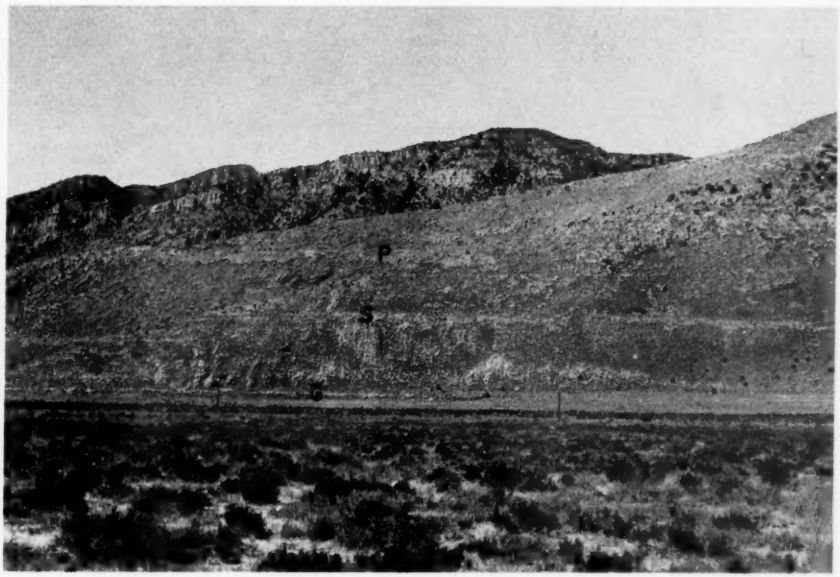

FIGURE 2

GILBERT BEACHES AT NORTH END OF STANSBURY RANGE

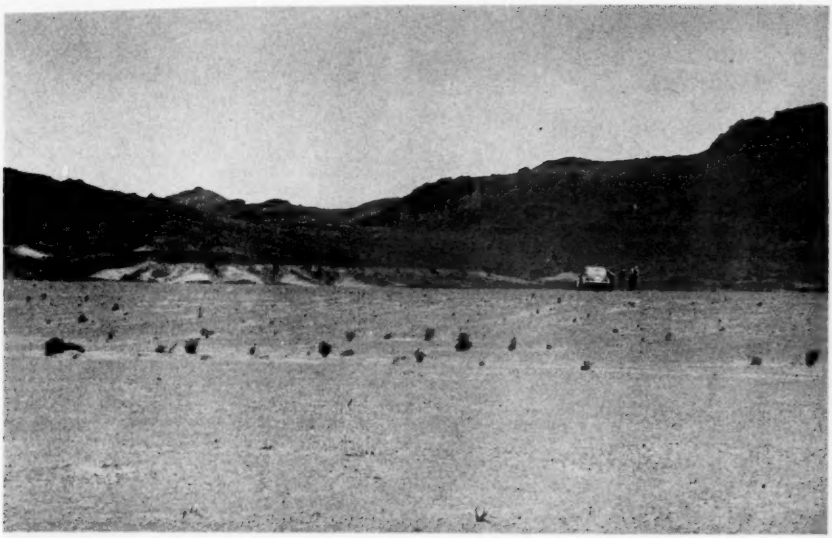

FIGURE 1

FIGURE 2

GILBERT BEACHES ON ANTELOPE ISLAND AND CRATER ISLAND

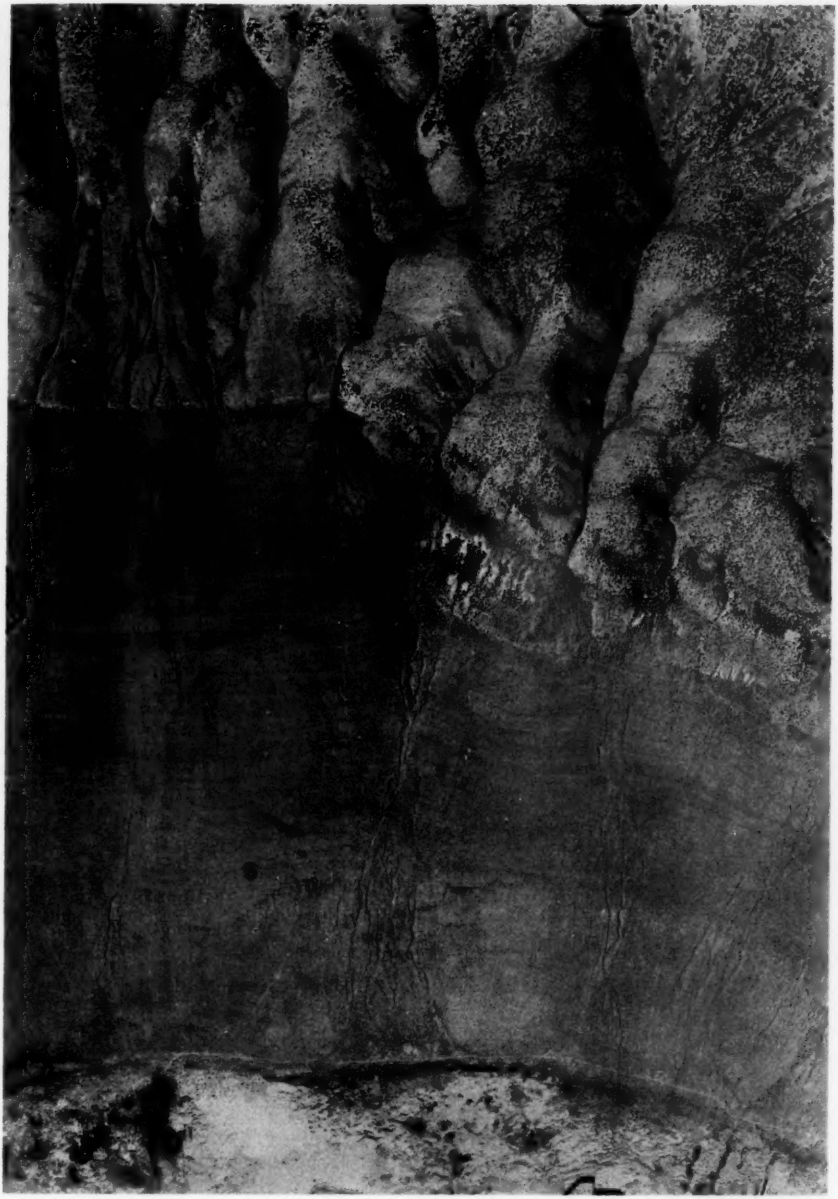

VERTICAL AERIAL PHOTOGRAPH OF LAKE BONNEVILLE BEACHES
ON EAST PIEDMONT OF PILOT RANGE

RED-BROWN SOIL IN EAST SALT LAKE CITY

incision would be deepened throughout the course. The presumed early incision as a distinct terrace can be recognized only in the valley from the Jordan Narrows northward for about 3 miles (Fig. 8, upper profile). North of this point the entrenchment of the last stage seems to have occurred without leaving a distinct secondary or lower terrace, except possibly in two places. The "64th South" road crosses a lower terrace which may mark the early entrenchment, and just south of the junction of Little Cottonwood Creek with the Jordan River is a similar lower terrace.

Thus, the entrenchment of the Jordan Valley is tied to two lowerings of the lake: one from the 4465-foot level to the 4245-foot level and one from the 4245-foot level to the present at about 4200 feet; this provides additional support to the postulation of a lake-stability level at 4240 feet. The writers here propose to name this lake stage the Gilbert stage and the shore features the Gilbert beach.

ELEVATION PROBLEM: A discrepancy exists between the elevation of the threshold for the expansion into the Great Salt Lake Desert (4221–4222 feet) and the lake level to which the expansion has been tied (4240–4245 feet). No recognizable beach features of any magnitude exist, as far as the writers have observed, between the 4240–4245 foot elevation and the present lake shore, except for the "meander line" at about 4205 feet. The meander line is a break in places between the saline, wet, lake-bottom deposits and the somewhat fresh water-flushed, vegetation-covered land beyond; it probably represents the upper limit of fluctuation of the lake in the last several hundred years.

Modern fault scarps 20–60 feet high occur along the Wasatch front and along part of the west side of the Oquirrh Range. The freshness of the scarps indicates that they are probably post-Gilbert in age. In no place does a fault cut the Gilbert beach, and therefore the effects of the faulting are difficult to analyze.

In addition to the possibility that the Gilbert beach has been displaced by vertical movements of the crust, it is recognized that beach features are built to variable heights by the same water plane. The discrepancy between the threshold and the Gilbert beach in Jordan Valley is small and of the magnitude of 18–23 feet. Possibly the amount is of no significance, and the main expansion over the Great Salt Lake Desert occurred at 4240–4245 feet, which became the stabilized level for the cutting of Gilbert beach. The topography of the desert floor, however, indicates that the threshold elevation should mark the stabilized level. There remains the possibility that the threshold elevation as designated is not correct, because level traverses have not been run over the desert floor west and southwest of Lakeside. From the air and from the ground the soggy salt-crusted clay bottom lands seem so flat that the threshold elevation could not be higher than 4221 feet.

Expansions Near the Stansbury Level

THE STANSBURY PROBLEM: The problem of the Stansbury shore line may be introduced by quoting Gilbert (1890, pl 134):

> "Upon any profile a considerable number of shores can be recognized below the Provo; it is probable that a system of levelings would enable these to be correlated in a consistent system. This has not been done, and only a single one has been recognized. That one is distinguished merely by the greater magnitude of its cliffs and embankments, but is not sufficiently accented to be everywhere identified. It is called the Stansbury shoreline. Its strongest delineation is upon Stansbury Island, where owing to local conditions it rivals the Provo shore in definition and surpasses the Bonneville. In abundance of tufaceous deposits it probably ranks next to the Provo."

Gilbert did not measure the height of the Stansbury shore on Stansbury Island, but by Paulin aneroid measurement the prominent tufa-crusted beach was found to be approximately 4460 feet above sea level.

After discussing the "Old River Bed" which leads from the Sevier basin to the Great Salt Lake Desert basin at about the Stansbury level and realizing the possibility of overflow basins as regulators which might cause "the oscillating lake to linger at a particular level each time it rose," Gilbert says:

PLATE 4.—RED-BROWN SOIL IN EAST SALT LAKE CITY

Living and fossil soils in cut at Foothill Boulevard and Skyline Drive, east Salt Lake City. A, B, and C, horizons of living soil. (1) Interbedded dull red sand and grit beds; (2) Red-brown fossil soil; (3) Nugget Sandstone. *See* Figure 13 for scale.

"The nature of the problem embodied in the Stansbury shore was not realized until the field examinations were so nearly complete that the opportunity had passed for visiting the localities important for its discussion. It therefore remains as one of the unanswered questions developed by the investigation."

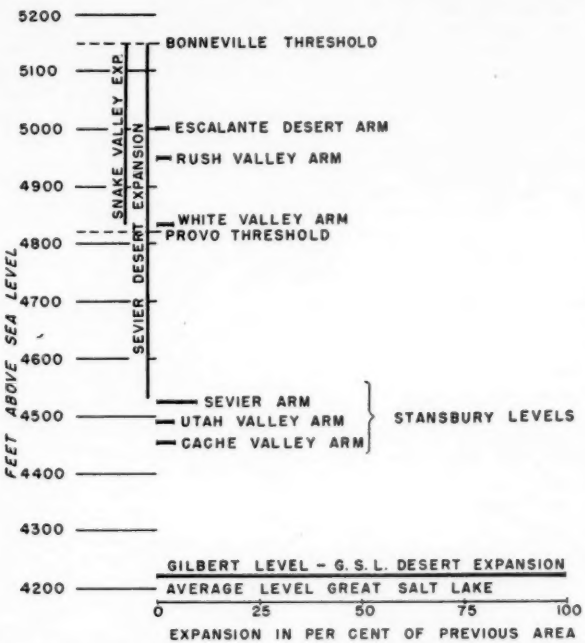

FIGURE 9.—THRESHOLD ELEVATIONS AND AREA OF EXPANSIONS OF LAKE BONNEVILLE

The principal problems concerning the Stansbury shores which are recognized at the present time are:

(1) Do the beaches represent one stabilized water plane, or several, or none?

(2) How many times has the lake stood at one level or at several?

(3) Is a climatic minimum indicated, or are the stabilized levels due to expansions into overflow basins? Is there a possibility of a combination of both?

These problems are considered first by a survey of the overflow basins; second, by a scrutiny of the elevations and sedimentary makeup of Stansbury beaches on the Salt Lake salient, the Jordan Valley, and the northern ends of the Stansbury and Oquirrh ranges; third, by a study of fossil soils related to the Stansbury shores; and fourth, by an analysis of cores from Great Salt Lake.

EXPANSIONS: The several major expansions of Lake Bonneville that may have served to regulate or stabilize the rise or fall of the water surface are tabulated in Figure 9. Of significance in the Stansbury problem are the three basins, Cache Valley, Utah Valley, and Sevier Lake basin. All three are near the eastern rim of the Bonneville Basin and receive major streams from the Wasatch Mountains and High Plateaus; Cache Valley receives the Bear River, Utah Valley receives the Provo River, and Sevier Lake basin receives the Sevier River. Cache and Utah valleys have outflowing streams today and in the early Pleistocene probably had outlets much like those of the present except for the beach and bottom deposits of Lake Bonneville. The Point of the Mountain spit closed or nearly closed Utah Valley at the Provo level for a short time, but the spit was trenched as the main body of water fell. The gorge known as the "Gates of the Bear River" by which Cache Valley is

drained was in existence before Bonneville history; judging from topographic maps the floor of the valley, although swampy in places today, was not closed at any time during the Pleistocene. Sevier Lake overflowed into the expanded over the broad Sevier Desert floor could there have been much of a stabilizing influence.

Considering expansions into Cache, Utah, and Sevier basins the writers conclude that

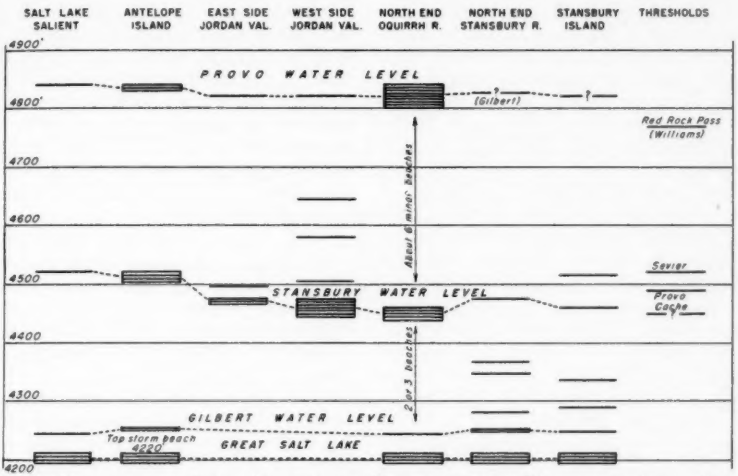

FIGURE 10.—ELEVATIONS OF SHORE LINES ALONG EAST AND SOUTH MARGINS OF GREAT SALT LAKE

main body of water when it stood at the Stansbury level (4479 feet approximately), but the present inflow is considerably less than sufficient to cause outflow.

If the lake rose from 4420 to 4470 feet it would flood Cache Valley; the increase in the surface and proportionate increase in evaporation would be 2.3 per cent. Utah Valley would be flooded at about 4500 feet, and the increase in area would be 2.2 per cent. It seems that the regulatory effects on the lake's surface elevation would be relatively negligible by expansions into these valleys because of major "through streams" and because of relatively small increase in evaporation area. The effect would probably be pronounced only if the imbalance of evaporation and precipitation were slight.

The "Old Channel" (Fig. 1) indicates that when the lake rose to about 4400 feet Sevier River had already filled the Sevier Lake basin to about 4520 feet; Sevier Lake was overflowing and about 75 feet deep. The relative area of Sevier Lake at this time would have been 11.2 per cent of the major lake, yet the increase of evaporation thus effected was already being sustained by the enlarged Sevier River inflow. Only as the lake rose above the threshold and they could have had only minor regulatory influence on the level of Lake Bonneville and that they are not a key to the Stansbury problem.

Elevations of Stansbury Water Planes

The elevations of shore lines along the east and south margins of Great Salt Lake are charted in Figure 10. The writers noted shore lines on the extreme west side of the Bonneville basin, but accurate topographic maps are lacking, and meaningful elevations have not been determined. Distances from benchmarks are too great to warrant dependence on aneroid readings where an accuracy within 10 feet is required. Nevertheless, the relations everywhere the writers observed them are exemplified by the elevation figures along the south and east margins of Great Salt Lake, and these data should be sufficient for an understanding and analysis of the problem.

It may first be observed that one dominant Stansbury shore line exists. Minor shore lines above and below may be noted, particularly on steep slopes facing the north, northwest, or west. Multiple shore lines on alluvial-fan piedmonts are conspicuous on aerial photo-

graphs. Yet in every place observed by the writers one beach stands out above the others. Its elevation is fairly uniform in Jordan Valley, the north ends of the Oquirrh and Stansbury ranges, and on Stansbury Island but conspicuously higher on the west face of the Salt Lake salient. Even on the new topographic maps elevations of the beach cannot be determined with certainty. Also, the water surface cannot be judged from the beach features consistently. These two factors may be the source of the 25-foot variation in the height of the water plane at localities other than the Salt Lake salient.

A third cause of variation in elevation of beaches is vertical movements of the earth's crust. Fault-block movements are most evident in the region, but warping movements may also have occurred. In the excavations of Utah Sand and Gravel Company pits on the Salt Lake salient an alluvial fan has been built over the Stansbury deposits which here are represented by a gravel spit with much material from the Farmington complex about 6–10 miles to the north (Jones and Marsell, 1955, p. 108). Faulting of 40–50 feet displacement has occurred since the bulk of the alluvial fan was built. The fault scarps are very crisp across the alluvial fan, and the gravel pits reveal the post-Pleistocene displacement. If the Salt Lake salient moved up 50 feet relative to sea level and the fault block on the west remained stationary, the dominant Stansbury shore along the Salt Lake salient should be 50 feet above the shore lines west of the fault. This relation is strongly suggested by the fact that the Stansbury water plane on the Salt Lake salient is 4520 feet in elevation and the others average about 4470 feet (Fig. 10). The Bonneville level is about 60 feet higher than normal on the Salt Lake salient; if this figure can be relied upon, about 10 feet of upthrow occurred before the Stansbury spit, and about 50 feet occurred afterward.

Gilbert (1890, p. 340) postulated isostatic adjustments in the Bonneville basin that were due to the filling and emptying of the basin with the waters of the great lake, but elevation control at present is too thin and inaccurate to judge the effects of warping.

CORRELATION OF THRESHOLDS AND SHORE LINES: The last column of Figure 10 shows the threshold elevations at the general Stansbury level in relation to the shore lines noted. From these relations and the above discussion it may be concluded that the three expansions have only a general relation to the shore lines. Because of their nature they could have had only a very slight regulatory control on the lake's surface. Since one strong beach exists in the range of 4445 to 4475 the lake fluctuated within this range for some time apparently uncontrolled by expansions.

CONCLUSIONS: One dominant beach with a water plane which fluctuated within the narrow range of about 30 feet was built during the last stand of the lake at the Stansbury level. The control of this surface elevation could not have been due to expansions into overflow basins, and therefore it must be assumed that nature reached a balance of precipitation and evaporation within the limits of fluctuation noted without special regulatory controls.

Meaning of Multiple Shore Lines

The prominence of multiple shore lines repeatedly referred to by Gilbert is emphasized by modern vertical aerial photographs. Plate 3 shows a succession of many regular small beaches. The small ones are scarcely recognizable on the ground, but the major ones, Bonneville, Provo, Stansbury, and Gilbert, stand out plainly. Multiple beaches like these are common around the Great Lakes and in places are sharply impressed on the aerial photos because of zones of vegetation. They are explained in that area as a succession of storm beaches as the lake level fell. A major storm every few years (perhaps 5–20) would result in a strong storm beach 5–15 feet above the normal level of the lake. With the lake level generally falling, this beach would be left free from waves until another pluvial maximum occurs. The photographic tone of the interval between the Bonneville and Provo is relatively dark, the interval between the Provo and Stansbury is medium, and the interval from the Stansbury down is light. As concluded below, the lake fell below the Provo level, rose back to it, fell below the Stansbury, rose to the Stansbury, and then fell to the Gilbert. This leaves each succession of storm beaches separated by a time interval, and because of subjection to subaerial weathering for different periods of time each succession would have a different photographic tone.

In places two, three, or four intermediate beaches are rather prominent. In a few places minor beaches exist between the prominent intermediate ones. In some places, however, especially on steep slopes, only the major beaches are discernible. A number of saddles have been noted, particularly tombololike con-

nections to former islands or remnants of headlands, which are particularly flat and look like major beach levels. These generally are not at a prominent level but are marked a mile away by an inconspicuous beach, if any. Thus, as the lake rose or fell, certain settings were very favorable for wave action, both erosional and depositional, and certain impressive levelings were formed quickly but are not necessarily indicative of a stabilized water surface.

Sedimentary Record

Preliminary Considerations

At the onset of the glacial and pluvial epoch the Bonneville basin looked much as it does now, especially in gross relief. The shore lines, the recent fault scarps, and a few conspicuous post-Pleistocene fans were not present, but ranges rising sharply from either alluvial fan or pediment piedmonts dominated the landscape. Major rivers from the Wasatch and High Plateaus had well-developed flood plains through some of the basins; bottom lands of the playa type dominated in others. As the lake waters accumulated the playas and river flood plains were flooded, and the waves played against either alluvial fan, pediment, or bedrock slopes. Although the beaches of Lake Bonneville are impressive, the amount of erosion and amount of material transported and deposited is insignificant except in a few places where sizable spits and deltas were built, or along the Wasatch where bottom deposits up to 100 feet thick accumulated (Hunt *et al.*, 1953, p. 17). The pre-Bonneville land forms dominate the scene and give the impression that the lake rose and fell rather quickly, reworked only a thin surface veneer of the pre-existing fan or pediment, and left a weak mark of its presence (Marsell and Jones, 1955, p. 115).

As in the Great Lakes region and along marine shore lines the highest water plane has generally left the most conspicuous impression, although the water surface may not have held at the maximum elevation as long as at some lower level. The writers conclude on following pages that the lake rose to the Provo level a second time and also rose from a lower level to the Stansbury; in such cases the elevation of maximum rise should be strongly marked.

During the first rise of Lake Bonneville the sediments deposited were different from those of later rises. The Alpine Formation (Hunt *et al.*, 1953, p. 17; Jones and Marsell, 1955, p. 93) is largely silt and is believed to be more voluminous than the post-Alpine sediments. It is commonly pink, rusty, or tan and differs from the gray sands and gravels of the younger lake deposits. An abundance of silt may have been present originally because of desert sands and silts blown high upon the mountain slopes or because of the development of a thick soil over the piedmont and lower mountain slopes. In either situation the waves of the Alpine lake stage would have found much more silty material to work on than those of later stages.

The writers follow Hunt *et al.* (1953, p. 17) in recognizing the Alpine as the first stage of the Bonneville Lake history. At least it was the first high-level lake. Jones and Marsell (1955, p. 92) recognize the "green clay series" under the Alpine; this series has nearly the same facies variations but not the same color. The green clays must represent an older lake, but any shore lines connected with them are obscure. Hunt describes two sequences of Pleistocene deposits, in the wells of Geneva steel plant in Utah Valley, that represent two lake stages older than the Alpine. Again the associated shore lines are obscure. Drainage into local basins before the Alpine was not necessarily the same as it is now, because in some areas of the Bonneville basin major displacements may have occurred along some of the Basin and Range faults in early Pleistocene time and changed the local drainage conditions perceptibly. It appears that the most detailed Pleistocene sedimentary record is preserved in the sediments of and under Great Salt Lake, but to date a continuous core has been taken only to a depth of 44 feet.

Alpine and Bonneville Deposits

The Alpine deposits are abundant up to an elevation of 5050 feet (Jones and Marsell, 1955, p. 97). Hunt *et al.* (1953, p. 17), Jones and Marsell (1955, p. 97), and Bissell (1952) believe that this elevation is about the upper limit to which the lake rose at the Alpine stage. Like Gilbert, they believe that the lake did not overflow and cut down its outlet at this time, because it fell and later rose again about 85 feet higher than the Alpine maximum to about 5135 feet, when it first overflowed at Red Rock Pass. The Bonneville shore line, conspicuous today, marks the 5135-foot stage (Bonneville stage), but the deposits of this lake are meager (Hunt *et al.*, 1953, p. 20; Bissell and Jones, personal communication). The broad and conspicuous Bonneville shore line on the Traverse Range and the associated spit may

seem anomalous to other parts of the shore line, but the writers have concluded that a pre-Alpine pediment served as a gently sloping base, first in Alpine time and later in Bonneville time, for the easy building of the wide beach. A cross section is shown in Figure 11. The Bonneville spit is compound; the portion below about 5000 feet is of Alpine growth, and lower Jordan Valley and adjacent areas, and the upper sketch of Figure 11 illustrates a common relation of the two features.

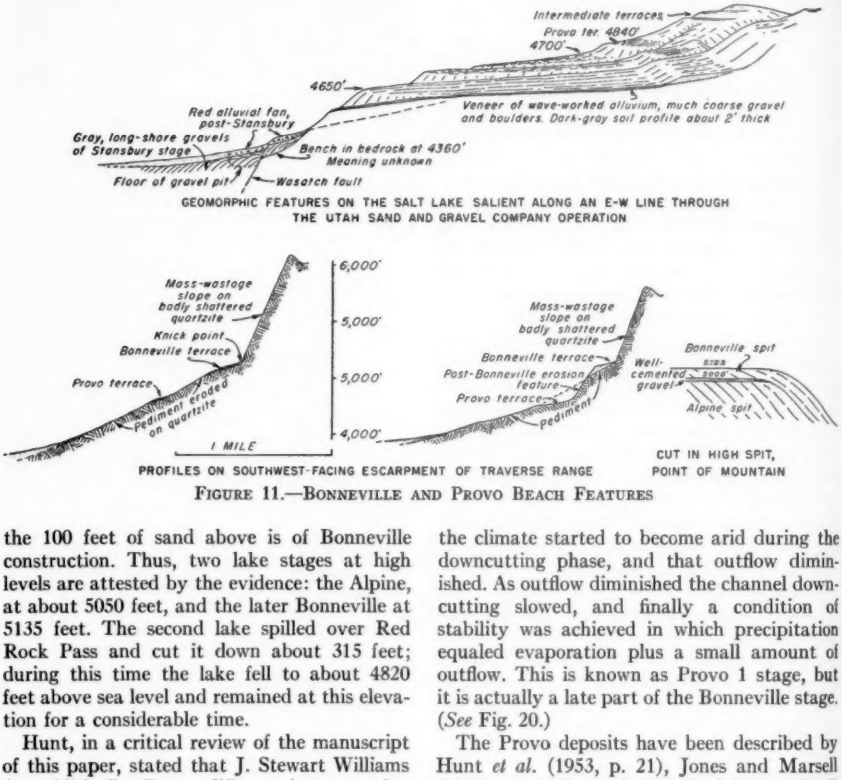

FIGURE 11.—BONNEVILLE AND PROVO BEACH FEATURES

Provo Deposits

Since the lake later fell below the incised Red Rock Pass outlet it can be assumed that the climate started to become arid during the downcutting phase, and that outflow diminished. As outflow diminished the channel downcutting slowed, and finally a condition of stability was achieved in which precipitation equaled evaporation plus a small amount of outflow. This is known as Provo 1 stage, but it is actually a late part of the Bonneville stage. (*See* Fig. 20.)

The Provo deposits have been described by Hunt *et al.* (1953, p. 21), Jones and Marsell (1955, p. 100), and Bissell (1952). Bissell particularly, and probably first, recognized the dual nature of deposits at the Provo level and concluded that the lake fell from the Provo 1 stage to drain Utah Valley and then rose again to within about 40 feet of the previous level.

Jones and Marsell describe the relations in the Lower Jordan Valley as follows.

"Many of the exposed shore features exhibit a dual nature, with nearly identical deposits superimposed one above the other . . . this is substantiated in the deposits [of the Draper spit] . . . by the

the 100 feet of sand above is of Bonneville construction. Thus, two lake stages at high levels are attested by the evidence: the Alpine, at about 5050 feet, and the later Bonneville at 5135 feet. The second lake spilled over Red Rock Pass and cut it down about 315 feet; during this time the lake fell to about 4820 feet above sea level and remained at this elevation for a considerable time.

Hunt, in a critical review of the manuscript of this paper, stated that J. Stewart Williams (unpublished) offers a different interpretation of the Alpine and Bonneville stages, as a result of his work in Cache Valley: "He feels that the Bonneville formation represents the culmination of the Alpine, that the unconformity between the Bonneville and Alpine is merely a minor diastem due to overlap of coarse clastic onto fine grained sediments. He shows Alpine and Bonneville formations undifferentiated."

Pediments are common on the middle and lower slopes of ranges of the Bonneville Basin and must be distinguished from the beaches. Figure 7 shows the pediments recognized in the

well-developed soil profile on the inclined beds of the lower delta lobe."

The high unit of the Draper spit stands at 4800–4820 feet, and a southward extension or terrace at 4760 feet, according to Jones and Marsell (1955, p. 103), marks the maximum rise of the second Provo stage. The proposal that the maximum rise of the lake during the Provo 2 stage was to the 4750– to 4760–foot level poses a problem, because little evidence of shore features is found at this elevation. The narrow terrace on the west side of the Draper spit to which Jones and Marsell refer may be traced for less than 1 mile, and no other terrace could be detected by the writers in the lower Jordan Valley at this elevation. At one or two places on the north end of the Oquirrh Range a bench of limited extent is noted below the one strong Provo terrace. The Provo terrace is generally sharp and strong and greatly outshadows any minor beaches immediately above or below.

According to the above evidence the Provo 1 stage is the late part of the Bonneville and represents a temporary stillstand in a falling lake. If the lake rose to a maximum in the Provo 2 stage, then the Provo 2 shore line probably should be stronger than the Provo 1, and if the two were not essentially developed at the same level, there should be two prominent beaches. The writers conclude that the second Provo rose to the same level as the previous Provo 1 lake and probably overflowed through the channel at Red Rock Pass.

Bissell (Personal communication) found an alluvial fan, in Utah Valley, built over the Provo 1 deposits and notched by the Provo 2 waters. The terrace is at 4750-foot elevation. Approaching Red Rock Pass in the north end of Cache Valley, Williams (1952) measures the elevation of the Provo terrace at 4770 feet (Utah Geological Society, Cache Valley, 1955, cross sections in road log). Here the Bonneville water surface is estimated at 5135, the same as in the Salt Lake City and Jordan Valley area, and thus the variation cannot be accounted for by faulting. Special attention in the field must be given to Bissell's and William's localities and the problems involved must be kept in mind. The observation of one strong beach is impelling evidence for the conclusion that Provo 2 lake rose to the same elevation as Provo 1, and this is the concept portrayed in Figure 20.

A second problem is the level to which the lake fell between Provo 1 and Provo 2. The concept of two lakes at the Provo level is relatively new, and previous workers have not sought to distinguish deposits of the two lakes. The principal observation has been that "Provo" deposits rest unconformably on Alpine (Hunt *et al.*, 1953, p. 21; Jones and Marsell, 1955, p. 100); since the unconformable relations are seen as low as 4300 feet (Lofgren, 1947, M.A. thesis, Univ. Utah, p. 43) in the lower Jordan River Valley, the lake fell below 4300 feet, either between the Alpine and Bonneville stages or between the Bonneville-Provo 1 and Provo 2. If the lake fell between Provo 1 and 2, then either no sediments were deposited during the Bonneville-Provo 1 stage, or they were deposited and locally removed where the unconformity is observed.

Jones (Jones and Marsell, 1955, p. 106) recognized four distinguishable assemblages of ostracodes in the lake deposits: the Green Clay fauna, the Alpine fauna, the Provo fauna, and the post-Provo fauna. On a field trip with Bissell in the low pass area between Utah Valley and Juab Valley Jones found a fifth fauna in a sizable deposit of Bonneville sands and silts; this fauna comes between his Alpine and Provo faunas. If the concept is correct that the lake rose to the Bonneville level, overflowed at Red Rock Pass, fell rather quickly to the Provo level, and lingered there as Provo 1 stage for some time, then at levels below 4800 feet the Bonneville and Provo 1 deposits would be conformable and part of one continuous sedimentary cycle. They should not be separated by a time interval long enough to produce conspicuous evolutionary changes, and therefore the Bonneville fauna would be the same as that of Provo 1. Since the new Bonneville fauna has not been recognized by Jones in Provo deposits in his numerous samplings, it seems probable that most of his identifications have been from Provo 2 deposits. Thus, deposits of the Bonneville-Provo 1 stage may not be very voluminous and in a number of places are absent. This agrees with all observers' notations of the Bonneville stage deposits but not the Provo deposits. The unconformity generally observed between "Provo" deposits and Alpine may commonly lie between Provo 2 and Alpine, and therefore the conclusion is drawn tentatively that the lake fell to a level well below 4300 feet between Provo 1 and 2 stages.

Hunt does not agree with the emphasis placed by the writers and by Jones and Marsell on the distinction between Provo 1 and Provo 2. He says in review of the manuscript of this paper:

"... the unconformity and overlap are real. However, the volume of sediment above the unconformity is nil compared with the rest of the formation. It approaches the ridiculous to give this thin and poorly defined deposit a rank equal to that of the Provo formation. As a matter of fact, there

salient and at the north end of the Oquirrh Range reveal the complex nature of the rock-cut benches and the silts, sands, gravels, and tufas of the lake, and the talus, alluvial fans, and slope wash of subaerial origin at this general elevation. As the lake rose and fell several times

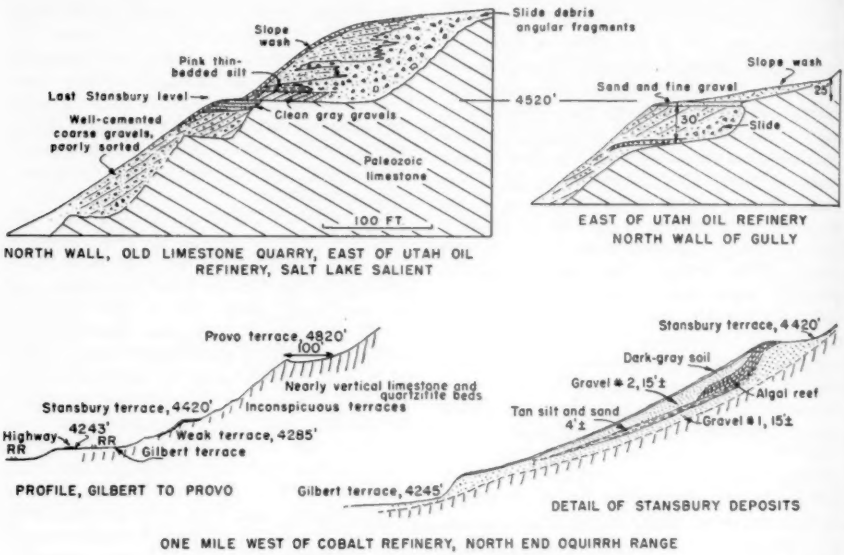

FIGURE 12.—STANSBURY BEACH DEPOSITS

may be several of these minor readvances because we cannot be sure about the correlation of the unconformities and overlapping deposits at isolated localities."

The fossil soil separating Provo 1 from Provo 2 deposits in the Reynolds gravel pit in the Cottonwood-Draper spit (Fig. 7; Jones and Marsell, p. 101, Fig. 30d) and the fossil soil in the Bacchus pit, also separating Provo 1 from Provo 2, support the concept of two lake stages separated by a long interval. At these two localities the volume of sediments is appreciable and evidently more than Hunt observed in Utah Valley.

Stansbury Deposits

Except for the near-shore spit along part of the west front of the Salt Lake salient (Jones and Marsell, 1955, p. 108) the beach deposits of the Stansbury levels have not been described. Numerous gravel pits along the Salt Lake

onlapping and offlapping deposits might have formed at the Stansbury level with each cycle; slight hesitations of the lake may have occurred at the Cache Valley, Utah Valley, and Sevier Lake basin expansion levels. If the deposits of each rise and fall were preserved they would be fairly thick and probably simple to interpret, but part or all of the previous deposit seems generally to have been cut away by the subsequent lake, and an unsystematic arrangement resulted (Fig. 12). A single cycle of onlap and offlap on certain steep slopes exists where perhaps previous lake stages removed the earlier deposits and only those of the last stand at the Stansbury level are present (Fig. 12). According to these lines of evidence, this last stage appears to be a post-Provo 2 episode:

(1) The single cycle of onlap and offlap deposits associated with the tufa deposits at the north end of the Oquirrh Range (Fig. 12) is tied to the dominant Stansbury level. Carbon-14 dates on the tufa indicate that it is younger than tufa of the Provo level and confirms the

concept of a Stansbury stage. (2) The last fresh-water stage of sedimentation in the sediments below Great Salt Lake relate by carbon-14 to the Stansbury tufas. (3) The river activity on the lake-bottom deposits below the Provo level and above the Stansbury presents the strongest evidence of a fall of the lake from Provo 2 to below the Stansbury and a later rise to, and maximum stand at, the Stansbury. Related to the stream activity are fossil soils which confirm the indication of the terraces. These points will be discussed below.

Gilbert Deposits

Most of the deposits of the Gilbert beach, where observed, are in the form of bars and spits. They consist of gravel and sand of local derivation. Cuts, either natural or artificial, are few; the structure is simple and points to the conclusion that the deposits were formed during the lake's last stand at the threshold elevation of 4245 feet. Figure 1 of Plate 2 illustrates an example.

Great Salt Lake Sediments

INTERPRETATION OF CORES: A barge was built with mast, windlass, pump, and accessories for procuring cores from the bottom of Great Salt Lake (Cohenour, 1952, M.A. thesis, Univ. Utah). The barge was towed to several places in the south-central part of Great Salt Lake between Stansbury and Antelope islands where a number of cores were procured. The deepest core hole penetrated 44 feet below lake bottom. Schreiber (Ph.D. thesis, Univ. Utah, in preparation), analyzed and interpreted the cores and sections of post-Stansbury sediments from a few places in the Jordan River area. Some of the conclusions of Schreiber are diagrammed in Figure 13. The sediments are gray limy silts and clays with fecal pellets and egg capsules of the brine shrimp to a depth of about 17 feet. From 17 to 30 feet is a layer of dark, organic-rich, foul-smelling, limy silt and clay. From 30 to 44 feet, the greatest depth penetrated, the sediments are gray, limy clays, silts, and sands, with fecal pellets. Schreiber concludes that the upper layer, from the bottom to 17 feet, is a brine deposit similar to the sediments accumulating in Great Salt Lake today, that the dark layer from 17 to 30 feet is a fresh-water lake deposit in the deepest part of the lake where foul reductive conditions prevailed, and that the layer from 30 to beyond 44 feet may again be a brine deposit.

Dr. Meyer Rubin of the U. S. Geological Survey offered to make a C^{14} analysis of the dark sediments of the fresh-water stage and two samples were submitted, as indicated in Figure 13. Because of a misunderstanding, the two samples were mixed together and run as one, and an age for the organic carbon of 16,850 ± 300 years was determined. Doctor Rubin also ran the carbon in the calcium carbonate of the sediment and determined an age of 16,680 ± 300 years. This nearly perfect agreement was not expected, but he writes (Personal communication) that he had already found a surprising agreement in a sample of trona from the Upper Salt of Searless Lake. His carbonate carbon age agreed closely with an age determined by Libby on the organic material.

About a year later Wallace Broecker of the Lamont Geological Observatory ran two samples from core 4 at the top and the bottom of the fresh-water sediment interval and obtained the following results:

14- to 16-foot interval (bulk inorganic CO_2) — 12,500 ± 250 years

31- to 33-foot interval (organic CO_2) — 26,300 ± 1100 years

(bulk inorganic CO_2) — 25,300 ± 1000 years

These results are consistent with themselves and with Rubin's intermediate analysis and appear to establish the age of the last fresh-water stage. It may be thought of as beginning about 23,000 years ago and ending about 13,500 years ago.

RELATION TO DANGER CAVE C^{14} DATES: Danger Cave is situated about 1 mile northeast of Wendover, Utah, at an elevation of 4310 feet. It is near the western margin of Lake Bonneville and would have been under water for all lake stages above 4310 feet, which is 110 feet above the present Great Salt Lake. The Gilbert shore lay immediately down an alluvial slope from the cave, a vertical distance below of about 65 feet. The cave has been excavated by Dr. Jesse D. Jennings and associates, and a remarkable record of ancient human occupation was uncovered. The stratigraphy and cultural levels in the cave are diagrammed in Figure 13. The drawing is taken from Jennings (1953, p. 179, Fig. 2).

Wave-washed gravels are at the base and mark the last time that the cave was flooded by the waters of Lake Bonneville. Carbon-14 dates were determined from the organic debris

FIGURE 13.—GREAT SALT LAKE SEDIMENTARY RECORD AND DEPOSITS OF DANGER CAVE

of the several cultural layers, and they range from 11,450 ± 600 years to 1930 ± 240 years before the present. It is immediately apparent that the Danger Cave date of 11,450 years marks the end of the last fresh-water lake and tallies closely with the carbon-14 date on the fresh-water sediments in the Great Salt Lake core.

RELATION TO TUFA C^{14} DATES: Realizing the possibility of dating by carbonate carbon, the writers obtained tufa samples from the shores of Lake Bonneville and submitted them to Doctor Rubin for analysis. The samples were collected at the north end of the Oquirrh Range 1 mile west of the cobalt refinery. Two samples were taken from the tufa of the Stansbury beach, one 40 feet below the other, and one sample was taken from the Provo. The two at the Stansbury level ran 14,000 ± 450 years, and the one at the Provo level ran "greater than 32,000 years."

The figure of 14,000 years for the Stansbury tufa is compatible with the Great Salt Lake core dates and the Danger Cave date.

Doctor Broecker recently ran more tufa samples taken from the Bonneville and Provo levels at the north end of the Oquirrh Range and from Utah Valley. The results are inconsistent, and, at present, baffling.

Feth and Rubin (1957, p. 17) recently announced (Unpublished) radiocarbon dates of four tufas at the Stansbury shore line; they range in age from 14,000 ± to 18,000 ± 1000 years. This is consistent with previous determinations. They also report on lower deposits as follows:

Wood in clay soil, Harrisville, elevation 4290 feet—8330 ± 300 years B.P.

Shells in clay soil, Harrisville, elevation 4290 feet—7720 ± 300 years B.P.

Plant stems in sand, Hooper, elevation 4235 feet—9730 ± 350 years B.P.

The plant stems at 4235 feet are just below the Gilbert level, and their age is consistent with deductions (Fig. 20), but the shells and wood from a locality 55 feet higher are dated as younger. The elevation, 4290 feet, is 20 feet lower than Danger Cave from which the waters last fell 11,450 years ago. If these three dates are correct, then the lake fell below 4310 feet about 11,450 years ago, sank to the 4245-foot (Gilbert) level, rose to about the 4290-foot level, then sank to the present. The analyses of the cores in Great Salt Lake and of the Jordan delta do not confirm this interpretation, and the writers regard the 4290-foot date as irregular and erroneous. The shells and the wood, deposited at the same time but analyzed separately, show ages 610 years apart. This difference suggests that carbonate carbon dates are not well understood. The same problem is emphasized in analyses of samples near Ogden at an elevation of 4650 feet, where a peat bed has an age of 9925 ± 300 (10,260 ± 300 on a rerun), and an overlying marl has an age of 12,960 ± 350. These dates at elevations above the Stansbury are younger and seem definitely irregular to the writers. Feth and Rubin date Provo level tufas from 11,380 ± 500 years to more than 32,000 years and one at the Bonneville level at 11,300 ± 300 years; these results are similar to Broecker's. The lake could not have been at the Bonneville level (5135 feet) at the same time as the Danger Cave level (4310 feet), and therefore the writers can place little reliance on carbonate carbon dates until the factors involved are better understood. Dates of organic carbon in contact with carbonates must be regarded critically, also. This is true of the dates of the samples of cores from Great Salt Lake, but here for some reason the several dates are consistent; they may be consistent with each other but still not an absolute measure of time.

Soils of Bonneville Basin

Significance and Scope of Investigation

Within and below the Bonneville deposits a number of soils have been noted in recent years whose significance as chronometers and climatic indicators has been called to the writers' attention by several investigators (Hunt and Sokoloff, 1950, p. 109; Hunt *et al.*, 1953, p. 42; Gvosdetsky and Hawkes, 1953, p. 9; Richmond *et al.*, 1952, p. 1369). Gvosdetsky spent three summers in the field and most of the associated winter months in the laboratory studying the soils of the Bonneville Basin, and the significant results follow.

Definitions

Soil is an independent natural body whose formation and development is based on five principal factors: (1) parent material, (2) biological activity, (3) climate, (4) relief, and (5) time. Under a given set of conditions (parent material, vegetation, climate, and relief) and during a certain time interval, soil becomes mature with a definite soil profile. Such a soil

is described as a normal or monogenetic soil (Bryan and Albritton, 1943, p. 472–477). If the variables of soil development are altered, however, by changes in climate, a new soil profile develops on the older profile. Such a soil is described as a complex or poligenetic soil. Both the monogenetic and poligenetic soils found on the surface of the land are living soils. The age of a living mature soil may range from hundreds and thousands of years in glaciated areas to millions of years under favorable relief conditions in unglaciated areas.

If a soil is buried its normal development is arrested, and it is subjected only to geological process of the subsurface. Buried soils are fossil soils. Profiles developed under subaerial conditions are usually preserved for a long time. The most stable part of the soil profile is the soil skeleton (particles over 1 mm in diameter); this persistent skeleton, with certain secondary minerals, is the "paleopedological bones" of the fossil soil (Nikiforoff, 1943, p. 197).

Podzols are soils of temperate and cool humid climates. In the upper light-gray or A_2 horizon all compounds except silica are removed or translocated to the underlying B horizon, which is enriched with sesquioxides of iron and aluminum. The colloidal sesquioxides are responsible for the clayey composition of the B horizon and make it red-brown. Carbonates and soluble salts are removed from the podzol profile. Mature mountain soils are largely podzols.

Laterites are soils of tropical and subtropical humid climates, usually red and very thick. In the process of laterization all minerals are decomposed, and all chemical components except the sesquioxides of iron and aluminum are removed.

Types of Soils Recognized

A number of different types of soils have been deciphered in the Bonneville Basin, and several classifications are possible. A classification based on physical and chemical characteristics without climate or age connotation is the most objective, but for informative headings a classification based either on genesis or on age would be better. The first of these last two is complicated by the fact that some soils are poligenetic and indicate the superposition of a profile of one climate on the profile of another. The age classification is not satisfactory either, because a soil that developed in the past may in places have been buried and preserved with little change, or in places it may have been left exposed to continued soil development. The buried soil would be a good marker between two stratigraphic units, but the exposed soil would serve only approximately for age determination.

For the present study divisions were set up based chiefly on stratigraphic position: post-Stansbury soils, post-Alpine pre-Stansbury soils, pre-Alpine soils, and mountain soils. The division of mountain soils is based on origin and therefore stands apart from the other three age groups. The mountain soils occur higher in elevation than the stratigraphic units of the several lakes and therefore are not generally significant in the lake history. In a study of the history of Lake Bonneville, the value of a discussion of the mountain soils lies chiefly in noting them and distinguishing them from the other groups of soils which are directly associated with the lake's stratigraphic units and history.

Post-Alpine Pre-Stansbury Soils

Characteristics and General Relations

The soils of post-Bonneville interpluvial times are dark-gray and light-gray grassland soils that were formed under semiarid or fairly moist steppe climates. They are sometimes called the prairie soils. They consist of an upper A horizon and an intermediate B horizon, both humified and leached of carbonates, and a lower C horizon, enriched in carbonates and consequently light gray. They are generally mature soils and if not partially removed by erosion range from 4 to 6 feet thick.

The dark-gray interpluvial soils in certain favorable situations separate deposits of one lake stage from those of another. A soil developed on lake-bottom sediments after the lake falls will generally be removed by the waves as the lake rises again, and thus no soil will separate the two sedimentary units. Where a stream has cut a shallow but fairly wide valley in the bottom sediments as the lake recedes to a new base, a soil will form on the stream flood plain and will be buried as the stream aggrades its valley as the lake rises. Finally, the lake submerges the flood-plain deposits, but the interpluvial soil is preserved. This is the common locale for fossil soils between stages of Lake Bonneville.

Some soils in unique places have had a beginning in post-Alpine time and are reddish-brown podzolic soils. They occur on the high,

cool, fairly humid piedmont and mountain slopes.

Soils of the Bacchus Area

SETTING: Fossil soils were observed at several localities in the Bonneville Basin, but the most striking exposures studied are about 20 miles southwest of Salt Lake City and 1.5 miles northeast of the settlement of Bacchus (Fig. 7, T. 2 S., R. 2 E). In this area a huge gravel pit in process of development afforded an opportunity to observe and examine for almost a year a constantly changing picture of fossil soils and buried topographic features. The gravel pit is situated between the elevations of 4550 and 4700 feet above sea level; within the worked zone is an array of unconsolidated deposits resting on the upturned and beveled strata of the Jordan Narrows unit of the Salt Lake group and possibly the Camp Williams unit, both Tertiary in age (Slentz, 1955, p. 25).

The variety and arrangement of Quaternary deposits will best be understood by reference to Figure 14. The older deposits have been incised by Coon Creek, and along its course an upper and lower terrace and flood plain are the prominent topographic features. The Provo lake terrace is above and the Stansbury below (Fig. 7). The locality in relation to the lake floor extends eastward from the pit, and the waves and longshore currents have made prominent spitlike terraces at several elevations. The source material, upon which the lake worked as it originally rose and probably reworked in part during future fluctuations, consisted principally of alluvial-fan and pediment-veneer material. The east bench of the Oquirrh Range was an extensive alluvial-fan bajada in early (?) Pleistocene time, and the alluvial fans were graded to an extensive pediment. In places the fanglomerate was removed and the Jordan Narrows unit exposed (Slentz, 1955, p. 23). A small amount of material that came to repose in the Bacchus pit area could have come from the rock mantle of the gullies and steep slopes of the northern end of the Oquirrhs, but the chief source was the fanglomerate and scattered exposures of Jordan Narrows tuffs and marls. The oldest alluvium that rests on the Jordan Narrows Formation in the Bacchus pit is regarded as shore sands and gravels of the lake at the Provo level. These underlie the upper terrace and in major part were formed as an offshore terrace or spitlike deposit without a complementary lagoon. The lower beds are sandy and dip gently; the middle beds are gravelly and appear as more steeply dipping foresets; the upper layer, also gently dipping, consists of pebbles and cobbles, some more than 1 foot in diameter. As explained below, these deposits are believed to be those of the Provo 2 stage. In another place in the pit (Gvosdetsky and Hawkes, 1953, Fig. 3) a reddish-brown loam underlies the gray sandy beach beds and may represent the Alpine Formation of Hunt *et al.*

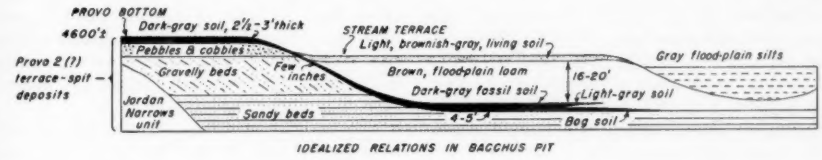

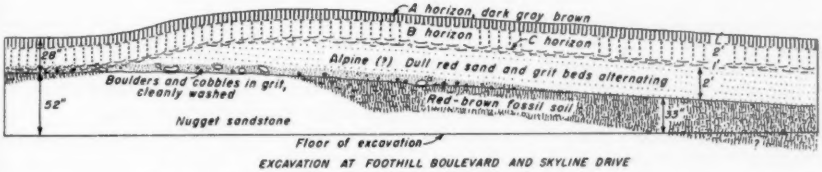

FIGURE 14.—SOILS AT BACCHUS PIT AND EAST SALT LAKE CITY

The deposits of the Provo 2 stage were thus dissected by Coon Creek after the lake fell, and the dissected valley was partly alluviated as the lake rose again; this was due to the changes in base level of the stream. The brown loam underlying the lower terrace is regarded as a flood-plain deposit. It was slightly dissected, and later the incisions were filled or nearly filled.

STRATIGRAPHY AND SOILS: The upper terrace is covered with a dark-gray living soil measuring 2½–3 feet in depth. The humified *A* and *B* horizons are leached of carbonates; the well-developed *C* horizon beneath, whitish from the carbonates above, measures 3 feet in depth. The lower boundary of the *C* horizon is well defined, since it coincides with the horizon of large cobbles measuring up to 1½–2 feet in diameter.

The dark-gray soil of the upper terrace extends along the slope until buried beneath the light-brown loam of the lower terrace. At this point the dark-gray soil becomes a fossil soil. On the slope the depth of the fossil soil decreases to several inches as a result of erosion, but downslope beneath the younger deposits of the lower terrace the depth of the dark fossil soil increases up to 60 inches. The uniform layer of brown loam overlying the fossil soil measures 16–20 feet thick.

The lower terrace exhibits a light-brownish-gray living soil on the brown loam, whose *A* and *B* horizons are about the same in thickness as those on the upper terrace. The lower-terrace soil is much lighter than the upper-terrace soil, and the *C* horizon is not so conspicuous, since the entire soil profile was developed on rather homogeneous loamy deposits, whereas the soil on the upper terrace was formed on a pebble and cobble layer. The carbonates in the *C* horizon of the upper terrace constitute 40–50 per cent of the soil, whereas in the *C* horizon of the lower terrace they make up only 5–10 per cent.

The 12- to 15-foot bluff between the upper and lower terraces gradually decreases northward or downstream. In a distance of 1250 feet both terraces are at the same level, and since there is no difference in relief at this point, the color of the soil and the stratigraphy distinguishes them.

Immediately west of the area sketched in Figure 14, which is on the west side of the flood plain, there are upper and lower terraces. A cross section in this area reveals a fossil soil 13–15 feet below the surface of the upper terrace. This soil is a brownish-gray humified silty loam more than 5 feet thick. Its location below a Provo 2 soil suggests a corollary of the Provo 1 soil exposed in the Reynolds gravel pit on the east side of Jordan Valley (Jones and Marsell, 1955, p. 101) which separates Provo 1 from Provo 2 deposits of a spit similar to that at the Bacchus pit.

MECHANICAL ANALYSIS: Sixty samples were taken from sections of the Bacchus pit, and from this group 10 were selected as representative of the area. These samples were analyzed in the laboratory for their mechanical, mineralogical, and chemical composition.

The analyses of the mechanical composition were divided into two phases: (1) The per cent of material in the total sample over 1 mm in diameter was computed. This portion of the sample was then further divided, and the per cent of each fraction was computed as a per cent of the entire sample. (2) The remaining material with a diameter of less than 1 mm, or soil proper, was considered as a unit, and each fraction was computed as a per cent of the unit rather than of the total sample.

The per cent of skeletal material in the representative 10 samples is tabulated in Table 2. The high per cent of skeletal material in the living and fossil dark-gray soils (53.4–61.9 per cent) indicates that the parent materials were of similar composition. The difference in percentage of skeletal material in the living (12–19 per cent) and fossil light-gray soil (0.5–2.5 per cent) suggests differences in the composition of the parent materials. This is consistent with the interpretation of the sediments on which the soils have developed —namely, that the dark-gray soil has evolved on the terrace-spit deposits of Lake Bonneville, and that the light-gray soil has developed on the flood-plain deposits of Coon Creek.

The mechanical composition of the same 10 samples as used in Table 2 is tabulated in Table 3. According to the analyses the differences between the soils are much less than the differences of the skeletal materials. All soils have a low amount of clay, ranging from 2.1 per cent to 8.1 per cent with the lowest amount in the *C* horizon of the light-gray fossil soil and the highest amount of clay in the *A* horizons of all soils. These findings are in general agreement with the principal properties of genetic horizons developed under the process of calcification. Since the most intensive soil processes take place in the *A* horizon, this horizon is enriched with inorganic and organic

clay minerals, whereas in the *B* horizon the soil processes are less intense, and the amount of clay is lower. In the *C* horizon, where soil processes are most limited, the amount of clay is negligible.

very low sand fraction (12 per cent) and the highest amount of silt (up to 74 per cent).

The mechanical composition of a soil is generally regarded as a function of parent material. Soil processes, however, change mechan-

TABLE 2.—SKELETAL COMPOSITION OF THE BACCHUS PIT SOILS
(In per cent)

Sample number	Genetic horizon	Soil		Skeleton (mm)				Soil < 1mm
				> 4	2-4	1-2	Total	
1	A	dark gray	living	32.0	11.6	11.7	55.3	44.7
2	B			39.2	5.1	0.1	53.4	46.6
3	A	light gray		3.5	3.3	5.2	12.0	88.0
4	B			8.4	4.7	6.1	19.2	80.8
5	A	dark gray	fossil	38.7	12.3	8.7	59.7	40.3
6	A			52.9	4.6	4.3	61.8	38.2
7	A	light gray		0.3	0.8	1.4	2.5	97.5
8	C				0.3	0.2	0.5	99.5
9	A	bog		0.8	0.4	0.8	3.0	97.0
10	A	brownish gray		0.9	0.6	0.5	2.0	98.0

TABLE 3.—MECHANICAL COMPOSITION OF THE BACCHUS PIT SOILS
(In per cent)

Sample Number	Genetic Horizon	Soil		Sand (mm)					Silt (mm)					Clay (mm)
				1 - 0.5	0.5 - 0.25	0.25 - 0.12	0.12 - 0.06	total 4	0.06 - 0.03	0.03 - 0.015	0.015 - 0.007	0.007 - 0.003	total	< 0.003
1	A	dark gray	living	25.0	5.8	5.0	6.8	42.6	15.5	18.4	10.4	6.4	50.7	6.7
2	B			23.0	4.8	4.0	9.1	40.9	10.7	24.4	13.7	7.3	56.1	3.0
3	A	light gray		10.3	11.7	17.7	21.1	60.8	16.3	11.8	2.7	2/3	33.1	6.1
4	B			9.0	12.2	17.6	20.9	59.7	16.0	14.0	6.4	1.0	37.4	2.9
5	A	dark gray	fossil	23.4	11.3	7.1	8.0	49.8	11.6	12.1	10.6	7.8	42.1	8.1
6	A			17.4	8.0	10.8	14.8	51.2	16.4	13.9	8.2	7.0	44.9	3.9
7	A	light gray		3.5	5.7	20.0	13.4	42.6	21.8	15.0	8.0	6.2	52.0	6.4
8	C			0.9	2.5	10.5	21.2	35.1	26.7	17.0	12.9	6.9	62.8	2.1
9	A	bog		5.3	8.1	13.2	13.3	40.0	16.1	18.8	14.1	7.1	56.1	3.9
10	A	brownish gray		0.4	0.6	2.9	8.2	12.1	37.8	22.0	15.8	8.4	74.0	3.9

According to the mechanical composition all the soils analyzed are loams of various types. The dark-gray soils are distinguished from the others by a high per cent of coarse sand. The brownish-gray humified soil, apparently separating the deposits of Provo 1 and Provo 2 stages, is a silty loam and is distinguished by a

ical composition considerably as a result of decomposition of larger particles into smaller ones and also as a result of the redistribution of material produced by soil development. If these facts are taken into consideration the implication is evident that the dark-gray soils of the upper terrace with a higher percentage

of clay, are older than the light-gray soils of the lower terrace; the inter-Provo (?) soil with the highest amount of clay and silt is older than the dark-gray soil.

MINERALOGICAL ANALYSIS: Individual identification of minerals was not undertaken in the analyses, since the results obtained would not contribute significantly to the immediate problem.[1] In this research, mineral composition is specified by groups of mineral separates based on specific gravity within four mechanical fractions ranging from 0.25 to 4 mm in diameter. The groups by orders of specific gravity were chosen as follows:

Lightest	<1.91
Very light	1.91–2.20
Medium light	2.20–2.51
Light	2.51–2.89
Heavy	>2.89

The general mineralogical composition of the four fractions is tabulated in Table 4. The data portray the inverse relationship between particle size and specific gravity. In the dark-gray living soil on the upper terrace the per cent of light particles with a specific gravity of 2.51–2.89 increases from 26.5 to 78.7 per cent, whereas the amount of very light particles decreases from 33.2 per cent to 6.3 per cent.

Most granules have no heavy particles but have a high per cent of very light particles which range from 12.8 to 79.6 per cent. Medium sand has a high per cent of heavy and light particles; the light particles range from 40.3 to 78.8 per cent.

These variations in composition of various particles are associated with the nature of the soil development and the time involved. The lighter the particles the easier they disintegrate and decompose by the soil-forming processes, and the longer the time involved the more thorough the process. Soil-forming processes attack the finer particles more intensely than the coarser ones. Thus the per cent of very light and lightest particles is highest in the granule group and decreases

[1] In pedology the clay minerals are usually of primary concern, but in paleopedology the unstable clay complex is less important than the stable skeletal portion of the fossil soil. In general the skeletal material in fossil soils is made up of quartz minerals, and this is particularly true in the Salt Lake Valley. Quartz minerals at different stages of weathering can be ascertained by analyses of specific gravity of skeletal fractions. The stage of weathering is in turn a direct expression of soil processes and time involved.

TABLE 4.—SPECIFIC GRAVITY OF SKELETON AND COARSE SOIL IN THE BACCHUS PIT
(In per cent)

Sample number	Genetic horizon	Specific Gravity	Skeleton										Coarse soil										
			Granules (2–4 mm)				Very coarse sand (1–2 mm)				Coarse sand (0.5–1 mm)				Medium sand (0.25–0.5 mm)						
			below 1.91	1.91–2.20	2.20–2.51	2.51–2.89	over 2.89	below 1.91	1.91–2.20	2.20–2.51	2.51–2.89	over 2.89	below 1.91	1.91–2.20	2.20–2.51	2.51–2.89	over 2.89	below 1.91	1.91–2.20	2.20–2.51	2.51–2.89	over 2.89
1	A	dark gray living	2.7	36.5	40.3	20.3	0.2	0	0.3	15.6	44.8	26.3	2.6	0.2	tr.	8.9	27.6	60.7	2.1	0.7	tr.	6.3	72.5	6.2	2.5
3	A	light gray	7.3	35.7	28.6	26.5	0.9	0	1.7	21.5	32.0	41.4	3.3	0.1	tr.	14.7	36.5	41.9	5.7	1.2	tr.	12.2	57.6	1.1	2.3
5	A	dark gray fossil	0.3	44.7	25.3	27.9	1.8	0	0.7	12.9	41.1	42.4	2.4	0.5	0	13.5	43.0	38.0	2.7	1.8	tr.	17.9	27.4	46.0	3.7	3.0
6	A		1.7	45.4	17.9	34.3	0.7	0	0.1	43.5	21.8	30.5	1.2	1.9	0.2	26.1	23.8	46.4	1.4	2.4	tr.	25.2	30.1	40.6	0.8	3.3
7	A		8.0	71.6	7.7	11.5	1.2	0	2.3	63.1	7.4	26.2	1.0	0	0.4	45.3	16.5	35.1	2.1	0.8	0	28.2	28.3	39.8	1.2	2.3
8	C	light gray fossil	28.0	17.2	14.9	17.2	3.1	0	5.1	53.3	20.8	20.8	0	0							tr.	41.6	31.0	25.8	0	0.6
9	A	bog brownish gray	3.8	45.3	23.9	28.0	0	0	0.8	36.6	26.0	26.0	1.2	0	0.4	43.4	41.6	14.6	tr.	0.1	0.1	48.8	23.9	15.1	1.9	0.3
10	A		2.9	8.9	53.0	32.2		0	1.3	6.8	53.4	53.4		0	2.3	8.3	32.0	56.7	0.8	tr.	tr.	10.0	30.0	30.5		0.5

gradually through coarse and very coarse sand. In the *A* horizon the soil processes are most intense, in the *B* horizon the intensity decreases, and in the *C* horizon the processes are most limited. Consequently the most intense disintegration and decomposition of light particles takes place in the *A* horizon, diminishes in *B*, and is almost negligible in *C*.

TABLE 5.—CHEMICAL ANALYSES OF THE BACCHUS PIT SOILS

Soil		Sample number	Genetic horizon	Per cent				pH
				Humus	Loss on ignition	Hygroscopic water	Carbonates	
Living	Dark gray	1	A	4.0	6.5	2.4	0	5.7
		2	B	1.9	3.5	3.0	0	7.3
	Light gray	3	A	2.9	2.7	1.4	0	6.4
		4	B	1.6	2.1	1.6	0	7.1
Fossil	Dark gray	5	A	4.4	5.9	2.5	3.6	8.4
	Light gray	7	A	1.9	3.8	1.7	0	9.5
		8	C	0	1.9	1.6	0	9.3
	Bog	9	A		8.1	2.3	5.0	8.5
	Brownish gray	10	A	1.9	8.2	2.9	0	7.5

The data of Table 4 may be summarized as follows: The degree of weathering of the soil skeleton and the time involved in the soil development decreases in the following order: (1) brownish-gray soil (on Provo 1), (2) dark-gray living soil, (3) dark-gray fossil soil (on Provo 2), (4) light-gray living soil, (5) light-gray fossil soil. These data suggest that the period of development was by far the longest for the brownish-gray soil and shortest for the light-gray fossil soil. The stratigraphic position (Fig. 14) indicates that the time required for the development of the dark-gray living soil was at least equal to and perhaps longer than the time required for the development of the dark-gray fossil soil and the light-gray living soil combined.

CHEMICAL ANALYSIS: The chemical analyses (Table 5) show a high per cent of humus in the *A* horizon in the dark-gray living and fossil soils; the highest amount is in the fossil soils. The pH of the dark-gray soil is 5.7, and the pH of the light-gray soil is 6.4. The light-gray fossil soil contains 3.6 per cent carbonates. The fossil bog soil has carbonates up to 5 per cent; the brownish-gray soil is noncalcareous and has a pH of 7.5.

Loss on ignition from the *A* horizon of the dark-gray and light-gray living soils is 6.5 and 2.7 per cent respectively; in the dark-gray and light-gray fossil soils the loss on ignition is 5.9 and 3.8 respectively. The highest loss on ignition, 8.2 per cent, is identified with the brownish-gray soil.

According to the data on humus, three groups of soils may be distinguished:

(a) Brownish-gray soil: high loss of ignition; low amount of humus; moderate amount of hygroscopic water

(b) Dark-gray living and fossil soils: moderate loss on ignition; high amount of humus; moderate amount of hygroscopic water

(c) Light-gray living and fossil soils: low loss on ignition; low to moderate amount of humus; low amount of hygroscopic water.

SUMMARY: The results of data dealing with the mechanical, mineralogical, and chemical composition of the Bacchus soils (living and fossil) are in accord with field observations of soil profiles and stratigraphic positions. These data may be summarized as follows:

(1) The brownish-gray soil was buried for a long time and subjected to subsurface processes. Thus the organic matter of the soil underwent profound changes. Most of the chemical components of the organic matter, except carbon, were released. The original amount of organic matter present in the soil was undoubtedly two or three times greater than indicated by present analysis. The considerable thickness of the soil (more than 5 feet) and the highly weathered nature of its skeleton suggest a long period of development, probably exceeding by several times that of the dark-gray living and fossil soil.

(2) The living dark-gray soil is second to the

brownish-gray soil in length of period of development. The coarse part of this dark-gray soil is highly weathered and consequently enriched by finer particles of silt and clay. The upper zones are leached and underlain by a well-developed caliche layer which gives evidence of a prolonged stage of dry-steppe or semidesert conditions. The dark color of the humified zones and the comparatively high amount of humus may be attributed to earlier and more humid climatic conditions.

(3) The dark-gray soil may be traced into a dark-gray fossil soil beneath the deposits of the lower terrace; thus its development where buried has been interrupted. The amount of humus in the dark-gray fossil soil is about the same or slightly more than in the living dark soil; the weathering is less pronounced, and the entire profile is slightly calcareous, which contrasts with the leaching in the upper horizons of the dark-gray living soil. The observed differences and similarities in the two soils (dark-gray living and dark-gray fossil) may be explained in terms of a comparable early history but with differences in later stages of development. The formation of both soils during the first stage, which lasted until the fossil soil became buried, was under a moist steppe climate, and during this early period a dark soil with considerable humus was formed. Later a portion of the dark soil was buried, and many of its original properties were preserved; the dark soil on the surface of the upper terrace continued its development until the present. This means that the interim of decreased precipitation between Provo 2 and the Stansbury was of short duration and made no detectable impression on the profile of the dark-gray soil. Only after the Stansbury stage were the arid climatic conditions effective in producing a leached upper zone and underlying caliche layer.

(4) The light-gray soil on the lower terrace was formed on the deposits that buried the previously developed dark-gray soil and therefore is much younger. The laboratory analyses corroborated the field observations: the data show less weathering of the coarse skeletal part of the light-gray soil, the amount of humus is less, and the development of a carbonate horizon is generally less pronounced than in the dark-gray soil.

RELATION TO LAKE BONNEVILLE HISTORY: A compatible relationship seems to exist between the history of Lake Bonneville and the soils of the Bacchus area:

(1) As the lake fell below the Provo 1 stage its shore-line and bottom deposits became exposed, and a soil started to form on them. The lake sank below the 4300-foot level, but a prolonged period of aridity did not occur, for the lake soon began to rise to the Provo level of the Provo 2 stage. Several thousand years of moist steppe climate passed, during which the mature brownish-gray soil formed. An interval of semiarid climate may have been interposed in the period of most steppe climate while the lake sank to the 4300-foot level and below; this interval could not have been long, because no impression is noted in the soil profile.

(2) As the lake rose again to the Provo level, most of the soil on the Provo 1 stage deposits was stripped away, but under certain conditions it was left and buried. These conditions obtain on stream flood plains and are explained as follows; as the lake rose the base level of the streams rose, and they consequently alluviated their flood plains. The lake eventually rose over the flood plains and spread cleanly washed sands and gravels over them, but the soil had been preserved.

(3) The lake held at the Provo level during the Provo 2 stage for a few thousand years and then began to fall again. As its deposits were exposed Coon Creek incised a valley about 20 feet deep in the lake deposits, and a new soil started to form both on the undissected lake deposits and on the valley floor of Coon Creek. For about 5000 years the climate was of the moist steppe type, and a dark-gray humus soil developed. For a brief time while the lake fell below 4470 feet the climate may have been semiarid, but no impression of it has been detected in the soil profile.

(4) The lake then rose to the Stansbury level at 4470 feet ±, which is below the Bacchus pit site; Coon Creek aggraded its flood plain, and the dark-gray soil was buried under the flood plain deposits but not on the higher lake deposits where it continued as a living soil.

(5) The lake held at the Stansbury level for a few thousand years, probably not more than 5000. Soon after it became stabilized Coon Creek ceased to aggrade its flood plain, and a soil started to develop on the flood-plain loam. The climate, while the lake held briefly at the Stansbury level, was probably of a moist steppe type. Then, about 12,000 years ago, the climate gradually changed to arid, and by about 6000 years ago the maximum of the arid climate cycle was reached (altithermal). Since then the climate has ameliorated somewhat to a semiarid one, at least in the Bacchus area. The light-gray soil, which developed as a re-

sult on the flood plain, lacks much humus, and its skeletal material is little weathered. The older, dark-gray soil, which on the higher lake deposits was not buried, continued as a living soil. As a result of the superposition of a dry steppe climate on it the upper zones are leached and underlain by a well-developed carbonate layer.

(6) During the altithermal the flood plain on which the light-gray soil developed was slightly dissected, and in the present stage, but before historical times, the incised channel was alluviated.

The above chronology provides suitable opportunity for the soils of the Bacchus area to evolve, and the soils are believed to support the history of Lake Bonneville as proposed from other lines of evidence.

Soils of Emigration Creek Valley

A soil believed to separate Alpine from Provo 2 deposits exists under a terrace at the mouth of Emigration Canyon, where the lake sediments are trenched by the stream. The soil is believed to mark the interpluvial between Provo 1 and Provo 2 and is similar in kind and position to the Bacchus dark-gray fossil soil. It is described on following pages in connection with a postpluvial soil in Emigration Canyon. Its occurrence is illustrated in Figure 18.

Soil at Mouth of Parleys Canyon

A deep gulley was cut southward in the high terrace on the south side of Parleys Canyon about where the new Wasatch Boulevard has been constructed. It was later filled in, but as observed and interpreted by Marsell, the relations are as shown in Figure 17. The deltas of the Provo 1 and Provo 2 stages had been recognized previously, but when the deep gully eroded into the high terrace an old, filled channel, cut in the Alpine silts, was exposed. Most of the fill is similar to the Alpine, and if it were not for a black soil and overlying muck deposit in the lower third of the channel the two deposits of silt may not have been recognized as separate. Marsell ties the channel fill to the lake at the Bonneville level, because it is evenly bedded as a lake deposit and is above the Provo level.

The soil is interpreted to mean a stage of low lake level which lasted at least several thousands of years and separates the Alpine and Bonneville-Provo 1 as distinct lake stages.

Soils of the Lower Sevier River Area

SETTING: In its lower course the Sevier River cuts through the Canyon Range (Sevier Canyon) and flows southwestward across a desert plain for about 60 miles to Sevier Lake. So much water is now appropriated for irrigation that the stream seldom discharges into the lake, but it has recorded an interesting erosional and depositional history.

Sevier Lake is the lowest part of the Sevier Desert basin which has a threshold outlet at about 4520 feet into the "Old Channel," a dry river bed leading into the Great Salt Lake Desert (Fig. 1). The basin has about 75 feet of closure below the outlet.

TERRACES: From Sevier Canyon at Leamington to the settlement of Delta the river has incised a relatively broad and shallow valley in the bottom sediments of the Provo stage. The valley ranges from half a mile to over a mile wide. Within the valley are two well-defined stream terraces: an extensive "middle-stream terrace" between the upper rim of the valley and the valley floor and the gently incised flood plain of the modern Sevier River (Fig. 15). Beyond the incised valley is a broad plain which extends to Sevier Lake.

The flood plain is 3–6 feet above the present stream channel and in places is a thousand feet wide. The river meanders across the entire flood-plain belt. The middle-stream terrace stands 20 feet above the flood plain at Leamington and is 35–40 feet above farther downstream at Delta. The Provo lake bed averages 70 feet above the middle-stream terrace, but the amount increases slightly from the Sevier Canyon downstream to Delta.

In longitudinal profile the terraces appear as illustrated in Figure 15. From Sevier Canyon the vertical distance between the Provo surface and middle-stream terrace increases downstream nearly to Delta, where the Provo surface merges with the terraces and probably lies buried under the Delta plain.

DELTA PLAIN: Below Delta the middle-stream terrace merges with a plain that slopes gently to Sevier Lake and for the most part is the desert floor of the lake at higher levels. From Delta to Deseret it is underlain by a rich black soil and is an area of irrigation and good crops. This section, the Delta plain, is dissected by the Sevier River, and the flood plain of the valley section continues westward through it (Fig. 15).

MEANDERS: Three sets of meanders are recognized. They are the small meanders

across the modern flood plain, the broad meanders of the modern flood-plain belt, which is incised in the middle-stream terrace, and the broader meanders of the flood plain of the

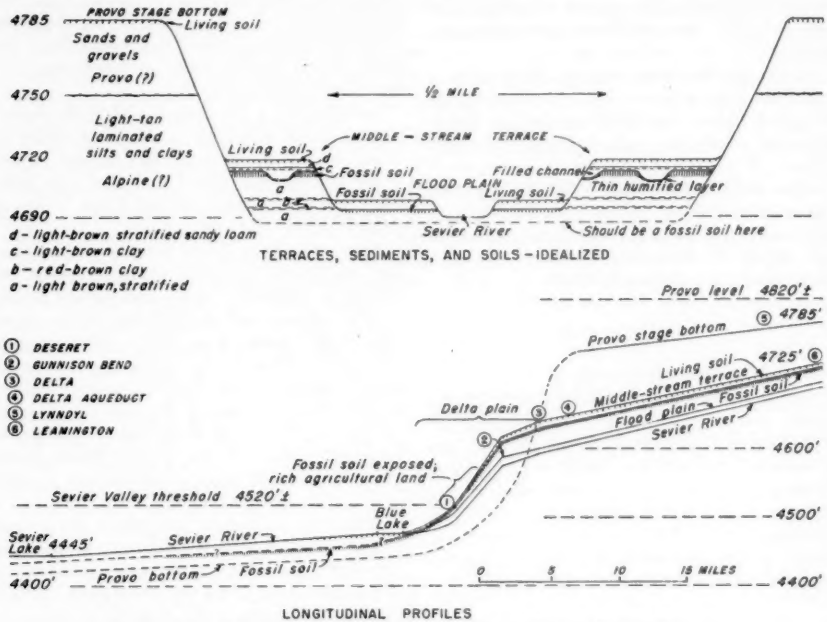

FIGURE 15.—TERRACES AND SOILS OF THE LOWER SEVIER RIVER VALLEY

middle-stream terrace. These are nicely displayed in the Delta-Melville reservoir area (Fig. 16).

STRATIGRAPHY: A deep meander cut-off (Fig. 16) exposes more than 100 feet of the sediments that underlie the old Provo lake bottom. At the base, 60 feet of tan, laminated silts and clays crop out which resemble the Alpine Formation in composition and appearance. Over these is a sheet of sand and gravel 50 feet thick. It is poorly exposed, but horizontal bedding is evident. It appears to be a deposit of the lake at the Provo stage.

The deposits under the middle-stream terrace in the area near Lynndyl are as follows: The surface layer is a sandy loam soil which has a humified gray horizon 6 inches thick. Beneath is a 2½-foot layer of light-brownish sandy loam, and beneath this is a 1½-foot layer of brown clay. A dark-gray fossil soil about 3 feet thick appears sharply beneath the upper alluvial deposits. The upper 2 feet of the soil are dark gray and well humified; the lower 1 foot is gray and less humified. The mechanical composition of the entire 3 feet is loamy.

Beneath the fossil soil a well-stratified brownish silty loam layer exceeds 5 feet in thickness. Two layers of red-brown laminated clay, each about 1 foot thick, occur 10 and 14 feet below the surface.

CHANNELS IN FOSSIL SOIL: Evidence of stream channeling through the fossil soil is especially plain in the banks beneath the middle-stream terrace in the Delta plain. Channneling was noted on the fossil-soil surface upstream in the valley section, but the depth of incision is probably much less there than in the Delta plain. The deepest channels observed on the fossil-soil surface were 6–8 feet, but most of the channels measured 3–4 feet deep; the width of the channels ranges from 10 to 15 feet. The bottom and slopes of these channels are made up of a thin humified soil horizon 1–5 inches thick. The humified layer does not decrease noticeably in thickness along the channel slope or near the channel edges and indicates that the channels were abandoned after they

were carved, grass grew abundantly, and soils developed on the surface; later the channel and soil were buried by the alluvial deposits that constitute the upper part of the middle-stream terrace.

Lake. Nine were selected as typical of the middle-stream-terrace deposits and were analyzed in the laboratory for their mechanical, mineralogical, and chemical composition. According to the mechanical analyses (Table 6)

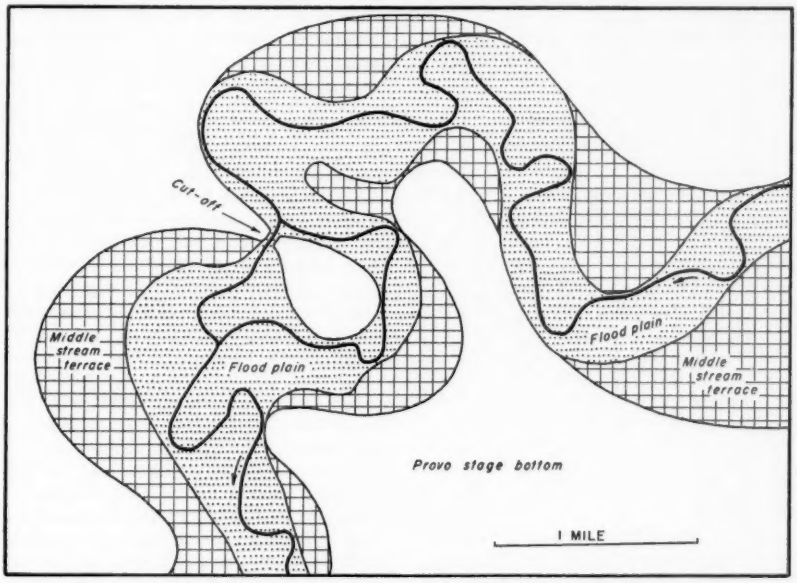

FIGURE 16.—MEANDERS OF SEVIER RIVER NEAR DELTA-MELVILLE RESERVOIR

The deposition of the upper alluvium leveled the dissected surface so effectively that the buried channels cannot be detected by the present configuration. The deposits range in depth from a few inches to 15 feet and have an average depth of 2–4 feet. The greatest depth of burial of the fossil soil occurs in the buried channels.

DEPOSITS OF DELTA PLAIN: In the area of the Delta plain the thickness of the upper alluvial deposits may be so limited that the living and fossil soils are merged and form a single profile. The upper 6–12 inches are light and slightly humified, whereas the lower portion is dark and well humified to a depth of 1–2 feet. In the area west of Delta the fossil soils are at the surface; they appear as old living soils that are highly humified and possess a granular structure. The soils of the area are noted for their fertility.

MECHANICAL ANALYSIS: More than 50 samples were taken from nearly all parts of the Sevier Valley, from Sevier Canyon to Sevier

the living and fossil soils as well as the alluvial layers are characterized by a fine-grained material with a large silt fraction. The paucity of skeletal material (particles with a diameter more than 1 mm) in the middle-stream terrace is strikingly characteristic. Only two samples taken at Leamington Bridge contained small amounts.

The living and fossil soils as well as the alluvial deposits of the middle-stream terrace are almost entirely silt loams. The only exception is found in the living soils at Leamington Bridge where the mechanical composition is that of a fine sandy loam—fine and very fine sand which constitutes 36.6 per cent, and coarse and medium silt which makes up 42.5 per cent. The mechanical composition of the fossil soil at Leamington Bridge is much finer than that of the overlying living soil; the predominant mechanical fractions are medium and fine silt (84.0 per cent); therefore the fossil soil at Leamington Bridge may be classified as a silt loam.

TABLE 6.—MECHANICAL COMPOSITION OF THE SEVIER VALLEY SOILS
(In per cent)

Sample number	Depth of sample from the surface	Soil or layer of deposits	Location	Sand (mm)						Silt (mm)					Clay (mm)
				1-0.5	0.5-0.25	0.25-0.12	0.12-0.06	Total	0.06-0.03	0.03-0.015	0.015-0.007	0.007-0.003	Total	0.003
1	2-7 inches	living soil	Leamington bridge	0.6	3.4	20.0	16.6	40.6	20.7	21.8	10.0	2.5	55.0	4.4
2	26-31 in.	fossil soil		0	0.2	1.7	3.9	5.8	5.9	40.4	43.6	0.5	90.4	3.8
3	1-6 inches	living soil	Lynndyl	0.1	0.6	4.2	18.1	23.0	28.0	30.1	9.8	6.0	61.9	3.1
4	25-30 in.	brownish layer		0	0.1	0.2	18.1	18.4	51.0	25.3	3.5	1.7	81.6	0.1
5	40-45 in.	reddish brown layer		0.1	tr.	tr.	0.2	0.3	11.5	71.2	3.4	9.8	95.9	3.8
6	60-65 in.	fossil soil		0.2	0.1	0.5	1.5	2.3	4.0	56.5	33.2	1.0	96.7	3.0
14	16-16½ feet	light brownish layer	Canal bridge	0	tr.	0.1	0.5	0.6	12.6	76.9	4.9	0	94.4	5.0
15	15-15½ feet	red layer		0	0	0	tr.	tr.	0.9	4.3	87.3	3.3	95.8	4.2
16	15-15½ feet	light brownish layer	Sevier Lake	0	0.1	0.6	0.3	1.0	19.0	72.0	4.0	0	95.0	4.0

About the same differences in mechanical composition between living and fossil soils are observed at Lynndyl. The predominant mechanical fractions of the living soil are: fine sand (19.1 per cent) and coarse and medium silt (58.1 per cent). Thus the living soils at Lynndyl are classed as a coarse silty loam. The mechanical composition of the underlying parent material is of the same nature, whereas the composition of the fossil soil is characterized by two predominant fractions, medium and fine silt (89.7 per cent); this identifies the soil as a silty loam similar to the fossil soil at the Leamington Bridge. Although the mechanical composition of the living soils at the two localities vary somewhat, the differences are of less magnitude than those existing between the living and the fossil soils. The fossil soils are made up of finer particles (silt) and are heavier than the living soils, which are composed of coarser particles (fine sand and coarse silt).

The alluvial deposits of the middle-stream terrace and the Delta plain are characterized mainly by a brownish silty loam with a very low amount of clay (1–2 per cent). Within the silty deposits are claylike layers whose mechanical composition is exemplified in sample 14 (Canal Bridge) and 16 (Sevier Lake). The predominant fractions of these layers are medium and coarse silt (69–91 per cent); amounts of clay range up to 5 per cent, and fine sand makes up 1 per cent or less. Thus the alluvium of the middle-stream terrace and Delta plain are silt deposits with small amounts of clay. Within the middle-stream terrace are also thin reddish-brown to red layers. The mechanical composition of these layers is shown in samples 5 (Lynndyl) and 15 (Canal Bridge). These layers resemble in mechanical composition the claylike layers; they are distinguishable, however, by a higher percentage of fine silt (87.3 per cent) and no sand.

The analysis of the mechanical composition of the soils and deposits that make up the middle-stream terrace and the Delta plain reveal that these deposits are characterized by their fineness of mechanical particles. Some fine-sand fractions are present, but very little skeletal material. The fossil soils are of a silty loam mechanical composition and somewhat heavier than the living soils which are coarse silty loam or fine sandy loam.

MINERALOGICAL ANALYSIS: A mineralogical analysis based on specific gravity was limited because of the lack of skeletal material in the middle-stream-terrace deposits and soils. Only

one sample was analyzed by the specific-gravity method, and this sample was taken from the living soil at Leamington Bridge. The data of this analysis (Table 7) portray the inverse relationship between particle size and specific gravity. Heavy minerals are present (1.4 per cent) only in the medium-sand fractions, whereas in the very coarse and coarse sand the heavy minerals are absent. All sand fractions have comparatively high amounts of the lightest minerals (specific gravity below 1.9). The absence of the heavy skeletal material indicates a relatively short period of soil development as well as limited soil-forming processes. The time required for the development of the living soil at Leamington Bridge, according to the state of weathering, is comparable with that of the living light-gray soil from the area of Bacchus, Utah, in Salt Lake Valley. Unfortunately there are no data on the weathering of fossil soils in the Sevier River Valley; field observations indicate, however, that the weathering of the fossil soils is much more advanced than that of the living soils. This is due not so much to the time involved as to the intensity of the soil-forming processes.

TABLE 7.—SPECIFIC GRAVITY OF SKELETON AND COARSE SOIL IN LIVING SOIL AT LEAMINGTON BRIDGE*

(In per cent)

Skeleton											
Granules (2-4 mm)						Very coarse sand (1-2 mm)					
below 1.91	1.91-2.20	2.20-2.51	2.51-2.57	2.57-2.89	over 2.89	below 1.91	1.91-2.20	2.20-2.51	2.51-2.57	2.57-2.89	over 2.89
-	100	-	-	-	-	5.8	0	17.7	29.4	47.1	0
Coarse soil											
Coarse sand (0.5-1 mm)						Medium sand (0.25-0.5 mm)					
below 1.91	1.91-2.20	2.20-2.51	2.51-2.57	2.57-2.89	over 2.89	below 1.91	1.91-2.20	2.20-2.51	2.51-2.57	2.57-2.89	over 2.89
0.8	6.3	20.4	18.7	53.8	0	1.7	6.7	9.8	3.3	77.1	1.4

* Table 6, sample 1.

CHEMICAL ANALYSIS: The chemical analyses of the soils in the Sevier area indicate comparatively low amounts of organic matter (humus) in the living and fossil soils. At the same time the analyses show that the amount of humus in the fossil soil (1–2 per cent) is twice that of the living soil (0.5–1 per cent). The color of the soil suggests a higher percentage of humus than the analysis reveals. This is probably due to the chemical changes in the organic matter of fossil soils: the amount of humus decreases, and the concentration of organic carbon increases. This process results in about the same dark soil which has the original amounts of carbon but a decreasing amount of total organic matter.

Hygroscopic water data, which reflect the amount of organic and inorganic matter and the nature of colloidal complex, are significant to an interpretation of the soils in the Sevier area. The results of the hygroscopic water analyses and the data for total amount of carbonates are tabulated in Table 8.

The fossil and living soils, as well as the different deposits of the middle-stream terrace, are highly calcareous. This is especially true of the red deposits that contain over 50 per cent carbonates and the light-brownish and red-brownish deposits with 32–39 per cent carbonates. The fossil soil has 25–31 per cent carbonates, and the living soil has 16–25 per cent. The least amount of carbonates is in the parent material underlying the living soil at Lynndyl. The amount of carbonates in the living and fossil soils at Leamington Bridge is the same (25.5 per cent), but at Lynndyl the fossil soil has twice (31.8 per cent) the amount of carbonates as the living soil (15.7 per cent). This distribution pattern does not assist in identifying the fossil soils.

The fossil soils are characterized by the highest hygroscopic moisture content; amounts range from 3.08 to 3.87 per cent, which is approximately three times greater than that found in the living soils. At the Leamington Bridge the hygroscopic moisture of the living soil was 0.87 per cent and that of the fossil soil 3.08 per cent; at Lynndyl the living soil contained 1.33 per cent and the fossil soil 3.87 per cent. At Lynndyl the living soil contains some-

what higher percentages of hygroscopic water (1.33 per cent) than the parent material (1.10 per cent). These differences in the amount of moisture in the living and fossil soils are due to differences in the mechanical compositions and especially to differences in intensity of soil processes which produce a much higher amount of organic matter and organo-mineral colloidal complexes in the fossil soil than in the living soil.

TABLE 8.—HYGROSCOPIC MOISTURE AND CARBONATES OF SEVIER VALLEY SOILS
(In per cent, dry soil)

Sample number	Depth from surface	Soil or layer of deposit	Hygroscopic moisture	Carbonates	Location
1	2-7 inches	Living soil	0.87	25.5	Leamington bridge
2	26-31 inches	Fossil soil	3.08	25.5	
3	1-6 inches	Living soil	1.33	15.7	Lynndyl
4	25-30 inches	Brownish layer	1.10	12.0	
5	40-45 inches	Reddish brown layer	2.81	31.8	
6	60-65 inches	Fossil soil	3.87	31.1	
14	16-16½ feet	Light brownish layer	2.06	39.0	Irrigation canal
15	15-15¾ feet	Red layer	1.37	52.6	bridge
16	15-15¾ feet	Light brownish layer	1.94	31.9	Sevier Lake

RELATION TO LAKE BONNEVILLE HISTORY: In the Sevier Desert basin a threshold basin of about 75 feet closure spills into Lake Bonneville at 4520 feet. Stabilized levels of Lake Bonneville above 4520 feet will represent base levels for the Sevier River, but when Lake Bonneville is below the threshold elevation, then Sevier Lake, at whatever elevation it may stand, becomes the controlling base level. The Stansbury level of the lake, 4470 feet ±, is about 50 feet below the outlet threshold. Base levels to which the Sevier River would therefore grade when Lake Bonneville stood at the Stansbury level would be to the threshold elevation or lower.

The Stansbury stage represents a climatic minimum; that is, the lake rose from a previous low to the Stansbury level, held there for a while, and then fell. At the time of the Stansbury stage Sevier Lake is presumed to have been overflowing for two reasons: (1) The middle-stream terrace, incised in the Provo bottom, seems to be graded to about the 4520-foot elevation (Fig. 15). The lake must subside to the present stand in order for the flood-plain terrace to have been incised into the middle-stream terrace; this would not be possible if the middle-stream terrace had been graded to the present lake. (2) The fossil soil below the surface of the middle-stream terrace indicates a moister climate than the present, and this tallies with the Stansbury stage and Sevier Lake up to overflowing. With these conditions assumed, the post-Provo 2 history is interpreted as follows:

(1) As Lake Bonneville sank from the Provo level Sevier River flowed over the evened bottom and started to trench the sediments. The main lake fell to the threshold elevation, then to the Stansbury, and finally possibly to the present Great Salt Lake level. Sevier Lake ceased to discharge and dried to its present state. A major valley was cut to the grade of the present stream or possibly a few feet lower. The bottom of the old channel has not been detected, but the writers believe that on its flood plain a soil would have formed like the fossil soil below the main terrace at Bacchus. Perhaps well records will reveal such a soil.

(2) Lake Bonneville rose to the Stansbury level at about 4470 feet, and the Sevier Basin filled to overflowing at 4520 feet. The base level of Sevier River, therefore, rose and its incised valley was graded (alluviated) to the 4520-foot level. A flood plain became stabilized for the duration of the Stansbury pluvial maximum, and in a rather moist climate a dark-gray soil of the moist-steppe variety developed on it.

(3) Near the end of the Stansbury maximum the flood plain was slightly dissected and then alluviated. Both dissection and alluvia-

tion were only a few feet. The channel sides supported a good growth of grass, but only a thin humified horizon developed on the new incision before it was filled with alluvium. The climate is assumed, therefore, to have remained somewhat as moist as before, and the cycle in the stream's eroding and depositing was small and short-lived. The three sizes of meanders in the lower Sevier Valley do not reflect the stream's activity at this time; again, the incident is probably not of major consequence and probably reflects a bobble in the climate and level of Sevier Lake near the end of the Stansbury pluvial maximum.

(4) Lake Bonneville then fell to the altithermal low, and Sevier Lake probably dried up. The middle-stream terrace flood plain was dissected, a new low-level flood plain became stabliized, and a gray soil formed on it.

(5) A slight increase in precipitation occurred after the altithermal; with the increase a slight alluviation of the flood plain, which buried the previous gray soil, also occurred. A new soil started to form on the fresh alluvium.

(6) Because of human occupation and possibly a subcycle of aridity the stream has recently cut a few feet below the flood plain.

Old Soils in the Alpine Area

SETTING: Reddish-brown soils have been noted and described in the Alpine area of Utah valley by Hunt and Sokoloff (1950) and Hunt *et al.* (1953). As pointed out by these authors the soils occur in two places: on a "pre-Wisconsin" moraine in the mouth of Dry Canyon (also called Alpine Canyon) and on an old fanglomerate half a mile northwest of the town of Alpine. The soil on the fanglomerate is buried by Bonneville level gravels and is hence a fossil soil, but the soil on the moraine, as interpreted by the writers, is a living soil.

The occurrence in both places is unique; other occurrences of such soils under similar conditions have not been noted. The soil on the old moraine was studied by the writers, and from a pit dug on a flat shoulder near the top of the old moraine the following description was obtained.

TYPE SECTION: The pit is located on the Lehi topographic quadrangle map 400 feet south-southwest from the closed contour marked 5770 feet, in the mouth of Dry Canyon on the north side of the creek. It is near the center of the nearly circular morainal area labeled Qmo, just below the fault on Hunt's map. The soil profile is as follows:

A horizon: 0–5 inches. Dark gray, well humified, granular, friable, loamy. Transition is well marked and fairly sharp to underlying horizon.

B_1 *horizon*: 5–19 inches. Red-brown clay, sticky when wet. Prismatic structure; units are very firm when dry. Grades gradually into B_2.

B_2 *horizon*: 19–35 inches. Reddish brown and a little less sticky than B_1. Prismatic structure. Grades into B_3.

B_3 *horizon*: 35–60 inches. Yellowish-brown clayey loam. Gradually changes downward from slightly yellowish brown to yellowish brown. Granite boulders are highly weathered in this horizon but slightly less than in upper horizons. The boulders can be cut through with difficulty with shovel but easily with pick. Bottom of pit.

By interpolation, B_3 horizon must go down another 3 feet at least and is underlain by the *C* horizon of leached and oxidized parent material. A short distance to the east Chipman Creek has cut a gorge through the old moraine along a recent fault zone, by which it has been diverted to Dry Creek. At the top of the gorge on either side the thick, reddish-brown soil can be seen in profile, and here it is at least 15 feet thick to the *C* horizon.

The above soil is podzolic; the illuvial *B* horizons are enriched in the clay minerals and the sesquioxides of iron and aluminum. The processes of decomposition are so intensive that the granite boulders of moraines are highly decomposed.

Typical podzols are developed in humid, subarctic climates, but the podzolic soils of the Wasatch piedmont, especially those here described, occur in the 5100- to 5800-foot interval. They have been noted much higher, however (Hunt and Sokoloff, 1950, p. 111). A marked change in climate sets in at about the 5100-foot elevation under the protection of the high peaks of the Wasatch: it is cooler, and there is greater precipitation. This is attested in the Alpine area of Utah Valley by the vegetation, where scrub oak about 4 feet high scattered with sage brush occur at 5100 feet and gradually change to a heavy growth of scrub oak about 20 feet high. In the spring-fed hollows at approximately 5400 feet, clumps of quaking aspen appear. During the week of March 3 to 10, 1957, the pit filled with enough rain water to indicate about 12 inches of rainfall. This was a rainy period, but it provides evidence of precipitation considerably greater here than 1000 feet lower down the piedmont.

The profile described above is regarded as a

living soil developed under the processes of podzolization during a long period.

CHANGE DOWNSLOPE: The well-developed soil on top of the old moraine, traced downslope to the west, changes fairly abruptly into a weakly developed brown podzol with a thick, dark-gray, humic *A* horizon and then to humic steppe soils, still on the old moraine of large granite boulders. Any knob and kettle topography that may have existed is gone, and several gullies drain the moraine effectively. Considerable slope wash is evident wherever pits are dug for soil examination, and it seems, that only the fairly flat top part of the old moraine has remained free from erosion; there over a long period, in a cool and humid climate a thick podzolic soil has developed.

INTERPRETATION: Hunt and Sokoloff (1950, p. 111) believe that the reddish-brown soil indicates considerable age. Because it resembles somewhat the gumbotils of the Middle West, which are developed on Illinoian and Kansan drifts, they regard it as pre-Wisconsin and therefore mark the underlying moraine as pre-Wisconsin. Horberg (1954, p. 1125) explains that this is a common practice and finds in southern Alberta that the podzolic soils belong clearly to the pre-Wisconsin drifts.

As far as the Wasatch piedmont is concerned the reddish-brown podzolic soil stands apart from the dark-gray steppe soils. The Alpine soil could be confused with only one steppe soil: the reddish-brown soil near the mouth of Parley's Canyon.

Soil of Terminal Reservoir

SETTING: The Terminal reservoir is situated at the north end of the Salt Lake City aqueduct and is just south of the mouth of Parley's Canyon on the east bench of Salt Lake City. The Bonneville beach is above and the Provo beach just below. The area is underlain by the Alpine dull-red silts with their sand and gravel lenses near the mountain front. Marsell recorded a thick red-brown soil on the bench at this location when the trench for the aqueduct was dug, and a new pit was dug to study the profile and if possible to recognize and describe an old soil developed on the Alpine Formation. The pit is just inside the fenced enclosure for the reservoir about midway from north to south on the west side and is at an elevation of about 4850 feet.

TYPE SECTION: The profile exposed in the pit is as follows:

A horizon: 0–5 inches. Brownish-gray calcareous silty loam.

B horizon: 5–12 inches. Reddish-brown calcareous silty loam.

A horizon: 12–18 inches. Dark-gray, leached, friable, silty loam. Only upper ½–1 inch, just beneath the upper very calcareous horizons, is slightly calcareous.

B horizon: 18–25 inches. Reddish-brown, clayey loam; leached and very compact with grayish humified streaks. When dry shows prismatic structure.

C horizon: 25–28 inches. Reddish-brown, slightly calcareous, compact, clayey loam.

Cca horizon: 28–45 inches and below. Horizon of carbonate accumulation; highly calcareous light-brown silty loam. Dense network of white carbonate veinlets.

INTERPRETATION: The soil-test pit is located on a gentle slope and shows two soils: (1) living, shallow calcareous steppe soil (0–12 inches); (2) fossil soil (12–45 inches). The fossil soil was probably truncated by slope erosion and the upper part of the *A* horizon removed. It was then buried and has remained so for a long time. It may be classified as a fossil-prairie soil.

Gvosdetsky believes that possibly it took as long to form as the reddish-brown podzolic soil on the Alpine moraine

It's reddish brown principally because of the reddish-brown Alpine silts upon which it has developed and not because of iron enrichment.

Post-Stansbury Soils

Occurrence and Nature

Soils in flood-plain areas are complicated as a result of frequent floods and shifting channels (Afanasiev and Gvosdetsky 1937, p. 158–159). The divisions of a well-developed flood plain are as follows: (1) a narrow belt of "by-stream" or levee deposits close to the stream channel and composed usually of sandy alluvium; (2) a wide belt of "central" flood plain bordering the levees composed largely of silty alluvium; (3) a narrow belt near the bounding terrace relatively far removed from the stream channel, composed of clayey deposits, and called the "by-terrace" zone. The periodical or seasonal water movement usually extends beyond the stream channel into all three parts of the flood plain or at least to some portion of them. The by-stream belts receive the thickest deposits,

and levees result; some deposition of finer particles takes place in the central area, and only insignificant deposition of very fine particles may take place in the by-terrace area.

The lateral movements of the stream channel usually are confined to the by-stream belt; consequently, the deposits on this part of the flood plain are constantly reworked and are very young. The finding of mature profiles and old buried soils in the by-stream belt is highly improbable. The stream channel shifts only occasionally into the central or by-terrace belts, and thus the alluvial deposits and buried soil profiles are most likely to be preserved there.

All the major streams of the Bonneville basin have well-developed flood plains, especially in their lower reaches; the least-developed flood-plain terrace is in the canyons proper. Regardless of the complexity of stratigraphy and soil cover on the flood plain, a definite two-part structure within the alluvial deposits was recognized in a number of places from the Bear River on the north to the Sevier River on the south. A similar structure was observed within the flood plain from the higher elevations adjacent to the glacial cirques down to the shore line of the present Great Salt Lake.

Lower Jordan River Flood Plain

DISTRIBUTION OF SOILS: In the Jordan Valley below the Gilbert terrace (Fig. 7) older alluvial deposits and a fossil and living soil are well preserved. The levees and the lower belts on either side have been pointed out; in the "central" belt the fossil soil has been observed and studied. A fossil soil was exposed in a trench along Redwood Road for 1.5 miles northward from North Temple Street. The soil is 3–6 feet beneath the present surface, which is only 10–15 feet above the present lake at 4200 feet. The flood plain slopes gently northward at 1 foot per mile for about 8 miles into the swampy delta area.

The boundary between the fossil soil and the upper deposit is abrupt. The fossil soil grades down into a fine, slightly weathered sandy loam 6 feet thick. The *A* and *B* horizons of the fossil soil together are 18–20 inches thick, but the depth of the two units in the living soil is 10–16 inches. This suggests that the time involved in the fossil-soil development was greater than that of the living soil.

TABLE 9.—MECHANICAL COMPOSITION OF LOWER JORDAN VALLEY FLOOD-PLAIN SOILS

(In per cent)

Soil	Horizon	Sand (mm)					Silt (mm)					Clay (mm)
		1–0.5	0.5–0.25	0.25–0.12	0.12–0.06	total	0.06–0.03	0.03–0.015	0.015–0.007	0.007–0.003	total	0.003
Living	A	0.5	0.6	0.4	2.5	4.0	7.1	19.2	23.9	15.5	65.7	29.3
	C	0.1	0.2	0.3	0.3	0.9	7.2	22.6	57.9	8.9	96.4	2.7
	D	0.1	0.6	0.8	0.6	2.1	2.5	15.6	74.3	3.4	95.8	2.1
Fossil	A	0.2	0.5	6.6	7.8	15.1	5.8	10.5	8.9	56.2	81.4	3.5
	C	0.8	2.0	19.4	33.1	55.3	17.0	9.3	8.4	6.7	41.4	3.3

MECHANICAL ANALYSIS: Mechanical analyses were made of the living- and fossil-soil profiles, and the results are tabulated in Table 9.

The living soil is composed of more than 90 per cent silt with appreciable clay (29.3 per cent) only in the upper horizon. The amount of sand and fine sand is negligible. The dominant fractions are fine silt. In the fossil soil the fine sand increases to 15.1 per cent, but the amount of silt decreases to 81.4 per cent. A greater difference is seen in the *C* horizon, where the amount of fine sand increases abruptly to more than 50 per cent.

HUMUS AND CARBONATES: The amount of humus in the living soil is nearly 3 per cent, and the amount in the fossil soil is 2.5 per cent. The percentage difference is not large, but the dark gray of the fossil soil is in contrast with the much lighter gray of the living soil.

The distribution of carbonates in both soils is significant. The living soil is highly calcareous throughout the profile, whereas the fossil soil in the *A* and *B* horizons is noncalcareous. The *C* horizon is calcareous but less calcareous than any horizon of the present soil. Results of the chemical analyses are listed in Table 10.

INTERPRETATION: The presence of a fossil soil in the deposits testifies to a relatively long and stable period without marked alluviation. The Jordan River spread a thin layer of

silt over the soil, and since then, without further alluviation in places, a new soil has formed. Gvosdetsky believes that the fossil soil was formed under climatic conditions slightly more arid than those of the present, and that the development of the soil took 1000–3000 years or more. The living soil is not so mature as the fossil soil and probably has not been developing so long.

TABLE 10.—CARBONATES IN LOWER JORDAN VALLEY FLOOD-PLAIN SOILS

(In per cent)

Soil	Horizon	Depth in Inches	Per Cent of Carbonates
Living	A	2 - 6	22.17
	C	14 - 17	22.49
	D	32 - 36	34.23
Fossil	A	41 - 57	0
	C	62 - 66	12.64

The authors have evolved two theories concerning the relation of the Lower Jordan Valley flood-plain soils to the Stansbury pluvial maximum and the Gilbert stand of the lake. One relates sediments, soils, and topography to the Gilbert stage on the basis of an expansion-stability level, and the other regards the Gilbert as a mild or small pluvial maximum following subsidence from the Stansbury pluvial. The expansion theory is presented first.

The Jordan Valley was the depositional and smoothed-out bottom of Lake Bonneville at the Stansbury level about 15,000 years ago. As the lake fell to the Gilbert level, from 4470 feet ± to 4245 feet ±, the bottom sediments were dissected (Figs. 8, 17). The material eroded from the incision was spread out over the Stansbury bottom sediments from about 33rd South Street northward; according to the expansion theory, it was in the form of bottom silts of the lake at the Gilbert level. The lake finally fell from the Gilbert level to 4200 ft (average of present) or possibly a few feet lower during the altithermal.

At the same time as the Gilbert lake bottom was exposed the Jordan River started renewed incison of its Gilbert level flood plain and spread the silts thus derived irregularly northward over the Gilbert bottom silts. The irregular spread is judged from the gentle nondescript irregularities shown on the new topographic maps. In places the Gilbert bottom sediments were not covered, and soil development continued uninterruptedly several thousands of years. The section of fossil soil and living soil along Redwood Road north of North Temple street, according to this chronology, is an area where the Gilbert bottom silts were not covered for about 3000 years. Then levee building spread a layer of silt 3–6 feet thick over the well-developed soil. The levee building was probably associated with the slight amelioration of climate from the dry altithermal and perhaps with the slight rise of Great Salt Lake. Levee building at this locality was short-lived, for reasons not clear, and another soil has been developing on the central flood-plain belt here for approximately 2000 years.

In diagramming the pluvial maximum theory (Fig. 17, climatic theory profiles) it is necessary to start with the lake as it sank and withdrew from the Stansbury shore, and to postulate that it fell to the present Great Salt Lake level, or even lower, because the bottom of this brine lake has been built up by about 16 feet of sediments since Stansbury time. As the lake sank the Jordan River dissected its broad valley not to a Gilbert level base, as the previous theory requires, but to a low brine-lake base (Fig. 17, cross profiles). The sediments derived from the dissection were spread as flood-plain and deltaic deposits over the lower bottom areas of Stansbury sediments. The Jordan River approached stability in its erosional and depositional activities during the dry interval that followed, and an arid soil formed over the lowland sediments and on the newly formed flood plain upstream from the deposits. This soil has not yet been found.

Then the lake rose to the Gilbert level because of a slight cooling of temperature, and a new layer of sediment was spread over its bottom. Upstream the Jordan River alluviated its flood plain and buried the soil that is assumed to have formed there.

The climate then turned to the arid altithermal, and the Gilbert stage waters disappeared. During the altithermal a soil formed on the Gilbert deposits. Upstream the Jordan River dissected the previously deposited sediments of the Gilbert stage, but the soil on the previous flood plain, now a terrace, continued to form.

With the amelioration of the climate from the arid altithermal, it is presumed that the Jordan River began a levee-building cycle over the lowlands and that the altithermal soil was buried where the levees accumulated. Since levee building is not uniform at all places

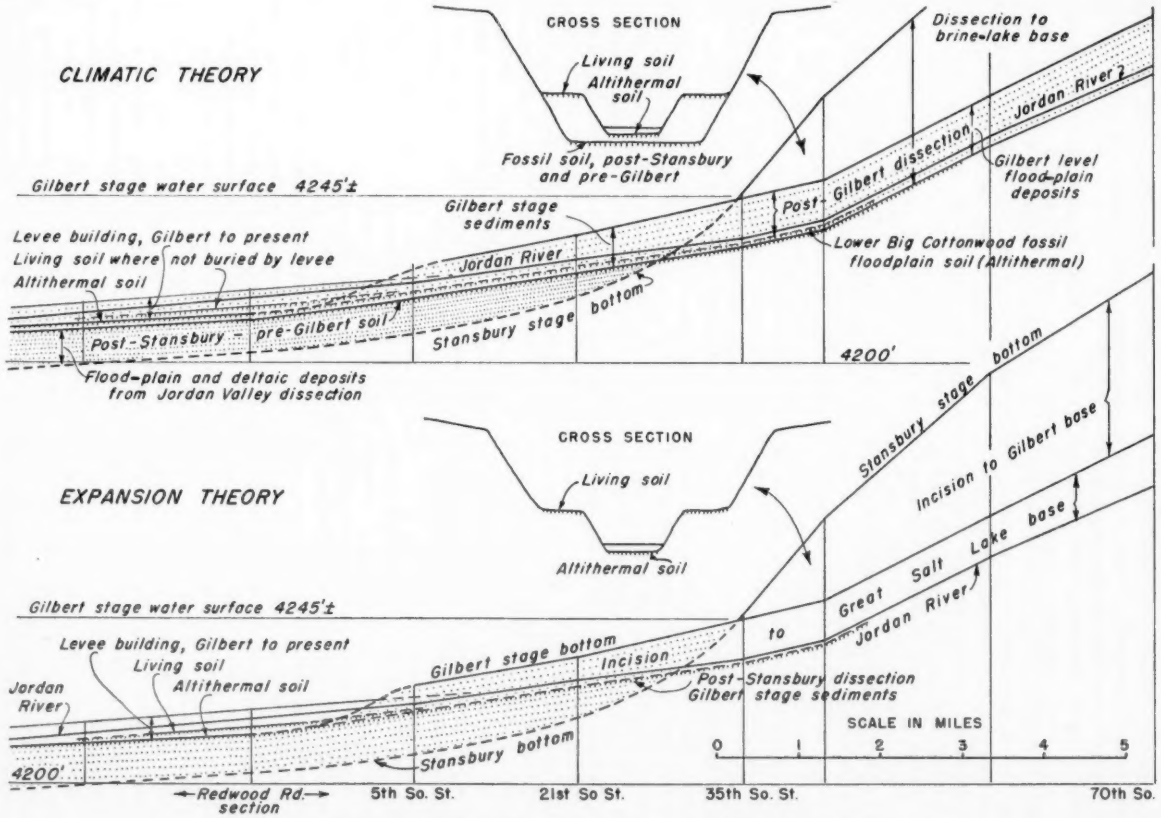

FIGURE 17.—SOILS, TERRACES, AND DEPOSITS OF LOWER JORDAN RIVER VALLEY

along the course of a river the altithermal soil was probably buried along the Redwood Road locality; for about the last 2000 years no further sedimentation has occurred, and a soil has formed during this period of time.

A comparison of the two theories helps to crystallize their similarities and differences. According to the expansion theory, river incision following the Stansbury stage was in two steps: first to the Gilbert base and then to the Great Salt Lake base. According to the pluvial-maximum theory, the Jordan River incised and graded first to a brine-lake stage, then alluviated to the Gilbert base, then dissected to the Great Salt Lake base. There could be no fossil soil between the Stansbury and Gilbert stages if the expansion theory holds, but a fossil soil could have been developed and preserved if the pluvial maximum theory is correct. Such a soil has not been detected as yet, but the possibility was not considered during the field work.

According to both theories the Gilbert stage preceded the altithermal, and the fossil soil on Redwood Road is of altithermal origin. Burial is probably due to levee building. An appreciable living-soil profile developed where the river has failed to flood and spread alluvium for some time.

The principal weakness of the expansion theory is that the threshold elevation does not jibe with the elevation of the beaches by 18–25 feet. This is too great to be overlooked, but because the exact elevation of the spillway is not known the significance of the discrepancy cannot be evaluated at present.

The climatic theory demands a pluvial maximum stabilized for some time by a balance of precipitation and evaporation. Considering Great Salt Lake and the present climate it is evident that the balance is not steady, and that the lake level fluctuates. However, the Stansbury and Bonneville stages require the same conditions, yet these pluvial maxima have not been seriously contended.

A third possibility exists—namely, some combination of the climatic and expansion theories. The writers have not attempted to analyze this possibility, because more field information seems required.

In a review of the manuscript of this article Ernst Antevs suggested that a fourth theory should be considered: the Gilbert lake stage could have been climatically controlled to the extent that it could reflect a halt in the trend toward aridity and not a rise to a maximum during a small climatic oscillation. The writers believe that the Gilbert beach is too strong to represent a halt of the lake recession because of a minor halt in climatic change and associate the beach with expansion over the Great Salt Lake Desert. Again, more data and study are needed.

Also, Antevs remarks that the pluvial-maximum theory requires a new dry stage about 12,000 years ago. He cites Clisby and Sears' (1956, p. 537, Fig. 1) plant-pollen graph from a study in west-central New Mexico, which records a drought at about this time.

Soils of the Big Cottonwood Creek Flood Plain

A flood plain, comparable in structure with that of the Jordan River lowlands, was observed along Big Cottonwood Creek. Two soils were observed 1.6 miles up from the junction with the Jordan River. The Big Cottonwood flood plain in this area grades westward to the Jordan at the rate of 30 feet per mile and lies only 70–80 feet above Great Salt Lake. At the surface is a living-soil profile which has a light-sandy loam composition; the gray humified horizon of the surface profile is 18–22 inches deep. In most places this humified horizon is underlain by a brownish horizon 15–20 inches thick that leaves the impression of a chestnut soil profile. A fossil-soil profile of very light sandy loam, 50–70 inches beneath the surface, grades downward into a fine sand. The dark-gray humified horizon is 20–25 inches thick. At certain localities the fossil soil comes close to the surface, so that the humified horizons of the fossil and living soil merge and form a very deep humified layer up to 50 inches thick. The upper and lower parts of this layer have a two-part structure by color as well as mechanical composition.

The living soil on the upper alluvial deposit is a silt loam with varying amounts of sand fractions (Table 11). The fossil soil is a silty clay loam with negligible amounts of sand. In the upper layer 1 per cent of the material consists of particles more than 1 mm in diameter (skeleton), whereas in the fossil soil none so large were observed. Profiles of the living and fossil soils are leached and non-calcareous. The reaction is strongly acid: pH for the living soil is 5.4 and for the fossil soil 5.1 to 5.6. Decomposition of organic matter is slow, and the amount of humus is 8.8 per cent and 4.7 per cent in the living and fossil soils respectively. The ignited portion in the living soil is 16.0 per cent and in the fossil soil is 13.7 per cent.

Soils of Emigration Creek Valley

Emigration Creek has trenched the sediments of the Bonneville-Provo 1 and Provo 2 stages westward to about 12th East Street, a distance of nearly 2 miles (Fig. 7). Here a fault scarp in the unconsolidated sediments exists, and since the incision is upstream from the scarp, faulting must be considered a cause in connection with the fall of the lake from the Provo 2 stage. The same applies to the entrenchment of Parleys Creek and Mill Creek. However, a terrace within the trenched valley near the canyon mouth, apparently unrelated to pluvial and postpluvial faulting, is clearly graded to the lake at the Provo level (Fig. 18). In the terrace a fossil soil occurs and separates deposits taken to be those of the Alpine lake from those of Provo 2. Beneath the fossil, dark-gray, loamy soil are reddish-brown silts and clays, and above are 23 feet of alternating layers of light-gray clay, silt, and gravel.

The sequence of events here is interpreted as follows: The lake receded from the Provo 1 stage level at about 4820 feet, and the stream trenched the thin deposits of the Bonneville-Provo 1 stage and exposed the Alpine silts on the flood plain. During the interpluvial stage a soil formed, and as the lake rose back to the Provo level (Provo 2) the flood plain was alluviated and the soil buried. With the fall of the lake from the Provo 2 level the alluviated flood plain was dissected.

A low, rather poorly defined terrace was observed below the main terrace. This also contains a buried soil. The soil is developed on beds of coarse sand and gravel and is dark gray and very calcareous. The thickness of the *A* and *B* horizons together ranges from 10 to 30 inches, and the profile is interpreted to signify a meadow type of soil.

The upper part of the flood plain is composed of a sandy loam or loamy deposits interbedded with gravels or humified layers. The entire upper section, even in the upper humified horizon of the living soil, is characteristically a bedded structure. In contrast, the fossil soil of the lower part in most places has no bedding and a well-developed granular soil structure. The percentage of carbonate in the *A* horizon of the living soil is 39.3 per cent, and in the fossil soil it is 25.3 per cent.

This lower flood plain, about 6 miles from the Jordan River, cannot be traced to the Jordan flood plain, but the writers assume that its soil is a product of the altithermal and that burial is due to the subsequent amelioration of climate.

TABLE 11.—MECHANICAL COMPOSITION OF FLOOD-PLAIN SOILS AT HEAD OF BIG COTTONWOOD CREEK

(In per cent)

Soil	Horizon	Sand (mm)					Silt (mm)					Clay (mm)
		1-0.5	0.5-0.25	0.25-0.12	0.12-0.06	total	0.06-0.03	0.03-0.015	0.015-0.007	0.007-0.003	total	0.003
Living	A (1"-15")	4.0	6.6	9.3	8.0	27.9	13.9	10.6	18.6	13.2	56.3	15.8
Fossil	A (17"-28")	0.1	0.3	0.8	1.8	3.0	18.3	21.0	10.6	21.0	70.9	26.1
	C (26"-28")	0.2	0.4	0.5	1.6	2.7	10.8	21.0	22.1	21.7	75.6	21.7

PRE-ALPINE SOILS

Occurrence

Reddish-brown soils up to 30 feet thick of pre-Alpine, possibly pre-Pleistocene, age and strikingly different from the post-Alpine steppe soils have been noted in Utah Valley by Hunt *et al.* (1953, p. 43) who write:

> "The ancient soils are restricted to the pre-Lake Bonneville deposits, and are further restricted to those areas where the surface had been preserved through the Lake Bonneville and post-Lake Bonneville time. The conditions are found at numerous places above the highwater mark of Lake Bonneville along the foot of the Wasatch, Traverse, and Lake Mountains."

Gvosdetsky found that the reddish-brown soils at a number of places in the Bonneville Basin are at least 5 times thicker than the fossil steppe soils; a great time interval was necessary for their formation. They were developed by the process of laterization under humid, subtropical conditions, whereas the steppe soils developed under a cool or temperate arid climate.

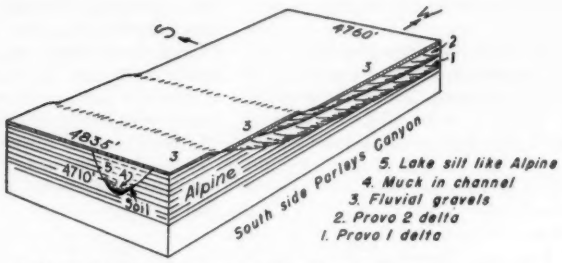

IDEALIZED RELATIONS AT MOUTH PARLEYS CANYON

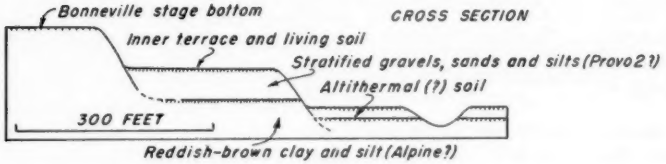

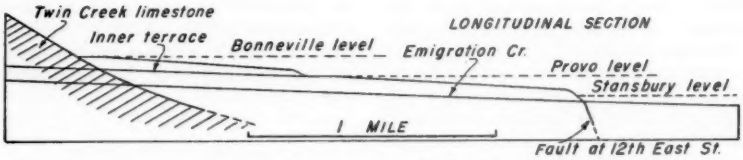

TERRACES OF EMIGRATION CREEK AT HOGLE ZOOLOGICAL GARDENS

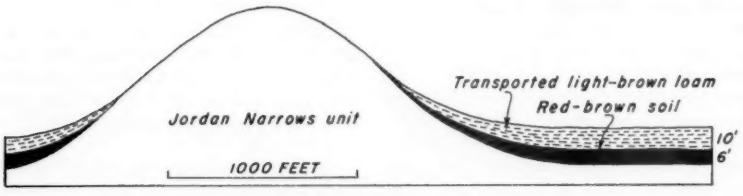

PRE-PLUVIAL SOIL SOUTH OF BACCHUS

FIGURE 18.—SOILS OF PARLEYS AND EMIGRATION CREEKS AND THE BACCHUS AREA

Spring Canyon Exposure

SETTING: An exposure of the red-brown fossil soil is located just above the Bonneville shore line and immediately north of the mouth of Spring Canyon between Parleys and Emigration canyons in the Wasatch Range. Eight feet of this fossil soil is exposed in a pit, but the total thickness is not known. It was formed on transported and mixed material derived from sandstone and limestone. The limestone boulders in the fossil soil are so deeply weathered that fragments can easily be cut with a knife. The red-brown fossil soil is covered by a transported colluvium derived from sandstone on the upper reaches of the steep mountain slope. At the surface on the colluvium is a mature, dark-brownish-gray living soil; its *A* and *B* humified horizons together are 2–3 feet thick.

FIELD CHARACTERISTICS: Remnants of the soil in the field are reddish brown or brown and of dominantly clayey composition. Distinctive well-developed columnar prismatic structures are elongated vertically. They measure about 2–3 inches in length and have a diameter of ½–1 inch. Some prisms may be 5 inches long and 2 inches in diameter. The surfaces of

the prisms are uneven and are covered with a film of colloids. (*See* Hunt and Sokoloff, 1950, Fig. 10.)

MECHANICAL ANALYSIS: The amount of skeletal material in the living soil and in the fossil red-brown soil is presented in Table 12 The living soil is 31.5 per cent skeletal material;

TABLE 12.—SKELETAL COMPOSITION OF RED-BROWN FOSSIL SOIL IN SPRING CANYON

(In per cent)

	Skeleton (mm)				Soil
	4	2-4	1-2	total	<1
Living soil	25.1	4.0	2.4	31.5	68.5
Fossil soil	3.5	0.6	0.7	4.8	95.2

most fragments are more than 4 mm in diameter and are composed of Nugget Sandstone. The fossil soil is less than 5 per cent skeletal material which is largely sandstone and limestone.

The mechanical composition of the living and fossil soils is also in striking contrast. The living soil is a loam with a total sand fraction (0.06 mm) of 49.5 per cent and only 18.5 per cent of fine silt and clay (0.15 mm). The fossil soil is characterized by a large amount of fine silt and clay (50.5 per cent) and a small amount of sand (10.3 per cent).

CHEMICAL ANALYSIS: Very little or no humus is present in the red-brown soils. Except near the limestone fragments the carbonates have been removed. The pH reaction of the red-brown soil ranges from below 6 to below 7, but near a limestone fragment it was 7 and over.

Foothill Boulevard Occurrence

Below the Spring Canyon exposure another striking example of the ancient red-brown soil was uncovered in an excavation for a service station at Foothill Boulevard and Skyline Drive, in Salt Lake City. This location is at an elevation of 4760 feet, or just below the Provo level. At the bottom of the cut (Fig. 14) is the Nugget Sandstone, badly shattered and crushed. The red-brown soil has developed on it, and the irregular lower limit of the soil grades rather abruptly into the light-pinkish-tan sandstone. The maximum exposed thickness is 3 feet, but much of the upper horizons has been eroded away, even where the thickness is maximum. All the soil is removed in places. (Compare Plate 4 with Figure 14.)

The soil has the same general characteristics as the Spring Canyon occurrence, but in addition a crude rectangular network of tiny rusty red veinlets is conspicuous, especially on the prism faces. Some veinlets penetrate the prisms as tubules; when veinlets are dry they leave a rusty red on the dull, olive-drab, clayey material.

On top of the red-brown soil is a cleanly washed boulder and gravel layer, and on top of this are dull reddish-tan sand and grit layers that resemble the Alpine lake deposits. Samples were submitted to Dr. D. J. Jones for examination, but no ostracodes were found in them. Possibly the reddish-tan sands are Alpine Formation sands reworked by the lake at the Provo level, but because the Alpine is extensively developed upslope from the locality the writers judge the sands to be Alpine.

If the sands are Alpine they indicate that as the lake rose during the Alpine stage it trimmed off irregularities of the slope and much of the thick red-brown soil and left a layer of coarse, clean gravel across the beveled surface. As the waters became deeper the ensuing deposits were finer sands.

Bacchus Exposure

About 3 miles south of the Bacchus pit and above the Bonneville shore line are outcrops of the Jordan Narrows Formation of the Salt Lake Group (Slentz, 1955). Road cuts across ridges reveal the red-brown soil (Fig. 18). The soil is 5–6 feet thick and of the same character as the Spring Canyon and Foothill occurrences. It grades below into the light-gray tuffs, marls, and gravels of the Jordan Narrows Formation and is therefore believed to have formed in place. Above the reddish-brown soil is a loamy deposit, probably a result of reworking of the soil.

Significance and Interpretation

Stratigraphic relations indicate that the red-brown soils in the Lake Bonneville Basin are pre-Alpine. The resemblance in color of the Alpine deposits to the reddish-brown soil, the large volume of silt characteristic of the Alpine, and the unusual thickness of the soil all point to the conclusion that the Alpine stage was the first high-water lake, that in places its waters found a very thick reddish-brown soil to work on, and that the extensive

red, pink, and tan silts and fine sands below the 5100-foot elevation were derived in part from the soil (Hunt *et al.*, 1953, p. 45).

The red-brown soils are lateritic but do not display the intensity of laterization found in true laterites which form in tropical and subtropical humid climates. Laterites are not so well known as podzols and chernozems, and the red-brown lateritelike soils are not easily interpreted. In subtropical latitudes where considerable elevations are reached the laterites apparently give way to lateritic soils because of somewhat cooler temperatures; and it may be inferred, therefore, that the red-brown soils of the Bonneville Basin formed under subtropical humid conditions, possibly at elevations somewhat above sea level.

The lateritic soils represent a climate considerably moister and warmer than the present climate. The distribution of redwoods indicates a gradual cooling from humid subtropical to glacial climates in northern North America from late Eocene to early Pleistocene (Chaney, 1940). Molluscan assemblages on the Pacific Coast suggest approximately the same change (Durham, 1951). The grass-covered prairies first appeared in Miocene time in places in the Bonneville Basin area. The presence of the lateritic soil cover is in accord with the paleogeographic evidence if it is assumed that the main period of deep-soil formation was Early Miocene, Oligocene, or even late Eocene. This involves considerations of the diastrophic volcanic, and geomorphic history during the Tertiary and is beyond the limits of the present report.

Mountain Soils

Soils of Mountainous Areas

The processes of denudation in mountains are responsible for partial or complete removal of soil cover; thus most soils in mountainous areas are young and immature, and the opportunity for fossil-soil development is limited. This is especially true in glaciated mountains where weathered rocks and soil cover are generally removed by the ice. In the lower portions of some mountain valleys, however, alluvial and morainic deposits are preserved. During interglacial times the soils formed on these deposits mature, and during the following glacial period the soil is buried. Several localities of this nature were observed in the Wasatch Mountains, and three are chosen as examples for description and analysis: the fossil soils of Deer Creek and Alpine canyons and of the Silver Lake cirque basin.

Soils of Deer Creek Canyon

SETTING: Deer Creek Canyon broadens near its mouth to a small valley three-tenths of a mile wide, with an average grade of 440 feet per mile. In the upper part of this small valley the grade is reduced to 200 feet per mile. The valley is filled with alluvial and morainic deposits that are cut 20–40 feet deep by the present stream, yet bedrock has not been exposed anywhere. Immediately above this small valley Deer Creek Canyon resumes the appearance of a typical mountain canyon with steep slopes and a grade of nearly 700 feet per mile. About three-fourths of a mile up Deer Creek Canyon in the small valley, at an elevation of 6760 feet, there is a good exposure of a fossil soil. This is probably the soil briefly descibed by Atwood (1909, p. 50).

FOSSIL SOIL: The fossil soil is overlain by fresh till with unweathered granite boulders. On the till is a well-developed mature soil with a dark-gray humified *A* horizon about 10 inches thick.

The upper 6–10 inches of the fossil soil is a dark-gray, well-humified *A* horizon, and sharply defined below this layer is 2 feet of red-brown soil resembling a podzol's *B* horizon; the latter has a prismatic columnar structure and feels very much like heavy clay. The red-brown *B* horizon gradually changes into a dark-red alluvium about 4 feet thick and composed of silt, sand and scattered sandstone cobbles. This rests on a gravel layer made up largely of red sandstone pebbles and a minor amount of dark porphyritic intrusive rocks.

ANALYSES OF FOSSIL SOIL: The skeletal and mechanical compositions of both the *A* and *B* horizons are very similar (Tables 13, 14). This similarity suggests that both horizons were developed *in situ* from the same parent material. The striking difference in appearance of the dark-gray *A* horizon and the red-brown *B* horizon is due to soil processes. A somewhat higher amount of clay and fine-silt (0/05 mm–0.003 mm) fractions in the *B* horizon is probably the result of alluviation of clay particles from the upper *A* horizon and the more intensive disintegration, by podzolization, of various particles in the *B* horizon. The amount of humus in the dark *A* horizon is 3.2 per cent; in the red-brown *B* horizon the humus is negligible. The soil profile is noncalcareous; the *A* and *B* horizons are leached and show a

slightly acid condition with a pH of 6.4 and 6.5 respectively.

The data on the general mineralogical composition according to specific gravity are tabulated in Table 15. The skeleton in the *B* horizon is more weathered than that in the *A* horizon. This is in agreement with the data on mechanical composition (Table 14) and is a result of podzolization. Both horizons are more highly weathered than are those of the inter-Provo soil at Bacchus. The two soils are not comparable, however, since the Deer Creek soil was developed under the influence of podzolization, whereas the Bacchus soil developed under the process of calcification. Minerals weather more rapidly under podzolization; this may explain the high degree of skeletal weathering in the Deer Creek soil. Yet the amount of organic matter in the *A* horizon of the Deer Creek locality seems too high for a soil much older than the inter-Provo soil. According to the humus content the Deer Creek soil might be classed as a Wisconsin "Brady" soil, but the skeletal weathering is not sufficient for this soil even under processes of podzolization. The stratigraphic position of the soil does not assist in the correlation.

TABLE 13.—SKELETAL COMPOSITION OF DEER CREEK FOSSIL SOIL

(In per cent)

Horizon	Skeleton (mm)				Soil
	4	2-4	1-2	Total	(1mm)
A (5-8 in.)	6.1	3.2	2.5	11.8	88.2
B (20-23 in.)	4.8	2.1	2.5	9.4	90.6

TABLE 14.—MECHANICAL COMPOSITION OF DEER CREEK FOSSIL SOIL

(In per cent)

Horizon	Sand (mm)					Silt (mm)					Clay (mm)
	1 - 0.5	0.5-0.25	0.25-0.12	0.12-0.06	Total	0.06-0.03	0.03-0.015	0.015-0.007	0.007 - 0.003	Total	0.003
A	5.8	5.5	6.7	7.6	25.6	18.4	16.9	7.1	17.6	60.0	14.4
B	5.3	5.4	6.7	7.4	11.7	11.7	16.1	11.7	18.9	58.4	16.8

TABLE 15.—SPECIFIC GRAVITY OF SKELETON AND COARSE SOILS IN DEER CREEK

(In per cent)

Specific gravity / Horizon	Skeleton											
	Granules (2-4 mm)						Very coarse sand (1-8 mm)					
	below 1.91	1.91-2.20	2.20-2.51	2.51-2.57	2.57-2.89	over 2.89	below 1.91	1.91-2.20	2.20-2.51	2.51-2.57	2.57-2.89	over 2.89
A (5-8 in.)	1.0	11.4	62.6	10.7	14.3	0	0.1	4.0	45.5	2.1	47.9	0.4
B (20-23 in.)	0	1.3	59.1	2.2	37.4	0	0	0.1	27.9	4.6	66.8	0.6
Specific gravity / Horizon	Coarse soils											
	Coarse sand (0.5-1 mm)						Medium sand (0.25-0.5 mm)					
	below 1.91	1.91-2.20	2.20-2.51	2.51-2.57	2.57-2.89	over 2.89	below 1.91	1.91-2.20	2.20-2.51	2.51-2.57	2.57-2.89	over 2.89
A (5-8 in.)	0.1	2.6	30.5	12.8	50.1	3.9	0.1	0.9	14.0	9.3	71.6	4.1
B (20-23 in.)	0.2	1.0	20.6	13.7	63.6	0.9	0.1	0.4	18.7	8.4	66.9	5.5

Soils of Silver Lake Cirque Basin

A flood plain is developed in the headwaters of Big Cottonwood Creek in the cirque basin of Sliver Lake just behind the last recessional moraine. The elevation at this locality is 8727 feet above sea level or 4528 feet above the level of Great Salt Lake. The characteristic two-part structure of the flood plain in the Jordan Valley is in evidence. The upper layer of 25 inches is a living mountain meadow soil with humified *A* and *B* horizons, which are together 16–20 inches thick. The lower alluvial deposit measures 20–25 inches and rests on a gravel base. Between the two layers is a fossil soil 12–14 inches thick.

Since the fossil soil is younger than the youngest moraine, it is probably of altithermal origin and related in time to the fossil flood plain soil of the lower Big Cottonwood Creek and the Jordan River lowlands.

Correlation of Soils

A number of exposures of the lateritic red-brown soil have been noted; they are almost certainly pre-Alpine in age and may be Tertiary. When more outcrops and exposures are recognized and studied, divisions of this soil may be set up, and one or more ages may be defined.

Two soils that separate Alpine from Bonneville sediments have been recognized. Both are near the mouth of Parleys Canyon; the one at the Terminal Reservoir probably took a long time to form before burial and marks the Alpine Formation as considerably older than the Bonneville.

The soil in Reynolds gravel pit (Jones and Marsell, 1955, p. 101) is here correlated with the oldest soil in the Bacchus pit, and both are believed to separate Provo 1 from Provo 2 deposits.

The dark-gray fossil soil under the lower-terrace alluvium in the Bacchus pit is regarded as a moist steppe soil of inter-Provo 2 and Stansbury age, whereas the fossil soil of the middle-stream terrace in the Sevier Valley presumably developed a little later, during the Stansbury pluvial maximum, and is also a moist steppe soil.

If the Gilbert stage was a minor pluvial maximum then a soil separating Stansbury deposits from Gilbert deposits might occur, but this has not yet been found.

The flood-plain fossil soils of both the lower Sevier and lower Jordan rivers reflect arid climates of short duration and are regarded as post-Gilbert and probably developed during the altithermal.

Various living soils have been evolving since Bonneville, Provo, Stansbury, and Gilbert times. The living soil above the Bonneville level in Spring Canyon probably dates from pre-Bonneville time but has suffered considerable erosion. The living soil at the Foothill Boulevard and Skyline Drive excavation, for instance, dates from Provo 2 time, and the living soil on the lower-terrace deposits of the Bacchus pit dates from Stansbury time.

Chronology of Lake Bonneville Stages

Succession of Stages

The chronology of lake stages as postulated by Antevs (1948; 1952), Bissell (1952), and the writers is shown in Figure 20. Supporting the theory proposed by the writers is the following summary.

The Stansbury shore at about 4470 feet is believed to mark a pluvial maximum and the last fresh-water lake, for several reasons: (1) The Stansbury terrace is outstandingly prominent and marks the boundary of an upper zone of somewhat eroded minor lake terraces from a lower zone of little weathered, minor terraces. (2) The river terraces and buried soils at Bacchus below the Provo beach and above the Stansbury are best explained by a fall of the lake below 4470 ft, consequent incision of the streams in the Provo bottom deposits, soil formation, rise of the lake to the Stansbury level, alluviation of the incised valleys and burial of the soil, fall of the lake, and entrenchment of the valley alluvium. (3) The tufa C^{14} analyses on the Stansbury beach correlate with the C^{14} dates of cores of the sediments of the last, fairly deep, fresh-water lake in the Great Salt Lake area.

The Gilbert level, 40–45 feet above Great Salt Lake, may mark an expansion-stability level of the lake in its general retreat from Stansbury to the present; it may also mark a minor pluvial maximum. Which theory is correct has not yet been established, but the lake never rose above the Gilbert level after the Stansbury. This is attested by the Danger Cave evidence and the sedimentary record under Great Salt Lake.

The lake stood at the Provo level (approximately 4820 feet above sea level) twice, as attested by the duality of deposits at the Provo level and in two known places by an intervening soil. Therefore, the lake presumably rose to the later Provo level after a low-level stage of several thousand years.

The Provo 1 stage is regarded as closely tied to the Bonneville stage because of the Red Rock Pass overflow situation. The authors believe, with Gilbert (1890, p. 171), that the lake here rose to overflowing, drained into the Snake River, and cut down its outlet channel about 315 feet with the consequent rapid lowering of the lake a similar amount to the Provo level. The lake held stationary at this elevation for some time, and the erosional

features and sediments of Provo 1 stage were formed. If this is the correct theory, the Provo 1 and Bonneville lake stages are part of the same climatic minimum. Bonneville from Provo 1 deposits have not been distinguished in most places, and Bonneville deposits are generally scarce.

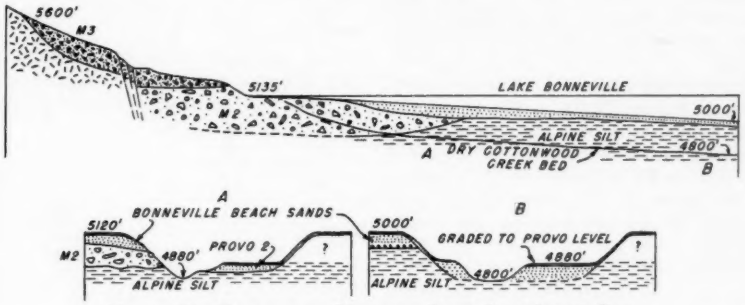

FIGURE 19.—RELATION OF MORAINES 3 AND 2 TO ALPINE SILT

Upper section is idealized from mouth of Little Cottonwood Canyon southwestward along Dry Cottonwood Creek. Cross sections A and B relate to points A and B of longitudinal section, and their vertical scale is somewhat greater.

The Bonneville and Provo 1 deposits overlie the Alpine deposits and hence are younger. The Alpine deposits are generally silts, in places pinkish tan to dull red and in other places pale gray green to gray tan, and are probably fairly voluminous. Wherever the overlying Bonneville or Provo 1 gray sands and gravels have been observed in contact with the Alpine, an unconformity is generally noted, and the break is striking. At two places a soil separates the two deposits. The Alpine lake is an older pluvial maximum, and its waves and currents worked on material which was of different character than succeeding lakes. The writers believe that this material over certain piedmont areas was a thick soil mantle reflecting in color the particular bedrock of the locality. If the Alpine lake ever rose to overflowing, the Bonneville lake could not have risen higher.

Microfossils are distinctive of the modern, the "Provo," the Bonneville, and the Alpine sediments (Jones and Marsell, 1955). A distinctive Stansbury fauna has not yet been recognized. The authors believe Jones' "Provo" fauna comes from Provo 2 sediments, and that his Bonneville fauna comes from Provo 1 and Bonneville which together represent a single pluvial maximum.

The steppe climates reflected by the interpluvial and postpluvial soils accord with the lake stages and interlake intervals as postulated.

Older lakes than the Alpine existed but did not rise as high, and their deposits are not yet well understood.

Ages of Younger Pluvial Maxima

Carbon-14 dates are consistent for the dating of the last major fresh-water stage, the Stansbury; accordingly this lake level was reached about 23,000 years ago and lasted until 13,500 years ago. Carbon-14 dates for the next older lake stage, the Provo 2, are inconsistent and have not yet been logically resolved. How much older the Provo 1-Bonneville and the Alpine are may be estimated only approximately by the separating soils and erosional unconformities. These seem to the writers real time breaks and equal to or greater than that which separates the Stansbury from Provo 2. The lake stages older than the Stansbury can be dated best by correlation with the glacial stages.

Age of the Alpine Formation

RELATIONS AT MOUTH OF LITTLE COTTONWOOD CANYON: The age of the Alpine Formation can best be determined by a study of the area around the mouth of Little Cottonwood Canyon (Fig. 7). Marsell (1947) recognized four ages of moraines and a relation of these to the Bonneville and Provo beaches. His note preceded the recognition of two lake stages at the Provo level, and the geologic setting here presented takes this condition into account.

The oldest moraine, here referred to as M1,

consists of large boulders strewn at elevations between 5200 and 6100 on the mountain front on the north side of the mouth of Little Cottonwood Canyon. All the finer matrix has been eroded away. Another remnant is found in Bell Canyon. In Mill D North Fork of Big Cottonwood Canyon a ridge is capped by it at least 500 feet above the next two younger moraines.

The next younger moraine, M2, is the "older" moraine of Atwood (1909, p. 82). It was deposited by an expanded foot glacier which extended at least a mile out from the canyon mouth and was later beveled by the waves of Lake Bonneville at the lake's highest level, 5135 feet. Its granite boulders are deeply weathered.

The third moraine, M3, is the "younger" moraine of Atwood and occurs as the crisp, faulted, lateral morainic ridge on the south side of the mouth of Little Cottonwood Canyon. The youngest moraine, M4, is an unmodified boulder pile about 1 mile down the canyon (west) of Alta at the head of Little Cottonwood. It is regarded as the terminal moraine of a short advance of the glacier.

Figure 19 shows the critical age relations of lake deposits to moraines. Inspection of the sides of Dry Cottonwood Creek valley reveals that the M2 moraine rests on the Alpine silts, and the Bonneville sands rest on both. The M3 moraine is clearly on M2.

Thus the Alpine silts were deposited and then dissected. Then the M2 moraine was deposited over the Alpine silts. The lake waters rose to the Bonneville level, beveled the moraine, and spread Bonneville stage sands and gravels over moraine and silts. Then the lake receded and rose to the Provo 2 level as the Provo 2 stage. This was contemporaneous with glacial stage M3. The writers believe that glacial stage M2 was contemporaneous with the Bonneville-Provo 1 pluvial stage, but that the rise of the lake lagged a little behind the advance of the glacier, so that the terminal moraine was deposited and soon afterward eroded by the lake's waves. (*See* Table 16.)

HUNT'S ANALYSIS IN THE ALPINE AREA: In the mouth of Dry Canyon northeast of Alpine village is a complex of glacial deposits. Atwood (1909, p. 78) recognized an "older" and a "younger" moraine there, the same as in the mouth of Little Cottonwood Canyon, which are here called M2 and M3. Hunt *et al.* (1953, p. 43) found the deep-reddish-brown podzolic soil on the "older" moraine of Atwood

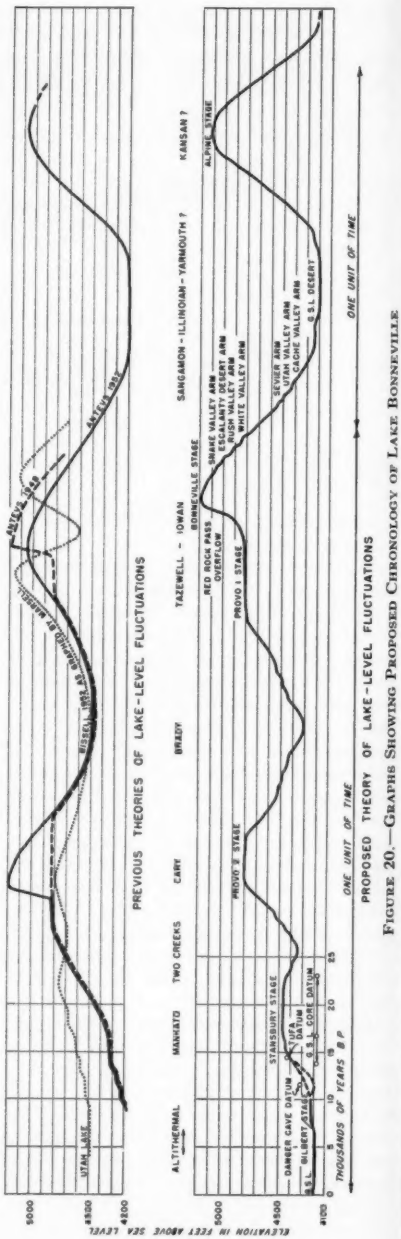

FIGURE 20.—GRAPHS SHOWING PROPOSED CHRONOLOGY OF LAKE BONNEVILLE

and decided that the evident antiquity of the soil dated the moraine as pre-Wisconsin. As explained above, the soil resembles somewhat the thick clayey gumbotils of the Middle West developed on the Illinoian and Kansan drifts. 15-foot reddish-brown soil is developed may be delineated by the soil blanket as a local mass on either side of the gorge of Chipman Creek, and it may be lapped upon by a moraine with deeply weathered granite boulders which

TABLE 16.—CORRELATION CHART OF PLUVIAL AND GLACIAL STAGES

The Wind River stages are from Holmes and Moss (1955), and the Waterton glacial chronology is from Horberg (1954). Wisconsin and Recent soils are of the steppe variety. The Bonneville-Provo 1 pluvial maximum lagged behind the moraine 2 maximum.

Time		Proposed Bonneville Chronology			Wind River Range	Waterton Region, Alberta, Canada
		Lake stages	Soil	Moraines		
Recent		Great Salt Lake			Cirque moraines	Cirque moraines
	Altithermal		Redwood Road			Colluvium, volcanic ash
		Gilbert				
Wisconsin	Mankato	Stansbury	Sevier Valley	Moraine 4	Temple Lake	
	Two Creeks		Bacchus pit			
	Cary	Provo 2		Moraine 3	Pinedale 1	Continental drift Late Wisconsin Mountain drift
	Brady		Reynolds pit and Bacchus pit			Drywood soil
	Tazewell and Iowan	Bonneville-Provo 1		Moraine 2	Bull Lake 2 Bull Lake 1	Upper till Lower till
Sangamon, Illinoian and Yarmouth			Thick steppe soil on Alpine fm. Podzolic soil on Moraine 1			Paleosol (Podzolic)
Kansan		Alpine		Moraine 1	Buffalo	Kennedy

FIGURE 20.—GRAPHS SHOWING PROPOSED CHRONOLOGY OF LAKE BONNEVILLE

Gvosdetsky is also impressed with the great age of the thick reddish-brown soil and regards it as dating back to pre-Wisconsin times. In dating the "older" drift of Atwood as pre-Wisconsin, however, the Alpine area becomes an exception, because elsewhere in the Wasatch and Uinta ranges the "older" and "younger" moraines have generally been regarded as early and late Wisconsin. It would seem that a morainal stage is missing in the Alpine area. If the M2 moraine in Little Cottonwood correlates with the "pre-Wisconsin" moraine in the Alpine area, then the Bonneville-Provo 1 lake stage is pre-Wisconsin. This seems unlikely.

The granite boulders in M2 of Little Cottonwood are deeply weathered, as in the "pre-Wisconsin" moraine at Alpine. There is no reddish-brown podzolic soil on M2, however, as on the old moraine at Alpine, but it may have been washed away by the waves at the mouth of Little Cottonwood.

Possibly three moraines exist in the mouth of Alpine Canyon, as at the mouth of Little Cottonwood. The moraine upon which the would be Atwood's "older" moraine. This "older," or early, Wisconsin moraine may be seen in fresh exposure on the south side of Dry Creek where a recent movement on the Wasatch fault occurred. There, no red soil is developed, although the steep slopes may not have been favorable for the development or preservation of such a soil. If the two old morainal masses are of different ages, then closer attention must be given to the degree of weathering of granite boulders in them. It has only been noted that the large boulders that protrude in part above the ground surface of both morains are fairly hard and fresh. The weathered outer zones have been removed, and the deeply weathered boulders are only found buried or freshly exposed.

If, in the Alpine area, the equivalent of the M1, M2, and M3 moraines in Little Cottonwood Canyon occurs, then the M1 is pre-Wisconsin, as are the Alpine silts. The deep steppe soil at the Terminal Reservoir on the Alpine silts confirms this conclusion.

Hunt *et al.* (1953, p. 41) tie the Alpine silts to the younger moraine, but their reasons are

not clear on this very important link. It is not evident to the reader why the gravels in the Alpine are tied to the younger moraine. They do not mention what the younger moraine fragments have in common with the Alpine gravels, and the writers failed to note any difference in the field in the general content of the two moraines.

Proposed Correlations

Table 16 shows the proposed correlations of the Bonneville lake stages, soils, and moraines of the Wasatch region and the correlation of these with the glacial stages of the Wind River Range and the Waterton region of Alberta. Horberg's (1954) time chart is used as a standard, since he was able to tie the mountain drifts to the continental drifts and establish a reliable relation. The proposed correlations seem compatible and logical. If they are correct, the Alpine lake stage would be Kansan or Illinoian, the Bonneville-Provo 1 would be Tazewell and Iowan, the Provo 2 would be Cary, and the Stansbury would be Mankato.

References Cited

Afanasiev, D., and Gvosdetsky, V., 1937, A contribution to the genesis of soils and vegetation in the floodplain of the Desna River: Jour. Botany, Ukranian Academy of Sciences, Kiev, p. 157–172 (in Ukranian with English summary, p. 170–172)

Antevs, Ernst, 1948, The Great Basin: climatic changes and prewhite man: Univ. Utah Bull., v. 38, no. 20, p. 168–191

—— 1952, Cenozoic climates of the Great Basin: Sonderdruck aus der Geol. Rundshau, Bd. 40, Heft 1, p. 94–108

—— 1953, Geochronology of the Deglacial and Neothermal ages: Jour. Geology, v. 61, p. 195–230

—— 1955, Geologic—climatic dating in the west: Antiquity, v. 20, p. 317–335

Atwood, W. W., 1909, Glaciation of the Uinta and Wasatch mountains: U. S. Geol. Survey Prof. Paper 61, 96 p.

Bissell, H. J., 1952, Stratigraphy of Lake Bonneville and associated Quaternary deposits in Utah Valley (Abstract): Geol. Soc. America Bull., v. 63, p. 1358

Bryan, Kirk, and Albritton, C. C., Jr., 1943, Soil phenomenon as evidence of climatic changes: Am. Jour. Sci., v. 241, p. 469–490

Chaney, R. W., 1940, Tertiary forests and continental history: Geol. Soc. America Bull., v. 51, p. 469–488

Clarke, F. W., 1942, Data of Geochemistry: U. S. Geol. Survey Bull. 770, 1005 p.

Clisby, K. H., and Sears, P. B., 1956, San Augustine Plains-Pleistocene climate changes: Science, v. 124, no. 3221, p. 537

Durham, John Wyatt, 1951, Cenozoic marine climates (Abstract): Geol. Soc. America Bull., v. 62, p. 1433–1434

Emiliani, Cesare, 1955, Pleistocene temperatures: Jour. Geology, v. 63, p. 538–578

Feth, J. H., and Rubin, Meyer, 1957, Radiocarbon dating of wave-formed tufas from the Bonneville basin (Abstract): Program, Geol. Soc. America Cordilleran Section, Los Angeles, Calif., April 19–20, p. 17

Flint, R. F., 1947, Glacial geology and the Pleistocene Epoch: N. Y., John Wiley & Sons, Inc., 589 p.

Gilbert, G. K., 1890, Lake Bonneville: U. S. Geol. Survey Mon. 1, 438 p.

Goldschmidt, V. M., 1954, Geochemistry: London, Oxford University Press, 730 p.

Grover, Nathan C., *et al.*, 1955, Surface water supply of the United States, 1933, pt. X, the Great Basin: U. S. Geological Survey Water Supply Paper 750, p. 105

Gvosdetsky, Vasyl, and Hawkes, H. B., 1953, Reappraisal of the history of Lake Bonneville: Utah Eng. Exp. Station Bull. 60, 70 p.

Gvosdetsky, Vasyl, and Hawkes, H. B., 1956, Middle stream terrace of the Bonneville Basin: Utah Engineering Experiment Station Bull. 81, 46 p.

Holmes, G. William, and Moss, John H., 1955, Pleistocene geology of the southwestern Wind River Mountains, Wyoming: Geol. Soc. America Bull, v. 66, p. 629–654

Horberg, Leland, 1954, Rocky Mountain and continental Pleistocene deposits in the Waterton region, Alberta, Canada: Geol. Soc. America Bull., v. 65, p. 1093–1150

Hunt, C. B., and Sokoloff, V. P., 1950, Pre-Wisconsin soil in the Rocky Mountain region, a progress report: U. S. Geol. Survey Prof. Paper 221-G, 15 p.

Hunt, C. B., and Varnes, H. D., and Thomas, H. E., 1953, Lake Bonneville: Geology of northern Utah Valley, Utah: U. S. Geol. Survey Prof. Paper 257-A, 99 p.

Hutchinson, G. E., 1953, The biochemistry of the terrestrial atmosphere, p. 371–433 *in* Kuiper, G. P., *Editor*, The Earth as a Planet: Chicago, Univ. Chicago Press, v. II, 751 p.

Jennings, Jesse D., 1953, Danger Cave, a progress summary: El Palacio, v. 60, no. 5, p. 179–213

Jones, D. J., and Marsell, R. E., 1952, Pleistocene lake sediments in the vicinity of Salt Lake City, Utah (Abstract): Geol. Soc. America Bull., v. 63, p. 1364

—— 1955, Pleistocene sediments of lower Jordan Valley, Utah, p. 85–112 *in* Eardley, A. J., *Editor*, Tertiary and Quaternary geology of the eastern Bonneville Basin: Utah Geol. Soc., Guidebook to Geology of Utah, no. 10, 132 p.

Marsell, R. E., 1947, The relations of the Little Cottonwood and Bell Canyon glaciers to Lake Bonneville (Abstract): Utah Acad. Sci. Proc. 1945–1946, v. 23, p. 18

Marsell, R. E., and Jones, D. J., 1955, Pleistocene history of Lower Jordan Valley, Utah, p. 113–120 *in* Eardley, A. J., *Editor*, Tertiary and Quaternary geology of the eastern Bonneville Basin: Utah Geol. Soc., Guidebook to Geology of Utah, no. 10, 132 p.

Nikiforoff, C. C., 1943, Introduction to paleopedology: Am. Jour. Sci., v. 241, p. 194–200.

Nolan, Thomas B., 1927, Potash brines in the Great Salt Lake Desert, Utah: U. S. Geol. Survey Bull. 795-B, 20 p.

Richmond, G. M., Morrison, R. B., and Bissell, H. J., 1952, Correlation of the late Quaternary deposits of the LaSal Mountains, Utah, and of Lakes Bonneville and Lahontan by means of interglacial soils (Abstract): Geol. Soc. America Bull., v. 63, p. 1368–1369

Slentz, Loren W., 1955, Salt Lake group in Lower Jordan Valley, Utah: Guidebook to Geology of Utah, no. 10, Utah Geol. Soc., Tertiary and Quaternary geology of the eastern Bonneville Basin, A. J. Eardley, editor, 132 p.

Thorne, James P., and Thorne, D. W., 1951, Irrigation waters of Utah; their quality and use: Agri. Exp. Sta. Bull. 346, Utah State Agri. Coll., 64 p.

Vishner, Stephen S., 1954, Climatic atlas of the United States: Cambridge, Mass., Harvard Univ. Press, 403 p.

Williams, J. Stewart, 1952, Red Rock Pass, outlet of Lake Bonneville (Abstract): Geol. Soc. America Bull., v. 63, p. 1375

University of Utah, Salt Lake City, Utah

Manuscript Received by the Secretary of the Society, October 29, 1956

BULLETIN OF THE GEOLOGICAL SOCIETY OF AMERICA
VOL. 68, PP. 1203-1224, 19 FIGS., 4 PLS. SEPTEMBER 1957

EFFECTS OF GAMMA RADIATION ON THE EXPERIMENTAL DEFORMATION OF CALCITE AND CERTAIN ROCKS

BY JOHN HANDIN, D. V. HIGGS, D. R. LEWIS, AND P. K. WEYL

ABSTRACT

Calcite single crystals, Yule marble, and certain other rocks were deformed dry at room temperature under constant confining pressures of 2000 or 2750 bars at a strain rate of 1 per cent per minute. Uniaxial compression and extension experiments were made; for the marble, parallel and normal to c_v fabric maximum; for the single crystals, parallel to c_v and normal to $m\{10\bar{1}0\}$. Yule marble exposed to 17 megaroentgens of gamma radiation before deformation turned from white to bright blue when deformed. Intensity of color varied with orientation and amount of strain. Irradiated single crystals changed from amber to ultramarine blue when the greatest principal stress paralleled c_v. No color change occurred when the least principal stress paralleled c_v. Irradiation resulted in small reductions in yield stress of most of the rocks, but not of the single crystals.

Petrographic studies of the single crystals revealed that established principal deformation mechanisms, twin gliding on $e\{01\bar{1}2\}$, and translation gliding on $r\{10\bar{1}1\}$, were still operative and confirmed that blue color was associated with translation gliding only. In Yule marble blue grains had deformed by translation, clear grains by twinning.

Thermoluminescence studies indicated that compression along c_v yielded a new peak in the glow curves (at 280°), not present in undeformed irradiated calcite. Extension along c_v increased the magnitude of the glow curve at about 240° but gave rise to no new peaks.

CONTENTS

TEXT

	Page
Scope of investigations	1204
Acknowledgments	1204
Previous work	1204
Experimental results	1205
Procedure	1205
Yule marble	1205
Calcite single crystals	1206
Limestones	1208
Hasmark dolomite	1210
Some sedimentary rocks	1210
Petrographic observations	1212
Notation	1212
Laboratory procedure	1213
Calcite single crystals	1213
General	1213
Extension Parallel to c_v	1214
Compression parallel to c_v	1214
Irradiated Yule marble	1214
Thermoluminescence studies	1216
General remarks	1216
Procedure	1217
Results	1217
Calcite single crystals	1217
Yule marble	1218
Marianna limestone	1219
"Devonian," Fusselman, and Wolfcamp limestone	1219
Dolomite	1220
Discussion	1221
Summary and conclusions	1223
References cited	1224

ILLUSTRATIONS

Figure	Page
1. Stress-strain curves for T cylinders of Yule marble	1206
2. Stress-strain curves for 1 cylinders of Yule marble	1207
3. Stress-strain curves for calcite single crystals deformed parallel to c_v	1208
4. Stress-strain curves for calcite single crystals deformed perpendicular to $m\{10\bar{1}0\}$	1209
5. Stress-strain curves for several limestones	1209
6. Stress-strain curves for Hasmark dolomite	1210
7. Stress-strain curves for some sedimentary rocks	1212
8. Stereogram of specimen 315	1215
9. Stereogram of specimen 314	1215
10. Glow curves of calcite single crystals	1217
11. Glow curves of T cylinders of Yule marble	1218
12. Glow curves of 1 cylinders of Yule marble	1219
13. Glow curves of Marianna limestone	1219
14. Glow curves of "Devonian" limestone	1219
15. Glow curves of Fusselman limestone	1220
16. Glow curves of Wolfcamp limestone	1220
17. Glow curves of Hasmark dolomite	1220

18. Glow curves of Luning dolomite..... 1220
19. Calcite crystal lattice..... 1222

Plate — Following page
1. Photograph of calcite crystals deformed parallel to c_v.....
2. Thin sections of calcite crystals extended parallel to c_v..... 1208
3. Thin sections of calcite crystals compressed parallel to c_v.....
4. Deformed irradiated Yule marble.....

TABLES

Table — Page
1. Summary of experiments..... 1211
2. Crystallographic notations of specific planes for common forms in calcite..... 1212
3. List of obsolete and corresponding current symbols for rotated lamellae..... 1213
4. Significant data for calcite crystals..... 1214
5. Color of grains as related to the gliding mechanisms in Yule marble..... 1216

Scope of Investigation

Our interests in the influence of high-energy radiations on the strength of crustal materials are of two kinds: geological, radiations of low intensity applied for a very long time; and technological, radiations in large doses given in a short time. Having been unable to find any published reports of quantitative measurement of the strength of artificially irradiated rocks, we thought it desirable to conduct a reconnaissance of the damage inflicted by a large (17 megaroentgen) but otherwise arbitrary exposure of gamma radiation from a cobalt-60 source. Recorded herein are the preliminary results of deformation experiments on calcite, Yule marble, four limestones, Hasmark dolomite, anhydrite, a sandstone, a shale, and a siltstone.

In an effort to learn something of the nature of the radiation effects, we have made petrofabric studies of calcite single crystals and Yule marble, and thermoluminescence studies of all the carbonate rocks.

This investigation was made possible by an unusual combination of research facilities: a radiological laboratory (Lewis and Weyl) providing the radiation source and equipment for thermoluminescence work, high-pressure apparatus (Handin) in which ordinarily brittle materials can be made to flow, and a petrographic laboratory (Higgs) in which universal stage and X-ray fabric studies can be carried out.

Acknowledgments

We are indebted to the Atomic Energy Commission for making available the cobalt-60 source. We gratefully acknowledge the assistance of R. V. Hager, Jr., J. N. Feather, T. V. Chan, and A. F. Roscoe and have enjoyed stimulating discussions with W. F. Bradley and M. C. Gutzwiller.

Previous Work

Pure electromagnetic radiation, in contrast to certain corpuscular bombardment, does not appear to disturb the structures of metal crystals sufficiently to influence the strength properties. We know of no previous measurements on rocks and could find no quantitative data on minerals other than metals.

There is a large literature, summarized recently by Przibram (1953, p. 38–42, 108–109, 140–143, 210), on coloration effected by radiation combined with deformation. Most experiments have been conducted on alkali halides which can be deformed permanently without rupture under atmospheric pressure.

Radium irradiation of pure, colorless halite results in a yellow coloration. After uniaxial compression of 100 kg/cm² normal to a cube face, the same dosage yields a deeper yellow. When the halite is loaded under 400 kg/cm², a blue color can be obtained whether the irradiation precedes or follows the deformation. Under very great loads (10,000 kg/cm²), however, no color change is effected. The color appears to be associated with translation gliding parallel to dodecahedral planes (T = {110}, t = [1$\bar{1}$0]).

Bluish-gray to violet coloration from Ra irradiation and uniaxial compression has also been observed in KCl, NaF, Na_2CO_3, K_2CO_3, $CaCO_3$, CaF_2, and several sulfates.

Natural colorless calcite acquires a yellow color under Ra irradiation and becomes blue gray under electron bombardment. Mechanical twinning, however, does not result in color changes. A cleavage fragment, twinned by pressing on an edge with a knife blade, turns yellow in both the twinned and untwinned portions. Natural yellow calcite can be made blue by uniaxial loading of several thousand kg/cm². Przibram felt, however, that the color of natural blue calcite must be due, if not to impurities, to intense radiation damage. He

did not associate the color with translation gliding in calcite; indeed, translation has been unequivocally demonstrated only recently (Turner, Griggs, and Heard, 1954, p. 931).

The only investigation of the effect of deformation on thermoluminescence appears to be that of Zeller (1954, p. 187), who subjected pellets of precipitated calcium carbonate to uniaxial compression of several thousand kg/cm². He observed that the alpha-activated glow-curve peak at 312°C. grew in height at the expense of the 110° peak with increasing pressure. No explanation for the behavior was offered, but it was pointed out that a deformation might introduce serious errors into age determinations based upon thermoluminescence measurements.

Experimental Results

Procedure

The apparatus, techniques, and procedures used in deforming ordinarily brittle rocks under high confining pressure in triaxial testing have been detailed in previous publications (Handin, 1953, p. 319–322; Handin and Fairbairn, 1955, p. 1261–1263). It is sufficient to say here that cylindrical specimens 1 inch long and half an inch in diameter, jacketed in thin copper tubes of negligible strength, are surrounded by kerosene under high pressure; then the axial, longitudinal pressure is made greater (compression test) or less (extension test) than the constant confining pressure. All tests were conducted at a constant strain rate of 1 per cent per minute at room temperature on dry specimens as soon as possible, never more than a few hours, after the specimens were removed from the radioactive source.

Yule Marble

Because it is pure, homogeneous, and relatively easy to deform with reproducible results, because it is naturally thermoluminescent, and because its experimental deformation had already been exhaustively studied by D. T. Griggs, F. J. Turner, and their collaborators, we chose Yule marble (Mississippian Leadville limestone of Colorado) as the first rock to be investigated. Specimens of two different orientations were cored from a slab provided by Griggs from his block number 5. *T* cylinders are cored parallel to the foliation of the rock; *l* cylinders are cut at 90° to *T* and normal to the foliation. Statistically the optic axes of the calcite grains tend to lie normal to the foliation (parallel to the long axes of *l* cylinders). The marble has a marked strength anisotropy (Griggs and Miller, 1951, Fig. 3).

Experiments were conducted under 2750 bars confining pressure, since data for unirradiated specimens were available from concurrent work. The first tests were made in compression on *T* cylinders, an orientation favoring mechanical twin gliding on $e\{01\bar{1}2\}$ in most grains (Handin and Griggs, 1951, Fig. 7). In this orientation the marble is very ductile, and none of the experiments was carried to fracture.

The first experiment (284) on irradiated marble revealed an unexpectedly large reduction in strength; the yield stress was only about 60 per cent of that of the unirradiated rock (188, 396) deformed under otherwise identical conditions (*see* Table 1). Being unaware at the time of the early work of Przibram (1953, p. 41) we were much surprised to find that the specimen which had assumed a faint pinkish cast during irradiation was bright blue after the 12 per cent compression. Closer scrutiny revealed that not all of the calcite grains had turned blue; some remained clear. These interesting effects, weakening and coloration, led us to a more complete investigation of the marble and also to a study of single crystals; our purpose was to relate the color to the flow mechanism involved.

Further compression tests on irradiated *T* cylinders (297, 390) revealed that the strength reduction was not as great as first supposed and that the reproducibility was very poor indeed. The stress-strain curves for Yule marble deformed at room temperature under a given pressure at a given orientation had been found by Griggs and Miller (1951, p. 861) to be reproducible within better than 5 per cent. Our curves for similar test conditions for specimens cored from the same block agree with those of Griggs to better than 5 per cent (Handin, 1953, p. 321). The maximum deviation for unirradiated specimens (188, 396) is only 3 per cent. The mean deviation for irradiated specimens (284, 297, 390) is, however, 25 per cent. The averaged stress-strain curves (Fig. 1) show that the probable strength is of the order of 80 per cent of that of the normal marble.

Extension curves for *T* cylinders (Fig. 1) show little or no difference for unirradiated specimens (averaged curve for experiments, 234, 389, and 398) and the irradiated specimen

(385). This orientation is unfavorable for twinning (Handin and Griggs, 1951, Fig. 7); and at the low confining pressure applied, the marble is still essentially brittle, so that very little permanent strain was achieved. All the specimens failed on incipient shear fractures inclined at about 70° to the least principal stress axis (in an extension test, the long axis of the

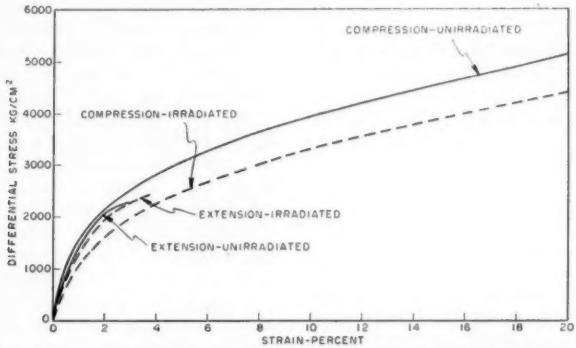

FIGURE 1.—STRESS-STRAIN CURVES FOR *T* CYLINDERS OF YULE MARBLE Deformed under 2750 Bars Confining Pressure at 24°C.

cylinder). Nevertheless, there was a small color change in the irradiated specimen from pink before deformation to blue gray after extension.

The extension of 1 cylinders favors twinning (Handin and Griggs, 1951, Fig. 7), and the specimens should be more ductile but weaker in this orientation than *T* cylinders in extension (Griggs and Miller, 1951, Fig. 3). That this is true can be seen by comparing the curves of Figures 1 and 2. Since there is no well-defined yield stress, it is preferable to compare the stresses at an identical small strain, say 2 per cent. The stress for 1 cylinders is then 1400 kg/cm² and for *T* cylinders 2100 kg/cm² in extension. Comparison of the averaged curve for irradiated specimens (370, 384) with that of unirradiated cylinders (235, 387) reveals a small strength reduction to 1320 kg/cm², about 5 per cent (Fig. 2). The reproducibility of experiments on both irradiated and unirradiated marble is excellent in this orientation, and the difference in strength, though small, is most probably significant. Radiation appears to have no effect on ductility. Again a color change from pink after irradiation to blue after deformation was observed.

The compression of 1 cylinders is unfavorable for twinning, and as Griggs and Miller (1951, Fig. 3) had already observed, the marble was found to be much stronger than in extension tests (Fig. 2). That it is also ductile in this orientation, in contrast to the case of *T* cylinders in extension, also unfavorable to twinning, is probably a result of the higher mean pressures obtaining in a compression test at the same confining pressure. In any event, none of the experiments was carried to fracture. The stress at 2 per cent strain of 4000 kg/cm² is nearly three times that of 1400 kg/cm² for an extension test in the same orientation. This difference is considerably larger than that of 3200 and 2000 kg/cm² respectively, reported by Griggs and Miller (1951, Fig. 3), but their experiments were conducted on Yule marble from a different block and under the much higher confining pressure of 10,000 bars. In compression the 1 cylinders are nearly twice as strong as *T* cylinders. The reproducibility of the curves for both unirradiated and irradiated material is good. The averaged curve for unirradiated specimens (233, 374) is about 10 per cent stronger at 2 per cent strain than for irradiated specimens (355, 369), and this difference is considered to be significant (Fig. 2). The deformed irradiated specimens were blue as usual. It is interesting to note that they were in fact a good deal bluer than the extended irradiated 1 cylinders for approximately the same strain, and this suggests that twinning results in a less pronounced color change. This is verified by single crystal studies.

Calcite Single Crystals

The mechanisms of deformation for unirradiated calcite, which were established by Turner, Griggs, and Heard (1954, p. 931), are

(1) twin gliding on $e\{01\bar{1}2\}$ with a positive sense of gliding in the direction $[e_1{:}r_2]$; (2) translation gliding on $r\{10\bar{1}1\}$, with a negative sense of gliding in the direction $[r_1{:}f_2]$; (3) translation gliding on $f\{02\bar{2}1\}$ with a negative sense of gliding in the direction $[f_1{:}r_2]$. Depending upon the crystallographic orientation relative to the yield stress is probable. Petrographic study has confirmed that twin gliding is responsible for all the permanent strain in both specimens, and the stress-strain curves of this paper are in good agreement with Griggs' (Turner, Griggs, and Heard, 1954, Fig. 3). Irradiation produced a light-amber color in the otherwise clear

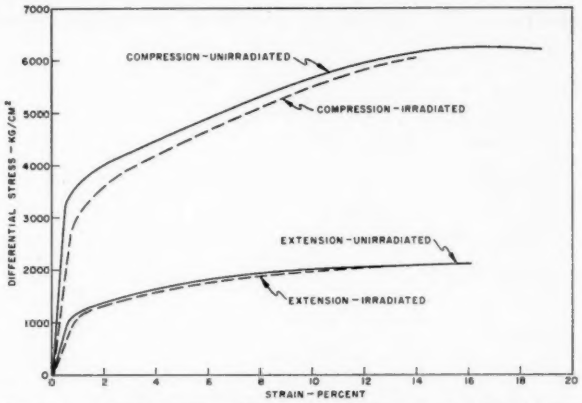

FIGURE 2.—STRESS-STRAIN CURVES FOR 1 CYLINDERS OF YULE MARBLE Deformed under 2750 Bars Confining Pressure at 24°C.

direction of loading, calcite may deform by twin gliding only or by translation gliding only. Twin gliding occurs to the exclusion of translation gliding in experiments where the least principal stress axis is parallel to c_v.[1] Translation gliding occurs to the exclusion of twin gliding where the greatest principal stress axis is parallel to c_v. In order to determine whether the color changes accompanying permanent strain of the marble are related to a particular flow mechanism, irradiated and unirradiated single crystals were loaded in compression and extension in two orientations, parallel to c_v, and normal to c_v and prism face $m\{10\bar{1}0\}$ under 2750 bars confining pressure (Table 1). In Plate 1 are specimens deformed parallel to c_v.

Extension parallel to c_i results in a high resolved shear stress coefficient of 0.40 on the mechanical twin plane in the correct (positive) sense for twin gliding (Turner, Griggs, and Heard, 1954, p. 902). The stress-strain curves (Fig. 3) of irradiated and unirradiated extended specimens (315 and 317) differ very little. Many more experiments would be required to test the statistical significance of the small difference observed, but a small increase of crystal, and deformation only caused the faint amber to disappear.

Compression parallel to c_v yields the maximum resolved shear stress coefficient of 0.50 on the cleavage plane $r\{10\bar{1}1\}$, and the sense on the twin plane $e\{01\bar{1}2\}$ is negative, so that mechanical twinning is impossible (Turner, Griggs, and Heard, 1954, p. 920). The stress-strain curves (Fig. 3) of compressed irradiated (314) and unirradiated (313) specimens again are much alike. In the absence of data on the reproducibility of experiments under identical conditions and on variations in mechanical properties to be expected from one single crystal to another, it can be said only that a small increase of yield stress is observed consistently. A fabric study has shown that translation gliding on $r\{10\bar{1}1\}$ accounts for all the strain in both specimens. The yield stresses of our curves are somewhat greater than that of the average curve given by Griggs (Turner, Griggs, and Heard, 1954, Fig. 3). A light-amber color resulted from irradiation, and compression then produced a dark ultramarine blue. Compression of unirradiated specimens causes no color changes; the crystals remain clear. Irradiation of previously unirradiated, but compressed, specimens does produce the same blue color, however.

[1] c_v is used to denote the optic axis (vertical in calcite). c denotes the form $\{0\bar{0}01\}$.

Twin gliding in irradiated calcite was not accompanied by color changes, whereas translation gliding did result in a remarkable color change. To confirm these results as well as the similarity in the stress-strain relations of irradiated and unirradiated calcites, four more experiments were conducted in which the differential load was applied normal to c_v and normal to the prism face $m\{10\bar{1}0\}$. Contrary to pression normal to m. Griggs gives no curve for m in extension at room temperature. His curve for m in compression (Turner, Griggs, and Heard, 1954, Fig. 3) is not unlike ours. The situation with regard to color would also be expected to be reversed. Indeed, specimen 391 compressed normal to m, twinning favorable, did not acquire a blue color. Number 392, irradiated and extended normal to m, trans-

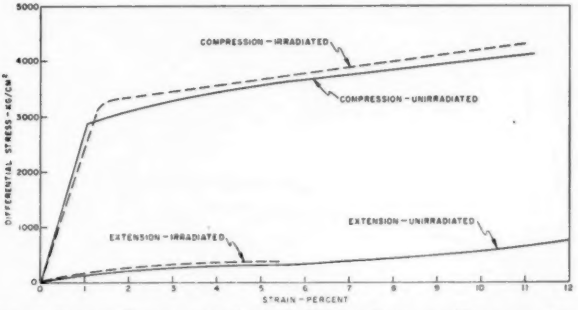

FIGURE 3.—STRESS-STRAIN CURVES FOR CALCITE SINGLE CRYSTALS DEFORMED PARALLEL TO c_v Under 2750 Bars Confining Pressure at 24°C.

the case of loading parallel to c_v, twin gliding is favored in compression where there is a high resolved shear stress coefficient (0.40) on one mechanical twin plane in the correct (positive) sense (Turner, Griggs, and Heard, 1954, p. 907). On the other hand, extension perpendicular to m favors translation gliding with a maximum resolved shear stress coefficient (0.50) on r and an incorrect sense (negative) on all three e twin planes. The stress-strain relationships would be expected to be reversed, and Figure 4 indicates that this is the case: the compression curves (376, 391), essentially similar again for irradiated and unirradiated material, are weaker than the extension curves (388, 392). For the experiments parallel to c_v (Fig. 3) the extension curves were the weaker, and are similar to those for com- lation favorable, would be expected to turn blue, but at 2750 bars pressure it was not ductile and broke after only a small elastic strain. There was no color change. Although the deformations were not checked microscopically, there is little doubt that this series of experiments confirms the lack of color change accompanying twinning as well as the virtual independence of the stress-strain curves of the irradiation.

Limestones

Data on the mechanical properties under confining pressure of a number of common sedimentary rocks, including several limestones, were available from an earlier study (Handin and Hager, 1957). We first chose one of these,

PLATE 1.—PHOTOGRAPH OF CALCITE SINGLE CRYSTALS DEFORMED PARALLEL TO c_v Under 2750 Bars Confining Pressure at 24°C. From left to right: unirradiated compressed, irradiated compressed (dark-blue color), unirradiated extended, irradiated extended (no color change).

PLATE 2.—THIN SECTIONS OF CALCITE SINGLE CRYSTALS EXTENDED PARALLEL TO c_v

A. Irradiated. 5.4 per cent strain (315). Plane of section contains c_v and parallels deformation plane.

B. Photomicrograph showing part of deformed band WXYZ in specimen 315. That twinning on e_1 is about 50 per cent completed is indicated by equal prominence of e_1 and e_1' lamellae.

C. Same as *B* but under polarized light at extinction position of e_1 lamellae.

D. Unirradiated. 12.6 per cent strain (317). Plane of section contains c_v and is normal to r_1.

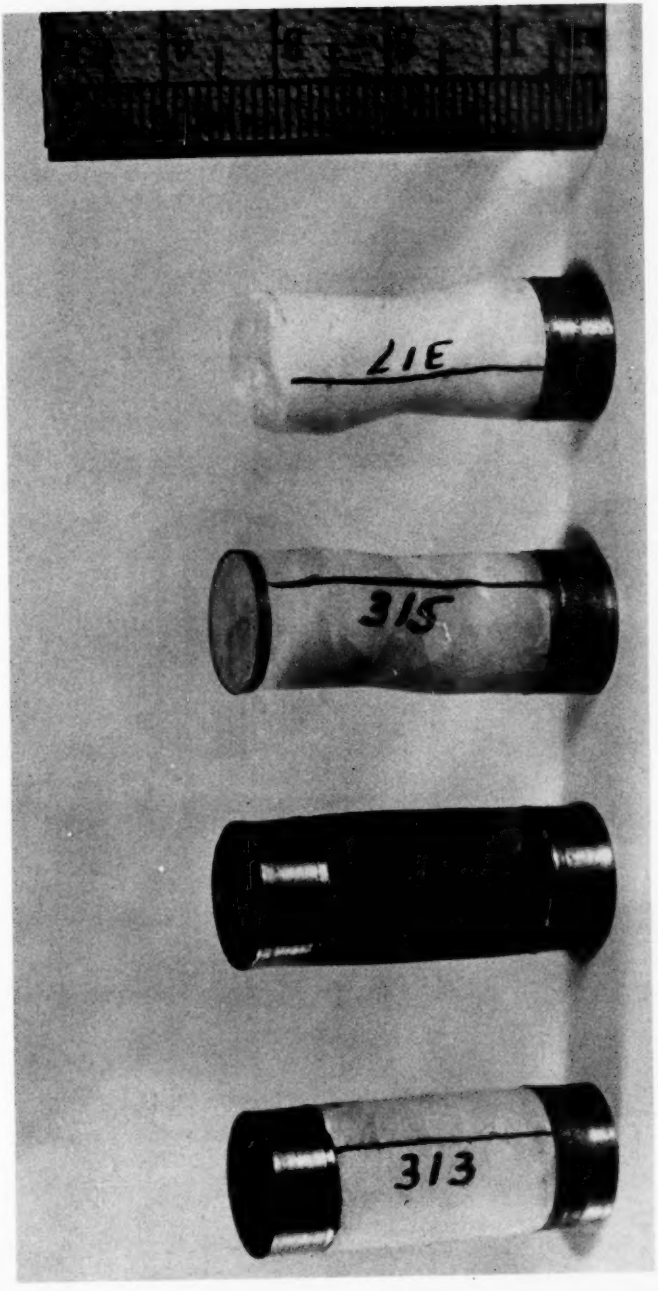

PHOTOGRAPHS OF CALCITE SINGLE CRYSTALS DEFORMED PARALLEL TO c_v

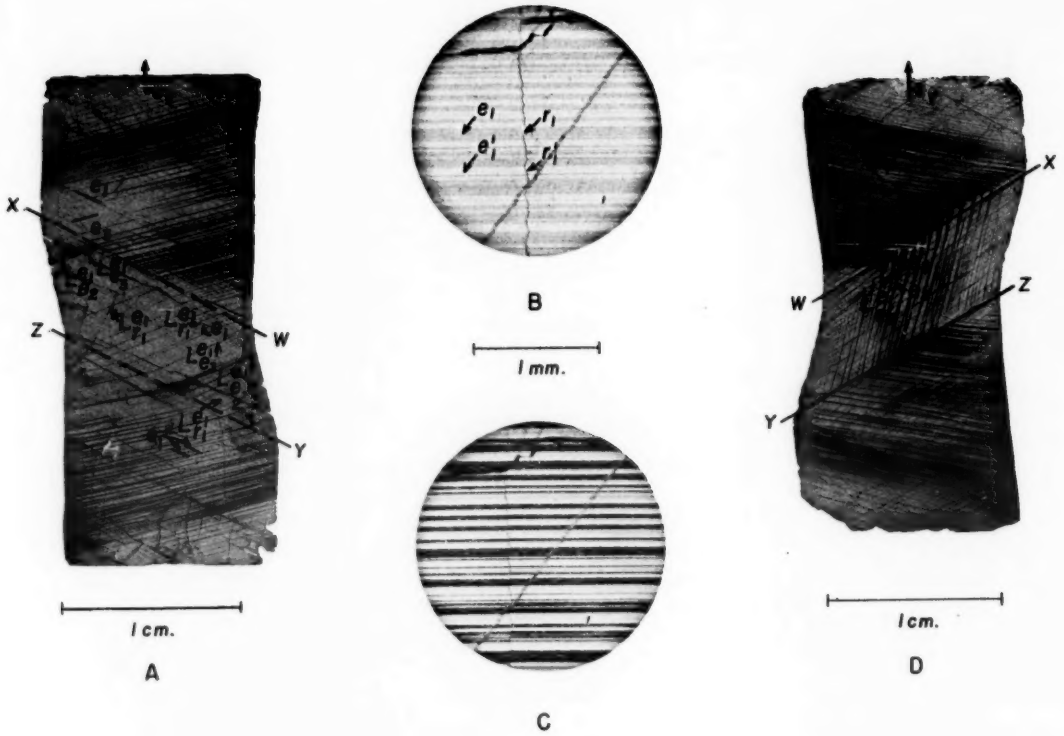

THIN SECTIONS OF CALCITE SINGLE CRYSTALS EXTENDED PARALLEL TO cv

1 cm.

A

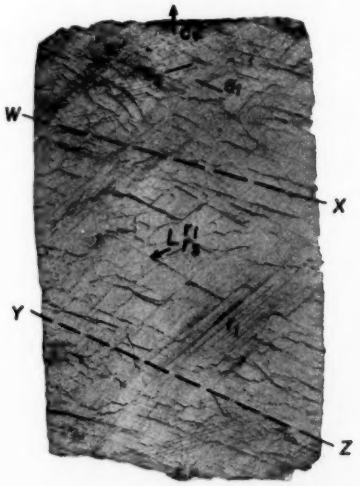

1 cm.

B

THIN SECTIONS OF CALCITE SINGLE CRYSTALS COMPRESSED PARALLEL TO cv

IRRADIATED *I* CYLINDER OF YULE MARBLE COMPRESSED 14.0 PER CENT

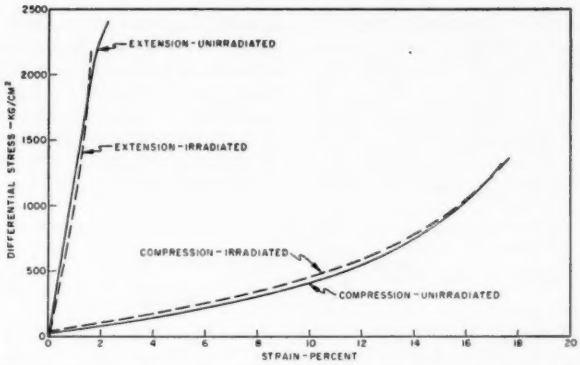

FIGURE 4.—STRESS-STRAIN CURVES FOR CALCITE SINGLE CRYSTALS DEFORMED PERPENDICULAR TO $m\{10\bar{1}0\}$
Under 2750 Bars Confining Pressure at 24°C.

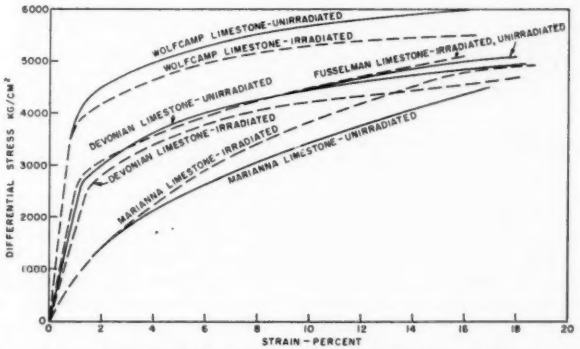

FIGURE 5.—STRESS-STRAIN CURVES FOR SEVERAL LIMESTONES
Deformed in Compression under 2000 Bars Confining Pressure at 24°C.

the Tertiary Marianna limestone of Florida, a chalky, porous, rather friable rock, for investigation with a view to determining whether the Yule marble was unusual in its response to gamma irradiation. A triaxial compression test was made on specimen 340 of irradiated Marianna limestone to be compared with tests on the two unirradiated specimens (394, 405) under a confining pressure of 2000 bars already used in the earlier work. We were surprised to find that no color change resulted from the deformation. The stress-strain curves (Fig. 5) for the unirradiated material are poorly reproducible, so that a comparison of the averaged curve with that for the single irradiated specimen very probably does not indicate that the strength has actually been increased by the radiation.

PLATE 3.—THIN SECTIONS OF CALCITE SINGLE CRYSTALS COMPRESSED PARALLEL TO c_v

A. Irradiated. 11.0 per cent strain (314). Plane of section contains c_v and parallels deformation plane.
B. Unirradiated. 11.2 per cent strain (313). Plane of section contains c_v and is normal to r_1.

PLATE 4.—IRRADIATED 1 CYLINDER OF YULE MARBLE COMPRESSED 14.0 PER CENT (369)

A. Grain boundaries and grain colors recorded from a study of a polished 2 surface.
B. Grain boundaries and gliding mechanisms recorded from thin section study of same polished surface.
C. Actual thin section from polished surface.

Three more limestones were chosen for testing on the basis of their high natural thermoluminescence. These are the "Devonian," the Fusselman, and the Wolfcamp; for a full description of which *see* Handin and Hager (1957, Appendix). All three acquired a pinkish-blue cast upon irradiation. Compression under 2000 bars confining pressure resulted in a loss of the pink, but no notable gain of the blue; the deformed specimens were gray or light blue gray. Any reduction of strength must be small, but not enough experiments were conducted to make it possible to give quantitative data. Each curve for unirradiated material (Fig. 5) is the average of two experiments, and the reproducibility is fair. The curves for irradiated specimens, however, are based on one experiment only. Ductility does not seem to be affected.

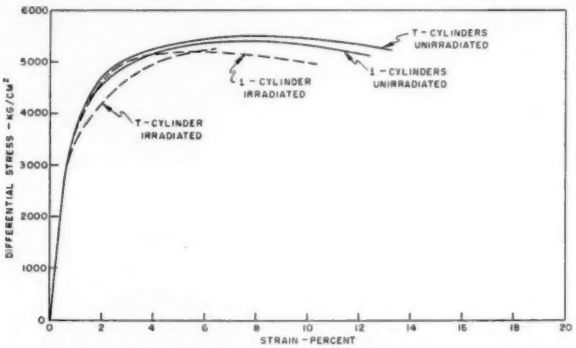

FIGURE 6.—STRESS-STRAIN CURVES FOR HASMARK DOLOMITE
Deformed in Compression under 2000 Bars Confining Pressure at 24°C.

Hasmark Dolomite

Again data were available from an earlier study for an unirradiated dolomite, the Cambrian Hasmark of Montana. Triaxial compression tests had been made in two orientations: parallel to the foliation (1 cylinders) and normal to the foliation (*T* cylinders). The optic axes of the individual dolomite crystal grains tend to lie normal to the foliation or parallel to the axis of a *T* cylinder (Handin and Fairbairn, 1955, Fig. 2). In spite of a high degree of preferred grain orientation, the dolomite has very little strength anisotropy. The stress-strain curves for unirradiated material (Fig. 6) are based on two experiments at 2000 bars confining pressure; the curves for irradiated specimens are based on only one. The Hasmark seems to be a little weaker after irradiation, but the data are insufficient to be certain. In any event the effect must be small, as is the color change accompanying the deformation of irradiated specimens (Table 1). It should be pointed out, however, that the dolomite is much less ductile than limestone at low pressures, so that the flow achieved is relatively small. Earlier studies of dolomite have indicated that the deformation mechanisms at room temperature are translation gliding on the base {0001} predominantly with minor twin gliding on $f\{02\bar{2}1\}$ (Higgs and Handin, 1954, p. 1263). Much more work would be required to relate the color change to a particular mechanism as has been done for calcite.

Some Sedimentary Rocks

A few experiments have been made on the following rocks for which data on unirradiated material were available: Blaine anhydrite, Barns sandstone, Muddy shale, and Repetto siltstone. This work was done merely as a rapid reconnaissance of any possible effects in several of the common sedimentary rock types. The stress-strain curves of Figure 7 indicate small reductions in strength but no apparent effects on ductility for all the rock tested. Again the data are insufficient to permit quantitative determinations, but the reproducibility of the experiments on unirradiated material, two for each rock, is good enough to allow us to state

TABLE 1.—SUMMARY OF EXPERIMENTS

		Experiment Number	Orientation	Confining Pressure Bars	Strain Percent	Ultimate Strength kg/cm²	Irradiated	Remarks
CALCITE SINGLE CRYSTALS		317	Ext. ∥ c_y	2750	12.6	800	No	Jacket failed probably.
		315	Ext. ∥ c_y	2750	5.4	370	Yes	Amber before. Clear after. Jacket failed.
		313	Comp. ∥ c_y	2750	11.2	4120	No	Not broken.
		314	Comp. ∥ c_y	2750	11.0	4330	Yes	Amber before. Dark blue after. Not broken.
		388	Ext. ⊥ a	2750	2.3	2150	No	Broken on 63° shear.
		392	Ext. ⊥ a	2750	1.6	2080	Yes	Gray before. No change after. Broke on one end.
		376	Comp. ⊥ a	2750	17.4	1320	No	Bent, but not broken.
		391	Comp. ⊥ a	2750	17.5	1290	Yes	Gray before. No color change after. Not broken.
YULE MARBLE		235	Ext. ∥ 1	2750	16.1	2260	No	Broke on "tension" fracture.
		387	Ext. ∥ 1	2750	15.3	2140	No	Necked. Not broken.
		370	Ext. ∥ 1	2750	16.0	2100	Yes	Pink before. Light blue after. Not broken.
		384	Ext. ∥ 1	2750	15.1	2140	Yes	Pink before. Light blue after. Jacket broke.
		232	Comp. ∥ 1	2750	18.8	6300	No	Bulged, but not broken.
		233	Comp. ∥ 1	2750	16.4	6060	No	Bent. Jacket broke.
		374	Comp. ∥ 1	2750	14.0	6250	No	Bent. Not broken.
		355	Comp. ∥ 1	2750	14.0	6110	Yes	Pink before. Blue after. Not broken.
		369	Comp. ∥ 1	2750	14.0	6050	Yes	No color before. Blue after. Not broken.
		398	Ext. ∥ 7	2750	3.0	2420	No	Broke on 70° shear.
		389	Ext. ∥ 7	2750	3.5	2170	No	Incipient shear.
		234	Ext. ∥ 7	2750	5.6	2490	No	Incipient shear.
		385	Ext. ∥ 7	2750	3.9	2280	Yes	Pink before. Blue-grey after. Incipient shear.
		188	Comp. ∥ 7	2750	19.7	5150	No	Bulged. Not broken.
		396	Comp. ∥ 7	2750	24.0	5750	No	Bulged. Not broken.
		284	Comp. ∥ 7	2750	25.4	4350	Yes	Pink before. Deep blue after. Incipient shear.
		297	Comp. ∥ 7	2750	11.9	1670	Yes	Pink before. Light blue after. Incipient shear.
		390	Comp. ∥ 7	2750	19.6	4720	Yes	Pink before. Blue after. Not broken.
LIMESTONES	Thermopolis	199	Comp. ∥ 7	2000	21.4	5680	No	Not broken.
		403	Comp. ∥ 7	2000	24.6	4800	No	Bent and bulged. Not broken.
		371	Comp. ∥ 7	2000	18.1	4700	Yes	Pinkish-blue before. Blue-gray after. Not broken.
	Paleozoic	231	Comp. ∥ 7	2000	22.1	5120	No	Incipient shear.
		404	Comp. ∥ 7	2000	25.5	5150	No	Bulged. Not broken.
		372	Comp. ∥ 7	2000	15.9	5080	Yes	Pinkish-blue before. Gray after. Not broken.
	Marianna	394	Comp. ∥ 1	2000	29.8	5300	No	Bent, but not broken.
		405	Comp. ∥ 1	2000	28.0	4680	No	Bulged. Not broken.
		340	Comp. ∥ 1	2000	18.7	4920	Yes	No color changes. Not broken.
	Bullfrog	223	Comp. ∥ 7	2000	17.5	6200	No	Bent. Incipient shear.
		402	Comp. ∥ 7	2000	12.6	5600	No	Bent. Not broken.
		373	Comp. ∥ 7	2000	16.4	5520	Yes	Pinkish-blue before. Gray after. Not broken.
DOLOMITE	Hasmark	237	Comp. ∥ 1	2000	12.4	5450	No	Broke on steep shear.
		301	Comp. ∥ 1	2000	11.4	5320	No	Broke on 60° shear.
		337	Comp. ∥ 1	2000	10.3	5160	Yes	Gray before. Bluish cast after. Not broken.
		300	Comp. ∥ 7	2000	11.8	5360	No	Not broken.
		312	Comp. ∥ 7	2000	13.3	5650	No	Bent, but not broken.
		336	Comp. ∥ 7	2000	6.4	5250	Yes	Gray before. Bluish cast after. Not broken.
	Ludwig	603	Comp. ∥ 7	2000	5.0	6450	No	Broke on 60° shear.
ANHYDRITE	Blaine	269	Comp. ∥ 7	2000	9.5	5050	No	Bent, but not broken.
		400	Comp. ∥ 7	2000	22.2	5270	No	Bent and bulged. Not broken.
		341	Comp. ∥ 7	2000	6.4	4540	Yes	No significant color changes. Not broken.
SANDSTONE	Berea	262	Comp. ∥ 7	2000	14.2	4600	No	Bent, but not broken.
		401	Comp. ∥ 7	2000	27.6	4050	No	Broke on 60° shear.
		334	Comp. ∥ 7	2000	14.1	3940	Yes	No color changes. Incipient shear.
SHALE	Muddy	399	Comp. ∥ 7	1000	14.1	2460	No	Incipient 57° shear.
		367	Comp. ∥ 7	1000	16.1	2500	No	Broke on 57° shear.
		354	Comp. ∥ 7	1000	14.2	2200	Yes	No color changes. Incipient shear.
SILTSTONE	Repetto	327	Comp. ∥ 7	1000	27.8	1700	No	Incipient shear.
		395	Comp. ∥ 7	1000	13.8	1830	No	Incipient 52° shear. Jacket split.
		353	Comp. ∥ 7	1000	26.1	1460	Yes	No color changes. Incipient shear.

that the effects are probably real though unspectacular. In no case was any color change involved.

Petrographic Observations

Notation

The crystallographic notation of Turner, Griggs, and Heard (1954) is used to designate specific planes. The common forms encountered for calcite and dolomite and their equivalent notations according to the new system described here are listed in Table 3.

Rotated lamellae are identified by the symbol L. Specific rotated lamellae are identified by subscripts (f_3, r, s, *etc.*) which relate them directly to their original rational positions in terms of accepted (Palache *et al.*, 1952) crystallographic notations for forms of the particular crystal involved. These crystallographic notations are used also as superscripts to identify

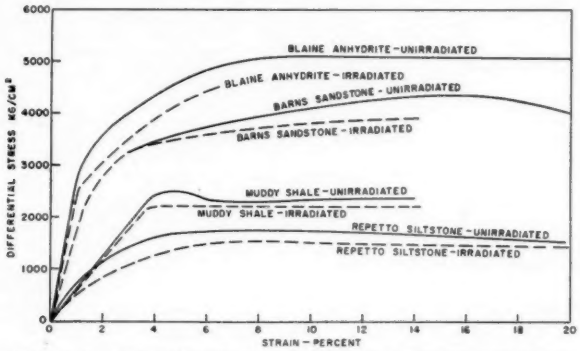

FIGURE 7.—Stress-Strain Curves for Some Sedimentary Rocks Deformed in Compression under 1000 or 2000 Bars Confining Pressure at 24°C.

TABLE 2.—Crystallographic Notations of Specific Planes for Common Forms in Calcite

Zone 1 a_2 = zone axis		Zone 2 a_3 = zone axis		Zone 3 a_1 = zone axis	
form	indices	form	indices	form	indices
e_1	$(\bar{1}012)$	e_2	$(1\bar{1}02)$	e_3	$(01\bar{1}2)$
r_1	$(10\bar{1}1)$	r_2	$(\bar{1}101)$	r_3	$(01\bar{1}1)$
f_1	$(\bar{2}021)$	f_2	$(2\bar{2}01)$	f_3	$(02\bar{2}1)$
m_1	$(10\bar{1}0)$	m_2	$(\bar{1}100)$	m_3	$(0\bar{1}10)$

in this study are listed with their symbols in Table 2.

The system of notation for rotated lamellae evolved during a conference[2] with I. Borg, D. T. Griggs, and F. J. Turner. It was agreed that their previous nomenclature (Borg and Turner, 1953; Turner, Griggs, and Heard, 1954) was inadequate and should be abandoned. Accordingly, the system agreed upon and described below was designed to provide maximum flexibility in future studies of deformed minerals of any species. The obsolete notations

[2] Conference at the Exploration and Production Research laboratory, Shell Development Company, Houston, Texas, November 12, 1955.

the active gliding planes. Hence $L_{m_i}{}^{n_j}$ identifies an m_i lamella that has been rotated by gliding on the n_j plane. The rotated lamella is identified by the subscript; the operator (or active gliding plane) by the superscript. Since a lamella may be rotated by successive or simultaneous gliding on two or more gliding planes, additional operators are added in superscript where the individual operations are identified, and they are separated by vertical bars. The quantity $L_{m_i}{}^{n_j|o_k|p_l}$, for example, identifies the lamella which results from successive rotations of an m_i lamella by gliding on each of the three planes, n_j, o_k, and p_l. Chronological order of gliding is not implied by sequences of

letters in the superscript because in many cases it cannot be determined. An *e* lamella in calcite, for example, may be rotated by twin gliding on another *e* plane followed by translation gliding on an *r* plane. The resulting rotated lamella would be identified as $L_{e_2}^{e_1/r_3}$, where the specific *e* and *r* planes are identified. This system does not distinguish between twin gliding and translation gliding. The type of gliding must be specified in the text.

less for planes inclined more than 70°. Probable maximum errors of 2° may exist for optic axis measurements when the axes are inclined 20° or less to the plane of the section. The error diminishes as the inclination increases.

TABLE 3.—LIST OF OBSOLETE AND CORRESPONDING CURRENT SYMBOLS FOR ROTATED LAMELLAE

Crystal	Symbol	
	Old	New
Calcite	L_1	$L_{e_1}^{r_1}$
	L_2, L_3	$L_{e_2}^{e_1}$
	L_4	$L_{r_1}^{e_1}$
	L_5	$L_{f_1}^{e_1}$
	L_6	$L_{e_1}^{r_2}$
	L_7	$L_{e_1}^{r_2}$
	L_8	$L_{f_1}^{r_1}$
Dolomite*	L_9	L_f^c

* Old symbol introduced in Turner, Griggs, Heard, and Weiss (1954).

Laboratory Procedure

Four thin sections of deformed calcite single crystals and one thin section of deformed Yule marble were studied. The petrographic examinations were made on a Zeiss microscope equipped with a universal stage and object traverser. Probable maximum error of measurement is 2° for planes inclined between 70° and 40° to the plane of the thin section. The error is

Turner's technique of establishing gliding mechanisms by studying rotation-of-lamellae phenomena was used in this work (Turner, Griggs, and Heard, 1954, p. 898–904). All stereograms were derived by plotting the measured optical data on a stereographic net. In all cases the lower hemisphere of the reference sphere was projected onto the horizontal plane.

Calcite Single Crystals

General.—The four specimens examined had been loaded parallel to c_y: two in extension, two in compression. For each type of experiment, one specimen had been irradiated, the other had

not. The planes of the thin sections are parallel to c_v and to the deformation plane for extension experiments; for compressed specimens they are parallel to c_v and normal to r_1. Each of the four thin sections was studied in detail, but since the deformation mechanisms were found to be identical in unirradiated and irradiated specimens, only the latter will be described in detail. The unirradiated specimens are illustrated for comparative purposes only. Significant data for all the crystals are summarized in Table 4.

wholly by twin gliding on $e\{01\bar{1}2\}$, and in these there were no color changes.

Compression parallel to c_v.—This orientation is most favorable for translation gliding on either $r\{10\bar{1}1\}$ or $f\{02\bar{2}1\}$ in unirradiated calcite (Table 4).

Deformation was fairly uniform throughout specimen 314 (Pl. 3*A*). There is a minor development of e lamellae near the ends of the specimen. Translation gliding occurred on r_2 and r_3 (Fig. 9). Gliding on r_2 caused internal rotation of e_3 and r_1 to the positions $L_{e_3}{}^{r_2}$ and

TABLE 4.—SIGNIFICANT DATA FOR CALCITE CRYSTALS.

Thin-Section Number*	Orientation	Load	Radiation	Strain (Percent)		Resolved Shear Stress Coefficient (S_{n1})**			Active System
				Measured	Calculated	$e\{01\bar{1}2\}$	$r\{10\bar{1}1\}$	$f\{02\bar{2}1\}$	
313	Parallel to c_v	Compression	None	11.2	8.2	.40-	.50-	.33-	$r\{10\bar{1}1\}$ TR***
314	Parallel to c_v	Compression	Gamma	11.0	10.4 14.8	.40-	.50-	.33-	$r\{10\bar{1}1\}$ TR***
315	Parallel to c_v	Extension	None	5.4	14.3	.40+	.50+	.33+	$e\{01\bar{1}2\}$ TW***
317	Parallel to c_v	Extension	Gamma	12.6	27.8	.40+	.50+	.33+	$e\{01\bar{1}2\}$ TW***

* Thin-section number corresponds to experiment number.

** Plus and minus signs refer to the positive and negative sense of shear as defined by Turner, Griggs, and Heard (1954).

*** TR = translation gliding; TW = twin gliding.

Extension parallel to c_v.—This orientation favors twin gliding (Table 4). Deformation (specimen 315) was confined almost entirely to the central sector (band *WXYZ*, Pl. 2*A*) where twinning on e_1 was about 50 per cent complete (Pl. 2*B*). The measurable lamellae are identified in Plate 2*A*, and all optical data are plotted on the stereogram (Fig. 8). Twin gliding on e_1 rotated e_2, e_3, and r_1 lamellae to the positions $L_{e_2}{}^{e_1}$, $L_{e_3}{}^{e_1}$, and $L_{r_1}{}^{e_1}$ respectively. These counterclockwise internal rotations amount to 14° and are in accord with the sense of shear for positive gliding on e_1. Although the calculated strain, $\epsilon = 14.3$ per cent, appears high compared to the measured strain of 5.4 per cent, there is actually good agreement because most of the deformation was restricted to one portion of the specimen that represents about one-third of its total volume.

The thin section of the unirradiated specimen (317) is illustrated in Plate 2*D*. The specimen was more highly deformed (12.6 per cent) than 315 which accounts for the difference in appearance. Both specimens deformed almost

$L_{r_1}{}^{r_3}$, respectively; and gliding on r_3 effected internal rotations of e_2 and $L_{r_1}{}^{r_2}$ to $L_{e_2}{}^{r_3}$ and $L_{r_1}{}^{r_2/r_3}$ respectively. In both cases the counterclockwise sense of internal rotation is in agreement with the sense of shear on r_2 and on r_3 (*see* inserts, Fig. 9). The rotations amount to 7°–10° resulting in calculated strains of 10.4–14.8 per cent which are in accord with the measured strain of 11.0 per cent.

The only significant difference between the irradiated and unirradiated (Pl. 3*B*) specimen was the blue color of 314 (irradiated). Translation gliding on $r\{10\bar{1}1\}$ was the only mechanism identified for either. Moreover, the close agreement between measured and calculated strains indicates that translation on $r\{10\bar{1}1\}$ accounts for almost all the strain. In the single crystals the blue color is clearly associated with translation gliding.

Irradiated Yule Marble

Experimentally deformed, irradiated Yule marble exhibits a color change similar to that

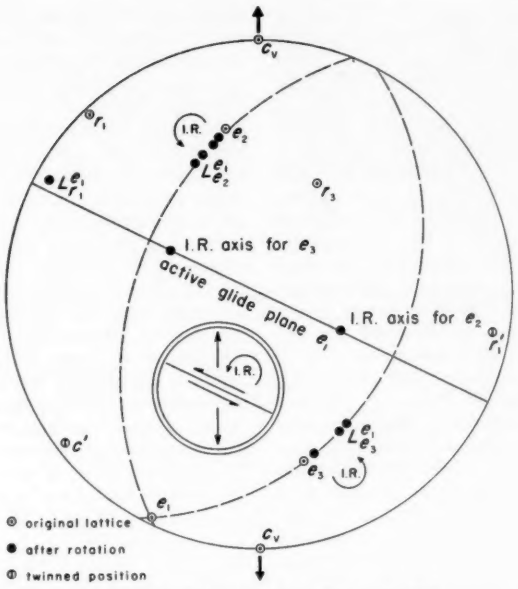

FIGURE 8.—STEREOGRAM OF SPECIMEN 315
Sense of Rotation and of Shear on the Gliding Plane Indicated in Insert. Rotated Lamellae in All Positions Cozonal with e_1.

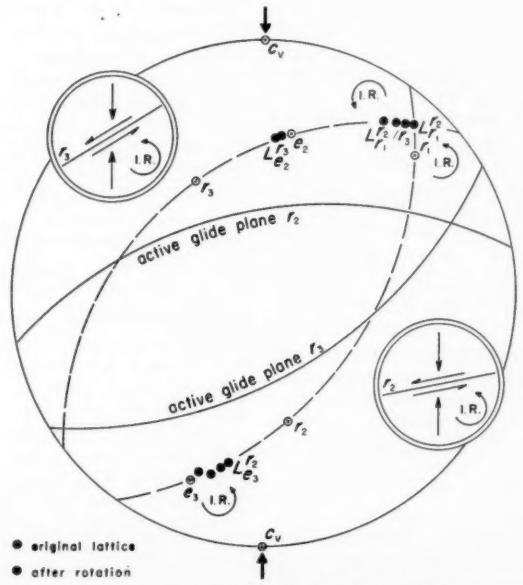

FIGURE 9.—STEREOGRAM OF SPECIMEN 314
Sense of Rotation and of Shear Indicated in Inserts.

of the calcite single crystals. The intensity of coloration, however, varies depending upon the relative number of blue and white grains present and upon the orientation of the cylinder relative to the load axis. This variation in intensity should be a function of preferred crystallographic orientation, since Yule marble has a well-developed c_v maximum. The blue color would be most intense in those cylinders that were oriented favorably for translation gliding in most grains if the color-gliding mechanism relationship established in the single crystals holds for the aggregate. Megascopically, this is the case—the most intense blue is associated with cylinders deformed in compression parallel to the c_v maximum.

The 2 surface (*see* Turner and Ch'ih, 1951, Fig. 1) of a 1 cylinder (specimen 369) was examined to test the color-gliding mechanism relationship in the aggregate. Since the color cannot be observed in thin section, it was necessary to record the colors of grains on a polished surface and then to make a thin section at this surface. The grain boundaries that could be identified on the polished surface under a binocular microscope were recorded (Pl. 4*A*) on an overlay of a color print of the surface, and the grain colors were noted as blue or white or as questionable blue or white. It could not be determined in some cases whether a faint blue was the color of a grain on the surface or was transmitted from a colored grain below the surface. The colors for such grains were noted as questionable.

The grains recorded from the polished surface that could also be identified in the thin section were examined microscopically, and the gliding mechanisms were identified and recorded (Pl. 4*B*). Two characteristic types of grains were observed. One type exhibits profuse development of $e\{01\bar{1}2\}$ twin lamellae, and in such grains the c_v axes are inclined at low angles to the plane of the thin section. The second type contains few or no twin lamellae, and the c_v axes are inclined at high angles to the plane of the thin section. That the clear grains deformed by translation gliding only and were not first completely twinned can be established unambiguously without making detailed measurements on each grain. This depends upon selection of the cylinder to be examined. As shown by Handin and Griggs (1951, Fig. 16) the 1 cylinder deformed in compression is one of the least favorably oriented for complete twinning one $e\{01\bar{1}2\}$. Measurements and identifications of the gliding mechanisms of a few grains using the technique of Turner confirm this. For the 2 surface examined, therefore, the clear grains, with their c_v axes at high angles to the plane of the thin section, reflect the translation gliding mechanism. Twin gliding is, of course, present in those grains exhibiting profuse development of twin lamellae. The observed colors of grains in the polished surface were related to the gliding mechanisms operative in those grains. Of the original grains, 122 were identified in the thin section. The results show (Table 5) that translation gliding was operative in the blue grains (58) and that twin gliding was operative in the white grains (38). Of the 122 grains, only 12 are anomalous.

The color-gliding mechanism relationship characteristic of the single crystals holds true for the aggregate; the blue color is associated with translation gliding. Study of the Yule marble provides additional evidence for the fact that individual calcite grains in the aggregate behave as though they are subjected to the same external forces that are applied to the specimen as a whole. Local stress concentrations are either unimportant or cancel out.

TABLE 5.—COLOR OF GRAINS AS RELATED TO THE GLIDING MECHANISMS IN YULE MARBLE

Color of Grains in Polished Surface	Thin-Section Examination		
	Number of Grains	Translation Gliding	Twin Gliding
Blue	63	58	5
White	44	6	38
Blue?*	13	12	1
White?*	2	0	2
TOTAL	122	76	46

* Estimated as questionable because the color may have been the color of a grain below the one on the surface.

THERMOLUMINESCENCE STUDIES

General Remarks

Thermoluminescence is the light emitted by some solids when heated at temperatures below incandescence. When samples are heated at a constant rate of temperature increase, light is emitted in a succession of maxima whose temperatures and magnitudes are related in some way to imperfections in the crystalline structure of the solids. Graphs of light intensity versus temperature are called glow curves.

The thermoluminescence of rocks results from the release by thermal agitation of electrons trapped in various metastable energy levels in the crystals which make up the rock. As the temperature is elevated, the chances

in crease for promoting an electron out of trap so that it can encounter a positively charged center with which it combines to give up some of its excess energy as a photon.

When a crystal absorbs gamma radiation, many energetic secondary electrons which are excited can populate any possible trapping sites at imperfections in the crystal structure. Any changes effected by a deformation in the kinds or numbers of imperfections will change the numbers and energies of electrons stores in traps associated with these imperfections. The effect of a deformation may, therefore, be reflected in the thermoluminescence glow curve.

The blue coloration accompanying translation gliding in irradiated calcite is another manifestation of the trapping of electrons in excited energy levels. The electrons are so coupled to their neighbors around a trap that oscillations occur which correspond in frequency to those of light in the optical absorption spectra.

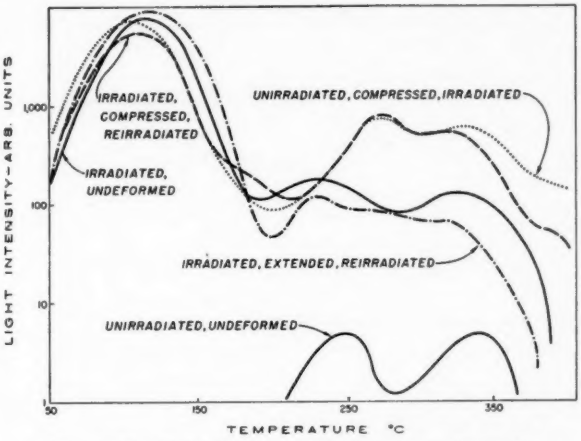

FIGURE 10.—GLOW CURVES OF CALCITE SINGLE CRYSTALS

Procedure

The material to be studied is ground and mixed, placed in a furnace, and heated at a constant rate of 80°C. per minute. The light emitted is measured photoelectrically, and its intensity is expressed in arbitrary units in terms of a standard light source in our laboratory. Glow curves are plotted on a semilogarithmic scale.

Since all materials must be ground for glow-curve measurements, the specimens were ground and then irradiated just before heating. The sequences of operation are then either deformation, grinding, irradiation, and heating, or irradiation, deformation, grinding, reirradiation, and heating. Samples are exposed for 164 hours in the nominally 100 curie cobalt-60 source. The dosage is computed as about 17 megaroentgens. Deformed specimens are reirradiated for 2 hours. For a detailed discussion of the thermoluminescence apparatus and technique, *see* Lewis (1956).

Results

Calcite single crystals.—The natural thermoluminescence of calcite is characterized by a glow curve with two similar peaks of relatively low intensity (Fig. 10). The effects of irradiation are to raise the average height of the curve and to introduce a large additional peak at about 120°C. We have found these two curves to be typical of a large number of natural calcites and limestones.

The effect of compression parallel to the optic axes (translation gliding) is to produce a new peak at approximately 280° (Fig. 10). Furthermore, this peak occurs whether or not the calcite is irradiated before deformation. The blue coloration also ensues in specimens compressed with or without prior irradiation. The glow-curve peak normally occurring at about 240° is somewhat reduced, but the 120° and 330° peaks are essentially unchanged in form.

Extension parallel to the optic axis (twin gliding) results in no new glow-curve peak (Fig. 10) nor in any color change. The 240° peak is somewhat enhanced relative to the 320° peak by the deformation. Again, similar glow curves are obtained whether or not irradiation precedes deformation.

Yule marble.—The natural thermoluminescence of the marble, typical of many limestones, is characterized by a glow curve with two peaks of relatively low intensity (Fig. 11). The effect of gamma irradiation is similar to that for the single crystals; the average intensity of the glow curve is increased, and a prominent new peak occurs at about 120°. The reasonable assumption that the thermoluminescence of the rock is the sum of that of the individual calcite grains appears to be valid.

The new glow curve resulting from the compression of a *T* cylinder (twinning favored in most grains) differs principally from that of the undeformed material in the appearance of a distinct shoulder at about 175°, not present in any of the single crystal curves. The new peak at 280°, associated with translation gliding in single crystals, also appears (Fig. 11). The glow curve of the specimen unirradiated before deformation is nearly identical to that of the irradiated and then compressed cylinder. The dark-blue color produced by a large shortening (about 25 per cent) and the light blue following a smaller strain (about 20 per cent) were observed upon irradiation following deformation whether or not the specimen had been irradiated previously.

It might be supposed that the glow curves for compressed *T* cylinders should resemble the curve for the extended single crystal (twinning favored). That they do not, and that there is a prominent color change, suggest that translation gliding is important even though most of the calcite grains are favorably oriented for twinning. The reason for this lies in the fact that most of the grains are completely twinned when the strain has reached about 10 per cent (Handin and Griggs, 1951, Fig. 16). Further strain to 20 per cent or more must then proceed by translation gliding in the completely twinned crystals.

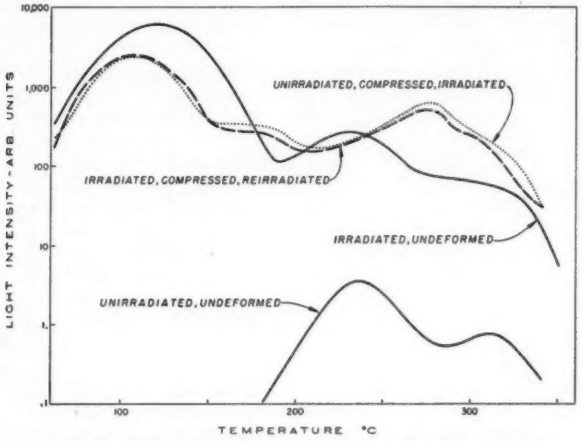

FIGURE 11.—GLOW CURVES OF *T* CYLINDERS OF YULE MARBLE

The glow curve for compressed 1 cylinders exhibits the prominent 280° peak associated with translation gliding as expected, since most grains are unfavorably situated for twinning (Fig. 12).

The extension of a 1 cylinder (twinning favored) to about 16 per cent effected a light-blue coloration in contrast to the dark blue of a 1 cylinder compressed a like amount. Furthermore, the glow curve is very much like that of the undeformed irradiated marble (Fig. 12) and of the single crystal extended parallel to c_p (*cf.* Figs. 10 and 12). This suggests that translation gliding has played a minor role in the deformation in accord with the prediction of Handin and Griggs (1951, Fig. 16) that although most grains are capable of twinning, few are completely twinned at strains of less than 20 per cent.

Since very little permanent strain was achieved in *T* cylinders in extension, no glow

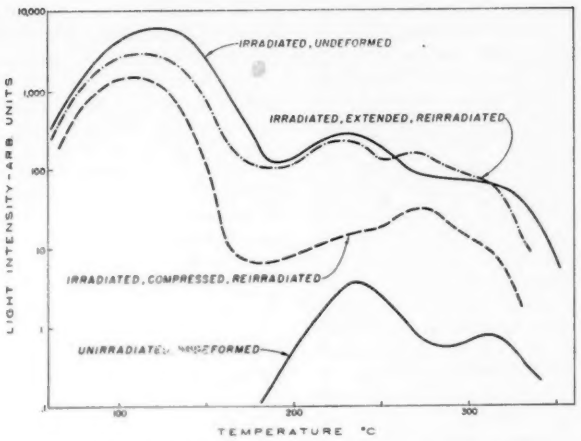

FIGURE 12.—GLOW CURVES OF 1 CYLINDERS OF YULE MARBLE

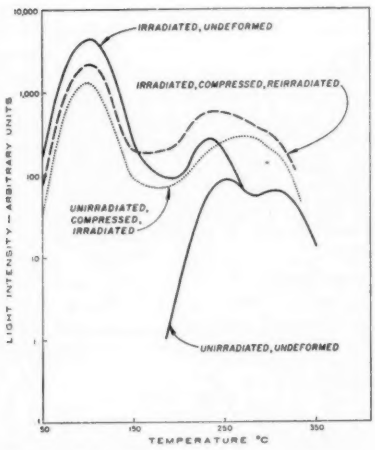

FIGURE 13.—GLOW CURVES OF MARIANNA LIMESTONE

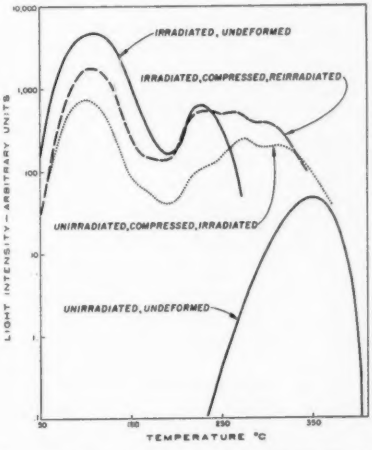

FIGURE 14.—GLOW CURVES OF "DEVONIAN" LIMESTONE

curves were determined for the marble in that orientation.

Marianna limestone.—The natural thermoluminescence of this rock is typical of many pure limestones collected, like the Yule marble, from at or near the surface where for a long time they had not been subjected to high temperatures. The undeformed irradiated specimen has a glow curve considered typical for limestone (Fig. 13). The effects of a 19-per cent compression are to introduce a shoulder in the glow curve at about 170°, to raise the intensity of the high-temperature portion of the curve, but to induce no new peak at 280°. No color change accompanied the deformation.

"Devonian," Fusselman, and Wolfcamp limestones.—These three rocks contain 95 per cent or more calcite. All were taken from well cores in flat-lying beds at depths of the order of 11,000 feet. The glow curves reflecting their natural thermoluminescence (Figs. 14, 15, 16) are characteristic of limestones which have been heated to about 100°, a temperature likely to be encountered at the depths men-

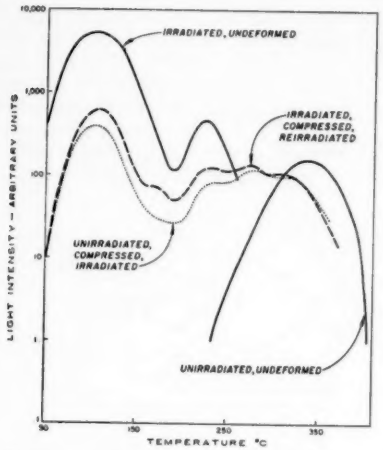

FIGURE 15.—GLOW CURVES OF FUSSELMAN LIMESTONE

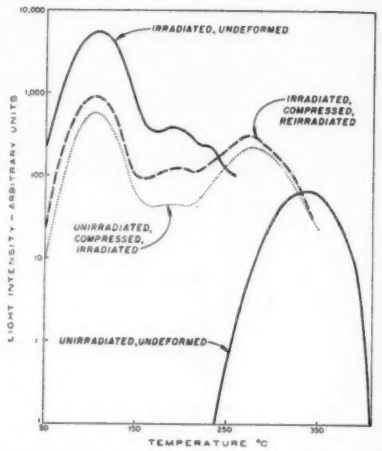

FIGURE 16.—GLOW CURVES OF WOLFCAMP LIMESTONE

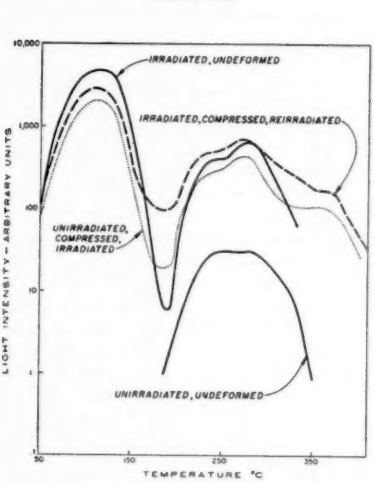

FIGURE 17.—GLOW CURVES OF HASMARK DOLOMITE

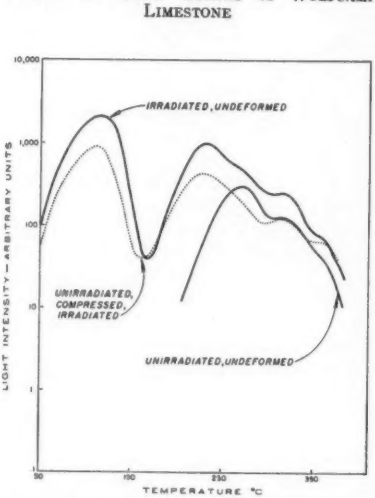

FIGURE 18.—GLOW CURVES OF LUNING DOLOMITE

tioned. The curves for irradiated undeformed samples of the "Devonian" and Fusselman are more or less typical of deeply buried limestones. The Wolfcamp curve exhibits a 170° peak, not ordinarily observed.

A compression of the order of 17 per cent introduces the new 280° peak found in Yule marble and calcite single crystal curves and associated with translation gliding. The 170° peak in the Wolfcamp is eliminated, but a new 170° peak appears in the Fusselman.

Dolomite.—The glow curve reflecting the natural thermoluminescence of the Hasmark dolomite (Fig. 17) is flat-topped over the region from about 240° to 280°, whereas a sharp peak at about 300° is typical of many naturally undeformed dolomites. The curve for the irradiated, experimentally undeformed specimens exhibits the commonly observed intense peak at 110°, characteristic also of limestones. The trough in the neighborhood of 170°, and another peak near 240° are also typical of many pure

dolomites. There is, however, a peak at about 280° which is not detected in the glow curves of dolomites collected from relatively undisturbed rock sections. Experimental compression of the order of 10 per cent under 2000 bars confining pressure does not materially alter the form of the glow curve. The glow curves for 1 cylinders are essentially similar to those for *T* cylinders; only the latter are shown. As was true for the limestones, the curves are similar whether or not the specimens were irradiated before compression. A bluish cast was observed in deformed irradiated specimens and also in normal cylinders irradiated after straining.

In an attempt to decide whether the 280° peak in the Hasmark might reflect the intense deformation to which the rock had been subjected in nature, glow curves were also obtained for Luning dolomite (Triassic) collected from an outcrop of nearly flat-lying beds. This rock, like the Hasmark, is a very nearly pure dolomite.

The glow curve reflecting the thermoluminescence of the irradiated but undeformed Luning is much like that of other dolomites from undisturbed, near-surface beds. The deformation of about 5 per cent has not significantly modified the glow curve (Fig. 18). Unfortunately, it is not possible to achieve large permanent deformation in dolomite in low-temperature tests, so that the experiment cannot be taken to mean that the 280° peak in the deformed Hasmark curves does not reflect a large natural deformation. It is therefore uncertain whether the 280° peak is due to a deformation or to impurity atoms in the dolomite crystals comprising the Hasmark rock.

Discussion

From the experiences of metallurgists it is known that large doses of electromagnetic radiation have no influence on the room-temperature strength of metals. In contrast, our results indicate that small but definite reductions of strength in certain rocks can be effected by gamma irradiation alone. This difference in behavior is understandable from the fundamental differences between electrical conductors (metals) and insulating solids (rocks). In metals the great mobility of free electrons even at room temperature permits rapid readjustments of those electrons which are momentarily excited by the scattering or absorption of gamma radiation by the metal atoms. On the contrary, the excited electrons in insulators have much less mobility and may encounter metastable energy states or traps in which they may remain at high energies for long times until released by, say, thermal stimulation when they may return to their normal lowest energy states. While the electrons are trapped in metastable levels, there is a redistribution of electrical charges which distorts the normal bonding of atoms near the trap. This is a possible mechanism of strength reduction in an ionic crystal.

It is also possible, but less likely, that the recoil from a very energetic electron emission produced by gamma absorption might actually produce dislocations in the lattice. The cross section for this process probably is, however, extremely low for gamma radiation compared to corpuscular radiation. Since the blue coloration and new peaks in the glow curves of calcite appear after deformation whether or not the material has been previously irradiated, it is concluded that most, if not all dislocations are generated during deformation and not during irradiation. The natural thermoluminescence of the undeformed materials is due probably to electrons trapped at growth imperfections: vacancies and interstitial atoms. Gamma irradiation increases the electron population of these traps but does not seem to create many new traps.

The geologically important alpha and beta particles could be expected to be much more effective than gamma rays in producing dislocations, but this very high efficiency of energy transfer to a crystal lattice means that the range of these particles is extremely short. The effect of neutrons would be of little geological interest, but the highly penetrating neutron radiation is of great technological importance for engineering materials.

The fact that the stress-strain curves of the irradiated marble are poorly reproducible compared with those of the unirradiated rock suggests that the radiation damage, whatever its nature, is not uniformly distributed throughout the material. This might mean that those imperfections sensitive to gamma radiation were unevenly apportioned and that the material could be locally weakened, in which event the strength reduction measured in a small sample might be misleading.

The facts that the strength of calcite single crystals is altered only slightly, or raised, if anything, whereas the yield stress of the marble is reduced by perhaps 20 per cent, suggest that most radiation damage is confined to grain boundaries. A further disordering of already relatively disordered regions may be involved.

It is known that high energy electromagnetic

radiations can create vacancies, mostly *F* centers (negative ion vacancies) in alkali halide crystals (Seitz, 1954). This process doubtless accounts for the slight coloration of the irradiated calcite before deformation. The mechanical properties of the halide crystals, for example, yield stress, internal friction, and hardness, as well as the elastic moduli, are influenced by X irradiation. Strength, hardness, and Young's modulus increase, and this has been attributed to the pinning of dislocations by vacancies which condense near dislocations in the crystals (Gordon and Nowick, 1956, p. 515). The small increase of strength of our gamma-irradiated calcite crystals may be due to the same process.

Several independent lines of evidence have demonstrated conclusively that the permanent deformation of halite results in the generation of vacancies by dislocations (Seitz, 1950, p. 1002). The blue coloration assumed by deformed halite upon Ra irradiation is further evidence (Przibram, 1953, p. 142). We have discovered blue coloration in a halite single crystal compressed 30 per cent under confining pressure and then gamma irradiated. The gliding mechanisms in halite and calcite are compared below.

In Figure 19 are shown the NaCl crystal structure and the calcite structure derived by distorting a cube by an extension along a space diagonal. The isometric forms in the halite are then analogous to the calcite forms expressed by rhombohedral indices (with reference to the cleavage rhomb).

There is no general theory relating the translation gliding elements—the plane *T* and the direction *t*—to a particular crystal structure. In metals, according to Schmid and Boas (1950, p. 86), "it is invariably the most dense atomic row that serves as a direction of glide, and usually the planes of highest atomic density are the glide planes." This means that planes and directions of low indices will form the commonest gliding elements. The gliding line is the zone axis of several possible gliding planes with low indices, and it is not always possible to predict which plane will be operative. In ionic crystals there appears to be a further restriction on translation. Ions of the same sign would not be likely to approach each other, since this would yield repulsions normal to the gliding line. There are, however, exceptions to this rule—the "forbidden" translation ($T = \{001\}$, $t = [100]$) taking place in galena (Buerger, 1930, p. 235).

In halite (Fig. 19) the lines containing the most closely spaced ions of like charge are the cube face diagonals $[1\bar{1}0]$, $[\bar{1}10]$, and four others comprising the three equivalent sets demanded by cubic symmetry. The common gliding plane is the dodecahedron $\{110\}$, but gliding on the cube $\{001\}$ can be achieved if the crystal is constrained and loaded so that the resolved

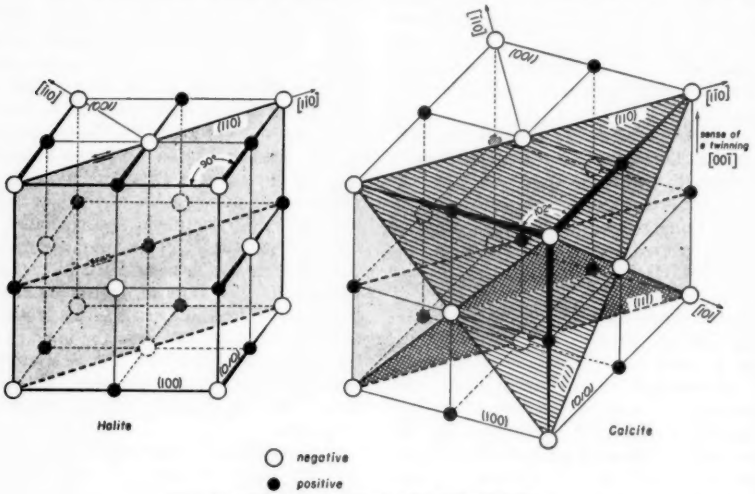

FIGURE 19.—CALCITE CRYSTAL LATTICE

shearing stress on {110} is low. Gliding on {111} at high temperatures has been claimed (Schmid and Boas, 1950, p. 229). In some crystals of the NaCl structural type, galena for example, translation occurs on {100} to the exclusion of {110}.

In calcite (110) is the familiar mechanical twin plane e_1 ($\bar{1}012$). [$1\bar{1}0$] translation might be expected but has never been observed probably because so little force is required for twinning along [$00\bar{1}$] = [r_2:r_3]. In the rhombohedron (001) = r_1 ($10\bar{1}1$). The diagonals [$1\bar{1}0$] and [$\bar{1}10$] are not equivalent as they were in the halite cube. We should expect translation to proceed with greater facility along the shorter of these lines [$\bar{1}10$] as has been observed (Turner, Griggs, and Heard, 1954, p. 931). In the cubic structure, translation in either sense is equally likely, but in calcite one sense may be preferred over the other, since the force field around a carbonate group is not spherical. Turner reports a negative sense, which is confirmed by our work.

In the rhombohedral structure the planes (111) = c (0001) and ($11\bar{1}$) = f_1 ($\bar{2}021$) are not equivalent. Translation on the base (111) has never been observed in calcite to our knowledge, though it is the common mechanism in dolomite at low temperatures (Higgs and Handin, 1954, p. 1263). Gliding on ($11\bar{1}$) has been observed by Turner, Griggs, and Heard (1954, p. 931) in the negative sense.

In our experiments on calcite we observed (001) translation along [$\bar{1}10$] in the negative sense as Turner did. This is analogous, then, to gliding in halite which is known to generate charge vacancies by dislocations, because of crowding of ions along rows containing all like charges. In calcite the blue coloration and appearance of new glow-curve peaks following deformation by translation gliding illustrate the same production of traps by dislocations. That twinning does not generate traps is due to the facts that (1) adjacent rows parallel to [$00\bar{1}$] are made up of ions of alternating sign, Ca and CO_3, so that any charge vacancies are likely to neutralize each other, and (2) in twin gliding the shear is fixed so that any one ion moves only a fraction of a periodic distance, never passing an ion of unlike charge. (The latter fact also explains why gliding occurs in an ordinarily "forbidden" direction. An ion does not move far enough toward its neighbor of opposite charge in an adjacent row to meet any appreciable repulsion.)

It is uncertain whether the coloration and thermoluminescence effects may be preserved in nature. The irradiation was ample, the dosage corresponding to that provided by the natural radioactive content of the surface rocks over a period of the order of 10 million years. Our blue calcite specimens have retained their color after storage in the dark for about 1 year. However, upon heating, the color disappears at about 290°C. The Yule marble is, of course, not blue, nor does the natural glow curve contain deformation induced peaks.[3] The rock, however, had almost certainly been heated above 300° during its metamorphism.

Summary and Conclusions

A 17-megaroentgen gamma irradiation does not influence the yield strength of calcite single crystals, but does result in a several per cent reduction of strength in Yule marble and probably slightly weakens anhydrite rock, dolomite rock, limestone, sandstone, shale, and siltstone.

Petrographic studies of experimentally deformed calcite crystals and Yule marble revealed that the principal deformation mechanism, translation gliding on r {$10\bar{1}1$} and twin gliding on e {$10\bar{1}2$}, established by Turner, Griggs, and Heard (1954), were active in both irradiated and unirradiated specimens.

Calcite deformed by translation gliding turns blue whether it is first irradiated, then deformed, or deformed and then irradiated. No color change accompanies deformation by twin gliding.

In calcite translation gliding leads to the appearance of a new peak at 280°C. in the thermoluminescence glow curve whether or not the material has been previously irradiated. Twin gliding enhances the 240° peak commonly found in calcite glow curves. Neither deformation much influences the typical 120° and 310° peaks which are probably related to traps associated with growth imperfections rather than disclocations.

We conclude that:

(1) Natural gamma radiation in the crust is not likely to affect the strength of rocks very much. Neither is the large gamma ray dose of these experiments important from the standpoint of the strength of the materials examined.

(2) Blue coloration and appearance of new

[3] Professor George W. Bain (Personal communication, May 1957) suggests that deformation effects may be related to grain size of limestones and reports that large (3 mm) aqua-blue crystals occur in some exposures of the Yule marble.

glow-curve peaks suggest the generation of vacancies (traps) by dislocations during deformation by translation gliding. The absence of color in calcite deformed by twin gliding is evidence for the lack of dislocations, at least of the kind providing traps for gamma-excited electrons.

(3) The alteration of the shapes of the thermoluminescence glow curves resulting from deformation may be preserved in naturally deformed rocks which have not been heated much above 200°C. If the natural thermoluminescence of a rock has been modified by folding or faulting, then caution must be observed in comparing glow curves for correlation or relative age determinations.

References Cited

Borg, Iris, and Turner, F. J., 1953, Deformation of Yule marble: Part VI—Identity and significance of deformation lamellae and partings in calcite grains: Geol. Soc. America Bull., v. 64, p. 1343–1352

Buerger, M. J., 1930, Translation-gliding in crystals of the NaCl structural type: Am. Mineralogist, v. 15, p. 174–187, 226–238

Gordon, R. B., and Nowick, A. S., 1956, The pinning of dislocations by X-irradiation of alkali halide crystals: Acta Metallurgica, v. 4, p. 514–527

Griggs, D. T., and Miller, W. B., 1951, Deformation of Yule marble: Part I—Compression and extension experiments on dry Yule marble at 10,000 atmosphere confining pressure, room temperature: Geol. Soc. America Bull., v. 62, p. 853–862

Handin, J., 1953, An application of high pressure in geophysics: Experimental rock deformation: Am. Soc. Mech. Eng. Trans., v. 75, p. 315–324

Handin, J., and Fairbairn, H. W., 1955, Experimental deformation of Hasmark dolomite: Geol. Soc. America Bull., v. 66, p. 1257–1274

Handin, J. W., and Griggs, D. T., 1951, Deformation of Yule marble: Part II—Predicted fabric changes: Geol. Soc. America Bull., v. 62, p. 863–885

Handin, J., and Hager, R. V., Jr., 1957, Experimental deformation of sedimentary rocks under confining pressure: Part I—Tests at room temperature on dry samples: Am. Assoc. Petroleum Geologists Bull., v. 41, p. 1–50

Higgs, D. V., and Handin, J., 1954, Experimental deformation of dolomite single crystals: Geol. Soc. America Bull., v. 65, p. 1263

Lewis, D. R., 1956, The thermoluminescence of dolomite and calcite: Jour. Phys. Chemistry, v. 60, p. 698–701

Palache, C., Berman, H., and Frondel, C., 1952, The System of Mineralogy, Vol. 1: 7th ed., New York, J. Wiley and Sons, Inc., 834 p.

Przibram, K., 1953, Verfärbung und Lumineszenz: Vienna, Springer-Verlag, 275 p.

Schmid, E., and Boas, W., 1950, Plasticity of Crystals: London, Hughes and Co., 353 p.

Seitz, F., 1950, The generation of vacancies by dislocations: Phys. Rev., v. 79, p. 1002–1003

Seitz, F., 1954, Color centers in alkali halide crystals. II: Rev. Modern Physics, v. 26, p. 7–94

Turner, F. J., and Ch'ih, C. S., 1951, Deformation of Yule marble: Part III—Observed fabric changes due to deformation at 10,000 atmospheres confining pressure, room temperature, dry: Geol. Soc. America Bull., v. 62, p. 887–905

Turner, F. J., Griggs, D. T., and Heard, H., 1954, Experimental deformation of calcite crystals: Geol. Soc. America Bull., v. 65, p. 883–934

Turner, F. J., Griggs, D. T., Heard, H., and Weiss, L. W., 1954, Plastic deformation of dolomite rock at 380°C.: Am. Jour. Sci., v. 252, p. 477–488

Zeller, E. J., 1954, Thermoluminescence of carbonate sediments, *in* Faul, Henry, Editor, Nuclear Geology: N. Y., John Wiley and Sons, 414 p.

Shell Development Company, Exploration and Production Research Division, Publication No. 118

Manuscript Received by the Secretary of the Society, March 21, 1957